Neural mechanisms of phantom limb pain



Victoria Root

Lady Margaret Hall & Nuffield Department of Clinical Neurosciences

University of Oxford

A thesis submitted for the degree of

Doctor of Philosophy

June 2022

Covid-19 Impact Statement

Note that during the Covid-19 global pandemic (from March 2020 onwards) my ability to collect data was severely affected. Data for *Chapters 1* and *2* (excluding passive case studies) were already collected, but data for *Chapters 3* and *4* had not yet been collected and could not be transformed to online studies due to requirement of physical equipment for the experimental protocols. When data collection resumed (between September 2020 – December 2020 and July 2021 onwards), recruitment of controls and acquired amputees was difficult. Amputees in particular, who are normally recruited from across the UK, were reluctant to travel and hesitant to participate understandably. This, unfortunately, led to only a small number of amputees being recruited for this thesis (n=4). Anecdotal conclusions only, will therefore be made throughout *Chapters 3* and *4*.

Victoria Root

Trinity Term 2022 Lady Margaret Hall

A thesis submitted in partial fulfilment of the requirements for the degree of Doctor of Philosophy at the University of Oxford

Thesis abstract

After limb amputation, the majority of amputees report the presence of phantom limb pain (PLP), whereby chronic painful sensations are localised in the missing limb. In this thesis I assessed the potential neural mechanisms underlying PLP, with a set of experiments which evaluated a popular theory of PLP – the maladaptive plasticity model, and then explored alternative hypotheses of PLP.

First, I assessed one of the long-held, implicit assumptions of the maladaptive plasticity model – that the cortical neighbour to the hand in the primary somatosensory cortex (S1) is the lips/lower face. Controls participated in active somatotopic mapping of the upper and lower face using functional magnetic resonance imaging. Univariate and multivariate analyses indicated that the likely cortical neighbour to the hand was the upper, not lower, face. Subsequent recruitment of amputees and congenital one-handers (positive control group) found little evidence for somatotopic shifts of the upper and lower face towards the deprived hand region in amputees, with no significant associations to PLP. Conversely, congenital one-handers, who do not experience PLP, displayed gross somatotopic shifts of all facial parts tested.

Next, the role of associative learning mechanisms in PLP was explored. Specifically, a novel behavioural task was designed to assess how amputees learn about nociceptive information in relation to phantom movement. Controls indicated significant learning of probabilistic cues with movements, validating the use of the behavioural paradigm for future studies with amputees. Anecdotal results from computational modelling and quantification of expectation biases indicated idiosyncratic learning styles and preserved placebo responses in amputees. Finally, a well-replicated task used in computational psychiatry demonstrated that ‘jumping-to-conclusions’, where individuals require little sensory information before belief formation, was tentatively related to pain catastrophising.

Taken together, these results not only assessed one of the most common explanations of PLP, but also offered novel behavioural paradigms that encourage the exploration of PLP outside of S1, with the aim to improve future treatment.

This thesis contains approximately 44,100 words.

Acknowledgements

Firstly, I would like to thank the limb-difference community and the one-handed participants that volunteered to take part in my studies. Thank you for answering my continuous questions about all things phantom-related.

Secondly, I would like to thank my funders: the Nuffield Department of Clinical Neurosciences and the Medical Research Council. Without their generosity I would not have been able to pursue this DPhil.

Irene Tracey and Tamar Makin, thank you both for being great co-supervisors and female role models. Irene, thank you for always finding time for me, I appreciated our chats about everything pain-related! And Tamar, you have been with me on my science journey since the beginning. Thank you for always pushing and challenging me – you have made me a better scientist because of it.

To all the plasticity lab members, past and present, I am grateful for all your support throughout the years, and for always being encouraging and thoughtful in your feedback after my lab presentations. In particular, I would like to thank Dollyane Muret and Roni Maimon-Mor. Thank you both for the time and kind mentorship, along with insightful academic advice, you have given me over the years.

Thank you also to the pain group at Oxford. You all helped me settle into not only a PhD but also a brand-new field at the beginning of my DPhil. I always enjoyed the inspirational journal clubs!

I wish to also thank the following students that I supervised during this time: Timothee Maniquet, Cecile Klinguer and Maite Arribas Ardura. Maite – we had a hell of a time with Covid-19 changing our plans. I couldn't have asked for a better student to go through that with.

I would also like to thank my collaborators: Hristo Dimitrov, Dario Farina, Suyi Zhang, Ben Seymour and Abby Tabor. In particular, thank you to Hristo for keeping me company in that B05 testing room and dreaming about all the cool studies we could do with EMG and phantoms – if only we had more time! Thank you to Suyi for answering my endless questions about reinforcement learning and for being my computational guru. Also, to Abby Tabor – our long chats about how to reconceptualise phantom limb pain within a predictive processing framework were one of the highlights of my PhD. Thank you for being a great mentor and friend – we will get that paper finished!

On a more personal note, thank you to my friends Alex, Jenny, Rob, Marie, Lilly and Paul, and all my Manchester friends up North (Sam, Megs and Mel!). You guys kept me sane during this journey with much needed beer, margaritas and gaming sessions. In particular thanks to Marie Müller – we met at UCL on the first day of our MScs, and look at us now! Thank you for giving me the best advice on all things statistics related and for proofreading my most complicated chapter.

Thank you to my Mum, Dad and Grandma for always asking me how the PhD was going, even if they didn't quite understand what I was talking about when I answered. Thank you also to my sisters – Katherine and Lucy. You guys have always had my back and I couldn't have done this without you.

And finally, thank you to my partner Hanna. This thesis is as much yours as it is mine. I could not have done this PhD without your continuous love and support. Here's to the next chapter.

Contents

List of Acronyms **9**

List of Figures **13**

Chapter 0 | Introduction **16**

0.1 What is pain? *16*

0.2 Phantom limb pain in acquired amputees *18*

0.3 The maladaptive plasticity theory of phantom limb pain *20*

0.4 Cortical representation of the phantom hand is preserved after amputation *25*

0.5 What about cortical reorganisation and phantom limb pain? *26*

0.6 Beyond the phantom – viewing phantom pain as chronic pain *29*

0.7 Aims of this thesis *31*

Chapter 1 | Face topography in the primary somatosensory cortex **34**

1.1 Introduction *34*

1.2 Methods *37*

1.2.1 Participants 37
1.2.2 Functional MRI sensorimotor task 39
1.2.3 Functional MRI passive stimulation task 40
1.2.4 MRI data acquisition 41
1.2.5 MRI pre-processing 42
1.2.6 Functional MRI analysis 43
1.2.7 Regions of Interest (ROI) definition 44
1.2.8 Winner-takes-all approach 46
1.2.9 Cortical distance analysis 47
1.2.10 Group-level visualisations 47
1.2.11 Multivariate representational analysis 48
1.2.12 Statistical analyses 49

1.3 Results *51*

1.3.1 The cortical neighbour of the hand representation is the forehead 51
1.3.2 The upper faces' activation patterns show greater similarity to the thumb than the lower face 54
1.3.3 Facial somatotopy is stable across time and paradigms 56

Chapter 2 | Reassessing face topography in the primary somatosensory cortex following hand loss **66**

2.1 Introduction *66*

2.2 Methods *69*

2.2.1 Participants 69
2.2.2 Phantom sensations rating 71
2.2.3 Functional MRI sensorimotor task 71
2.2.4 Functional MRI analysis 72
2.2.5 Surface area calculation 72
2.2.6 Group-level visualisations 73
2.2.7 Multivariate representational analysis 74
2.2.8 Statistical analyses 74

2.3 Results *76*

2.3.1 The upper face borders the deprived hand area in amputees and one-handers ... 76

2.3.2 One- handers, but not amputees, show lip remapping in the deprived cortex based on univariate topographic mapping 77
2.3.3 One-handers, but not amputees, show forehead remapping in the deprived cortex, based on univariate topographic mapping 80
2.3.4 Tongue movements produce different topographic maps across groups 83
2.3.5 Brain decoding in the deprived hand area reveals stable facial representational pattern for amputees, and increased facial information in one-handers 85

2.4 Discussion *90*

Chapter 3 | How does sensorimotor engagement influence learning of novel nociceptive stimuli? **97**

3.1 Introduction *97*

3.2 Methods *102*
3.2.1 Participants 102
3.2.2 Experimental procedures 104
3.2.3 Pain familiarisation and thresholding 104
3.2.4 Electromyographic recording 108
3.2.5 Aversive learning paradigm 110
3.2.6 Questionnaires 114
3.2.7 Learning measures 115
3.2.8 Behavioural data modelling 118
3.2.9 Statistical analyses 122

3.3 Results *124*
3.3.1 Participants were able to successfully learn pain contingencies with and without movements 124
3.3.2 Participants demonstrate a generalised bias towards their initial learning 129
3.3.3 Movement enhances placebo responses during acquisition 133
3.3.4 Participants learn pain probabilities quicker without movement 138

3.4 Discussion *143*

Chapter 4 | Is learning of novel nociceptive stimuli associated with probabilistic reasoning? **153**

4.1 Introduction *153*

4.2 Methods *158*
4.2.1 Participants 158
4.2.2 Experimental procedure 159
4.2.3 Questionnaires 164
4.2.4 Pain learning measures 164
4.2.5 Statistical analysis 165

4.3 Results *167*
4.3.1 Catastrophising beliefs about pain are tentatively related to 'jumping-to-conclusions' 167
4.3.2 No significant relationship was found between nociceptive learning rates and 'jumping-to-conclusions' 171
4.3.3 Amputees demonstrate similar responses to the Beads Task as controls 173

4.4 Discussion *175*

Chapter 5 | Discussion **184**

5.1 Thesis overview *184*

5.2 Maladaptive plasticity model – where do we go from here? *186*

5.3 Phantom limb pain beyond the primary somatosensory cortex *189*

5.4 Future treatment avenues for phantom limb pain *196*

5.5 Concluding remarks *199*

References **202**

Appendices **233**

6.1 Supplementary Materials Chapter 1 ..... *233*
6.1.1 Supplementary Methods 233
6.1.2 Supplementary Figures 235

6.2 Supplementary Materials Chapter 2 ..... *239*
6.2.1 Supplementary Figures 239
6.2.2 Supplementary Tables 240

6.3 Supplementary Materials Chapter 3 ..... *248*
6.3.1 Supplementary Figures 248
6.3.2 Supplementary Tables 257

6.4 Supplementary Materials Chapter 4 ..... *262*
6.4.1 Supplementary Figures 262
6.4.2 Supplementary Tables 263

List of Acronyms

δ	Prediction error
50-50	Cue with 50% probability of receiving warm or painful temperatures
95% CI	95% Confidence interval
3T	3 Telsa
a	Learning rate (alpha)/Associability
ACC	Anterior cingulate cortex
ANOVA	Analysis of variance
BAs	Brodmann's area
BDI	Beck's Depression Inventory
BET	Brain extraction tool
BF	Bayes Factor
BIC	Bayesian Information Criterion
BOLD	Blood oxygenation level dependent
CoG	Centre of gravity
CS	Conditioned stimulus
DTC	Draws to Certainty
DTD	Draws to Decision
EMG	Electromyography
FEAT	fMRI Expert Analysis Tool
FILM	FMRIB's Improved Linear Model
FLIRT	FMRIB's Linear Image Registration Tool
FNIRT	FMRIB's Nonlinear Registration Tool

fMRI	Functional magnetic resonance imaging
FSL	FMRIB Software Library
FWHM	Full-width half maximum
GABA	gamma-aminobutyric acid
GLM	General linear model
H-L	Cue starting at high-pain probability (acquisition block) and switching to low-pain probability (reversal block)
Hz	Hertz
IED	Inter-electrode distance
JTC	Jumping-to-conclusions
K	Kappa
KPa	Kilopascal
L	Left
L-H	Cue starting at low-pain probability (acquisition block) and switching to high-pain probability (reversal block)
LMM	Linear mixed model
M1	Primary motor cortex
MATLAB	Matrix laboratory
MCFLIRT	Motion Correction using FMRIB's Linear Image Registration Tool
MDS	Multidimensional scaling
MEG	Magnetoencephalography
mm	millimetres
MNI	Montreal Neurological Institute
MR	Magnetic Resonance
MVC	Maximum voluntary contraction

η	Eta
NHS	National Health Service
n.s.	Non-significant
OLP	Open-label placebo
PCS	Pain catastrophising scale
PLP	Phantom limb pain
PLS	Phantom limb sensations
R	Trial's actual sensory outcome
R	Right
RLP	Residual limb pain
RDM	Representational dissimilarity matrix
RF	Radio frequency
RMS	Root mean square
ROI	Regions of interest
RSA	Representational Similarity Analysis
RW	Rescorla-Wagner
s	Seconds
S1	Primary somatosensory cortex
S2	Secondary somatosensory cortex
SD	Standard deviation
SE	Standard error of the mean
t	Trial
TE	Echo delay time
TFCE	Threshold free cluster enhancement
TMR	Targeted muscle reinnervation

TMS	Transcranial Magnetic Stimulation
TR	Repetition time
US	Unconditioned stimulus
V	Model predicted value
x_t	Cue shown on trial t

List of Figures

Figure 0.1. A schematic description of the maladaptive plasticity model……..22

Figure 1.1. Experimental design for active sensorimotor task…….39

Figure 1.2. Regions of interest and winner-takes-all analysis in the primary somatosensory cortex for an example participant……..46

Figure 1.3. Average activity maps for each facial movement and cortical geodesic distances……52

Figure 1.4. Representational Similarity Analysis in face region-of-interest in two-handed controls……55

Figure 1.5. Representational dissimilarity matrices (RDMs) for Active 1, Active 2 and Passive for CTR 01……..57

Figure 1.6. Representational dissimilarity matrices (RDMs) for Active 1, Active 2 and Passive for CTR 02.……58

Figure 1.7. Graphical summary of main findings and methodologies for Chapter 1……..59

Figure 2.1. Group-level activity maps for each facial movement…….77

Figure 2.2. Characterisation of lip (re)mapping in the primary somatosensory cortex……..79

Figure 2.3. Forehead topography in the primary somatosensory cortex……82

Figure 2.4. Tongue remapping in amputees and one-handers in the primary somatosensory cortex……..85

Figure 2.5. Representation Similarity Analysis (RSA) in the deprived/non-dominant hand area across all groups……..87

Figure 2.6. Representation Similarity Analysis (RSA) in the deprived/non-dominant face area across all groups……...89

Figure 2.7. Graphical summary of main findings and methodologies for Chapter 2……..90

Figure 3.1. Thermode stimulation sites and pain thresholding procedures…….106

Figure 3.2. Schematic outline of aversive learning paradigm……113

Figure 3.3. Average expectancy and intensity ratings per cue and block……128

Figure 3.4. Acquisition biases for high- and low-pain probabilities……...131

Figure 3.5. Nocebo and placebo responses for Active and Passive conditions…….135

Figure 3.6. Correlations between nocebo and placebo responses in Active and Passive conditions……138

Figure 3.7. Model comparison statistics and individual correlations between actual and predicted ratings……140

Figure 3.8. Average learning rates in Active and Passive conditions and the relationship between learning rates and placebo responses……..142

Figure 3.9. Graphical summary of main findings and methodologies for Chapter 3……143

Figure 4.1. Experimental design for Draws to Decision……..160

Figure 4.2. Experimental design for Draws to Certainty……162

Figure 4.3. Draws to Decision and Disconfirmatory Evidence for control participants and amputees……168

Figure 4.4. Regressions between questionnaire and bead measures in controls and amputees……170

Figure 4.5. Relationship between Draws to Decision and pain learning measures in control participants……173

Figure 4.6. Graphical summary of main findings and methodologies for Chapter 4……175

List of Tables

Table 2.1. Demographic details for amputees (A01-17) and congenital one-handers (C01-21). 70

Table 3.1. Demographic details for amputees..... 103

Table 3.2. Model fitting parameters means and standard deviations. 121

Table 3.3. Temperatures used for warm and painful trials for controls and amputees..... 124

Table 4.1. Task and questionnaire details for amputee sample. 174

Chapter 0 | Introduction

> *"Verily it is a thing wondrous strange and prodigious, and which will scarce be credited, unlesse by such as have seen with their eyes, and heard with their ears the Patients who have many months after the cutting away of the Leg grievously complained that they yet felt exceeding great pain of that leg so cut off." (p. 338, Paré 1649).*

0.1 What is pain?

Pain is defined as "an unpleasant sensory and emotional experience associated with, or resembling that associated with, actual or potential tissue damage" (*p*.1977, Box 2, Raja et al., 2020), according to the International Association for the Study of Pain. It is notably different from nociception, which refers to activity that occurs in the nervous system in response to a noxious stimulus. Pain, by definition, is subjective – it is "always a personal experience… influenced to varying degrees by biological, psychological and social factors", and learnt across an individual's lifetime (*p*.1977, Box 2, Raja et al., 2020). Pain usually serves an adaptive role, signalling to the individual actual or potential threat to the body. However, it can also have adverse effects on function, social and psychological well-being. For example, if pain persists beyond the expected healing period, usually around 3 months, it is deemed to be chronic (Treede et al., 2019; Cohen et al., 2021).

Chronic pain holds little evolutionary benefit and has been associated with a wide-range of negative impacts for the individual, ranging from biological and neurological changes, development of co-occurring mental disorders (e.g.,

depression, anxiety), loss of sleep, social withdrawal and financial difficulties due to the loss of work (Cohen et al., 2021). A recent systematic review and meta-analysis found that between one-third and one-half of the UK population (~28 million adults) are affected by chronic pain, with 10.4 – 14.3% of people, rising to 19% across Europe (Breivik et al., 2006), suffering from moderate to severely disabling pain (Fayaz et al., 2016). Chronic pain may arise secondary to an injury or condition (e.g., osteoarthritis) where the pain may be viewed as a symptom, or it can emerge independently from any known cause, in the case of conditions such as fibromyalgia and complex regional pain syndrome (Treede et al., 2019).

Chronic pain has previously been categorised into three types: nociceptive, neuropathic and nociplastic. Broadly speaking, nociceptive pain arises from activity in neural pathways, neuropathic pain arises from damage/disease to those pathways and nociplastic pain from the abnormal processing of pain signals without evidence of clear damage to the system (Cohen et al., 2021). Despite these categorisations, it is generally accepted that the manifestation of chronic pain in individuals is not so clear cut, and usually presents as a mixture of these phenotypes. Pain, and chronic pain, can therefore be viewed as a continuum, with the exact characteristics of the pains' presentation dependent on each individual's prior experience and/or injury. These factors can also inform the treatment of chronic pain, which can comprise of the following: physical exercise, cognitive behavioural therapy, pharmacological management (including opioids), surgery, neurostimulation to the spinal cord or cortex and alternative therapies (e.g., acupuncture), to name a few. Treatment efficacy, however, has been questioned (Barroso et al., 2021; Knotkova et al., 2021; Morley et al., 2013; Turk, 2002), with

total pain relief and high-quality evidence for effectiveness lacking. A possible reason is that treatment for chronic pain is usually targeted towards the management of symptoms, aiming to improve quality of life rather than pain reduction per se (Cohen et al., 2021). Understanding the mechanisms that underlie chronic pain, however, may better inform future treatment approaches and improve the lives of individuals who suffer from such a condition.

0.2 Phantom limb pain in acquired amputees

The motivation for this thesis was to explore, and design novel paradigms to assess, potential neural mechanisms underlying a chronic pain condition – phantom limb pain (PLP). PLP is a chronic neuropathic pain syndrome, characterised by painful sensations in the missing limb after amputation. It is notably different to residual limb pain (RLP), which is defined as pain residing in the stump only, and to non-painful phantom sensations (PLS). PLS are usually described as innocuous, involving tingling, itching or numbness sensations in the missing limb. They are very common after amputation, usually beginning instantaneously (Ehde et al., 2000; Henderson & Smyth, 1948; van der Schans et al., 2002). Many amputees also report the ability to voluntarily move their phantom limb. This is supported by reports of detailed kinaesthetic sensations regarding the degree and extent of phantom movement (Henderson & Smyth, 1948; Shukla et al., 1982b).

PLP sensations, however, are most commonly described as feeling sharp, shooting, stabbing, throbbing, burning, aching, and/or cramping (Ehde et al., 2000; Schley et al., 2008), with PLP episodes varying in intensity, duration, and

frequency (Whyte & Niven, 2001). The prevalence of PLP is relatively high after amputation, with a recent meta-analysis citing incidence rates between 50 – 85% (mean 63%; 95% CI[58.23, 67.05]; Limakatso et al., 2020; also see Stankevicius et al., 2021 who reports a lifetime prevalence of PLP at 76% – 87%), and is thought to be relatively constant over time, at least up to 2 years after amputation (Schone et al., 2022). Factors associated with the development of PLP range from preoperative pain, RLP, proximal site of amputation, lower limb amputation, affective disorders prior to amputation (e.g., depression and anxiety) and the presence of PLS (Balakhanlou et al., 2021; Diers et al., 2022; Larbig et al., 2019; Limakatso, Bedwell, et al., 2020; Schone et al., 2022). Despite the high prevalence of PLP it is notoriously difficult to treat (Makin, 2021; Schone et al., 2022). Treatment options range from typical pharmacological drugs (Erlenwein et al., 2021; Hall & Eldabe, 2017; McCormick et al., 2014), sensory discrimination training (Flor et al., 2001; Graham et al., 2020), graded motor imagery (Limakatso, Madden, et al., 2020; Moseley, 2006; although see Thieme et al., 2016), mirror therapy (Barbin et al., 2016; Moseley et al., 2008; Ramachandran et al., 1995; Wang et al., 2021), virtual and augmented reality (Herrador Colmenero et al., 2018; Ortiz-Catalan et al., 2016; Osumi et al., 2019; Rajendram et al., 2022), peripheral nerve blocks (Borghi et al., 2014; Ilfeld et al., 2021; Vaso et al., 2014), targeted muscle reinnervation (Dumanian et al., 2019; Valerio et al., 2019), spinal cord stimulation (Aiyer et al., 2017), non-invasive brain stimulation (Bolognini et al., 2013, 2015; Damercheli et al., 2022; Gunduz et al., 2021; Kikkert et al., 2019), motor cortex stimulation (Garcia-Pallero et al., 2022; Nguyen et al., 2011) and deep brain stimulation (Abreu et al., 2022; Bittar et al., 2005). Despite the range of treatment options available, complete eradication of PLP is rarely achieved and

the quality of evidence for existing treatments and their effectiveness is questionable (Aternali & Katz, 2019; Makin, 2021; Richardson & Kulkarni, 2017), akin to other chronic pain conditions. Larger sample sizes, double-blind placebo-controlled clinical trials and wide-spread agreement on therapeutic targets, be that reduction in PLP intensity (and if so, clarity on accepted measures) or improved quality of life, are needed in order to assess treatment efficacy accurately. Most importantly, we need a thorough mechanistic understanding of PLP before we are able to develop optimal treatments that provide adequate pain relief for individuals.

0.3 The maladaptive plasticity theory of phantom limb pain

One of the most influential models describing the neural mechanisms of PLP, commonly called the maladaptive plasticity model, proposes that pain arises as a perceptual consequence of cortical reorganisation in the primary somatosensory cortex (S1) following limb loss (Flor et al., 1995). Cortical reorganisation reflects changes in the functional organisation of a cortical map and is usually signified by shifts in boundaries between cortical representations. In terms of S1, body parts are arranged somatotopically, with neighbouring body parts often represented adjacently in the cortical map (although note some exceptions e.g., the hand and face; Penfield & Boldrey, 1937; Penfield & Rasmussen, 1950). The hand area itself contains a detailed somatotopy of the hand, with each digit represented separately and adjacently (Merzenich et al., 1983). The cortical topography of body parts is somewhat less defined, however, within the primary motor cortex (M1; Graziano & Aflalo, 2007; Schieber, 2001), causing the majority of the cortical reorganisational research in primates and humans to focus on changes, and shifts

in, somatotopic boundaries within S1. However, previous work has demonstrated that dense anatomical connections exist between S1 and M1 in primates and rodents (Bedwell et al., 2014; Stepniewska et al., 1993). In addition to this, during skilled movements (e.g., hand grasps) it is known that M1 receives tactile and proprioceptive feedback from S1 (Gardner et al., 2007) and, conversely, S1 receives inputs from M1 to aid in online processing of sensory signals, e.g., corollary discharge (Crapse & Sommer, 2008; Umeda et al., 2019), akin to the feedforward model of motor control (Miall & Wolpert, 1996). Thus, cortical activity profiles of body parts in S1 and M1 are not isolated from one another, but interact in a richly informative and detailed manner. Therefore, despite the focus on S1 somatotopy in cortical reorganisation in humans and primates, the role of M1 cannot be ruled out and subsequent findings should be viewed within a sensorimotor (i.e., joint) context.

Influential work first looking at cortical reorganisation after amputation was carried out in non-human primates using electrophysiology. Here authors found that 2 – 6 months after digit amputation, the deprived finger area was subsequently invaded by cortically adjacent fingers (Merzenich et al., 1984). It was later shown that after long-term sensory input loss (~12 years) from the entire hand and arm in macaque's, extensive cortical reorganisation was observed: the missing hand area in S1 become responsive to touch on the lower part of the macaque's face (Pons et al., 1991). Several mechanisms have been proposed to underly cortical reorganisation (see Collins et al., 2018 for an overview), including axonal sprouting (Florence et al., 1998; although see Chand & Jain, 2015), changes in subcortical organisation projecting to the cortex (Jones & Pons, 1998; Jain et al.,

2008), and the unmasking of inhibited cortical connections (Harding-Forrester & Feldman, 2018; Li et al., 2014; Muret & Makin, 2021). Since the body part representations that expanded into the deprived S1 region in these non-human primate studies were cortical neighbours, it was subsequently established that cortical reorganisation likely follows the neighbourhood relationships in the native somatotopy (Kaas et al., 2008; although see Hahamy & Makin, 2019).

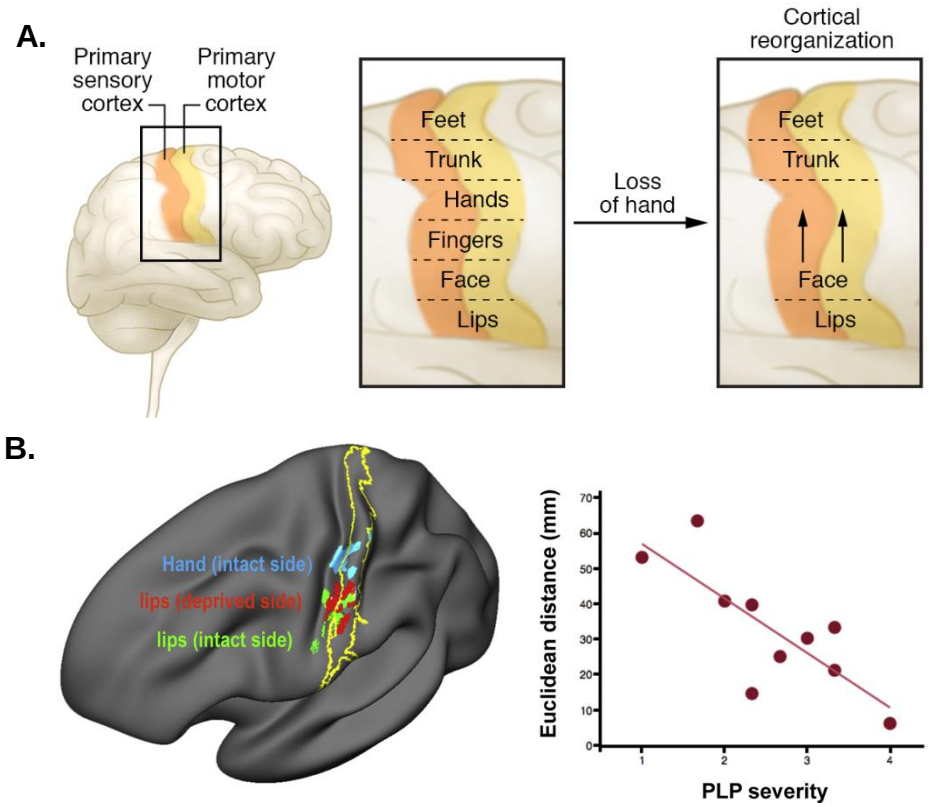


Figure 0.1. *A schematic description of the maladaptive plasticity model.* **(A)** The maladaptive plasticity model proposes that the sensorimotor (primary sensory cortex in orange and primary motor cortex in yellow) cortical representation of the neighbouring body part to the hand (depicted in the left-hand side box) – the face – reorganises into the deprived hand region (shown in the right-hand side box) after upper limb loss. Resulting 'mismatches' between hand and face cortical activity are thought to produce an 'error signal' which is interpreted as painful. Adapted from Collins et al., (2018). **(B)** Functional neuroimaging results in n=10 upper-limb amputees with phantom limb pain who underwent sensory stimulation (air-puffs) of the intact thumb (blue) and lips (red=deprived hemisphere; green=intact hemisphere). Euclidean distances between activity for the deprived lips and intact thumb (flipped into the deprived hemisphere) demonstrated a replication of Flor et al.'s (1995) findings – amputees who reported higher levels of PLP intensity also displayed shorter distances between lip and thumb activity. Adapted from Makin & Flor (2020).

In terms of cortical reorganisation in humans, this led to a plethora of studies using changes in the representation of the lower face – usually denoted by lip movement or stimulation – as a marker for cortical reorganisation (although see *Chapter 1* for a thorough investigation into the lips, and the face in general, as a suitable cortical neighbour to the hand). Specifically, the maladaptive plasticity model was based on the idea that S1 sensory deprivation after an amputation leads to degradation of the missing hand area, which is consequently 'invaded' by the neighbouring representation of the lips (Flor, Nikolajsen, & Staehelin Jensen, 2006; Ramachandran & Hirstein, 1998; see *Figure 0.1.A*). As a result, the deprived hand area now responds to input intended for adjacent cortical territories, and the mismatch between the body part representations generates an 'error' signal, which is subsequently interpreted as pain arising from the phantom hand.

A seminal study by Flor et al., (1995), using magnetoencephalography (MEG), found that the cortical distance between the lip and the missing hand area was reduced in amputees compared to controls. Importantly, amputees with worse PLP had greater shifts in the lip representation towards the missing hand area (see *Figure 0.1.B*). This correlation between S1 reorganisation and PLP has subsequently been supported by various studies using different paradigms (including active) and participant groups (Diers et al., 2010, 2015; Karl et al., 2001; Lotze et al., 2001; MacIver et al., 2008; see Flor et al., 2006 or Andoh et al., 2018 for an overview). The idea that pain arises from perceptual uncertainty as a result of maladaptive plasticity is also prominent in other theories of PLP, such as sensorimotor incongruence (Harris, 1999) and the stochastic entanglement hypothesis (Ortiz-Catalan, 2018). Here amputation is hypothesised to trigger

incongruences within the sensorimotor system, or cross-firing and ‘retuning’ of the sensorimotor and pain network. Both explanations, including that of cortical reorganisation, rests on the assumption that the level of sensory noise within the system is interpreted by higher-order areas as erroneous and therefore painful (Flor, Nikolajsen, & Staehelin Jensen, 2006; Harris, 1999).

A key implication of the maladaptive plasticity model and other theories, is that by reversing cortical reorganisation and ‘re-establishing’ the missing hand representation, PLP should be alleviated (Moseley & Flor, 2012). In fact, this is the assumption underlying a range of treatments aimed to engage with the phantom limb visually or through motor execution, ranging from mirror box and graded motor imagery to virtual and augmented reality, which have all reported mixed effectiveness (Barbin et al., 2016; Thieme et al., 2016). This throws the validity, and the reliability, of such theories into doubt – if the premise of the theory does not adequately translate to pain relief, what are they missing?

0.4 Cortical representation of the phantom hand is preserved after amputation

Recent work has started to contest the fundamental assumptions of the maladaptive plasticity model. By taking advantage of amputees’ ability to voluntarily move their phantom hand researchers have been able to demonstrate that the phantom hands’ cortical representation perseveres – not degrades – after amputation. For example, phantom limb movements have been shown to elicit both central and peripheral motor signals, different to that of imagined movements

(Raffin, Giraux, & Reilly, 2012; Raffin, Mattout, Reilly, & Giraux, 2012). It has also been shown that phantom movements evoke comparable neurophysiological responses to real movements during both action execution and action inhibition (Bruno et al., 2019). The activity subsequently elicited in the missing hand area in the sensorimotor cortex has also been shown to be similar in amplitude to controls non-dominant hand movements (Kikkert et al., 2018; Makin, Scholz, et al., 2013), along with a detailed somatotopy of the phantom hand, up to decades after amputation (Kikkert et al., 2016; Wesselink et al., 2019). Preserved cortical representation of the phantom hand has been found using both active (Bruurmijn et al., 2017) and passive (Serino et al., 2017) neuroimaging, including MEG (Yanagisawa et al., 2016), paradigms, intracortical stimulation of the deprived hand area (Flesher et al., 2016, 2019), and stimulation of the phantom hand area with transcranial magnetic stimulation (TMS) (Bestmann et al., 2006; Cohen et al., 1991; Hess et al., 1986; Mercier et al., 2006; Reilly et al., 2006). These studies are also consistent with findings at the periphery. Here peripheral nerve stimulation of amputees' residual nerves evoked phantom sensations (Anani & Körner, 1979; D'Anna et al., 2017; Dhillon et al., 2004; Granata et al., 2018), which were highly localised to spatially restricted regions of the phantom hand (Tan et al., 2014). This indicates that the entire somatosensory pathway associated with the missing hand are functionally preserved despite amputation.

0.5 What about cortical reorganisation and phantom limb pain?

Work demonstrating the persistence of the cortical representation of the phantom hand after amputation sits in contrast to traditional reorganisational accounts (although see Boström et al., 2014). In support of this, recent research has shown

that the amputees missing hand area is not likely remapped by an ‘invasion’ of the lips, relative to controls (Kikkert et al., 2018; Makin, Scholz, et al., 2013; Valyear et al., 2020). Any reported shifts in the lip representation have been found to be smaller than previously thought, and limited to the face region itself (Makin et al., 2015; although see Raffin et al., 2016). *Chapter 2* will further provide a comprehensive assessment of the extent of somatotopic changes in the face representation as a whole, beyond solely the lips, after amputation, and whether any remapping is associated with PLP.

Indeed, it has been shown that the preservation of the cortical sensorimotor activity of phantom hand itself that correlates with PLP reports, rather than the reorganisation of this cortical representation, with greater preserved activity in the missing hand area related to greater chronicity of the PLP (Kikkert et al., 2018, 2019; Makin, Scholz, et al., 2013). But perhaps the strongest empirical evidence against the notion of maladaptive S1 reorganisation is that, as stated before, when stimulating the missing hand region painful percepts are never evoked (Flesher et al., 2016; Mercier et al., 2006), leading to the question as to what does this persisting phantom activity represent?

To answer this, we must go back to earlier theories on PLP which suggested that PLP arises from peripheral aberrant signals as a result of nerve injury (Nystrom & Hagbarth, 1981). Due to difficulties in administering anaesthetic nerve blocks and the inability to eliminate PLP completely (Borghi et al., 2010; Nystrom & Hagbarth, 1981; potentially due to difficulties in blocking nociceptive C-fibres; Serra et al., 2015), this theory was disregarded in the favour of more cortical explanations

(e.g., maladaptive plasticity). However, a recent study has re-emphasised the importance of the periphery in PLP. Here authors injected the dorsal root ganglion with local anaesthetic, thereby preventing ectopic signals from reaching the central nervous system. They found that this consistently led to a rapid and reversible attenuation, and often complete elimination, of PLP (Vaso et al., 2014). Thus, the persisting activity in the missing hand area could reflect this aberrant firing at the periphery, and would explain why those with greater activity of the deprived hand area also report greater chronicity of their PLP. This is further evidenced by a significant relationship between motor control over the phantom hand and chronic PLP, whereby those with worse motor control over the phantom reported greater PLP and greater cortical activity in the missing hand area (Kikkert et al., 2017). Thus, the extent of engagement with the periphery, via phantom movement, is linked to the resulting PLP, a relationship which will be explored further in *Chapter 3* by designing a novel behavioural paradigm to explore such association. Phantom motor control, therefore, seems to be inextricably linked to the experience of PLP and cortical activity beyond that of S1. For example, reports of activity in typical pain-processing regions, such as the second somatosensory cortex (S2) and posterior insula, have been found during phantom hand movements (Makin, Scholz, et al., 2013). Additionally, a reduction in missing hand activity and PLP, via the use of non-invasive brain stimulation during phantom hand movements, has been linked to preceding upregulation from these same pain-processing areas (Kikkert et al., 2019). It is currently unclear as to whether the relationship between phantom motor control and PLP is causal, especially as the relief of PLP via phantom limb movement techniques, e.g., mirror therapy, reports mixed effectiveness (Thieme et al., 2016). One possible explanation is that

the correlational relationship reflects the optimality of reinnervation after amputation, with either (or both) increased aberrant and nociceptive firing at the periphery leading to increased levels of PLP (Kikkert et al., 2017) or poorer efferent retargeting after injury leading to deteriorated motor control of the phantom (Gagné et al., 2009). Crucially, however, characterising phantom limb movements has demonstrated that PLP may extend beyond that of (re)organisation in S1, encompassing a system branching from the periphery to processing in cortical pain networks.

0.6 Beyond the phantom – viewing phantom pain as chronic pain

It is now widely accepted that the experience of pain is not merely a reflection of peripheral input, but arises as a result of prior knowledge and current sensory information (Wiech, 2016), suggesting that ascribing PLP solely to aberrant peripheral firing may be too simplistic. As mentioned earlier, the mechanisms underlying the development of chronic pain are debated, but recent theories suggest that the role of cognitive factors, especially expectations, and how they are integrated with nociceptive information, are likely to be important (Büchel et al., 2014; Hechler et al., 2016; Ongaro & Kaptchuk, 2018; Tabor & Burr, 2019). For example, prior expectations, or predictions, relating to pain can modulate the resulting subjective rating of a noxious stimulus, e.g., placebo analgesia and nocebo hyperalgesia (Grahl et al., 2018; Tracey, 2010). Recently, computational work has shown that the influence of expectations on pain perception is likely through perceptual decision-making rather than altered sensory processing (Wiech et al., 2022; Wiech, Vandekerckhove, et al., 2014), highlighting again the role of higher-level inferences in pain.

Research into the role of cognitive factors and PLP, however, has rarely been addressed (see Fuchs et al., 2018 for an overview). Little work that has been done has shown that preoperative pain, as well as prior depression and anxiety, have later been linked to the development of PLP (Larbig et al., 2019). It has also been shown that amputees who report a high level of bothersomeness of PLP were also almost three times more likely to report depressive symptoms (Darnall et al., 2005). As very little work exists exploring the relationship between depression and anxiety and PLP, however, it is difficult to draw robust conclusions. For example, a study comparing depression and anxiety between those with PLP and those with non-phantom neuropathic pain disorders found those with PLP reported lower levels of depression and anxiety in comparison (Fuchs et al., 2015; Kazemi et al., 2013). It could be that depression and anxiety are more important predictors during the early stages of amputation (Shukla et al., 1982), or are more related to the disability and social aspects of the condition after amputation (Horgan & MacLachlan, 2009; Senra et al., 2012). Interestingly, a key longitudinal study of depression/anxiety in lower-limb amputees at 3, 6, 12 and 24 months after amputation found that anxiety, but not depression, predicted pain (Castillo et al., 2013; although note this study also included non-amputees). Future research is therefore needed to draw robust conclusions between depression/anxiety and PLP. Pain catastrophising, a cognitive, psychological trait, or 'prediction', however, has been shown to be particularly important in PLP. For example, catastrophising has been shown to account for 35% of the variance in PLP reports (Vase et al., 2011, 2012). It has also been significantly related to wind-up pain, a measure used to assess central sensitisation (Vase et al., 2011), indicating that PLP may

emerge from a combination of peripheral changes, altered processing of pain in cortical networks, and higher-level, cognitive biases. How pain expectations and sensory information are weighted, including the role of cognitive factors, and especially in regards to learning about pain, and whether this may change (anecdotally) in instances of PLP, will be further explored in *Chapter 3* and *Chapter 4*.

0.7 Aims of this thesis

To explore the neural mechanisms behind PLP fully is beyond the scope of this thesis, but my work will aim to push the concept of PLP beyond that of cortical reorganisation in S1 by asking: **what are the potential neural mechanisms behind phantom limb pain?**

Firstly, in *Chapter 1*, I will begin by reassessing the suitability of using the lips as a cortical marker of reorganisation in S1. To do so, I recruited two-handed controls to participate in a detailed somatotopic mapping of the face using both an active and passive (case study control) functional magnetic resonance imaging (fMRI) paradigms. This allowed me to assess the cortical orientation of the face in S1, which has previously been debated in humans. By using univariate and multivariate analyses, I found that the lips were not, in fact, the likely neighbour to the hand, but the upper face (or forehead) was.

Subsequently, in *Chapter 2*, I then utilised the active fMRI paradigm to assess the extent of cortical reorganisation in amputees and a positive control group – congenital one-handers (individuals born without a hand). To assess cortical

reorganisation several measures were used, including cortical (geodesic) distances, surface coverage indices and multivariate Representational Similarity Analysis (RSA). By using a combination of univariate and multivariate techniques, I was able to draw a detailed, and sensitive, picture of the extent of cortical reorganisation after limb loss in the neighbouring representation to the hand. Here I found that amputees reported very little cortical reorganisation in the deprived hemisphere (although see *Chapter 2* for exceptions) when compared to controls, and that no measures of reorganisation were significantly related to PLP. Extensive reorganisation, however, was found in the congenital one-hander group, validating the use of the active paradigm.

As *Chapter 1* and *Chapter 2* provided evidence against the maladaptive plasticity model, *Chapter 3* began to explore alternative explanations for PLP. In particular, it focused on using a novel behavioural paradigm designed to quantify the influence of movement on associative learning of nociceptive stimuli. As chronic pain development has been theorised to rely on associative learning mechanisms, and amputees have reported a significant relationship between phantom motor control and PLP, it aimed to assess the relationship between the two. Note that as Covid-19 prevented recruitment of a full sample of amputees (see *Covid-19 Impact Statement*), the *Chapter* subsequently focused on the suitability of the paradigm for learning in two-handed controls and a small sample of amputees (for anecdotal comparisons). Computational modelling of the participant responses, as well quantification of the influence of expectations on pain, were used to measure overall learning. It was found in two-handed controls that movement did not benefit the overall rate of learning, but may have particular benefits when

individuals are learning about relief. Importantly, amputees showcased anecdotally similar placebo responses to controls. Divergences to controls were noted for two amputees with PLP, but further work with larger samples is encouraged to explore these findings further.

Finally, *Chapter 4* employed a well-known task used in computational psychiatry to assess how individual's weight sensory evidence when making a decision. It measures a replicated bias termed 'jumping-to-conclusions' (JTC), whereby those with delusions require less evidence to form a belief. Evidence for this bias has also been shown in those with depression (Sastre-Buades et al., 2021), anxiety (Bensi & Giusberti, 2007), functional neurological disorders (Pareés et al., 2012) and chronic pain (Parkes et al., 2019). Again, due to Covid-19 recruitment issues in regards to amputees, this *Chapter* will focus on the relationship between JTC and cognitive, affective traits such as depression, anxiety and pain catastrophising, making anecdotal comparisons only to the small sample of amputees. It was found that a proportion of controls, and two amputees, reported a JTC bias, which was tentatively related to pain catastrophising in controls. Specifically, those who tended to catastrophise more often, and were less anxious, were more likely to JTC. No relationships were found between JTC and depression, or to the pain learning measures reported in *Chapter 3*.

Taken together, these studies as a collective aim to probe, and offer novel tasks for exploring, the various hypotheses relating to the underlying neural mechanisms of PLP.

Chapter 1 | Face topography in the primary somatosensory cortex

1.1 Introduction

Cortical representations of different body parts in the primary somatosensory cortex (S1) are known to be topographically organised in a highly structured, map-like fashion. A particular feature of S1 is that adjacent body parts are represented (broadly) next to each other – in other words, S1 is arranged somatotopically. This body atlas is commonly termed the cortical homunculus, and is draped in a medial-to-lateral fashion across S1 and the primary motor cortex (M1) (Penfield & Boldrey, 1937; Penfield & Rasmussen, 1950). The largest and most detailed representation within S1's homunculus is the hand – here each individual finger displays a segregated cortical representation, producing a highly detailed cortical map. A multitude of studies has replicated the detailed somatotopy of the hand in both humans (Ejaz et al., 2015; Kolasinski et al., 2016) and non-human primates (Merzenich et al., 1987), using a wide range of methodologies. However, results on somatotopic mapping of other body parts in S1, and in particular, the hands' cortical neighbour the face, are mixed.

Here, a plethora of electrophysiological work in non-human primates has demonstrated that the face representation is likely organised in an 'upside-down' (or inverted) manner, with the chin and lips bordering the hand area in S1 (Cerkevich et al., 2013; Coq et al., 2004; Cusick et al., 1986; Dreyer et al., 1975; Jain et al., 2001; Lin & Sessle, 1994; Manger et al., 1995; Merzenich et al., 1978; Nelson et al., 1980; Sur et al., 1982; Toda & Taoka, 2004). However, only a

handful of neuroimaging studies in humans has subsequently supported this inverted somatotopic organisation of the face (Servos et al., 1999; Yang et al., 1993). Indeed, seminal work carried out by Penfield & Boldrey (1937), using direct electrical stimulation of cortical fields in S1, found evidence for a contrasting, upright orientation, with the upper – not lower – face bordering the hand. This has been further replicated in recent studies using intraoperative optical imaging (Sato et al., 2002, 2005; Schwartz et al., 2004), electrostimulation (Roux et al., 2018; Sun et al., 2021), and functional magnetic resonance imaging (fMRI) paradigms using passive stimulation and active movements (Huang & Sereno, 2007; Kikkert et al., 2022; Schellekens et al., 2022; Willoughby et al., 2021). Yet other studies have also suggested more complex representations of the face in S1, following the segmental division of the trigeminal nerve into an 'onion skin' pattern, manifesting in a rostro-caudal cortical representation (Borsook et al., 2004; DaSilva et al., 2002; Schellekens et al., 2022). For this 'onion skin' model, the nose representation would be found more inferior in S1 than the lower jaw or forehead (Moulton et al., 2009), following neither an upright or inverted orientation. Adding to the complexity, several studies have also reported gross somatotopy and overlap of the facial parts in S1, unable to distinguish between individualised representations of the upper and lower face (Iannetti et al., 2003; Kopietz et al., 2009; Nguyen et al., 2004).

An accurate somatotopic mapping of the face is therefore needed, which would advance our understanding of basic topography in S1. Clarity on facial somatotopy would also have implications for the maladaptive plasticity model of phantom limb pain (PLP). Here, despite the current conflicting findings on facial

somatotopy, researchers have commonly used the lips as a marker of cortical remapping after upper limb loss (see Flor, Nikolajsen, & Staehelin Jensen, 2006) for an overview). This is based on the implicit assumption that the face in humans follows that in non-human primates (Pons et al., 1991), with the lower face neighbouring the deprived hand area, i.e., an inverted representation. It also rests on the belief that subsequent remapping is determined by cortical proximity, therefore any identified remapping in S1 after upper limb loss is likely to be found in the lower face (or residual arm; the hands' more medial neighbour). However, if the face is organised in an upright (or more complex) manner in humans, by focusing on remapping of the lips only, researchers may either be overestimating the extent of shifts of the lip representation and/or neglecting more significant shifts of the hand's actual cortical neighbour.

Detailed mapping of the upper and lower face is therefore needed to assess typical topography of facial sensorimotor organisation. Here, we conducted a mapping of face cortical organisation to determine facial orientation (upright versus inverted) in the primary sensorimotor cortex in 22 two-handed controls. We employed an active motor paradigm during fMRI to map somatotopy of the face (Schellekens et al., 2022), due to the ease of administration and avoidance of practicality issues faced with passive stimulation protocols (Kikkert et al., 2022; also see *Discussion*). Participants were instructed to move their forehead, nose, lips and tongue, providing a thorough mapping of both the upper and lower face, as well as their dominant/non-dominant thumbs. We then calculated the centre-of-gravity (CoG) for each movement, as well as the cortical geodesic distances from each CoG to a pre-defined anatomical cortical anchor, in order to infer somatotopy

of each facial part. We subsequently carried out multivariate analysis (e.g., Representational Similarity Analysis; RSA) within the face region, which is more sensitive to representational overlaps and subtleties in activation patterns, to rigorously assess and inform the facial somatotopy suggested by our univariate results. Furthermore, to validate our use of an active paradigm for probing facial somatotopy, we also developed a passive stimulation paradigm using an optimal vibrotactile device safe for MRI usage (Kikkert et al., 2022; Sonar et al., 2021). Here, case studies were carried out on two controls who completed two active sessions ~12 months apart, as well as a passive stimulation session, allowing us to assess the reliability of the face representation over time, and the consistency of facial somatotopy across active and passive paradigms. Taken together, we aimed to provide a detailed and comprehensive somatotopy of the face representation of S1 in controls, before assessing the extent of changes within this representation after upper limb loss (see *Chapter 2*).

1.2 Methods

1.2.1 Participants

Twenty-two two-handed controls (age; *M*=45.55, *SE*=2.02, women; *n*=10, left-handers; *n*=6) were recruited (note the same control sample was also used in *Chapter 2* for group comparisons). Two individuals (aged 33 and 29, 2 women, 1 left-handed) also participated in the passive validation procedure (hereafter Passive; see below for description of task). These individuals also underwent two sessions of the sensorimotor active task used in the main analyses (hereafter Active 1 and Active 2). This allowed us to i) assess the consistency of our data between the two active sessions and ii) account for the fact that a different

scanner was used for the passive task (and thus one of the active sessions, namely Active 2, to be compared to the Passive session). Procedures were in accordance with NHS National Research Ethics Service approval (18/LO/0474), and written informed consent was obtained.

1.2.2 Functional MRI sensorimotor task

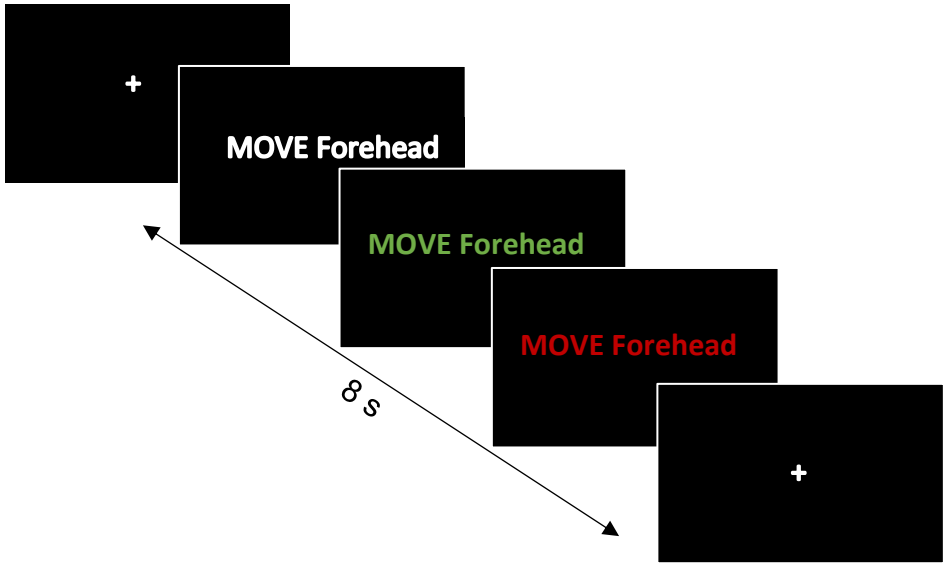


Figure 1.1. *Experimental design for active sensorimotor task.* Participants were first shown a fixation cross for ~8 seconds (s). The first movement (pseudo-randomised) was then displayed on the screen, with the instructions "MOVE", followed by the chosen body part (forehead, nose, lips, tongue, left thumb, right thumb). Participants were then required to move the chosen body part for 8 s. Note that the instruction "~~~Rest~~~" was presented five times throughout each run. The text flashed green every ~1.2 s to provide the pace in which the movement should be enacted. As the block ended the text would flash red, indicating the end of that block and that the text would subsequently change showing the next movement. Once all the movements had been displayed a fixation cross was presented on the screen for 8 s indicating the end of the run. Each run lasted for ~244 s, with a total of 3 runs within each scan. Note that the passive sensorimotor task utilised the same trial structure, however, the instruction "MOVE" was removed and the participant completed 4 runs instead of 3.

We used an active motor paradigm (Active 1 and Active 2), where participants were visually instructed to move their forehead, nose, lips or tongue. This paradigm was chosen because it enabled bilateral activation of S1 simultaneously, allowing us to directly compare activity patterns between the two hemispheres. Participants were also instructed to move their left and right thumb, resulting in 6 conditions. Baseline (i.e., rest) was included as a 7th condition. Specific instructions involved: raising eyebrows (forehead), flaring nostrils (nose), puckering lips (lips), tapping tongue to the roof of the mouth (tongue), flexing and extending (thumb). The protocol comprised of 8 s blocks, with each condition repeated 4 times per run (5 times for baseline), over 3 functional runs. Before entering the scanner, participants practised each movement with the experimenter to ensure that the movement could be executed and to standardise each movement across participants (e.g., specificity and pace). Performance during scanning was visually monitored online with the use of an eye-tracker camera and an experimenter dedicated to this task. Note that multiple participants reported during the experimenter briefing that they could not successfully flare their nostrils, and were therefore instructed to attempt moving their nose in the scanner.

1.2.3 Functional MRI passive stimulation task

Soft pneumatic actuators (SPA-skin; Kikkert et al., 2022; Sonar et al., 2021) were placed on the participants' forehead, nose, lips and tongue on the body midline, and on the thenar eminence of each thumb (see *Supplementary Methods and Supplementary Figure 1* for thorough description of device and additional considerations for tongue stimulation). Once the actuators had been attached and the participant was inside the scanner bore, a short thresholding procedure was

carried out, whereby the pressure (KPa) of the actuators was adjusted to reach above-threshold subjective equality across body parts. The procedure began by defining the pressure for the least sensitive body part – the nose. Here pressure began at 35 KPa and was increased or decreased in step-sizes of 5 KPa. Stimulation length was 8 seconds and participants had 3 seconds to make their response, e.g., pressing a button to either increase/decrease the pressure or state that the pressure was 'ideal' (clearly perceived). The nose was then used as a reference body part, whereby 8 seconds of stimulation was administered to the nose followed by 8 seconds of stimulation to one of the other body parts (forehead, lips, tongue, left and right thumb), i.e., the target body part. The participant then had 3 seconds to respond via button-press in order to adjust the pressure (increasing or decreasing by 5 KPa) of the target body part in order to generate a similar tactile experience to that of the nose. Throughout thresholding, if the participant responded with 'ideal' twice, or if 5 trials had been administered, the resulting pressure was chosen for that body part. During the functional MRI task, each body part was stimulated using the thresholded KPa and a stimulation frequency of 5 Hz. The same block design (with similar time-course) as for the Active sessions was used (i.e., 8s stimulation blocks, each condition repeated 4 times per run, 5 times for baseline), but over 4 functional runs instead of 3.

1.2.4 MRI data acquisition

Functional and anatomical MRI data were obtained using a 3 Tesla Prisma MRI scanner (Siemens, Erlangen, Germany) with a 32-channel head coil. Functional and anatomical MRI data for the Passive and Active 2 sessions were obtained with the same MRI parameters as for the Active 1 session, but on a different 3T

Prisma scanner. Anatomical data was acquired using a T1-weighted sequence (MPRAGE), with the following parameters: TR = 2530 ms; TE = 3.34 ms; flip angle = 7°; voxel size = 1 mm isotropic resolution. Functional data based on the blood oxygenation level dependant (BOLD) signal were acquired using a multiband T2*-weighted pulse sequence, with a between-slice acceleration factor of 4 and no in-slice acceleration (TR = 1450 ms; TE = 35 ms; flip angle = 70°; voxel size = 2 mm isotropic resolution; imaging matrix = 106 x 106; FOV = 212 mm). 72 slices were oriented in the transversal plane. A total of 172 whole-brain volumes for each of the three runs were collected per participant. Field-maps were acquired for field unwarping. Passive and Active 2 functional data were pre-processed and analysed as described below for the main analyses.

1.2.5 MRI pre-processing

Functional data was first pre-processed using FSL-FEAT (version 6.00). Pre-processing included motion correction using MCFLIRT(Jenkinson et al., 2002), brain extraction using BET (Smith, 2002), temporal high-pass filtering with a cut-off of 119 s and spatial smoothing using a Gaussian kernel with a FWHM of 3 mm. Field maps were used for distortion correction of functional data.

For each participant, we calculated a midspace between the three functional runs, i.e., the average space in which the images are minimally reorientated. Each functional run was then aligned to the midspace and registered to structural images (within-subject) using FMRIB's Linear Image Registration Tool (FLIRT), and optimised using Boundary-Based Registration (Greve & Fischl, 2009). Where specified, functional and structural data were transformed to MNI152 space using FMRIB's Nonlinear Registration Tool (FNRIT; Andersson et al., 2010).

1.2.6 Functional MRI analysis

Time-series statistical analysis was carried out using FMRIB's Improved Linear Model (FILM). Task-based statistical parametric maps were computed by applying a voxel-based General Linear Model (GLM), as implemented in FEAT. The design was composed of 6 explanatory variables for each movement, convolved with a double-gamma hemodynamic response function (Friston et al., 1998), and its temporal derivative. The six motion parameters were included as regressors of no interest. Motion outliers (> 0.9 mm) of large movements between volumes were included as additional regressors of no interest at the individual level. For our main comparisons 6 contrasts were set up, corresponding to the facial movements' (forehead, nose, lips, tongue and left/right thumb) relative to rest. Since the nose condition yielded weak activity relative to baseline, we excluded it from the univariate analysis (see *Supplementary Figure 2*).

The estimates from the three functional runs were then averaged voxel-wise using a fixed effects model in participants structural space, with a cluster forming z-threshold of 2.3 and family-wise error corrected cluster significance threshold of $p < 0.05$. Each estimates' average was masked prior to cluster formation with a sensorimotor mask, defined as the precentral and postcentral gyrus from the Harvard Cortical Atlas. The sensorimotor mask was registered to the individuals structural scan using an inversion of the nonlinear registration by FNIRT. All functional MRI analysis was carried in individual's native anatomical space.

1.2.7 Regions of Interest (ROI) definition

Facial topography was studied using anatomical ROIs for the hand and face areas in S1. Although M1 and S1 are expected to activate during facial movement we primarily focused on S1 due to the traditional focus in the maladaptive plasticity literature on S1 representational shifts (Flor, Nikolajsen, Jensen, et al., 2006). Furthermore, M1 topography tends to be less well-defined (Graziano & Aflalo, 2007; Schieber, 2001), and so characterisation of typical facial topography may be more apparent in S1. Nevertheless, we wish to note that due to the proximity of S1 to M1, it is possible that marginal contribution from M1 may have affected our S1 activity profiles.

Firstly, S1 was defined on the average surface using probabilistic cytoarchitectonic maps, by selecting nodes for Brodmann areas (BAs) 1, 2, 3a and 3b (Wiestler & Diedrichsen, 2013). The S1 hand ROI (hereafter hand ROI) was defined by selecting the nodes approximately ~1 cm below and ~2.5 cm above the anatomical hand knob. In contrast to earlier work (Wesselink et al., 2019), we defined a conservative lateral boundary of the hand ROI (~1cm below the hand knob) to ensure there was limited facial activity captured. From the remaining parts of S1, the medial region was discarded and the lateral region was selected as the preliminary approximation for the S1 face ROI (hereafter face ROI; *Figure 1.1*).

Structural T1-weighted images were then used to reconstruct pial and white-grey matter surfaces using Freesurfer (version 7.1.1) at the individual level. The hand and preliminary face ROIs were then projected into individual brains via the

reconstructed individual anatomical surfaces. As the secondary somatosensory cortex (S2) contains a crude somatotopy (Ruben et al., 2001), the preliminary face ROI was further trimmed in participant's structural space by removing the overlap with S2. S2 was defined in MNI152 space using the Juelich Histological Atlas and thresholded at 25% (Wiech, Jbabdi, et al., 2014). The S2 ROI was registered to participants' structural space using an inversion of the nonlinear registration carried about by FNIRT. The remaining preliminary face ROI with the overlap from S2 removed was used as the face ROI for all univariate analyses. We note that due to the probabilistic nature of these masks, there could be some marginal contribution from S2 in our estimated face area.

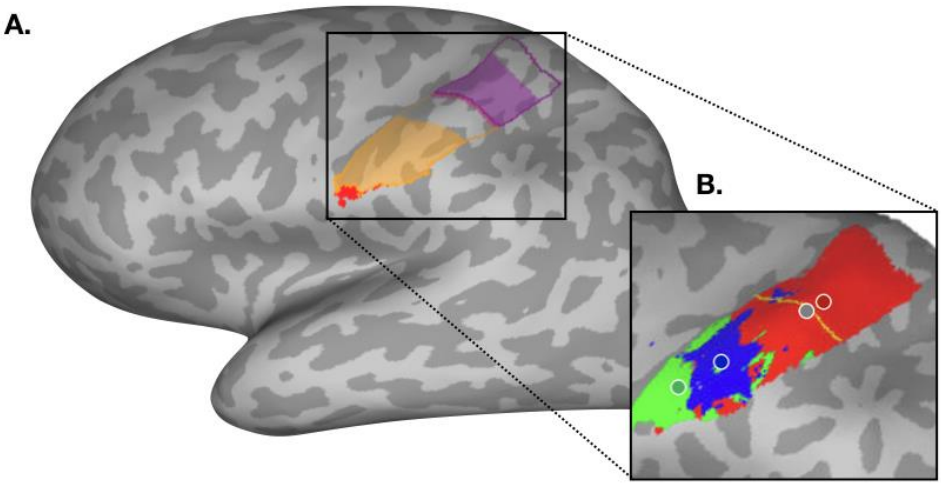


Figure 1.2. *Regions of interest and winner-takes-all analysis in the primary somatosensory cortex for an example participant.* **(A)** Regions of interest (ROI) used for univariate analyses are outlined in purple for the hand, and in orange for the face. Shaded areas of each region of interest denote the trimmed ROIs used for multivariate analyses. ROI overlap with the secondary somatosensory cortex (S2) is highlighted in red, and was removed from the face ROI in order to minimise somatotopic contribution from that region. **(B)** A typical winner-takes-all map from an example participant, with forehead activity in red, lip activity in blue and tongue activity in green. The centre-of-gravity for each movement is signified by a coloured dot outlined in white. The hand-face border is outlined in yellow, with the midpoint denoted by a grey dot. Cortical geodesic distances were measured from each facial parts CoG to the hand-face border midpoint.

1.2.8 Winner-takes-all approach

To characterise S1 facial topography, the hand and face ROIs were combined to produce an overall S1 ROI (minus the medial region), and a winner-takes-all approach was used (see *Figure 1.1.B*). For each participant, thresholded z-statistics averaged across the three functional runs were assigned to one of three

face parts (forehead, lips, tongue), dependent on which facial movement relatively showed maximal activity within the S1 ROI. Face-winners (i.e., the output of the winner-takes-all) were then projected to the individual's anatomical surface. Note that we excluded the thumb, which covered ~66% of the deprived hand ROI surface area in controls (see *Supplementary Figure 3*). All subsequent analyses at the individual's anatomical surface level were computed using Connectome Workbench (v1.4.2).

1.2.9 Cortical distance analysis

To assess facial somatotopy in relation to the hand area, the centre-of-gravity (CoG, weighted by cluster size; Makin et al., 2015) of each face-winner map was calculated in each hemisphere and the geodesic cortical distance between each movement's CoG and a predefined cortical anchor computed. The cortical anchor was defined as the midpoint of the lateral border of the hand ROI (see *Figure 1.1.B*). The border was drawn manually and the midpoint calculated for each participant, and were visually confirmed by a second experimenter. The geodesic distance was assigned a negative value if the movement's CoG was located below the hand border (i.e., laterally).

1.2.10 Group-level visualisations

Prior to group-level visualisations, participant information regarding hand dominance (controls) were used to sagittal-flip raw pre-processed data, such that the brain activity corresponding to the non-dominant hand is always represented in the left hemisphere. Group-level statistical parameter maps were then created with a threshold-free cluster enhancement (TFCE) approach using FSL's Randomise tool (Winkler et al., 2014). TFCE is a nonparametric, permutation-

based method for cluster formation, and has been shown to demonstrate improved sensitivity when compared to typical thresholding methods (Smith & Nichols, 2009). Group activity mixed-effect maps were calculated for each fixed-effect (i.e., averaged across the three functional runs) parameter estimate of a face movement (forehead, lips, tongue) contrasted to baseline. Prior to permutation (n = 5000), parameter estimates were masked with a sensorimotor mask, defined as the precentral and postcentral gyrus from the Harvard Cortical Atlas. A family-wise error correction of $p < 0.05$ and variance smoothing of 5 mm (as recommended for datasets with less than 20 participants) were used. Resulting clusters were thresholded at $p < .01$ and projected to a group cortical surface (Glasser et al., 2016) using Connectome Workbench (v1.4.2), and activity is visualised in BAs 1, 2, 3a, 3b and 4.

1.2.11 Multivariate representational analysis

Representational Similarity Analysis (RSA; Nili et al., 2014) was used to assess the multivariate relationship between activity patterns generated by each face part. RSA was conducted in the face ROI only to explore relative similarity across face parts, and whether these would be in line with our univariate somatotopy. To ensure the selectivity of the face area, the face ROI used for univariate analyses was further trimmed medially by ~1cm, creating a 1cm gap between the hand and face ROIs (see *Figure 1.1.A*). For each participant, parameter estimates for the four facial movements (forehead, nose, lips and tongue) and the contralateral thumb were extracted from all voxels within the chosen ROI, as well as residuals from each runs' first-level analysis (three runs in total). Due to the increased sensitivity to subtle changes in activity patterns afforded by the multivariate

approach, we included the nose movement. Multidimensional noise normalisation was used to increase reliability of distance estimates (noisier voxels are down-weighted), based on the voxel's covariance matrix calculated from the GLM residuals. Dissimilarity between resulting facial activity patterns were then measured pairwise using cross-validated Mahalanobis distances (Walther et al., 2016). Due to cross-validation, the expected value of the distance is zero if two patterns are not statistically different from each other. Distances significantly different from zero indicate the two representational patterns are different; negative distances indicate noise. Larger distances for movement pairs therefore suggest greater discriminative ability within the ROI. The resulting 10 unique inter-facial representational distances were characterised in a representation dissimilarity matrix (RDM). Multidimensional scaling (MDS) was also used to project the higher-dimensional RDM into lower-dimensional space, whilst preserving inter-facial dissimilarity, for visualisation purposes only. Analysis was conducted on an adapted version of the RSA Toolbox in MATLAB (Nili et al., 2014), customised for FSL (Wesselink & Maimon-Mor, 2018).

1.2.12 Statistical analyses

All statistical analyses were carried out using jamovi (v1.6.23.0). Outliers were classified as +/- 3 standard deviations to the mean. We chose to not remove outliers in our analyses and checked that the significance and direction of the results did not change if identified outliers were removed. When appropriate, univariate analyses was compared using parametric statistics. To assess normality for parametric tests, Shapiro-Wilk tests were run on residuals in combination with inspection of Q-Q plots. Where stated, non-parametric test

statistics are reported where the assumption of normality has been violated. Analysis of Variance (ANOVA) was used to assess cortical distances across the different facial movements, with two within-subject factors of Hemisphere (Dominant x Non-Dominant) and Movement (Forehead x Lips x Tongue). Post-hoc comparisons were conducted with a Bonferroni correction for multiple comparisons (corrected alpha=.016; reported uncorrected *p*-values in text).

We reported the corresponding Bayes Factor (BF_{10}), defined as the relative support for the alternative hypothesis, for all reported results (excluding post-hoc comparisons, which were conducted on estimated marginal means whilst controlling for brain size volume). Note that Bayes Factors reported for interactions reflect the model as a whole (main effects and interactions). Subsequent Bayes Inclusion Factors were reported for main effects and interactions individually, which quantify how much the observed data are more probable under models that include the predictor relative to models that do not. While it is generally agreed that it is difficult to establish a cut-off for what consists sufficient evidence, we used the threshold of $BF<1/3$ as positive evidence in support of the null, consistent with others in the field (Dienes, 2014; Wetzels et al., 2011; though see Kass & Raftery, 1995). The Cauchy prior width was set at 0.707 (jamovi's default).

For multivariate analyses, the average pairwise distances for the face parts and thumb were first assessed for the significance of information content in the face ROI using a One-Sample *t*-test in each hemisphere (dominant and non-dominant). To next quantify whether the upper face demonstrates greater similarity to the

hand than the lower face, a Paired Samples *t*-test was used to compare the forehead-to-thumb pairwise distance to the lips-to-thumb pairwise distance in the face ROI. Where assumptions of normality were violated, the rank biserial correlation was used as a measure of effect size instead of Cohen's *d* (Kerby, 2014). Pearson correlations were then used to assess the relationship between pairwise distances in the face ROI across Active 1, Active 2 and Passive sessions in the non-dominant hemisphere (see *Supplementary Figure 4* for intact hemisphere results).

1.3 Results

1.3.1 The cortical neighbour of the hand representation is the forehead

When looking at facial organisation at the group-level we found a qualitatively upright orientation of the face in the primary sensorimotor cortices (see *Figure 1.2.A* and *1.2.B*), with the forehead located closest to the hand area, followed by the lips, and the tongue located laterally. These facial maps also displayed preserved symmetry across the dominant and non-dominant hemispheres. The facial somatotopy presented here therefore suggests that the hand's cortical neighbour is the forehead (or upper face), in contrast to the inverted facial somatotopy in non-human primates (Cerkevich et al., 2013; Coq et al., 2004; Cusick et al., 1986; Dreyer et al., 1975; Jain et al., 2001; Lin & Sessle, 1994; Manger et al., 1995; Merzenich et al., 1978; Nelson et al., 1980; Sur et al., 1982; Toda & Taoka, 2004). This further highlights the need to reassess the often-cited, traditional lip-to-hand marker of cortical remapping.

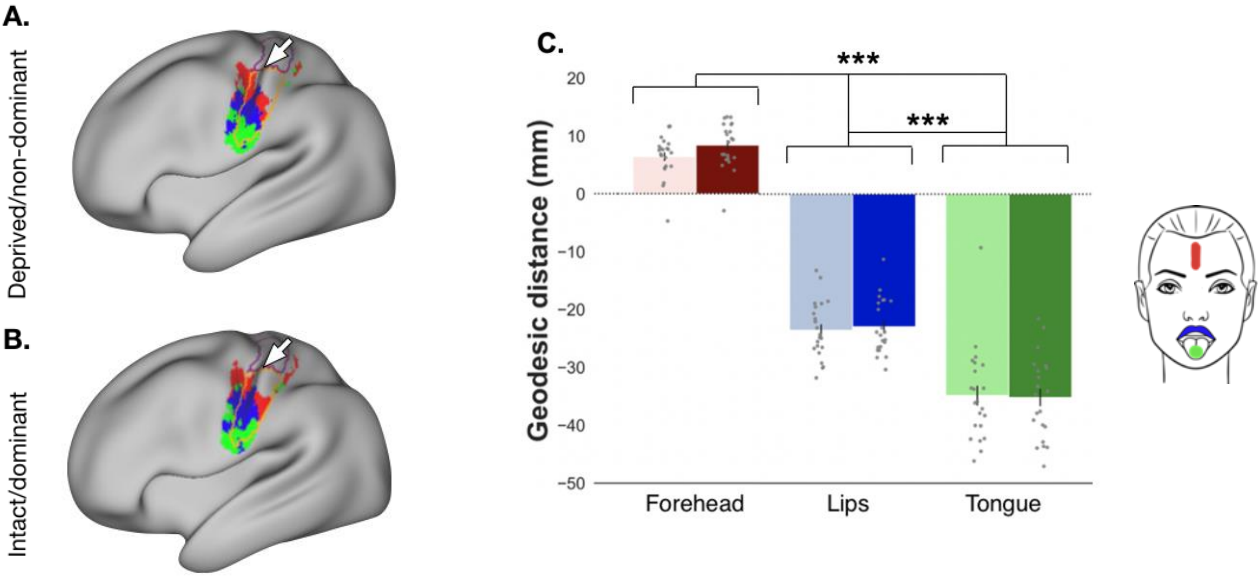


Figure 1.3. *Average activity maps for each facial movement and cortical geodesic distances.* Average activity for the forehead (red), lips (blue) and tongue (green) movements, contrasted to rest, in the **(A)** deprived/non-dominant (darker colours) and **(B)** intact/dominant hemisphere (lighter colours) for controls (n = 22). All clusters were created using a threshold-free cluster enhancement procedure with a sensorimotor pre-threshold mask (defined using the Harvard Cortical Atlas), and thresholded at $p < .01$. The hand and face ROIs are outlined in purple and orange respectively, and the central sulcus is denoted with a white arrow. For average activity maps in controls with nose movements, see *Supplementary Figure 2*. **(C)** Cortical geodesic distances (y-axis) in the intact (darker colours) and deprived (lighter colours) hemisphere for forehead (nose), lips (blue) and tongue (green). Individual data points and standard error of the mean are plotted in grey. ******* $p<.001$; note *p*-values are uncorrected.

Subsequently, to support these qualitative conclusions we next assessed facial somatotopy by looking at the cortical geodesic distances in relation to the predefined cortical anchor. Note that the majority of the distances for the forehead (see *Figure 1.2.C*) were positive (apart from one participant), indicating that the

CoG for this movement was located above the lateral border of the hand ROI. This was in comparison to the lips and tongue, which both reported negative distances, with greatest negativity reported for the tongue, indicating again that the tongue is likely to fall more laterally in S1, followed by the lips, then forehead, i.e., in an upright orientation. To confirm that the forehead displayed significantly shorter distances to the cortical anchor than the other two face parts, we calculated the absolute value of the geodesic distances and carried out a Repeated Measures ANOVA, with two within-subject factors of Hemisphere (Dominant x Non-dominant) and Movement (Forehead x Lips x Tongue). We first found a non-significant main effect of Hemisphere ($F_{(1,21)}$=0.859, p=0.364, n^2_p=0.039, BF_{10}=0.190, $BF_{Inclusion}$=0.212), and a non-significant interaction for Hemisphere x Movement ($F_{(2,42)}$=2.157, p=0.128, n^2_p=0.093, BF_{10}=5.388e+45, $BF_{Inclusion}$=0.221) indicating that the cortical distances for each movement (and overall) were similar across the two hemispheres, confirming our qualitative interpretation of preserved hemispheric symmetry of the facial somatotopic map. Importantly, we did find a significant main effect of Movement ($F_{(2,42)}$=153.720, p<.001, n^2_p=0.880, BF_{10}=1.148e+47, $BF_{Inclusion}$=1.169e+47), with post-hoc comparisons demonstrating significantly shorter distances for the forehead when compared to the lips (t=-9.943, p<.001, d=-2.120) and tongue (t=-17.479, p<.001, d=-3.726). Thus, the upper face is likely to be located closer to the lateral border of the hand ROI than the lower face. Furthermore, the lips subsequently showed shorter distances than the tongue (t=-7.536, p<.001, d=-1.607), suggesting, again, an upright orientation of the face in S1.

1.3.2 The upper faces' activation patterns show greater similarity to the thumb than the lower face

To further inform the facial somatotopy suggested by our univariate results, we also conducted a multivariate analysis in the face ROI across the dominant and non-dominant hemispheres (see *Figure 1.3*). As RSA takes into account the similarity between activation patterns, rather than the localisation of the activity, it allows us to quantify facial somatotopy more subtlety. For example, if the upper face does border the hand area, like our univariate analysis suggests, we would predict that activation patterns for the forehead movements would be more similar to thumb movements than the lips, due to cortical proximity. Firstly, as a sanity check, we assessed that we had significant information content for facial movements within the face ROI by confirming that the overall average distances were significantly different from zero in the dominant ($t_{(21)}$=24.2, p<.001, d=5.15, BF_{10}=5.29$_{e+13}$) and non-dominant ($t_{(21)}$=24.4, p<.001, d=5.20, BF_{10}=6.41$_{e+13}$) hemisphere (see *Figure 1.3.A* and *1.3.B*). Secondly, to test our key prediction, we then assessed whether the pairwise distances for the thumb and forehead were significantly smaller, indicating greater similarity, than the thumb and the lips. When doing so, we did find significantly shorter distances in the dominant ($t_{(21)}$=-13.15, p<.001, d=-2.80, BF_{10}=6.33$_{e+8}$) and non-dominant hemisphere (W=-0.00, p<.001, r_{bs}=-1.00, BF_{10}=359614) for the forehead-to-thumb distances (non-dominant: M=0.621, SE=0.0406; dominant: M=0.593, SE=0.0371) when compared to lips-to-thumb distances (non-dominant: M=0.959, SE=0.0491; non-dominant: M=0.956, SE=0.0502) (see *Figure 1.3.A* and *1.3.B*). Thus, both our univariate and multivariate analyses in two-handed controls indicates that not only does the upper face seem to be localised closer to the hand area than the lower

face, but it also displays more similar activation patterns to the hand. Our results therefore point towards an upright orientation of the face in S1.

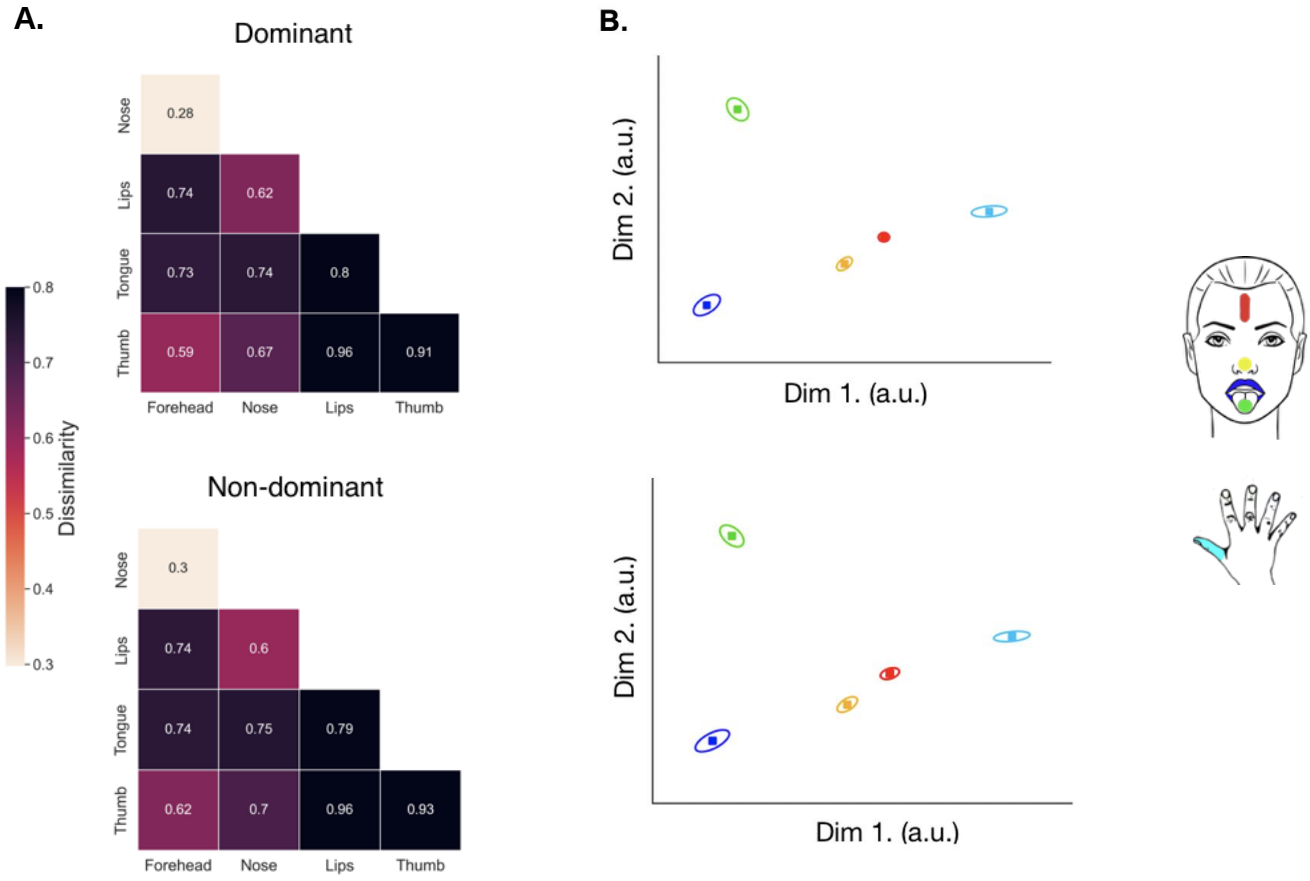


Figure 1.4. *Representational Similarity Analysis in face region-of-interest in two-handed controls.* **(A)** Average Representational Dissimilarity Matrices (RDMs) for *n*=22 two-handed controls in the face region-of-interest in the dominant and non-dominant hemisphere. Note that the pairwise forehead-to-thumb distances are significantly smaller than the lips-to-thumb distances, indicating greater similarity in activation patterns of the upper face and thumb, than the lips (lower face) and thumb. **(B)** Multi-dimensional scaling plots for each hemisphere (dominant and non-dominant), projecting the average RDM distances into a lower dimensional space. Distances between each marker reflect dissimilarities, with closer markers indicating greater similarity. Forehead movements are plotted in red, nose in yellow, lips blue and tongue green, with the standard error plotted around each data point.

1.3.3 Facial somatotopy is stable across time and paradigms

However, it could be argued that active movements may produce different cortical maps to those with passive stimulation. To counter this, we had two participants return ~12 months later from the first active session (Active 1), to re-do the active motor paradigm (Active 2) as well as a passive stimulation protocol (Passive; see *Methods*). We were then able to compare facial representational structure in the face ROI across all three sessions, and thereby quantify not only the stability of the face representation across time, but also the consistency of the representation between active and passive paradigms (see *Figure 1.4* and *1.5*).

When doing so, we found a significant positive relationship between the two active sessions for both participants (see *Figures 1.4.B* and *1.5.B*), indicating a relatively stable representational pattern of facial activity in the face region across time (CTR 01: $r_{(8)}$=0.9140, p<.001, 95% CI[0.67, 0.98], BF_{10}=132.84 ; CTR 02: $r_{(8)}$=0.862, p=.0013, 95% CI[0.51, 0.97], BF_{10}=32.665). We also found a trend for a positive correlation between the Active 2 and the passive paradigm in one participant (CTR 01: $r_{(8)}$=0.6238, p=.0540, 95% CI[-0.01, 0.9], BF_{10}=1.997), that is significant in the second participant (CTR 02: $r_{(8)}$=0.665, p=.0358, 95% CI[0.06, 0.91], BF_{10}=2.695). This indicates a broadly similar representational structure of the face when evoked using both movements and passive stimulation, validating the use of our active paradigm to explore facial somatotopy in S1. Furthermore, we can again see (anecdotal) evidence for greater similarity between the pairwise distances of the forehead and thumb than the lips and thumb, across both participants and time, providing support for a relatively stable upright facial orientation in S1. We do note, however, smaller dissimilarity values for the passive

paradigm, indicating a reduction in facial information available overall when using this stimulation protocol.

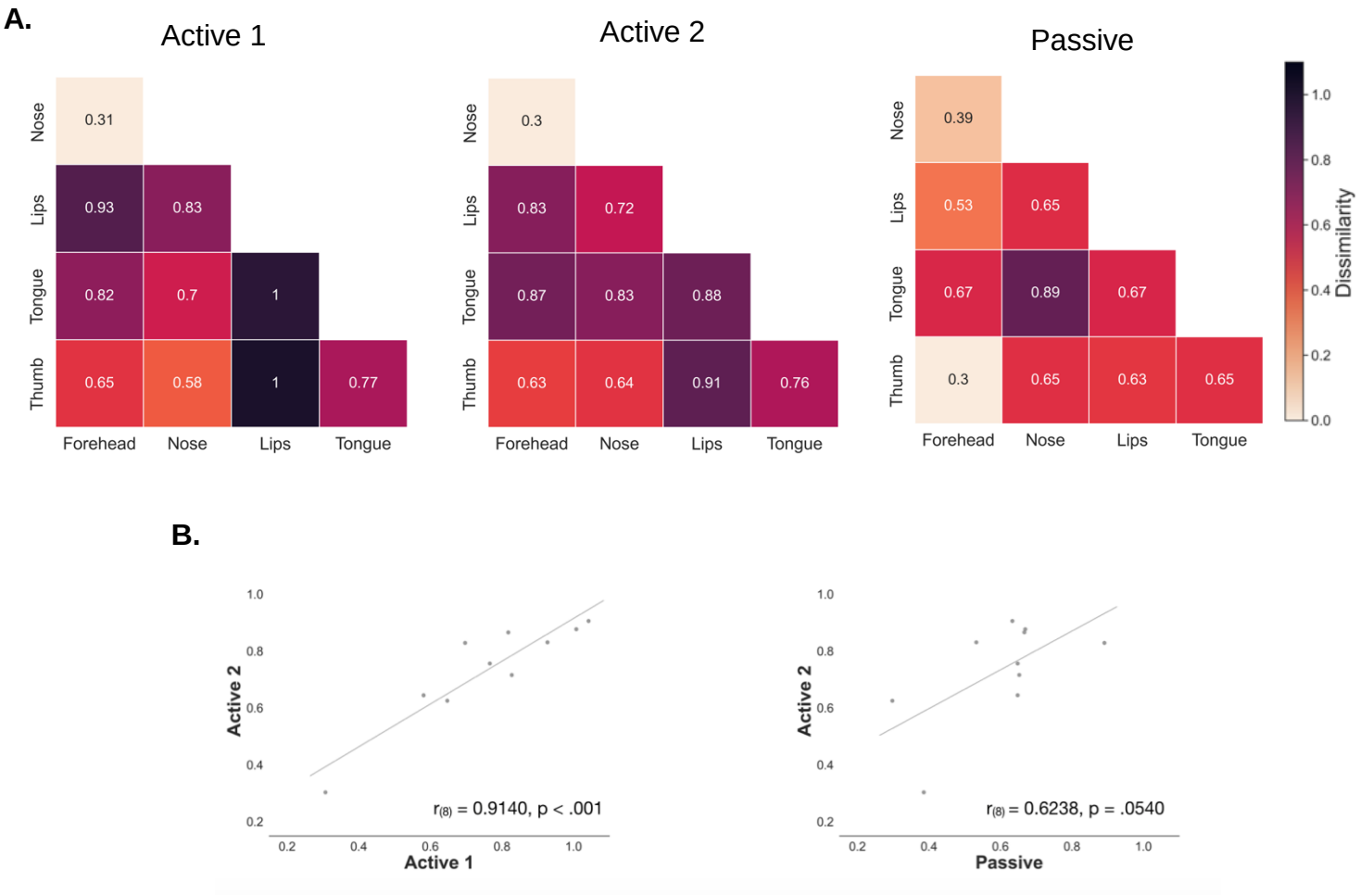


Figure 1.5. *Representational dissimilarity matrices (RDMs) for Active 1, Active 2 and Passive for CTR 01.* **(A)** RDMs for the first control participant (CTR 01) who participated in a second active somatotopic mapping (Active 2) of the face (and thumb) ~12 months after the first active session (Active 1), as well as participating in a passive stimulation replication protocol (Passive). Pairwise distances are shown for all facial movements (forehead, nose, lips and tongue), as well as the thumb, in the face region-of-interest in the non-dominant hemisphere. Larger distances indicate greater dissimilarity between activation patterns and smaller distances indicate greater similarity between patterns. Note smaller distances for the forehead-to-thumb than the lips-to-thumb. **(B)** A significant correlation was found between facial (and thumb) pairwise distances in the non-dominant hemisphere between Active 1 and Active 2, and a strong positive trend was found between Active 2 and Passive.

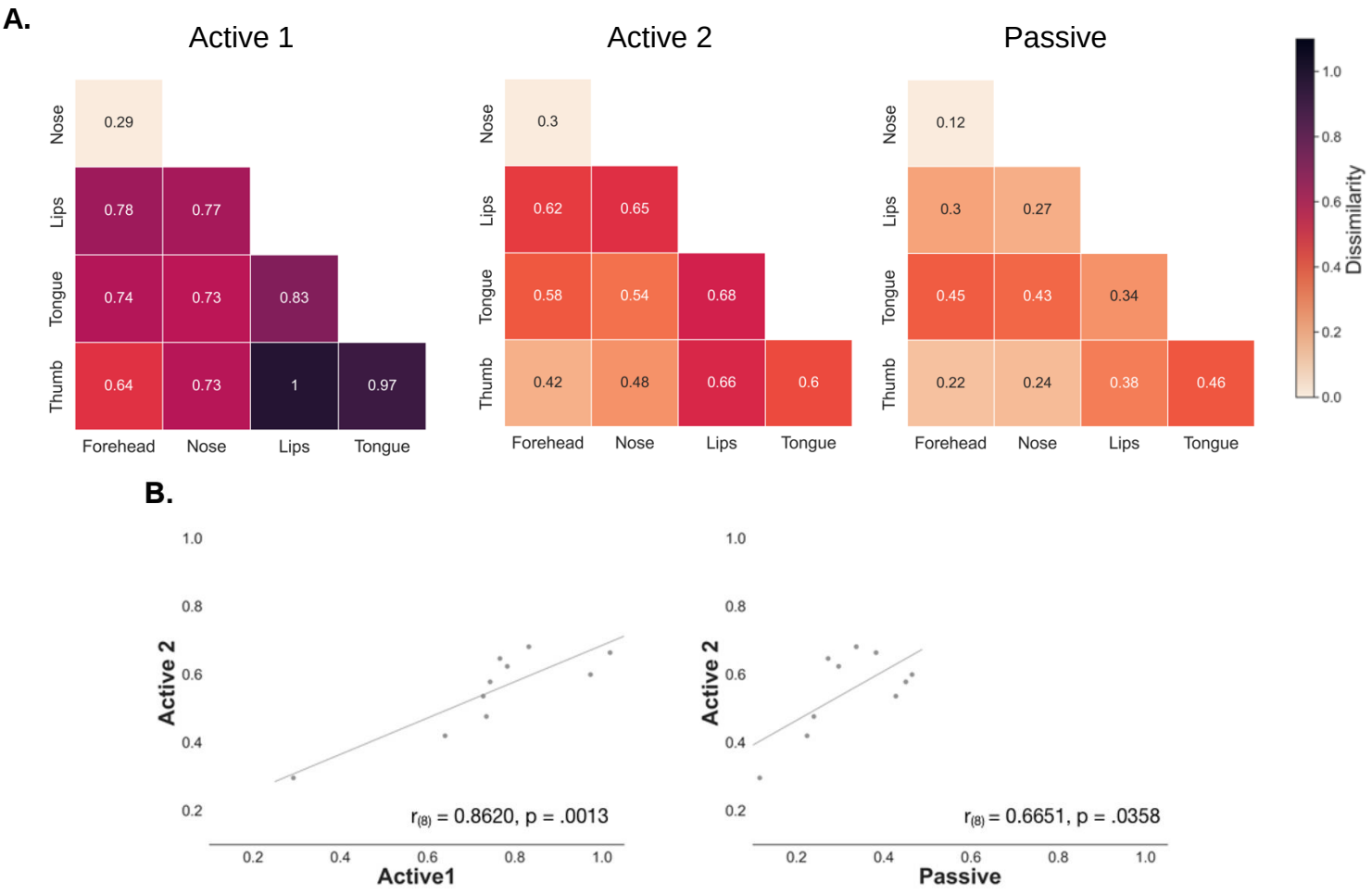


Figure 1.6. *Representational dissimilarity matrices (RDMs) for Active 1, Active 2 and Passive for CTR 02.* **(A)** Annotations as in *Figure 1.4*. Note pairwise distances shown are for the second control participant (CTR 02). **(B)** For this control participant significant correlations were found between Active 1 and Active 2, as well as Active 2 and Passive, indicating fairly stable facial somatotopy across time and paradigms for this individual.

1.4 Discussion

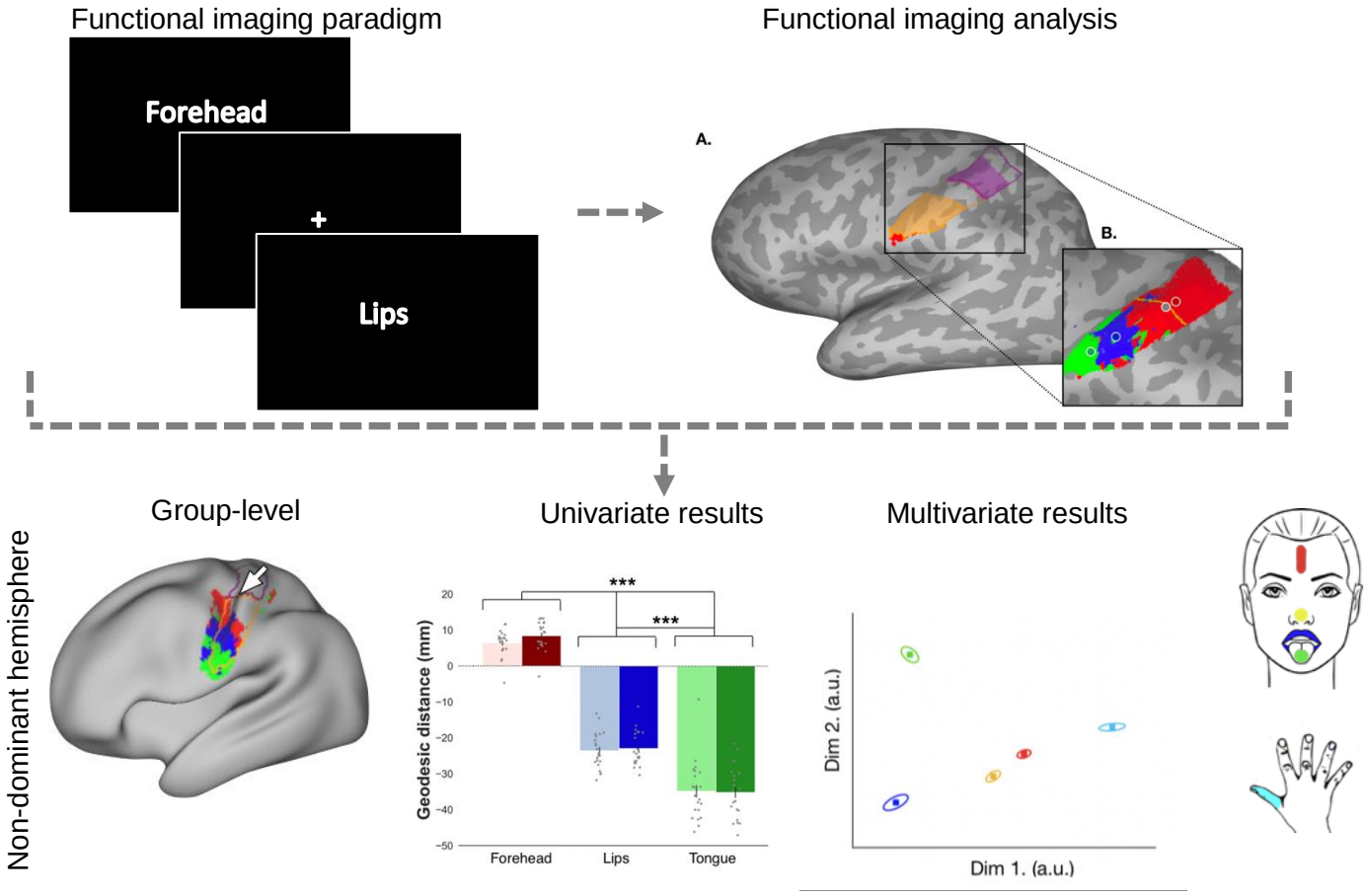


Figure 1.7. *Graphical summary of main findings and methodologies for Chapter 1. N* = 22 two-handed controls completed either an active or passive (pneumatic stimulation; *n*=2 controls only) functional neuroimaging paradigm, moving/stimulating the forehead, nose, lips, tongue and thumbs (dominant and non-dominant). Two regions-of-interest – the primary sensory hand and face region – were then defined and a winner-takes-all analysis was conducted. Centre-of-gravities (CoG) for each movement was then computed and geodesic distances calculated from each CoG to a predefined cortical anchor, as well as a Representational Similarity Analysis (RSA) in the face region. Main univariate and multivariate results for the active paradigm indicated that the cortical neighbour to the hand is likely to be the forehead, followed by the lips and tongue. Furthermore, passive stimulation multivariate results indicated a similar pattern of activation to the active paradigm (i.e., an upright orientation of the face), with a significant and strong positive trend for face-face pairwise distances across paradigms.

Unlike the hand, the somatotopy of the face in humans has long been debated. Some studies have suggested that it is organised in an 'upside-down' manner, with the lower face bordering the hand area, similar to that found in non-human primates (Servos et al., 1999; Yang et al., 1993). However, contrasting work has offered multiple conflicting somatotopies, including an upright orientation (Huang & Sereno, 2007; Kikkert et al., 2022; Roux et al., 2018; Sato et al., 2002, 2005; Schellekens et al., 2022; Schwartz et al., 2004; Sun et al., 2021; Willoughby et al., 2021), rostro-caudal representation (Borsook et al., 2004; DaSilva et al., 2002; Moulton et al., 2009) and one of gross somatotopic overlaps, with no clear orientation at all (Iannetti et al., 2003; Kopietz et al., 2009; Nguyen et al., 2004). These mixed results have implications for the maladaptive plasticity model of PLP. Here the lips have traditionally been used to measure topographic shifts after upper limb loss, based on the implicit assumption that the face is inverted in S1 and that the lips border the hand area. To address these somatotopic inconsistencies in the current literature, we conducted a thorough mapping of the upper and lower face in two-handed controls using an active functional sensorimotor task during fMRI (see *Figure 1.7*). Our subsequent univariate and multivariate analyses demonstrated that the face was likely organised in an upright manner in S1, with the forehead (or upper face) bordering the hand area, followed by the lips, then the tongue. We also had two participants complete the active sensorimotor task ~12 months apart, as well as participating in a passive stimulation protocol. Here we found that the faces' representational structure, including its upright orientation, was relatively stable across time and also across active and passive paradigms, thereby validating our choice of an active task in order to probe facial somatotopy in S1.

Firstly, our univariate analyses at both group and individual level confirmed an upright orientation of the face in two-handed controls. Specifically, we found that the forehead representation borders the hand area, followed by the lips, and tongue located more laterally. Unfortunately, due to the difficulty in obtaining consistent nostril flaring movements across all participants, we were unable to find reliable activation for the nose in the univariate somatotopic maps. This has particular implications for the 'onion-like', rostro-caudal representation of the face, which would be signified by the nose located more inferior to the forehead and lower jaw (Moulton et al., 2009). Similar uncertainties regarding inference of a segmental, rostro-caudal representation have also arisen in other instances using an active sensorimotor task to map facial somatotopy (Schellekens et al., 2022), indicating using such a paradigm may not be sensitive to more fine-detailed cortical representations. Indeed, it may be argued that it is difficult to achieve isolated execution of specific facial muscles when performing movements without impacting sensory processing of neighbouring facial parts. For example, a recent paper demonstrated that prior to movement execution (e.g., a finger press), finger-specific activity patterns were found in S1 which predicted the final planned finger action (Ariani et al., 2022). Thus, engagement of M1 will undoubtedly influence resulting activity in S1, possibly leading to a more gross somatotopy (although see Edin & Abbs, 1991 and Prsa et al., 2019 whereby Pacinian receptors are found to activate during stimulation of remote sites). In support of this, recent work has suggested a 'double-representation' for the larynx in the primary sensorimotor cortices, with a dorsal (closer to the hand) and ventral (below the tongue) representation (Eichert et al., 2020). As our tongue movement may be considered a holistic inner mouth

movement (participants were required to touch the tip of the tongue to the roof, saying ‘tut’), it is likely that we ‘tapped in’ to this double-representation. However, when looking at our univariate results, we do not see evidence of such a cortical ‘double’ representation for the tongue/mouth. When using active paradigms, therefore, the resulting map may be cruder and broader in somatotopy in S1, and at the loss of more fine-detailed representations of the nose. Furthermore, the resulting gross somatotopic maps may have been compounded by our use of a ‘winner-takes-all’ analysis which negates the representation of overlapping representations. However, the addition of our multivariate analyses aimed to reduce the influence of this confound by taking into account the more subtle relationships between activation patterns of facial parts, rather than the amplitude of overall cortical activity. Indeed, our multivariate analyses showed that we were successful in isolating sensorimotor representations of the various movements (forehead, nose, lips and tongue) within our regions of interest. Thus, even if somatosensory information is overlapping across movements, there was still enough distinct information to separate the representational patterns. Interestingly, our multivariate results also indicated very similar activation patterns between the forehead and nose, suggesting that it may be considered as part of, or more similar to, the upper face, therefore potentially in line with an upright orientation of the face. However, future research is needed to confirm the exact location of the nose and larynx within the somatotopic map, involving participants who are able to move them adequately and reliably.

It must also be noted that we only targeted 4 facial movements in total to generate the facial somatotopic maps, therefore inferring the orientation of the face based on

these results is inherently limited to the facial parts that we tested. However, mapping the face comprehensively within an MRI setting has been historically tricky. The majority of previous research here has focused on using passive stimulation protocols using pneumatic devices (to avoid MR interference and RF heating of metallic components). While some of these devices are promising, allowing high spatiotemporal control and safe stimulation of facial parts within the MR head coil (Chen et al., 2017; Custead et al., 2017; Huang et al., 2017), they often require custom masks built for each individual subject to allow full stimulation coverage of the face, an inability to fit underneath narrower head coils or to fix stimulators on participants with larger heads, and are also expensive. Furthermore, these devices either utilise air puffs (Chen et al., 2017; Huang et al., 2017) or stimulators (Custead et al., 2017; Willoughby et al., 2021), which are unable stimulate facial parts such as the tongue or to attach properly to curved body parts (particularly crucial for face stimulation, e.g., the nose). A device which may overcome these issues is the SPA-skin system, which was used within this study for the passive stimulation case studies. Here the SPA-skin actuators are made of soft MR-safe silicone and are 1 mm thick, and thus can be deployed without MR interference artefacts inside the head coil (Kikkert et al., 2022) and has the flexibility to attach to curved facial parts (see *Supplementary Methods* and *Supplementary Figure 1* for full description). Indeed, we developed the device a step further by creating a flexible disposable pouch to contain an SPA actuator which would be placed on the tongue for stimulation, thereby passively mapping the tongue for the first time (to our knowledge). Although a recent study also conducting facial mapping (of the forehead, upper lip and chin) using this device reported significant information content for the face in a face region of interest, this was significantly lower than digit-

to-digit pairwise representational distances in the hand region. It is difficult to state with certainty why this was the case, and may reflect the density of mechanoreceptors in the face compared to the hand, which also varies dependent on the facial area, e.g., the upper face has a lower density of mechanoreceptors than the lips (Corniani & Saal, 2020), or simply noisier (and thus unreliable) stimulation. This is also anecdotally in line with our case study results, whereby the overall amount of information content (i.e., average pairwise distances for facial parts) were also (qualitatively) considerably reduced in the Passive session. Interestingly, both of the Active sessions (1 and 2) displayed increased pairwise distances for the face in the two case studies. As we were able to show consistency in representational structure of the face between Active and Passive sessions (although note a strong positive trend for one participant), the use of an active sensorimotor task may circumvent the above issues regarding passive stimulation of the face in an MR environment, albeit with more gross somatotopic maps.

In support of active somatotopic mapping, previous work has also demonstrated that active tasks may produce greater overall activation of S1 (Berlot et al., 2019; Wiestler et al., 2011), and produce greater separability between multivariate activity patterns of the fingers (Sanders et al., 2019), when compared to passive stimulation, possibly due to the increased 'richness' of input, e.g., efferent and top-down inputs. Indeed, although passive paradigms offer greater control over stimulation parameters, they may actually reflect a more constrained view of S1 somatotopy. For example, recent work has shown that the topography of S1's hand representation reflects habitual patterns of action across digits of the hand (Ejaz et al., 2015; Ingram et al., 2008). This is in line with the recent work

suggesting that the organisational principle of M1 may be behaviour itself – M1 may not just reflect a map of isolated body parts, but behavioural repertoires, or 'action maps' (Graziano, 2016). Thus, by utilising a paradigm that is more reflective of naturalistic tactile inputs in everyday life, may indeed be a more suitable, and ecologically-valid way, of assessing facial somatotopy. Crucially, recent studies have directly compared representational structure of the hand and S1 topography between active and passive paradigms, finding a high level of consistency in somatotopy across the two tasks (Berlot et al., 2019; Sanders et al., 2019), akin to our passive stimulation case studies.

As the face has one of the largest innervation densities and cortical representations, second to the hand, these results inform and advance our understanding of basic topography in S1. Furthermore, they have clear implications for the maladaptive plasticity model of PLP, where researchers have historically used the lips as a marker of cortical remapping after upper limb loss due to its cortical proximity to the hand in S1. However, as we have demonstrated in this *Chapter*, the cortical neighbour to the hand is actually likely to be the upper, not lower, face, thus if cortical remapping of neighbours does exist after upper limb loss, we would therefore expect to see the forehead shifting towards and into the hand area – not the lips. We must therefore revisit these findings and provide a comprehensive mapping of the face (upper and lower) in amputees to discern the extent of somatotopic changes after upper limb amputation, and most importantly, whether these are related to PLP (see *Chapter 2*).

Chapter 2 | Reassessing face topography in the primary somatosensory cortex following hand loss

2.1 Introduction

Our brains capacity to adapt, known as cortical plasticity, is integral to our successful functioning in daily life, as well as rehabilitation from injury. A key model for exploring the extent, and consequences of, cortical plasticity is upper limb loss (via amputation or congenital absence). Here, the cortical hand territory in the primary somatosensory cortex (S1), suffers an extreme loss of sensory input in tandem with dramatic alterations of motor behaviour (Makin, Cramer, et al., 2013; Muret & Makin, 2021). The functional and perceptual correlates of amputation-related plasticity are currently debated (Makin & Bensmaia, 2017; Ortiz-Catalan, 2018). In particular, it is not clear whether functional cortical reorganisation is restricted to early life development or can also occur in adults.

Traditionally, research assessing cortical plasticity after upper limb loss has followed the tenet that neighbouring body parts of the missing hand, and lower face in particular, shift and encroach into the deprived hand area. This emphasis on the lip representation stems from early electrophysiological work in non-human primates, where numerous studies have demonstrated an ‘upside-down’ facial somatotopy (see *Chapter 1*), with the lips and/or lower-chin inputs remapping into the deprived hand area after sensory loss (Jain et al., 1997; Pons et al., 1991). This therefore led to the well-accepted assumption that remapping is determined by cortical proximity (Buonomano & Merzenich, 1998; Nardone et al., 2013). Thereafter, the measurement of topographic shifts in humans has tended to focus

on that of the lips, where researchers have reported that the shifted lip representation towards and into the deprived hand area after amputation is significantly associated with phantom limb pain (PLP) intensity (Birbaumer et al., 1997; Flor et al., 1995; Foell et al., 2014; Grüsser et al., 2001; Lotze et al., 2001). PLP is a neuropathic pain syndrome experienced in the missing, amputated limb by the majority of amputees (Limakatso et al., 2020; also see *Introduction*). This condition is commonly thought to arise from maladaptive cortical plasticity in S1 (although see Makin, 2021), specifically from a signal mismatch between the missing hand representation and the remapped inputs of the lips in the deprived hand area (Ramachandran & Hirstein, 1998).

The research focus on remapping of the lips in amputees is based on this assumption that the lips neighbour the hand area. As we discussed in *Chapter 1*, however, recent research has suggested that the face may in fact be orientated in an upright manner in humans in S1, with the upper face bordering the hand area, not the lips (Huang & Sereno, 2007; Kikkert et al., 2022; Roux et al., 2018; Sato et al., 2002, 2005; Schellekens et al., 2022; Schwartz et al., 2004; Sun et al., 2021; Willoughby et al., 2021). In line with this, recent work has reported that the shift in the lip representation towards the missing hand in amputees was minimal, and likely to reside within the face area itself, with no relationship to PLP (Makin et al., 2015). Surprisingly, there is currently no research that considers the representation of other facial parts, including the upper face in particular (e.g., the forehead), in relation to plasticity or PLP.

Remapping after upper limb loss has also been documented in individuals born without a hand (hereafter one-handers), who do not experience PLP (Makin, Scholz, et al., 2013). Here it has been shown that the representation of multiple body parts, including the residual arm, legs and mouth, remapped into the missing hand territory (Hahamy et al., 2017; Hahamy & Makin, 2019). Importantly, cortical remapping in this group does not depend on cortical proximity of the body parts. With regards to the lips, a recent transcranial magnetic stimulation (TMS) study has reported functionally-relevant lip activity in the deprived hand area of one-handers (Amoruso et al., 2021), showcasing that reported remapping may also be functional. It was proposed that the observed remapping of various body parts could have been shaped by compensatory behaviour (Hahamy et al., 2017), as these body parts are all used by one-handers to compensate for their missing hand function, but this hypothesis awaits validation.

Here, we conducted a mapping of face cortical organisation to determine the extent of somatotopic shifts in the primary sensorimotor cortex in 22 two-handed controls, 17 amputees and 21 one-handers. We used surface-based comparisons, including cortical (geodesic) distances, to measure the extent of cortical remapping of the upper (forehead) and lower face (lips) in relation to the deprived (or non-dominant) hand area across all groups. We also explored the representation of the tongue, which has not been previously studied in the context of deprivation-triggered brain plasticity. Furthermore, we used multivariate representational similarity analysis (RSA) in order to characterise more subtle alterations in the relationship between facial activity patterns (forehead, nose, lips, tongue) in the deprived hand and face areas, independent of gross spatial

somatotopic shifts. We predict that the extent of cortical remapping in amputees will be minimal, in line with previous work utilising cortical geodesic distances (Makin et al., 2015). We further predict that if cortical remapping does exist in amputees, then this will be restricted to the cortical neighbour of the hand – the upper face (based on our results in *Chapter 1*). Finally, we predict that we will find no evidence of a significant relationship between cortical remapping and PLP within our amputee group. Furthermore, we predict to find evidence of extensive cortical remapping in the one-handers, validating our methodology as suitable for identifying remapping effects.

2.2 Methods

2.2.1 Participants

Seventeen individuals with acquired unilateral upper-limb amputation (age; *M*=53.71, *SE*=2.69, women; *n*=4, missing right hand; *n*=9), twenty-one individuals with unilateral congenital transverse arrest (age; *M*=42.67, *SE*=3.04, women; *n*=13, missing right hand; *n*=8) and twenty-two two-handed controls (age; *M*=45.55, *SE*=2.02, women; *n*=10, left-handers; *n*=6) were recruited (note the same control sample was used in *Chapter 1*). Two additional amputees who were recruited for the study did not participate in the scanning session due to MRI safety concerns, and further recruitment was stalled due to Covid-19 restrictions. The proportion of participants with intact/dominant right hand, as well as gender, were matched across groups ($\chi^2_{(2)}$=2.674, *p*=.263; $\chi^2_{(2)}$=5.593, *p* =.061). While significant differences between groups were observed for age ($H_{(2)}$=7.689, *p*=.021), post-hoc comparisons confirmed non-significant differences between amputees and one-

handers relative to controls. Age covariates were therefore only included in statistical analyses when direct comparisons between amputees and one-handers were carried out. Procedures were in accordance with NHS National Research Ethics Service approval (18/LO/0474), and written informed consent was obtained.

Participants	Age	Gender	Handedness (prior to amputation for amputees)	Affected limb	Level of limb deficiency	Years since amputation	PLS intensity	PLS frequency	Chronic PLS	PLP intensity	PLP frequency	Chronic PLP	Cause of amputation
A01	60	M	R	R	2	43	100	5	100	60	5	60	Trauma
A02	34	M	R	R	1	3	50	2.5	14.6	70*	2	17.5*	Trauma
A03	58	M	R	R	1	33	90	5	90	100	1	20	Trauma
A04	59	M	R	L	2	16	40	1	8	0	1	0	Trauma
A05	54	M	A	L	1	36	100	5	100	80	4	40	Trauma
A06	47	F	R	L	2	18	80	4	40	0	0	0	Electrocution
A07	40	F	R	R	1	10	40	3	13.3	0	0	0	Trauma
A08	47	M	R	R	2	5	70	4	35	10	4	5	Trauma
A09	53	M	R	L	2	34	20	0	0	0	0	0	Trauma
A10	56	F	L	L	1	12	90	5	90	80	5	80	Tumour
A11	66	M	R	R	1	38	60	5	60	0	0	0	Trauma
A12	65	F	L	L	1	10	90	5	90	80	4	40	Trauma
A13	66	M	R	L	1	35	80	2	20	100	2	25	Trauma
A14	64	M	R	R	1	18	75	5	75	65	5	65	Trauma
A15	65	M	R	R	1	8	70	5	70	0	0	0	Trauma
A16	48	M	R	R	1	23	85	5	85	65	5	65	Trauma
A17	31	M	R	L	2	14	30	5	30	25	1	5	Trauma
C01	32	F	R	L	2								
C02	32	F	R	L	2								
C03	35	M	R	L	2								
C04	48	M	R	L	2								
C05	22	F	L	R	2								
C06	54	F	R	L	2								
C07	56	F	L	R	2								
C08	53	M	R	L	1								
C09	54	F	R	L	2								
C10	58	M	L	R	2								
C11	22	M	R	L	2								
C12	30	F	R	L	2								
C13	24	M	L	R	2								
C14	33	F	L	R	2								
C15	39	F	L	R	2								
C16	55	F	R	L	2								
C17	67	F	L	R	2								
C18	30	F	L	R	2								
C19	43	M	R	L	2								
C20	63	M	R	L	2								
C21	46	F	R	L	2								

Table 2.1. *Demographic details for amputees (A01-17) and congenital one-handers (C01-21).* Level of limb deficiency is as follows: 1 = limb loss above elbow (transhumeral), 2 = limb loss below elbow (transradial); L = left, R = right; PLS & PLP frequency: 0 = no sensation or pain, 1 = once or less per month, 2 = several times per month, 3 = once a week, 4 = daily, 5 = all the time. *PLP intensity rating was on average. PLS = phantom limb sensations; PLP = phantom limb pain.

2.2.2 Phantom sensations rating

Amputees were asked to rate the frequency of PLP experience within the last year. They also rated the intensity of their worst PLP experience during the last week (or in a typical week involving PLP; 0 = no pain, 100 = worst pain imaginable). A chronic measure of PLP was calculated by dividing the worst PLP intensity in the last week by PLP frequency (1 = all the time, 2 = daily, 3 = once a week, 4 = several times per month, 5 = once or less per month). This approach which takes into account the chronic aspect of PLP has been used successfully before (Draganski et al., 2006; Kikkert et al., 2016, 2017, 2018; Lyu et al., 2016; Makin et al., 2015; Makin, Scholz, et al., 2013), and has high inter-session reliability (Kikkert et al., 2018). We also asked amputees about the vividness and frequency of non-painful phantom sensations (see *Table 2.1*).

Please note that the **Functional MRI sensorimotor task** (see *p.*39-40), **MRI data acquisition** (see *p.*41), **MRI pre-processing** (see *p.*42), **Functional MRI analysis** (see *p.*43), **Regions of Interest definition** (see *p.*44), **Winner-takes-all approach** (see *p.*46), **Cortical distance analysis** (see *p.*46), and **Multivariate representational analysis** (see *p.*48-49) were the same as that carried out in *Chapter 1*. Please see below for any further additional analyses/information regarding group-specific comparisons of facial somatotopic remapping:

2.2.3 Functional MRI sensorimotor task

An active sensorimotor task only was used for facial somatotopic mapping across groups. Note for thumb movements, amputees were asked to flex/extend their

phantom thumb to the best of their ability, and one-handers were asked to imagine such movement.

2.2.4 Functional MRI analysis

Here we noted that the number of motion outliers of large movements were similar across groups (of total *n* volumes per group: amputees: 0.36%; controls: 0.36%; one-handers: 0.42%). Again, since the nose condition yielded weak activity relative to baseline, we excluded it from the univariate analysis.

2.2.5 Surface area calculation

To assess possible remapping into the hand area specifically, a secondary winner-takes-all analysis was restricted to the hand ROI only. The surface area coverage (mm^2) for each face-winner were computed on the individual anatomical inflated surface. We next calculated the proportion of the hand ROI occupied by each face part by dividing each face-winner's surface area by the total hand ROI surface area for each individual. From the resulting percentages, we produced a laterality index for each movement with the following formula:

$$laterality\ index = \frac{(deprived_m - intact_m)}{(\sum deprived_m, intact_m)} \qquad (1)$$

whereby $deprived_m$ and $intact_m$ represent the percentage of surface area coverage for the facial movement *m,* respectively in the deprived and intact hemisphere. A subsequent laterality index of +1 indicates surface area coverage of that movement solely within the deprived hemisphere (or the hemisphere contralateral

to the non-dominant hand in controls), whereas a value of 0 represents an equal balance of surface area coverage across both hemispheres. Note that this approach characterises cortical remapping in relation to the intact hemisphere and has been used in numerous previous studies on amputees (Birbaumer et al., 1997; Flor et al., 1995; Foell et al., 2014; Grüsser et al., 2001). It assumes that the intact hemisphere reflects baseline (i.e., that it is truly 'intact'), which may not be the case due to inter-hemisphere plasticity and/or homeostatic mechanisms (Muret & Makin, 2021; Philip & Frey, 2014; Valyear et al., 2020) and so we also compared our results to the control group.

2.2.6 Group-level visualisations

Prior to group-level visualisations, participant information regarding hand dominance (controls) and deprived hemisphere (one-handed participants) were used to sagittal-flip raw pre-processed data, such that the brain activity corresponding to the non-dominant/missing hand is always represented in the left hemisphere (note that a similar proportion of participants were flipped across groups).

As well as activity maps, we also visualised the winner-takes-all output at the group-level. Here the 'winners' for each face movement within the S1 ROI (the hand and face region combined) in MNI152 space were concatenated into a single volume per group to produce a consistency map for the individual movements (i.e., how many participants maximally activated the same voxel when moving a given facial part). Resulting consistency maps were then projected to a group

cortical surface (Glasser et al., 2016) using Connectome Workbench (v1.4.2) for visualisation only.

2.2.7 Multivariate representational analysis

RSA was conducted in the hand and face ROIs to explore possible remapping across representational features between groups. Note 6 unique inter-facial representational distances (10 unique distances when including the thumb for controls and amputees only), were characterised in the representational dissimilarity matrix (RDM) for group comparisons.

2.2.8 Statistical analyses

All statistical analyses were carried out using JASP (Version 0.14). Outliers were classified as +/- 3 standard deviations to the mean. We chose to not remove outliers in our analyses and checked that the significance and direction of the results did not change if identified outliers were removed. When appropriate, univariate analyses was compared using parametric statistics. To assess normality for parametric tests, Shapiro-Wilk tests were run on residuals in combination with inspection of Q-Q plots and reporting of Levene's Test for Equality of Variances. Where stated, non-parametric test statistics are reported where the assumption of normality has been violated. Analysis of Variance (ANOVA) was used to explore group differences to controls in cortical distances. Each mixed ANOVA had a between-subject factor of Group (Controls x Amputees; Controls x One-handers) and a repeated-measures factor of Hemisphere (Intact/Dominant x Deprived/Non-dominant), and was run separately for each facial movement (forehead, lips and tongue). We controlled for brain size volume

when comparing cortical distances between groups. Post-hoc comparisons were conducted with a Bonferroni correction for multiple comparisons (corrected alpha = .025; reported uncorrected *p*-values in text). If assumptions of normality were violated, the difference between cortical distances in the intact and deprived hemisphere were calculated, and the group difference between one-handed groups and controls was computed using a Mann-Whitney *U* test. Resulting statistics are reported alongside the mixed ANOVA output. Independent *t*-tests were used to calculate laterality indices group differences.

We reported the corresponding Bayes Factor (BF_{10}), defined as the relative support for the alternative hypothesis, for all results (excluding post-hoc comparisons as these were based on estimated marginal means). Note that Bayes Factors reported for interactions reflect the model as a whole (main effects and interactions). Subsequent Bayes Inclusion Factors were reported for main effects and interactions individually, which quantify how much the observed data are more probable under models that include the predictor relative to models that do not. While it is generally agreed that it is difficult to establish a cut-off for what consists sufficient evidence, we used the threshold of $BF<1/3$ as positive evidence in support of the null, consistent with others in the field (Dienes, 2014; Wetzels et al., 2011; though see Kass & Raftery, 1995). The Cauchy prior width was set at 0.707 (JASP's default). To investigate whether remapping measures were related to PLP, we used a one-tailed Mann-Whitney *U* tests to compare laterality indices of amputees with (n=11) and without PLP (n=6) for relevant facial parts, under the hypothesis that PLP should result in greater remapping (see *Supplementary Figure 5* for the analogous analysis for the cortical geodesic distances).

For multivariate analyses, in order to quantify the dissimilarity, or 'information', each ROI holds for the face across groups, a linear mixed model (LMM) analysis was used, allowing us to consider the distinct contribution of face-thumb or face-face pairs. The face-face LMM contained fixed factors of group (controls, amputees and one-handers), hemisphere (intact, deprived) and facial pairs (6 unique representational distances). A random effect of participant, as well as covariates of age and gender, were also included in the model. An additional LMM was used to explore potential remapping in the hand ROI in relation to the non-dominant/phantom thumb in controls and amputees. Here the LMM contained the fixed factors of group (controls and amputees), hemisphere (intact, deprived) and face-to-thumb pairs (4 unique representational distances), as well as a random effect of participant. All LMM's were carried out in jamovi (version 1.6.15) under restricted maximum likelihood (REML) conditions with Satterthwaite adjustment for the degrees of freedom.

2.3 Results

2.3.1 The upper face borders the deprived hand area in amputees and one-handers

When looking at facial organisation at the group-level we found qualitatively similar activity maps across groups (see *Figure 2.1*), highlighting a robust somatotopy of the face with preserved symmetry across the two hemispheres. These facial maps also indicated an upright orientation of the face in S1, with the forehead located closest to the hand area, followed by the lips, and the tongue located laterally, across all groups. Thus, the facial somatotopy presented in the

amputees and one-handers (as well as controls, see *Chapter 1*) suggests that the deprived hands' cortical neighbour is the upper face. However, conclusions based on group averages may be misleading as they ignore inter-individual differences.

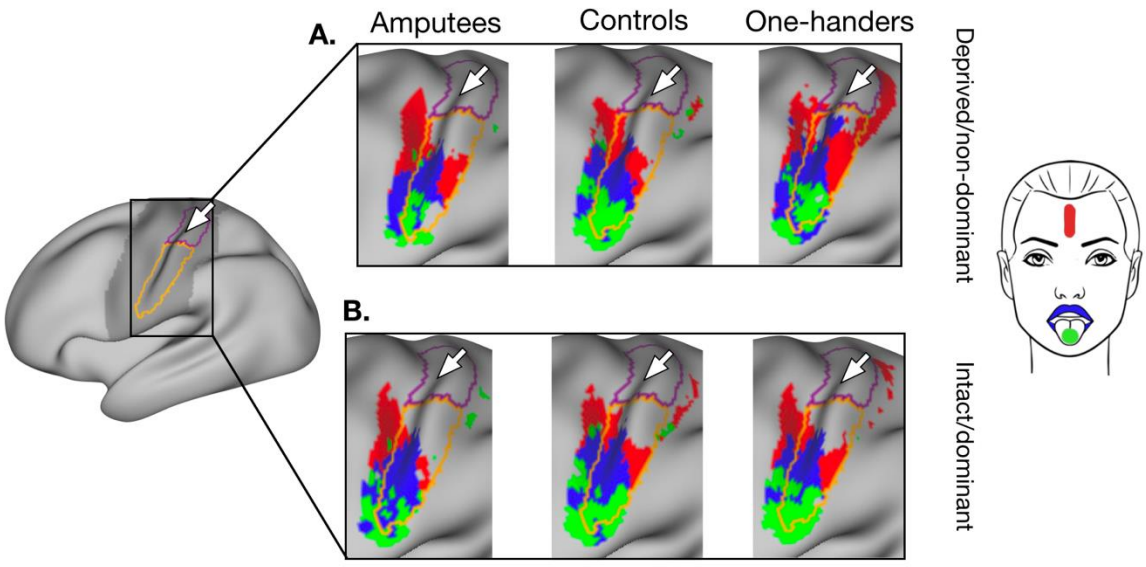


Figure 2.1. *Group-level activity maps for each facial movement.* Group average activity for the forehead (red), lips (blue) and tongue (green) movements, contrasted to rest, in the **(A)** deprived/non-dominant and **(B)** intact/dominant hemisphere for controls (*n*=22), amputees (*n*=17) and one-handers (*n*=21). All clusters were created using a threshold-free cluster enhancement procedure with a sensorimotor pre-threshold mask (defined using the Harvard Cortical Atlas; shown in grey), and thresholded at $p<.01$. The hand and face ROIs are outlined in purple and orange respectively, and the central sulcus is denoted with a white arrow.

2.3.2 One- handers, but not amputees, show lip remapping in the deprived cortex based on univariate topographic mapping

To account for inter-individual differences in functional topography and brain topology, we first explored changes in the cortical (geodesic) distance between the

lips and the lateral border of the hand ROI of amputees and controls. Here we found no statistically significant main effects or Group x Hemisphere interaction ($F_{(1,36)}$=0.003, p=0.954, n^2_p=9.566$_{e-5}$, BF_{10}=0.427, $BF_{Inclusion}$=0.321; controlled for brain size volume; *Figure 2.2.B*; for main effects see *Supplementary Table 1*), indicating that the lip area in amputees is not located differently to that of controls. This is further supported by a lack of evidence for significant remapping of the lips (i.e., greater surface coverage) in the missing hand ROI for amputees when compared to controls (U=171.000, p=0.660, d=-0.086, BF_{10}=0.355; see *Figure 2.2.C*). These results suggest, contrary to popular theories on brain plasticity in amputees (Flor, Nikolajsen, Jensen, et al., 2006), that the lips do not remap into the deprived hand area after upper limb loss. However, as the reported Bayes Factors indicated only anecdotal evidence for the null, we next compared the lips laterality index between those individuals who reported suffering from PLP (n=11) and those who no longer experienced chronic PLP (n=6) and found no significant differences (U=36.000, p=0.404, d=0.091, BF_{10}=0.545).

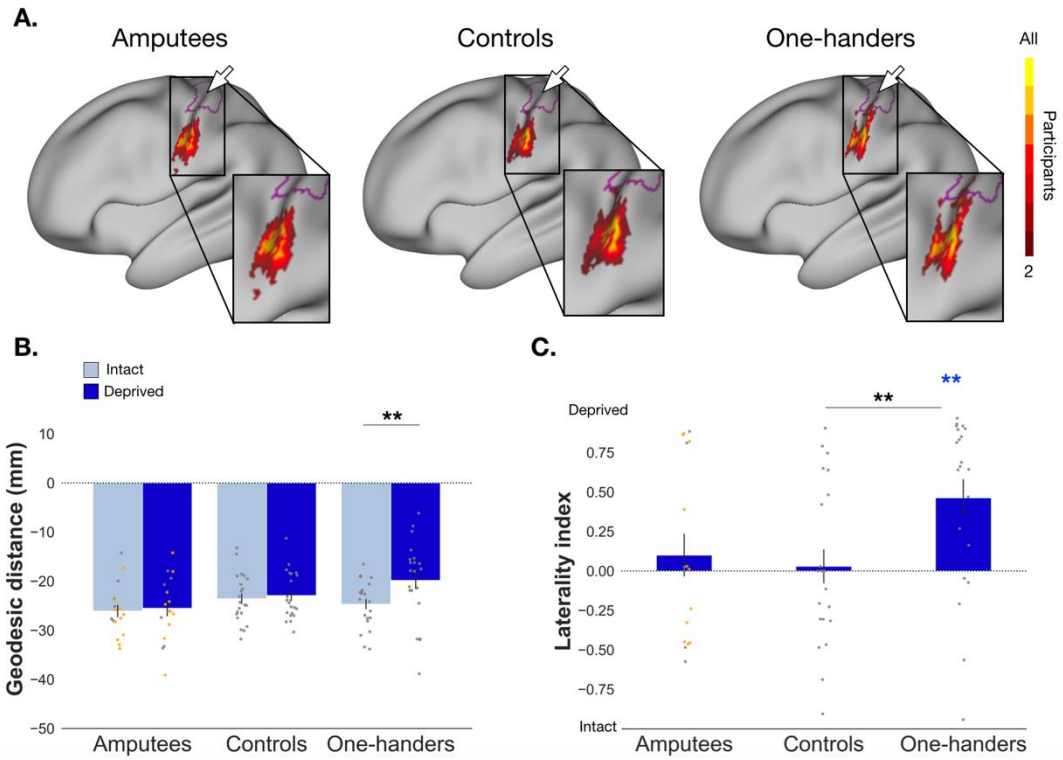


Figure 2.2. *Characterisation of lip (re)mapping in the primary somatosensory cortex.* **(A)** Group-level consistency map for the lips in the S1 ROI (hand and face combined) across groups. The colour gradient represents participant agreement for maximally activating that particular voxel, relative to other face movements (winner-takes-all approach). The hand ROI is outlined in purple and central sulcus denoted by the white arrow. **(B)** Cortical geodesic distances from the lip CoG to the lateral border of the hand ROI are plotted for amputees (*n*=17), controls (*n*=22) and one-handers (*n*=21). Distances in the intact/dominant hemisphere are plotted in light blue, and distances in the deprived/non-dominant hemisphere are plotted in darker blue. Positive distances indicate the lips CoG is located medial to the lateral border of the hand ROI, and negative distances indicate the lips CoG is located laterally to the hand ROIs' border, in the face ROI. The lateral boundary of the hand ROI itself equates to a geodesic distance of zero. **(C)** Laterality indices for the proportion of surface area coverage of the lips in the hand ROI for all groups (amputees, controls and one-handers). Positive values indicate greater surface area coverage in the deprived/non-dominant hemisphere, and negative values reflect greater surface area coverage in the intact/dominant hemisphere. Standard error bars and all individual data-points are plotted in grey and uncorrected for brain size. Amputees with PLP (yes/no) are plotted in orange. * $p < .05$; ** $p < .01$ (please note p-values are uncorrected); coloured asterisk's indicate values are significantly different from zero.

When looking at lip plasticity within the one-handers group, however, we did note a slight qualitative shift in the location, and spread, of the lip activity within the deprived hemisphere (see *Figure 2.1.B*). This is further supported by a visible shift of the one-handers lip group-level consistency map towards, and into, the deprived hand area (see *Figure 2.2.A*). These changes in the lip representation were statistically significant, with a significant Group x Hemisphere interaction for the lips cortical distance to the hand-face border in one-handers and controls ($F_{(1,40)}$=5.419, p=0.025, n^2_p=0.119, BF_{10}=343.133, $BF_{Inclusion}$=2.163; controlling for brain size; see *Figure 2.2.B*; see *Supplementary Table 2* for main effects). Confirmatory comparisons indicated no statistically significant shifts of the lip CoG in the deprived hemisphere when compared to the controls non-dominant hemisphere ($t_{(40)}$=-1.414, p=0.165; see *Figure 2.2.B*). However, shorter distances from the lips to the hand area were found in the deprived hemisphere of the one-handers when compared to their intact hemisphere ($t_{(40)}$=-3.760, p<.001), indicating substantial evidence for lip remapping. These shifts in the deprived hemisphere were also reflected in significantly greater surface area coverage of the lips in the hand ROI when compared to controls (U=119.000, p=0.007, d=-0.485, BF_{10}=3.480; see *Figure 2.2.C*), which was significantly different from zero (W=197.000, p=0.003, d=0.706, BF_{10}=14.415). This evidence of lip remapping is in line with previous work in one-handers (Amoruso et al., 2021; Hahamy et al., 2017).

2.3.3 One-handers, but not amputees, show forehead remapping in the deprived cortex, based on univariate topographic mapping

As we note a qualitative upright orientation of the face (see *Figure 1* and *Chapter 1*), the question remains as to whether the neighbour to the hand – the forehead –

would reorganise after limb loss in amputees, as hypothesised by traditional theories (Flor, Nikolajsen, Jensen, et al., 2006). Again, we found no significant evidence for cortical remapping of the neighbouring forehead in amputees when assessing changes in cortical distances (Group x Hemisphere: $F_{(1,36)}$=0.935, p=0.340, n^2_p=0.025, BF_{10}=0.139, $BF_{Inclusion}$=0.537; controlled for brain size volume; non-parametric equivalent: U=231.000, p=0.221, d=0.235, BF_{10}=0.498; see *Figure 2.3.B*). A significant difference was found, however, of reduced forehead surface area coverage in the deprived hand ROI when compared to controls ($t_{(37)}$=2.048, p=0.048, d=0.661, BF_{10}=1.572; see *Figure 2.3.C*). Interestingly, the direction of results indicates less, not more, remapping of the forehead in the deprived hand ROI of amputees. However, note the inconclusive Bayes Factor. We subsequently found non-significant differences when comparing the forehead laterality index for amputees with and without PLP (U=26.000, p=0.769, d=-0.212, BF_{10}=0.322). Taken together, these results suggest that if remapping of the cortical neighbour – the forehead – does occur, this effect is small in comparison to controls, away from the hand area, and is not related to PLP.

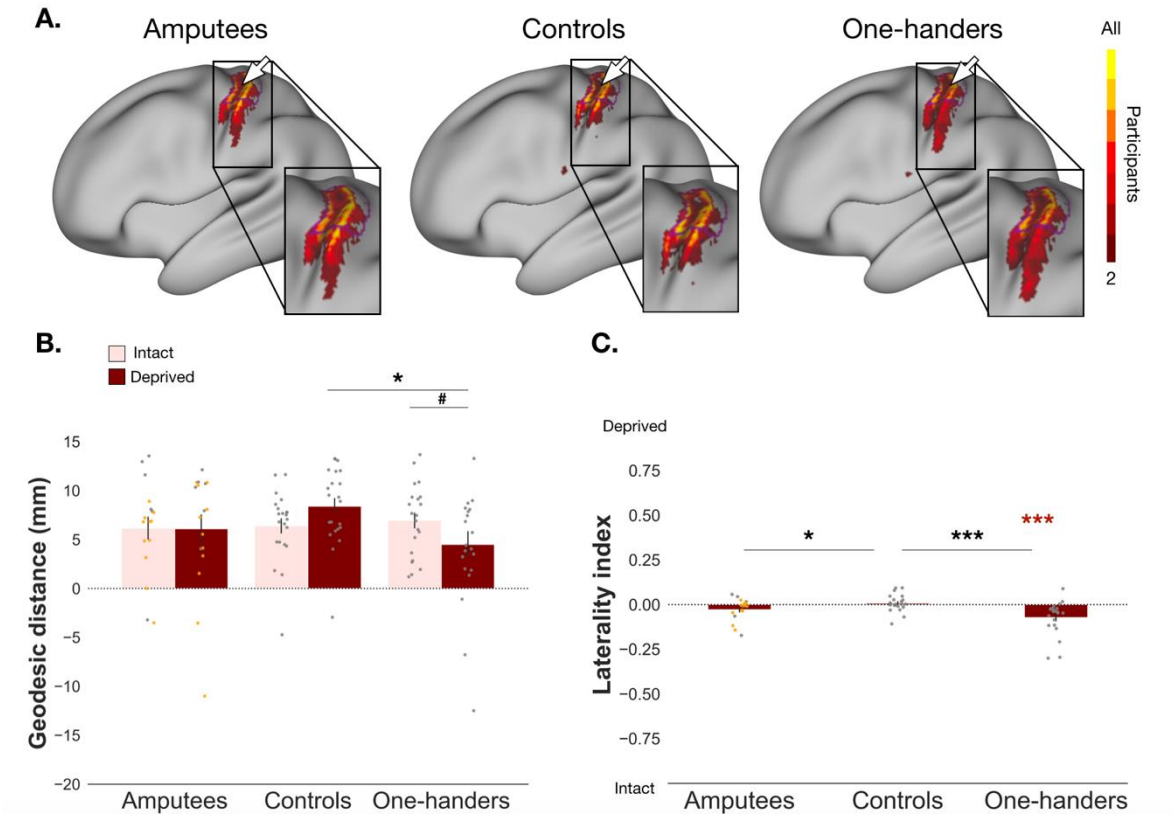


Figure 2.3. *Forehead topography in the primary somatosensory cortex.* All annotations are as in Figure 2.2. For main effects of cortical geodesic distance comparison between amputees and one-handers versus controls, see *Supplementary Tables 3-4*. Distances in the intact hemisphere are plotted in pink and deprived hemisphere in red. # strong positive trend; * p < .05; *** p < .001; coloured asterisk's indicate values are significantly different from zero.

When looking at the one-handers group we did find significant evidence of forehead remapping with a Group x Hemisphere interaction ($F_{(1,40)}$=8.287, p=0.006, n^2_p=0.172, BF_{10}=1.470, $BF_{Inclusion}$=11.273; controlled for brain size volume; non-parametric equivalent: U=343.000, p=0.006, d=0.485, BF_{10}=4.264; see *Figure 2.3.B*). Confirmatory comparisons indicated a positive trend for shorter distances of the foreheads' CoG to the lateral boundary of the hand ROI in the deprived hemisphere when compared to their intact hemisphere ($t_{(40)}$=2.208, p=0.033) and

significantly shorter distances when compared to the controls non-dominant hemisphere ($t_{(40)}$=2.558, p=0.014). As the forehead's CoG tended to be located above the hands' lateral border (see *Figure 2.3.A*), these results indicate a significant shift of forehead activity away from the deprived hand ROI. This is further supported by a significant decrease of surface area coverage for the forehead in the deprived hand ROI when compared to controls (U=381.000, p<.001, d=1.069, BF_{10}=25.816), which was significantly different from zero (W=19.000, p<.001, d=-0.835, BF_{10}=181.656; see *Figure 2.3.C*). Remapping of the cortical neighbour in one-handers, therefore, manifests in a shifting away of the upper face from the deprived hand area, possibly due to increases in activity of other facial movements, e.g., lips.

2.3.4 Tongue movements produce different topographic maps across groups

We also assessed changes in the tongue representation, which is not an immediate neighbour to the hand in S1 (see *Figure 2.4.A*). We did not find significant evidence for shifts in the tongue's CoG towards the hand ROI in amputees when compared to controls (Group x Hemisphere: $F_{(1,36)}$=2.546, p=0.119, n^2_p=0.066, BF_{10}=0.176, $BF_{Inclusion}$=0.513; controlled for brain size volume; non-parametric alternative: U=126.000, p=0.087, d=-0.326, BF_{10}=0.882; see *Figure 2.4.B*). Nevertheless, the tongue did show significantly greater surface area coverage in the deprived hand ROI of amputees when compared to controls ($t_{(37)}$=-2.759, p=0.009, d=-0.891, BF_{10}=5.414; see *Figure 2.4.C*), which was also significantly different to zero ($t_{(16)}$=2.302, p=0.035, d=0.558, BF_{10}=1.941). As tongue remapping is not reflected consistently across analyses, and due to the lack of pre-existing hypotheses, this

preliminary result should be interpreted with caution (also note the inconclusive Bayes Factor for the One-Sample *t*-test). However, it does indicate that some level of cortical remapping may occur in amputees after upper limb loss. We next explored whether this increase in tongue activity within the deprived hand ROI, as captured by the laterality index of amputees, was related to PLP (see *Figure 2.4.C*), and found a non-significant difference ($t_{(15)}$=1.223, p=0.120, d=0.620, BF_{10}=1.169). These results suggest that amputees with PLP do not report greater instances of tongue remapping, when compared to amputees without PLP.

We also found greater surface area coverage of the tongue in the deprived hand ROI of one-handers (see *Figure 2.4.A*) that was significantly different from zero (W=180.000, p=0.024, d=0.558, BF_{10}=1.651) and from controls (U=109.000, p=0.003, d=-0.528, BF_{10}=2.763; see *Figure 2.4.C*). This increased tongue activity in the one-handers deprived hand area was also reflected in a significant Group x Hemisphere interaction ($F_{(1,40)}$=7.149, p=0.011, n^2_p=0.152, BF_{10}=13.801, $BF_{Inclusion}$=5.584; controlled for brain size volume; non-parametric equivalent: U=140.000, p=0.027, d=-0.394, BF_{10}=2.351; see *Figure 2.4.B*) of the cortical distance between the tongues' CoG and the lateral boundary of the hand ROI. Confirmatory comparisons indicated significantly shorter distances to the lateral hand ROI border for the tongue in the deprived hemisphere compared to intact ($t_{(40)}$=-3.5808, p<.001), and a strong positive trend when compared to the controls' non-dominant hemisphere ($t_{(40)}$=-2.119, p=.040). These results tentatively suggest that cortical remapping in one-handers may extend further to include tongue facial movements.

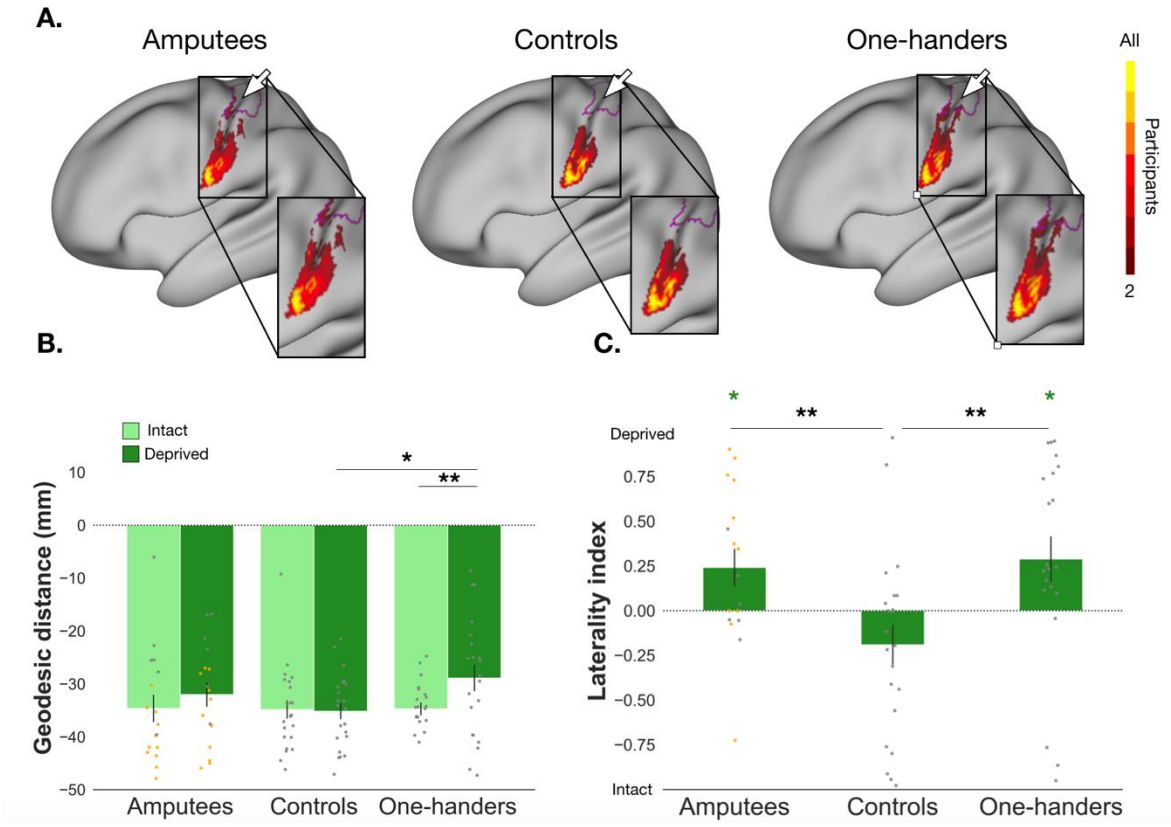


Figure 2.4. *Tongue remapping in amputees and one-handers in the primary somatosensory cortex.* Distances in the intact hemisphere are plotted in light green and distances in the deprived hemisphere in dark green. For main effects of cortical geodesic distance comparison between amputees and one-handers versus controls, see *Supplementary Tables 5-6*. All other annotations are as in *Figure 2.1*.

2.3.5 Brain decoding in the deprived hand area reveals stable facial representational pattern for amputees, and increased facial information in one-handers

The analyses described above focused on the topographic relationship of the three facial parts, but cortical remapping could potentially manifest subtly, without disrupting the spatial distribution of the face representation. RSA identifies statistical (dis)similarities across activity patterns, providing a more sensitive measure of

representational changes (Diedrichsen et al., 2018). To further explore any possible remapping in the deprived hand area of the amputees, we first looked at the pattern of dissimilarity for each face part relative to non-dominant/phantom thumb in the hand ROI for controls and amputees. Here we found a non-significant Group x Hemisphere x Face-Thumb interaction ($F_{(3,259.0)}$=0.569, p=0.636), as well as a non-significant Group x Hemisphere interaction ($F_{(1,259.0)}$=0.057, p=0.811; see *Figure 2.5.A*). The pattern of facial activity in relation to the thumb is therefore statistically comparable between amputees and controls, indicating similar representational structure of the face, relative to the hand, between the two hemispheres and groups.

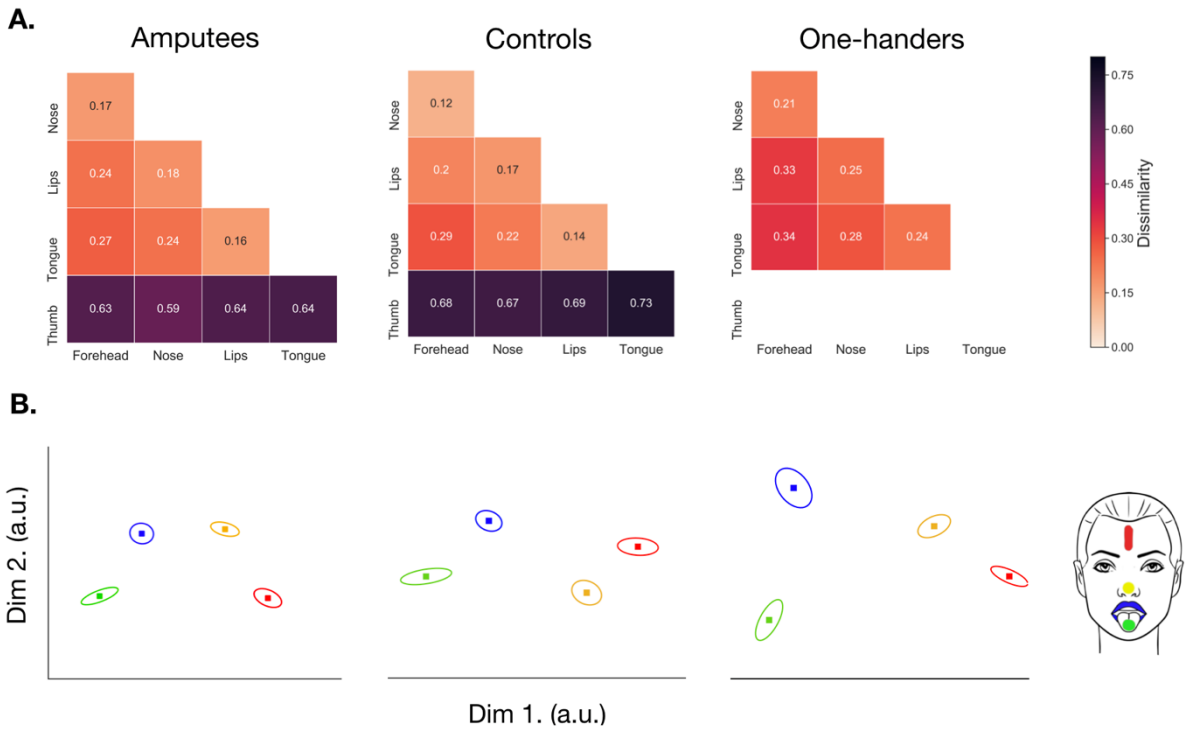


Figure 2.5. *Representational Similarity Analysis (RSA) in the deprived/non-dominant hand area across all groups.* **(A)** Representational Dissimilarity Matrices (RDMs) for amputees (*n*=17), controls (*n*=22) and one-handers (*n*=21). Greater dissimilarity between activity patterns for the chosen pairwise comparison indicates more information for that facial part within the hand area. Smaller dissimilarity values of facial (and thumb) activity patterns indicate a reduced ability to discriminate between the chosen movements in the hand area. Face-thumb distance values are only shown for the controls and amputees. (**B)** Multi-dimensional scaling plots for each group, which projects the RDM distances into a lower-dimensional space. Here the distances between each marker reflects the dissimilarity, with more similar activity patterns represented closer together, and more distinct activity patterns positioned further away. Forehead movements are plotted in red, with the nose in yellow, lips blue and tongue green, and the standard error is plotted around each data point. Please note, a different scale was used compared to the face ROI (see *Figure 2.6*). For main effects and interaction for face-thumb and face-face pairwise distances in hand ROI *see Supplementary Tables 7-8*.

We also found a non-significant Group x Hemisphere x Face-Face interaction when looking at face-face pairwise dissimilarity in the hand ROI across all three groups ($F_{(10,627.0)}$=0.572, p=0.837; controlled for age; see *Figure 2.5.B*), suggesting a similar representational structure of the face across hemispheres and groups. However, when we looked at the average amount of facial information within the hand ROI, we did find a significant Group x Hemisphere interaction ($F_{(2,627.0)}$=14.544, p<.001), indicating potential differences in facial information content in the hand area. Post-hoc comparisons (corrected alpha=0.0125; uncorrected *p*-values reported) exploring this effect reported significantly greater dissimilarity between facial-part representations in the deprived hemisphere of the amputees (M=0.214; SE=0.021; $t_{(627.0)}$=-4.401, p<.001) and one-handers (M=0.273; SE=0.018; $t_{(627.0)}$=-5.668, p< .001), when compared to their respective intact hemisphere (amputees: M=0.152; SE= 0.021; one-handers: M=0.202; SE=0.018). When comparing to the controls non-dominant hemisphere (M=0.191, SE=0.017), we only found significantly greater facial information in the one-hander's deprived hand area ($t_{(72.8)}$=-3.297, p=0.002) and a non-significant effect for amputees ($t_{(71.7)}$=-0.828, p=0.411). These results are in line with our univariate analyses, which demonstrate significant cortical remapping of facial parts in the one-handers group. It also suggests that there may be inter-hemispheric changes in facial information in the intact hand ROI of amputees (M=0.152 SE=0.021; controls: M=0.207, SE=0.017), though this latter result awaits further confirmation.

For completion, we also looked at facial activity patterns (i.e., face-face pairwise dissimilarities) within the face ROI across all three groups. Here we found non-significant differences for a Group x Hemisphere x Face-Face interaction

($F_{(10,627.0)}$=0.136, p=0.999) and Group x Hemisphere ($F_{(2,627.0)}$=0.626, p=0.535), suggesting a similar representational pattern of facial activity, i.e., facial information content, across hemispheres and groups (see *Figure 2.6*).

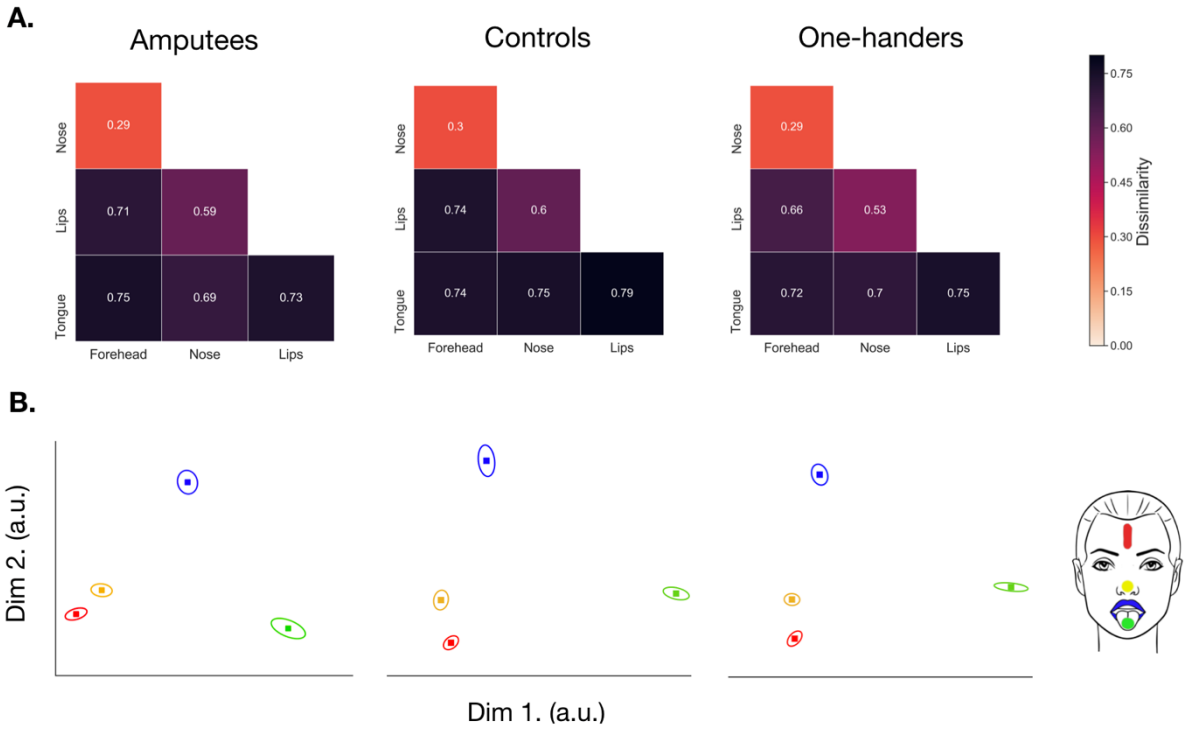


Figure 2.6. *Representational Similarity Analysis (RSA) in the deprived/non-dominant face area across all groups.* All annotations are as in *Figure 2.5*. For main effects and interaction for face-face pairwise distances in face ROI see *Supplementary Table 9*.

2.4 Discussion

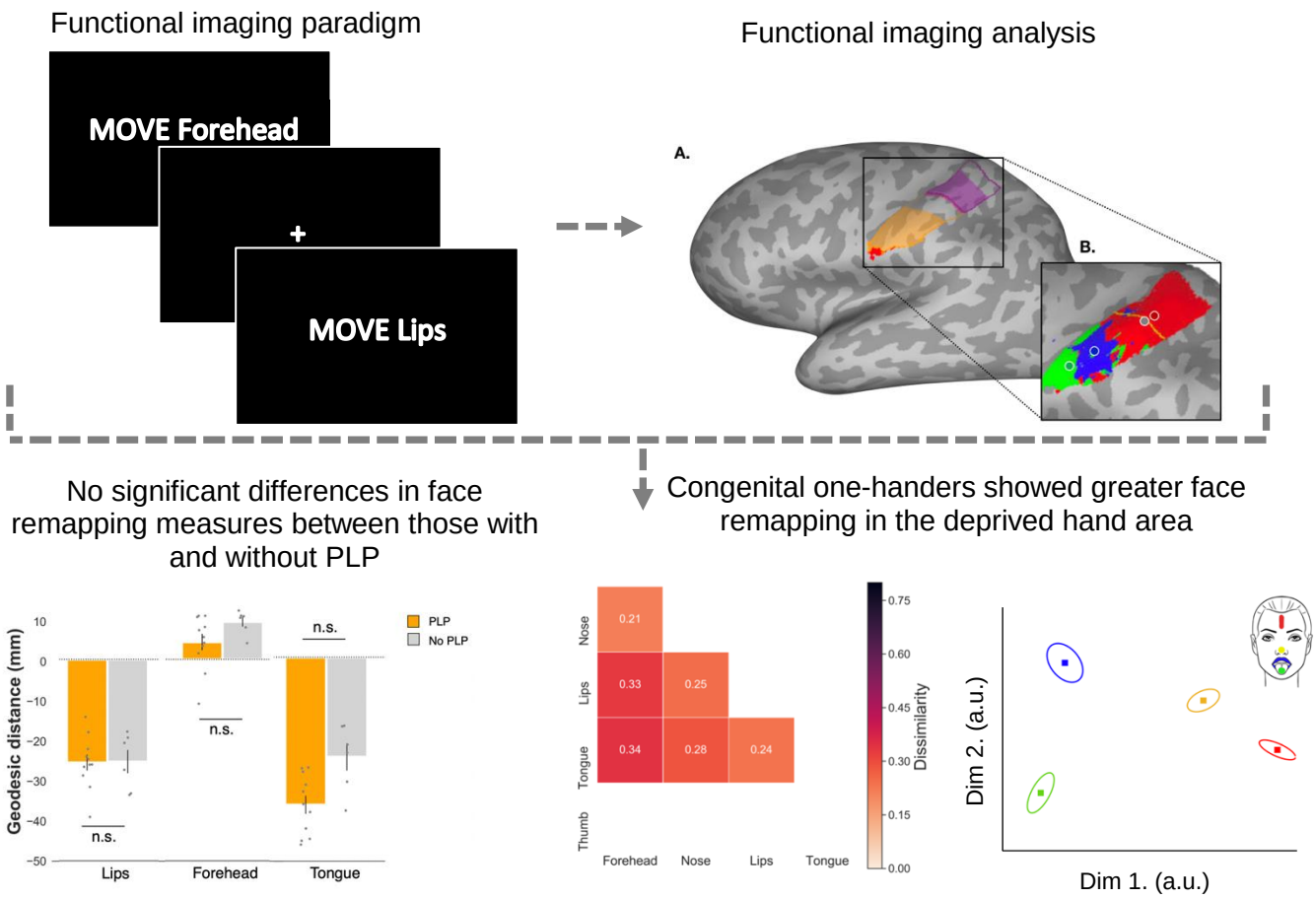


Figure 2.7. *Graphical summary of main findings and methodologies for Chapter 2.* Two-handed controls (*n* = 22), upper-limb acquired amputees (*n* = 17) and congenital one-handers (*n* =21) completed an active functional neuroimaging paradigm, moving their forehead, nose, lips, tongue and thumbs (intact and phantom). Univariate and multivariate analyses were then conducted in hand and face regions-of-interest. No significant differences were found between amputees with and without PLP for the calculated geodesic distances between each movements centre-of-gravity and a predefined cortical anchor, contrary to the maladaptive plasticity model. In contrast, extensive findings of cortical remapping were found for congenital one-handers across all movements, with significantly greater information content for the face in the deprived hand region of interest compared to the controls non-dominant hand area, suggesting that cortical remapping may extend beyond cortical neighbours in certain populations. Further research characterising mouth representations and inter-hemispheric imbalances in amputees is needed, however.

It is a well-accepted notion, rooted in non-human primate electrophysiological data, that upper limb amputation triggers cortical remapping of the assumed neighbour – the lower face – into the missing hand area. This previous work predominantly characterised remapping by investigating shifts of the lip representation (Birbaumer et al., 1997; Flor et al., 1995; Foell et al., 2014; Grüsser et al., 2001; Karl et al., 2001; Lotze et al., 2001; MacIver et al., 2008). However, by focusing on only one face part, activity elicited by other facial parts (such as the forehead) in areas of interest in S1 (i.e., the hand-face border) are not taken into account (see Muret & Makin, 2021). Here we explored the relationship of face-to-hand remapping in controls and one-handed groups, and used both univariate (topographic) and multivariate (representational structure) methods to investigate in detail the information content of the face in both the deprived and intact hand and face areas. We found little evidence for remapping of all tested facial parts in amputees, with no significant relationship to the presence of PLP. As a positive control, we also recruited individuals that were born without a hand (one-handers), who have previously shown cortical remapping across multiple body parts (Amoruso et al., 2021; Hahamy et al., 2017; Hahamy & Makin, 2019). Across all facial parts, one-handers showed evidence for a complex pattern of face remapping in the deprived hand area, with consistent and converging evidence across analysis approaches. Together, our findings demonstrate that the face representation in humans is highly plastic, but that this plasticity is restricted by the developmental stage of input deprivation, rather than cortical proximity, and is not likely to be related to PLP.

When looking at face-to-hand remapping in amputees, where the remapping of cortical neighbours has been the prevalent explanation for PLP, we find little

evidence of shifts of locality and remapping in the deprived hand area for facial parts, including the neighbour (forehead) and hypothesised neighbour (lips). Our univariate results are further supported by our multivariate analysis, where we find no significant changes in the relationship between face-to-thumb activity in the deprived hand area. These results support previous work reporting a lack of cortical remapping after amputation (Kikkert et al., 2018; Makin, Scholz, et al., 2013; Raffin, Mattout, et al., 2012), suggesting that in amputees this area might be functionally unipotent – pertaining to hand-related activity alone and lacking the ability to rescope after hand loss. Indeed, the idea of unipotency parallels previous work demonstrating the remapping of the intact hand only, not the lower face (Valyear et al., 2020), into the deprived hand area after upper limb loss, which was not associated with PLP (Bruurmijn et al., 2021; Makin, Cramer, et al., 2013; Raffin et al., 2016). This, and our current results, lends support to work suggesting that maladaptive plasticity is not likely to underlie the emergence of PLP, and that the hand and face representation are relatively stable after upper limb loss (Kikkert et al., 2016, 2018; Makin et al., 2015; Makin, Scholz, et al., 2013; Wesselink et al., 2019). It therefore highlights the need to consider and explore explanations of PLP outside of maladaptive mechanisms in S1 (see *Chapter 3* and *Chapter 4*), and in particular, a revision of treatments for PLP which are based on reversing such maladaptive plasticity, e.g., mirror-box therapy (Moseley & Flor, 2012).

However, due to the inconclusive Bayes Factor in our key analyses, we cannot strongly conclude that remapping does not occur in amputees. This could be attributed to our relatively small sample (further recruitment was prevented due to Covid-19 restrictions), and in particular, the small proportion of amputees

experiencing PLP (11 out of 17). However, pain is not a necessary condition for deprivation-triggered remapping (Andoh et al., 2020; Recanzone et al., 1992; Wang et al., 1995) and vice versa, PLP can be experienced in absence of remapping (De Nunzio et al., 2018). Moreover, previous studies reporting significant differences between amputees who experienced PLP and those who do not, often employed a similar sample size (Lotze et al., 2001), indicating that the expected effect of remapping should be substantial (if it exists). It should also be noted that our chosen measure of chronic PLP – dividing the worst PLP intensity in the *last week* by PLP frequency – may also provide a skewed assessment of PLP, as the intensity of the pain is only measured from the previous week. For example, individuals who may have recently experienced a 'flare up' of PLP intensity would report subsequently higher levels of chronic PLP, and vice versa. Although this is countered somewhat by dividing the PLP intensity by PLP frequency, and it has been successfully used in previous research (Draganski et al., 2006; Kikkert et al., 2016, 2017, 2018; Lyu et al., 2016; Makin et al., 2015; Makin, Scholz, et al., 2013), this criticism is worth noting. Future measurements of PLP, therefore, may want to consider estimating PLP intensity over a similar time period to the estimated PLP frequency, i.e., average PLP intensity from the previous year.

We did also find anecdotal evidence for remapping of the tongue within the deprived hand area in amputees. This was a surprising result, as the tongue is not a cortical neighbour to the hand, and was not specifically hypothesised to remap in amputees. We also found that amputees reported a different amount of facial information across the two hand areas. Although this multivariate result was not significantly different to that of controls in the deprived hemisphere, it demonstrates the

plausibility that cortical remapping in amputees may exist to a certain degree (e.g., an inter-hemisphere imbalance; see Bramati et al., 2019; Makin, Scholz, et al., 2013; Valyear et al., 2020), albeit any relationship to PLP is tenuous. While these latter results require further validation, they support our premise that cortical proximity of representations may not be a necessity for remapping to occur. In this context, as mentioned in *Chapter 1*, our tongue condition could also be classed as an 'inner mouth' movement, with the potentiality of both lateral and more medial 'hotspots' of the mouth and larynx (i.e., a 'double' representation; Eichert et al., 2020). The potential tongue remapping we found in amputees, therefore, may reflect changes in the medial mouth representation, but this would need to be investigated further by separating the relative contributions of the tongue and larynx.

Our findings, however, may seem contradictory to the many previous studies reporting lip remapping in amputees (Birbaumer et al., 1997; Flor et al., 1995; Foell et al., 2014; Grüsser et al., 2001; Karl et al., 2001; Lotze et al., 2001; MacIver et al., 2008). One possible explanation is that it has been claimed that active movements may produce different cortical maps to those with passive stimulation (Andoh et al., 2018; Flor et al., 2013; although see *Discussion, Chapter 1* and Berlot et al., 2019; Sanders et al., 2019), and previous work demonstrating a relationship between cortical remapping and PLP tended to use passive stimulation (Birbaumer et al., 1997; Flor et al., 1995; Foell et al., 2014; Karl et al., 2001). However, we do not think this methodological difference underlies our contrasting results as movement-induced lip activity has been shown to demonstrate lip remapping before (Lotze et al., 2001; MacIver et al., 2008; Striem-Amit et al., 2018), indicating that an active paradigm is suitable for

demonstrating cortical remapping (if it exists). Conversely, a recent study using passive lip stimulation in amputees also did not find any evidence for remapping (Philip et al., 2017). Furthermore, previous remapping studies predominantly focused on a single part of the face. We are one of the first studies (to our knowledge) to assess the mapping and potential remapping of multiple facial parts at once. By focusing on the lips only, previous designs excluded other facial parts which may have elicited greater activity in certain areas of S1, resulting in a less accurate delineation of the lip-selective representation. Such down-sampling of body maps, therefore, can lead to biased results and interpretation (Muret & Makin, 2021). While our design is not completely exempt from this limitation, the fact that we assessed other parts of the face may explain why our results diverged from previous findings.

We did find converging and conclusive evidence for cortical remapping of all facial parts (neighbours and non-neighbours) in our (congenital) one-hander group. Here the pattern of remapping is strikingly different to that of cortical neighbourhood theories. Specifically, the location of the cortical neighbour – the forehead – is shown to shift away from the deprived hand area, which is subsequently 'taken over' by the lips and the tongue. The increase of facial activity in the deprived hand area is in turn supported by our multivariate results, whereby significantly greater information content for the face was found in the deprived hand area for one-handers when compared to controls. One-handers' deprived hand area, therefore, seems to have increased discriminability between different facial movements. It is difficult to ascertain from our study the drivers of this remapping. It has been suggested previously that remapping within this group may be driven by

functionally-relevant behaviour substituting the loss of the limb (Amoruso et al., 2021; Hahamy et al., 2017). Alternative explanations relate to an overall and unspecific release of inhibition (i.e., decreased GABA) in the missing hand area, allowing for latent activity of other body parts to be detected (Hahamy et al., 2017). While speculative, our results tend to support the former, as we report remapping for facial parts which have the ability to compensate for hand function, e.g., using the lips and/or mouth to manipulate an object, and a lack of remapping for those that cannot (the forehead). This increased activity from body parts compensating for hand function may represent a stabilising mechanism, aimed at preserving the integrity of the sensorimotor network and its function (Muret & Makin, 2021). The deprived hand area in one-handers, therefore, may be deemed pluripotent – suitable for adapting to multiple body parts (Amoruso et al., 2021), which may preserve the role of the hand area by sustaining its hand-function related information content.

In summary, our use of both univariate and multivariate analyses found consistent evidence for a complex pattern of face remapping in congenital one-handers, in line with the theory suggesting remapping in this group reflects compensatory behaviour (Hahamy et al., 2017; Muret & Makin, 2021). This is in contrast to amputees, where we find little evidence for cortical remapping, indicating a relative stability of both the hand and face representation after upper limb loss, with no significant evidence of remapping measures associated with PLP. Our results therefore call for a reassessment of traditional remapping theories based on cortical proximity, and future research into potential alternative mechanisms of PLP, outside of maladaptive plasticity in S1.

Chapter 3 | How does sensorimotor engagement influence learning of novel nociceptive stimuli?

3.1 Introduction

Pain is not an isolated sensory phenomenon – it results from interactions with the world and promotes a range of protective behaviours and actions learnt from past experience to preserve bodily integrity (Tabor et al., 2017; Vlaeyen, 2015). Pain, in this light, can be viewed as a learning signal (Seymour, 2019), encouraging the formation of associations between external and internal stimuli to learn about recovery from injury and potential threat (Phelps et al., 2021). Once these associative memories are formed, they may generalise to perceptually or functionally similar events, allowing not only the prediction of future pain experience, but also having a direct influence on pain perception itself (e.g., if you are expecting pain within a certain context, you are more likely to report that a stimulus is painful; Franke et al., 2022; Vlaeyen, 2015).

Associative learning is therefore key in the development and maintenance of chronic pain. For example, individuals suffering from chronic pain have been found to over-generalise their predictions about pain to innocuous stimuli and events (Meulders et al., 2014). They have also reported reduced extinction rates (Flor et al., 2002; Sandström et al., 2020), indicating prolonged stubbornness of initially formed associations, as well as showcasing sub-optimal learning strategies e.g., greater precision on prediction errors (Brown et al., 2020), and impairments in threat and safety learning (Schlitt et al., 2021).

Associations between the sensory consequences of movements and actions are particularly important. For example, sustained practice of avoidance and safety behaviours has long been theorised to contribute to the formation of chronic pain (i.e., the fear-avoidance model; (Meulders et al., 2011; Vlaeyen, 2015; Vlaeyen et al., 2016; Vlaeyen & Linton, 2012). The resulting adapted motor repertoire may maintain a chronic state through impeding movement that may relieve pain, thus disallowing the creation of new associations between movement and innocuous outcomes (Barnes et al., 2021; Hodges & Smeets, 2015). The majority of research, however, addressing the formation of pain expectations use classical conditioning paradigms, whereby external visual stimuli (CS+) or simplified movements suited to experimental settings (e.g., a button press (Bräscher et al., 2016); joystick movement (Meulders et al., 2011); robotic manipulandum (Meulders et al., 2016)) are paired with a stationary painful response (US). In reality, pain is usually preceded by a naturalistic movement (e.g., bending down in chronic lower back pain patients), with proprioceptive and interoceptive cues more salient in the prediction of pain (Alaiti et al., 2020; Meulders et al., 2011, 2016).

Movement not only acts as a conditioned stimulus, but recent work has shown it can impact on the subsequent perception of pain itself. For example, several studies have highlighted that increased levels of perceived controllability of pain, usually associated with an action such as a button press, leads to reduced levels of pain (Becker et al., 2015; Salomons et al., 2007; Wiech, Edwards, et al., 2014; Wiech et al., 2006). It has also been reported that self-induced stimulation reduces perceived pain (Borhani et al., 2017; Bräscher et al., 2016; Lalouni et al., 2021), highlighting the importance of the motor efference copy and the execution of

movement itself (e.g., sensory attenuation; Seymour & Mancini, 2020). These aspects of movement and controllability are also key in the development of chronic pain. For example, uncontrollable and unpredictable pain (e.g., increased uncertainty) has been shown to have hyperalgesic effects (Meulders et al., 2011; Yoshida et al., 2013).

An extreme example of the loss of movement and controllability in chronic pain is from individuals who lose a limb later in life (hereafter amputees) and subsequently develop phantom limb pain (PLP). The majority of amputees retain some degree of voluntary motor control over the phantom limb (Kikkert et al., 2017; Raffin, Giraux, et al., 2012; Raffin, Mattout, et al., 2012), with preserved representation of the limb in the primary sensorimotor cortices (Kikkert et al., 2016, 2018; Makin, Scholz, et al., 2013; Wesselink et al., 2019) and motor commands at the periphery (Dhillon, 2005). The engagement of the phantom limb sensorimotor loop, including generation of motor predictions in relation to phantom actions, therefore likely persists after amputation. However, the sensory feedback from a phantom movement and the somatosensory landscape of the phantom itself is impoverished, interspersed with spontaneous fluctuations of PLP (Henderson & Smyth, 1948).

How does this severely affected motor repertoire of the phantom limb impact on the development and maintenance of PLP? As previously suggested, the formation of chronic pain may rest on associative learning between an action and the sensory outcome. Amputees cannot update or change their motor prediction due to the robustness (or ‘stubbornness’) of the central (and peripheral)

representation of the phantom limb. Nor can they gather new sensory information efficiently to confirm or form a new prediction due to the stochastic nature of the current sensory input and the absence of a physical limb. Their ability to learn and utilise sensory information, as well as to update and change predictions, is therefore likely impaired, and may result in a vulnerability to the development of chronic pain. Despite a wealth of neuroimaging research addressing the cortical origins of PLP (see Makin & Flor, 2020 for an overview), very little work has been done on how amputees with PLP learn about pain and the interaction of this with motor control over the phantom limb. One study has reported a significant positive relationship between the motor control of the phantom limb and PLP (Kikkert et al., 2017), yet the subsequent impact on associative learning is yet to be addressed.

We therefore designed a novel behavioural aversive learning paradigm in order to explore the relationship between the role of movement and associative learning in 28 healthy controls and a small sample of amputees with varying levels of chronic PLP. Here three cues were each associated with different probabilities of receiving heat pain (80%, 20% and 50% initial pain probabilities), with the high- and low-pain probability cue switching contingencies halfway through. In contrast to previous learning paradigms (Meulders et al., 2011, 2016), our cues were familiar everyday items which each afforded a different naturalistic grasp that participants were required to execute in order to receive the sensory outcome of the trial. Crucially, amputees were required to execute the grasps with their phantom limb. Control participants also completed a Passive condition of the task where the trials' sensory outcome was automatically delivered, without the need of

movement. This study design allowed us to answer our key predictions with a two-pronged approach: 1) within-group comparison of pain learning in healthy individuals both with and without movement, 2) how this pain learning may differ in amputees with chronic pain (anecdotally).

We hypothesise that movement inclusion in the experimental paradigm will promote an increased rate of learning, due to enhanced levels of attention, perceived controllability and contextual information of the stimuli. We predict that this may manifest in a generalised 'boosting' of expectancy effects, e.g., placebo and nocebo responses, when compared to the Passive condition. We further hypothesise that learning will be sub-optimal in amputees with chronic PLP, in line with previous work in other chronic pain patient groups (Brown et al., 2020; Schlitt et al., 2021). We predict that suboptimality of learning in amputees will be reflected in a slower rate of learning and biases towards expecting painful outcomes (e.g., a heightened nocebo response), reflected in over-generalisation of pain expectations to innocuous cues (e.g., a decreased placebo response). Furthermore, we predict that initial learning of cue associations within the amputee group will be more stubborn and cue-specific, with a reluctance to 'forget' the high-pain probability cue, and a quicker 're-learning' of the low-pain probability cue with a high-pain probability after the cue contingency switch. Note only anecdotal conclusions will be drawn for the amputee group due to the small sample size.

3.2 Methods

3.2.1 Participants

Twenty-eight two-handed controls (age, *M*=36.7, *SE*=2.85; women, *n*=16; left-handers, *n*=2) were recruited. Exclusion criteria included history of psychosis, the presence of a chronic pain condition or the current administration of medication known to influence, or treat, pain. Six additional controls who were recruited for the study did not participate in the task due to pain thresholding issues (*n*=3), lack of understanding of task instructions (*n*=2) and technical issues (*n*=1). Four individuals with acquired unilateral upper-limb amputation (age, *M*=41.0, *SE*=6.42; women, *n*=2; missing right hand, *n*=4) were also recruited (see *Table 3.1* for demographic details). One amputee who was recruited for the study did not participate in the aversive learning paradigm due to lack of understanding of task instructions. Procedures were in accordance with NHS National Research Ethics Service approval (18/LO/0474), and written informed consent was obtained.

ID	Age	Gender	Handedness (prior to amputation)	Affected limb	Level of limb deficiency	Years since amputation	PLS intensity	PLS frequency	Chronic PLS	PLP intensity	PLP frequency	Chronic PLP	Current medication
AA01	50	M	R	R	1	7	70	1	70	25	1	25	Gabapentin
AA02	31	F	R	R	1	13	80	1	80	20*	5	4	Pregabalin
AA03	54	M	R	R	1	27	30	2	15	40	3	13.33	None
AA04	29	F	R	R	2	2	70	5	14	90	1	90	None

Table 3.1. *Demographic details for amputees.* Level of limb deficiency is as follows: 1 = limb loss below elbow (transradial), 2 = limb loss at elbow; L = left, R = right; phantom limb sensations (PLS) and phantom limb pain (PLP) frequency: 1 = all the time, 2 = daily, 3 = once a week, 4 = several times a month, 5 = once or less a month. Chronic ratings of PLS and PLP were calculated by dividing the intensity of their worst PLP experience (or PLS vividness) during the last week (or in a typical week) by PLP/PLS frequency over the last year. Cause of amputation for all recruited amputees were due to trauma. *PLP intensity rating was on average.

3.2.2 Experimental procedures

After completing informed consent, controls and amputees were first introduced to the thermal stimuli during a familiarisation and thresholding session (see *Section 3.2.3*). They were then familiarised with the movements used within the aversive learning paradigm and the electromyographic (EMG) equipment used to record movement initiation and muscular activity (see *Section 3.2.4*). Participants then completed 96 trials of the Active (aversive learning with movements) and Passive (aversive learning without movements; controls only) learning paradigm (see *Section 3.2.5*). Order of presentation was determined by counterbalancing across participants. Our experimental design, therefore, contained the followed factors of Group (controls versus amputees) and Condition (active versus passive). Although, note our amputee group only completed an Active version of the task. Learning was quantified (see *Section 3.2.7*) using the following outcome measures: acquisition bias (see *Section 3.2.7.1*) – the degree of bias towards initial learning of the cues, placebo and nocebo responses (see *Section 3.2.7.2*) – the influence of expectation on perceptual ratings, response latency and muscular activity during movement preparation (see *Section 3.2.7.3*), and the model parameters (e.g., learning rate) following an application of a reinforcement learning model to participant trial-by-trial predictions (see *Section 3.2.8*). Questionnaires evaluating anxiety, pain catastrophising and depression (see *Section 3.2.6*) were completed after the aversive learning paradigm.

3.2.3 Pain familiarisation and thresholding

The experiment began with a temperature familiarisation and thresholding session. We used two in-house-developed thermal resistors (30°C rise in 0.8 seconds), each with two thermodes (15 x 20 mm), to deliver the thermal stimuli.

The device is internally self-calibrating to ensure the correct temperature is delivered, and has been used in several previous studies within our group (Brooks et al., 2005; Fairhurst et al., 2007; Leknes et al., 2008; Wise et al., 2002). The two thermodes were attached to the participant's non-dominant upper arm, or the upper portion of the residual limb for amputees (see *Figure 3.1.A*) using self-adhesive bandages. We then calibrated for each participant one painful and one warm temperature to be used in the main task. The painful temperature was thresholded to reflect a rating of '6' on the pain intensity scale (0=no pain at all; 10=worst pain imaginable; hereafter target pain rating), i.e., it was moderately painful. The warm temperature was thresholded to be perceptible, but not painful, for the participant. To achieve this, we first began with a temperature familiarisation session. The aim of the familiarisation session was to reduce task anxiety and to practice rating the thermal temperatures on the intensity scale for participants. During familiarisation, participants were sat in a relaxed position in front of the testing desk, with their hands placed in their laps. A warm temperature (~42°C) was initially administered and participants were told to rate verbally on the pain intensity scale how painful that temperature was (0=not painful at all; 10=worst pain imaginable). Participants were then informed that the temperature would increase linearly until their pain threshold was reached. Thermal stimulation lasted for 3 seconds (s), and temperatures were increased in step-sizes of ~1°C until participants neared the target pain rating of '6', which then reduced to ~0.5°C.

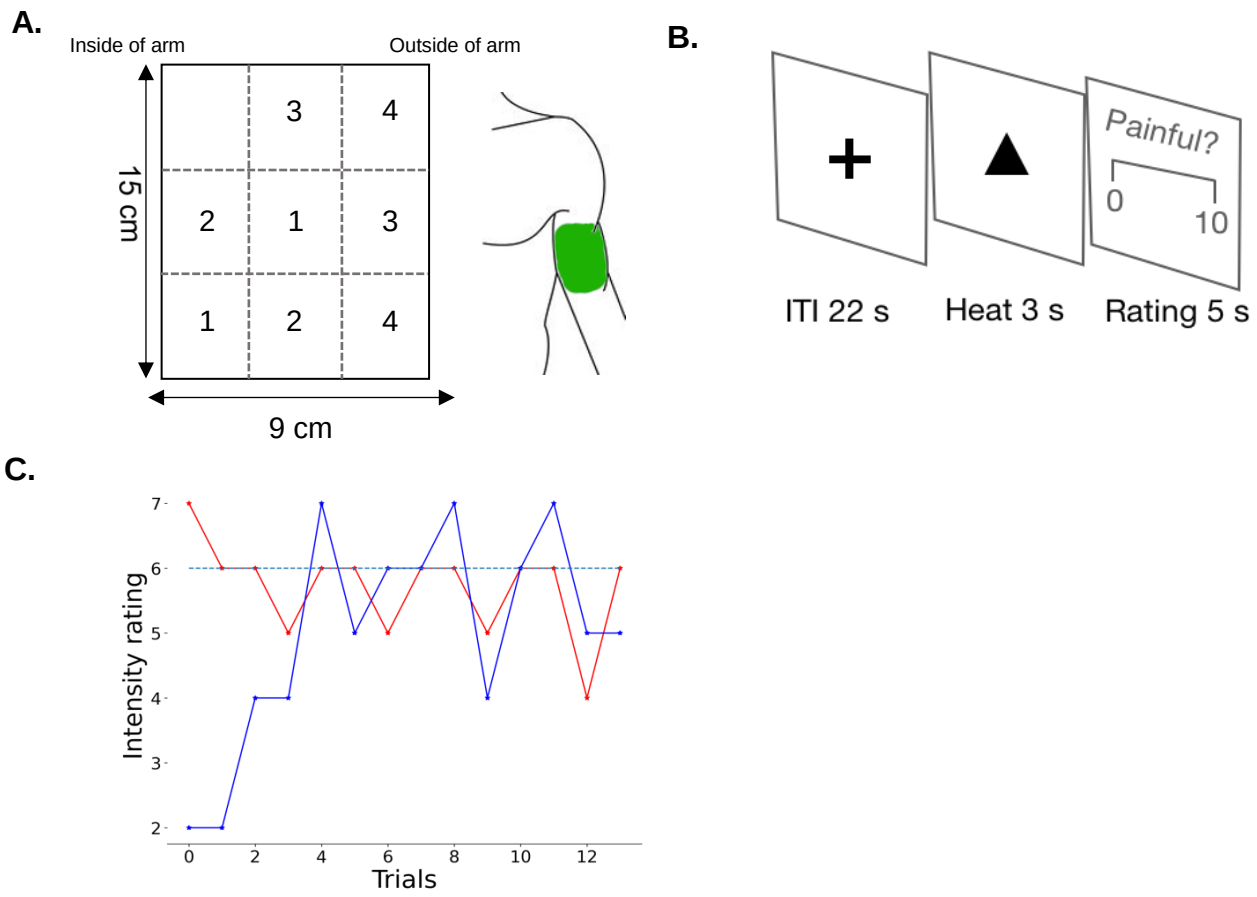


Figure 3.1. *Thermode stimulation sites and pain thresholding procedures.* **(A**) A diagram detailing placement of the thermodes on the upper arm (shaded green area). Sites (1) were used for familiarisation and thresholding; sites (1) and sites (2) were used for one condition of the aversive learning paradigm and sites (3) and (4) were used for the other condition (Active or Passive, dependent on counterbalancing). **(B)** Example of the pain thresholding paradigm presented to participants and trial timings. They were first shown a geometric shape during thermal stimulation followed by a verbal intensity rating and inter-trial-interval with a fixation cross. **(C)** Plotted intensity ratings from the pain thresholding procedure from an example control participant. The target pain rating of '6' is highlighted by the dashed line, with the ascending staircase in blue and the descending in red. Trials are along the *x*-axis and intensity ratings on the *y*-axis. As you can see both staircases reported intensities of '6' on multiple trials. An average of these trials was then used as the painful temperature in the main task.

Familiarisation runs continued until participants were rating one or two points above the target pain rating. This allowed the experimenter to estimate an acceptable thermal range of stimulation for each participant, and the likely temperature needed to achieve an intensity rating of '6'. There was a ~30 s inter-stimulus interval and thermal stimulation was alternated across two thermodes in order to minimise sensitisation/habituation. The familiarisation procedure was repeated 3 times, with a break of ~5 minutes between each familiarisation run.

We then used an interleaved staircasing procedure (Gracely et al., 1988), with one ascending and one descending staircase, to calibrate the temperature required for the target pain rating. The starting temperature for each staircase was calculated as the average maximum temperature, or the average temperature which was perceptible and mildly painful, across the three familiarisation runs for the descending and ascending staircase respectively. The thresholding task itself was presented on a computer screen, with each trial first showing a geometric shape during thermal stimulation, followed by text prompting for an intensity rating and a fixation cross (see *Figure 3.1.B-C*). Participants were required to make their rating verbally, which was in turn recorded via a key press by the experimenter. The staircase deployed three different step-sizes (2°C, 1°C and 0.5°C), dependent on the current rating. The closer the current intensity rating was to the target pain rating of '6', the smaller the step-size change (increase or decrease, dependent on staircase) in temperature. There were 28 trials in total, with 14 trials per staircase. Trial order was pseudo-randomised and the task took ~13 minutes to complete. To calculate the painful temperature used in the aversive learning paradigm, the temperature which was rated as the target pain rating of '6' across the ascending

and descending staircases' was chosen. If the participant had only reported the target pain rating in one of the staircases, or the temperatures across the two staircases did not agree, an average of the painful temperature was chosen across these trials. For 5 participants, the thresholding procedure was stopped as the staircases reached the maximum, ethically-allowed temperature of 57°C, which was subsequently used as the painful temperature. The warm temperature was defined as ~8.2°C (5.5°C – 10.5°C) below the painful temperature, so it was perceptible, but not painful (see *Table 3.3* for average temperatures). Note that as the chosen warm temperature was perceptible to participants, and reflected an increase in thermal sensation on the skin from baseline, the majority of participants rated the stimulus as ~1-2 on the intensity rating scale, despite the lack of painful sensation. Importantly, resulting warm and painful temperatures used in the aversive learning paradigm were significantly different from each other in both experimental conditions (Active: $t_{(27)}$=-32.7, p<.001, d=-6.18, BF_{10}=9.65e+19; Passive: $t_{(27)}$=-31.9, p<.001, d=-6.02, BF_{10}=4.96e+19). Once the thresholding task had been completed, the chosen pain and warm temperatures were administered to each stimulation site on the upper arm (see *Figure 3.1.A*) to check for site sensitisation differences. Here the chosen temperatures were tweaked by 0.5 – 1°C, if necessary, to obtain consistent perceptual intensity ratings across the arm.

3.2.4 Electromyographic recording

After pain thresholding and familiarisation, a 64-channel electrode array (52 mm x 20 mm; 4 mm inter-electrode distance (IED)) was placed on the forearm, over the belly of the flexor radialis muscle of the non-dominant arm with conductive paste.

For amputees, two 32-channel electrode arrays (80 mm x 40 mm; 10 mm IED) were placed at the end of the residual limb, dependent on areas of maximal muscle contraction when opening and closing the phantom hand. Consistent electrode placement based on anatomy across amputees is difficult to achieve due to idiosyncrasies of reinnervation. A reference electrode was attached to a wet leather band on the non-dominant wrist for controls, and a single electrode (36 mm x 40 mm) was placed on the olecranon (elbow) of the residual limb of the amputees.

Once the electromyographic (EMG) arrays had been placed, the signal was sampled at 2000 Hz, filtered (common-mean; high-low pass: 20 – 500 Hz; bandstop: 45 – 55 Hz) and transformed online using the root mean square (RMS). The maximum voluntary contraction (MVC) was calculated online by verbally instructing participants to clench their fist, or phantom hand, as hard as they could followed by short period of rest. This was repeated several times over ~20 seconds, and the maximal activity was recorded as the MVC (controls: M=0.176 mV, SD=0.090 mV; amputees: M=0.127 mV, SD=0.033 mV). For amputees, as two arrays were used to record muscular activity, the MVC was calculated by selecting a sub-sample of electrodes placed over the belly of the muscle which maximally contracted during closing of the phantom hand.

The experimenter then outlined three hand grasps (global hand, pinch, and two-fingered hook) necessary for the Active condition of the aversive learning paradigm. Here the three physical object cues (see below), each affording a different grasp, were placed in front of the participant on the testing desk (n=7 had

pictures of the objects only). The participants were then verbally guided to grasp each one in turn for ~60 s. During grasp execution, the experimenter emphasised that the control participants must not physically touch the object, but to complete the grasp ~5 cm away from the object/object's handle. This was to allow comparisons between controls and amputees, who cannot touch the objects with their phantom hand. A second experimenter also qualitatively monitored the range of EMG activity during grasp execution. Afterwards, an EMG threshold was calculated at ~10% of the participant's MVC (controls: *M*=0.014 mV, *SD*=0.004 mV; amputees: *M*=0.011 mV, *SD*=0.005 mV), which corresponded to activity levels recorded at grasp initiation during the practice.

3.2.5 Aversive learning paradigm

Participants were then outlined instructions for the aversive learning paradigm. The task itself was split into two conditions (within-subjects design), termed 'Active' and 'Passive' (see relevant sections below), which were counterbalanced across participants. Amputees participated in the Active condition only. For each condition, there were 96 trials in total split into two learning blocks of 48 trials each (see *Figure 3.2*), termed acquisition and reversal. Both conditions were presented to participants on a computer screen using PsychoPy v3.2.3. Four different stimulation sites were used on the upper arm for the thermal stimuli (see *Figure 3.1.A*). During the paradigm, a painful temperature was not delivered twice in a row on the same stimulation site, and the thermode positions were switched halfway through each condition to minimise sensitisation/habituation. Before beginning the task, six practice trials were administered to ensure participants understood, and that the chosen EMG threshold (Active only) was appropriate,

i.e., it triggered the resulting temperature successfully. As the practice trials were for task comprehension only, the sensory outcome of each trial was warm, not painful. Throughout the task, all participant ratings were made verbally and the experimenter recorded each rating via a key press.

3.2.5.1 Active condition

Active trials began with a fixation cross followed by a picture of one of three different everyday objects – a travel mug, an espresso cup, and a mug – that were also placed physically in front of participants (*n*=7 had pictures of the object only). Each object, or cue, was associated with a different probability of receiving a painful temperature during that trial. After initial cue presentation, participants were required to verbally rate the likelihood (0=no pain; 10=definitely expecting pain) that they would receive a painful temperature on this trial (hereafter expectancy rating). This allowed us to assess, trial-by-trial, whether participants could explicitly learn the pain probability associated with each cue.

During the acquisition block, the travel mug cue was associated with an 80% probability of receiving pain, and a 20% probability of receiving a warm temperature, i.e., a high-pain probability. This was switched in the reversal block to a low-pain probability – with a 20% probability of receiving pain and an 80% probability of receiving a warm temperature (see *Figure 3.2*). Hereafter this cue will be referred to as the H-L cue, reflecting that it changed from a high to a low pain probability from the acquisition to the reversal block. In contrast, the espresso cup was first associated with a low-pain probability (20% painful; 80% warm) in the acquisition block, which switched to a high-pain probability (80% painful; 20% warm) in the reversal block. This cue will therefore be referred to as L-H. In order

to control for floor/ceiling effects in participants' expectancy ratings, the mug cue had a 50% probability of receiving painful temperatures across the acquisition and reversal blocks, and will therefore be referred to as 50-50 hereafter. There were 16 cue repetitions per block, with cue order presentation pseudo-randomised throughout. As each cue's associated pain probability was not explicitly outlined to participants, the acquisition block allowed us to explore the initial extent of learning these pain probabilities. The reversal block subsequently allowed us to explore the extent of adaptation to the new cue-pain associations, as well as assessing the robustness of the initial learning.

After participants had made their expectancy rating, a green box appeared around the cue indicating to participants to initiate a hand grasp (with their non-dominant or phantom limb) towards the corresponding physical object in front of them. Each of the objects afforded a different grasp. For example, the travel mug (H-L cue) required a global hand grasp, the espresso cup (L-H cue) a pinch grasp, and the mug (50-50 cue) a two-fingered hook grasp. The execution of the object-specific hand grasp then triggered the resulting temperature (painful or warm) to the non-dominant/residual limbs' upper arm. The cue, therefore, was not only a visual cue but also an action cue, with the sensory outcome of the trial related to the specific action performed. Participants were then required to verbally rate the intensity of the thermal stimuli on a 0-10 scale (0=no pain at all; 10=worst pain imaginable).

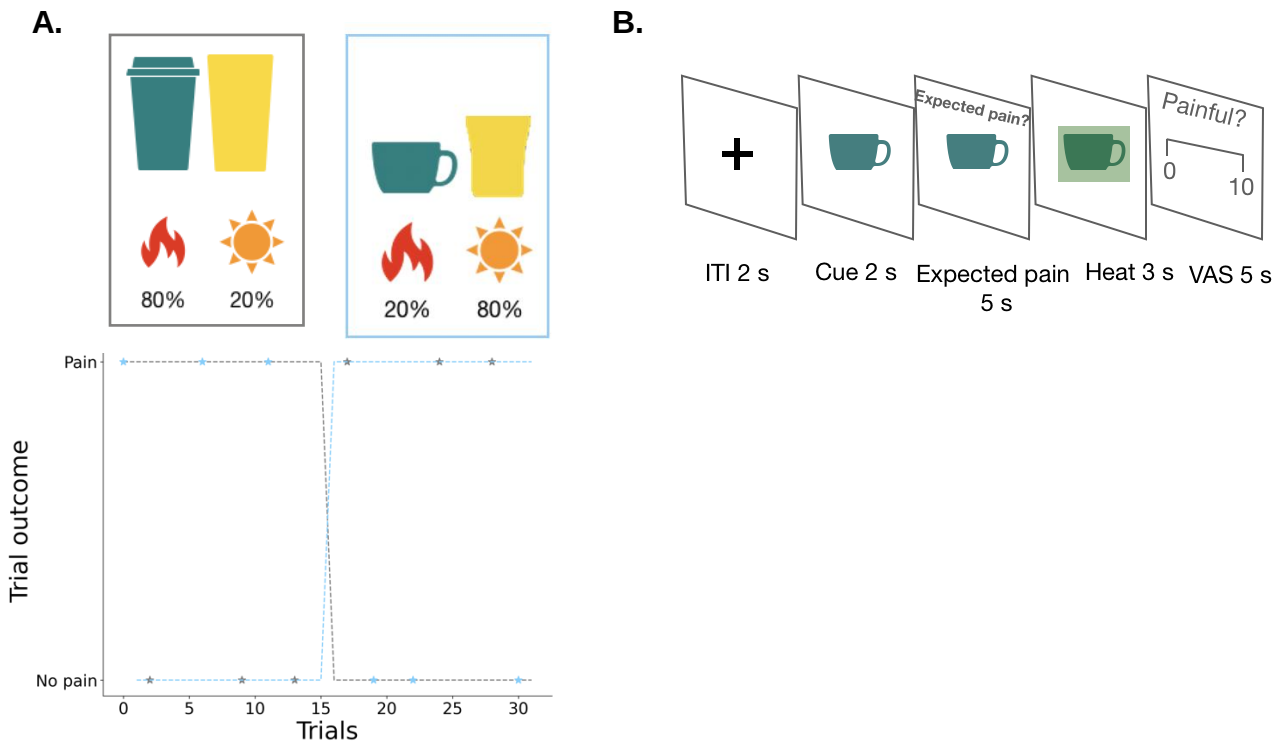


Figure 3.2. *Schematic outline of aversive learning paradigm.* **(A)** Pictorial diagram of the H-L (grey outline) and L-H (light blue outline) cues, with the associated pain probabilities for the Active (teal) and Passive (gold) conditions. The fire symbol reflects the associated probability of painful temperatures, and the sun symbol reflects the associated probability of warm temperatures. **(B)** Schematic outline of the aversive learning paradigm presented to participants on the computer screen, with associated trial timings. Participants were first presented with a picture of the object, followed by an expectancy rating (0=no pain; 10=definitely expecting pain). A 'Go' cue then appeared in the Active condition (green box around the object), which disappeared when the participant started moving. The thermal temperature was then administered to the non-dominant/residual arm (or was automatically delivered after the expectancy rating in the Passive condition), followed by a verbal intensity rating (0=no pain at all; 10=worst pain imaginable). **(C)** A diagram of the H-L (grey) and L-H (light blue) sequence presented in the aversive learning paradigm. Note the H-L cue switches to a low-pain probability halfway through, i.e., after 16 cue repetitions. Conversely, the L-H cue switches to a high-pain probability at the halfway point. 'Surprise' trials (see *Learning measures*) are denoted by a star, and trial outcome (pain/no pain) is on the *y*-axis and trial number on the *x*-axis. See *Supplementary Figure 6* for surprise trials in the unmatched Passive sequence.

3.2.5.2 Passive condition

Participants also completed a variation of the above learning paradigm, termed the 'Passive' condition. Here participants were explicitly instructed not to move during the task. Instead, the thermal stimuli were automatically administered to the participant's upper arm after the expectancy rating had been made. As in the Active condition, there were three object cues each associated with a different pain probability – H-L, L-H and 50-50. Again, the H-L cue switched from a high- to low-pain probability from the acquisition to the reversal block, and vice versa for L-H. However, different objects were presented in order to prevent learning transfer between conditions, yet they were still everyday objects that afforded different hand grasps – a pint glass (H-L), a shot glass (L-H), and a wine glass (50-50). The order of cue presentation was also pseudo-randomised and different to that of the Active condition (although see *Learning measures* for surprise trial matching.).

3.2.6 Questionnaires

We initially aimed to use these questionnaires in order to control for potential group differences between controls and amputees. However, as Covid-19 restrictions hindered and stalled recruitment of our patient sample (amputees), we subsequently assessed whether aversive learning was related to depression, anxiety and pain catastrophising. Three questionnaires were administered to participants after the main experimental paradigm, consisting of: Beck's Depression Inventory (BDI; Beck et al., 1961), Trait Anxiety (Spielberger, 1983) and the Pain Catastrophising Scale (PCS; Sullivan et al., 1995).

3.2.7 Learning measures

Two main learning measures were quantified from participants' expectancy and intensity ratings – acquisition biases and placebo/nocebo responses (see below). In order to quantify these measures, we delineated between two types of trials for the H-L and L-H cues, which we termed expected and surprise trials (see *Figure 3.2*). For example, an expected trial for the H-L cue would be a painful temperature in the acquisition block, and a warm temperature in the reversal block. As there were 16 cue repetitions per block, 13 of these would be classified as expected trials, reflecting the associated probabilities.

In contrast, surprise trials corresponded to the trials that were unexpected. For example, for the H-L cue this would be the 3 warm trials in the acquisition block, and the 3 painful trials in the reversal block. Note that when considering intensity ratings, surprise trials were the same trial on which the unexpected temperature occurred. For expectancy ratings, as these were made prior to the administration of the thermal stimulus, surprise trials were classified as the trial immediately following the unexpected temperature. The placement of the surprise trials within the H-L and L-H sequence were the same across Active and Passive conditions. However, for eleven participants, the surprise trials in the Passive condition occurred at different points in the cues' sequence (see *Supplementary Figure 6*). The type of passive sequence administered (matched x unmatched surprise trials) was therefore included as a covariate in analyses when directly comparing Active and Passive learning (see *Statistical analysis*).

3.2.7.1 Acquisition bias

Our first measure aimed to assess the stubbornness of the learning in the acquisition block of the H-L and L-H cues, as reflected in participants' expectancy ratings (excluding surprise trials). We specifically looked at how this initial learning influenced expectancy ratings once each cue's associated pain probability had changed in the reversal block. As the H-L and L-H cues began with a high- and low-pain probability respectively, this allowed us to quantify two types of bias; that towards a high-pain probability or towards a low-pain probability.

To calculate the bias towards high-pain we took the average expectancy ratings of the H-L cue in the reversal block and subtracted the ratings of L-H cue in the acquisition block ($\overline{H-L}_{\text{Reversal}} - \overline{L-H}_{\text{Acquisition}}$). Here both cues were matched in their associated low-pain probabilities. Crucially, however, H-L$_{\text{Reversal}}$ was originally associated with a high-pain probability, therefore a resulting positive value indicates an increase in the expectancy rating scale towards expecting pain. In contrast the low-pain bias was calculated as follows – $\overline{L-H}_{\text{Reversal}} - \overline{H-L}_{\text{Acquisition}}$ – whereby the cues are matched in their associated high-pain probabilities, with the L-H$_{\text{Reversal}}$ originally associated with a low-pain probability. Here a resulting negative value indicates a decrease in the expectancy rating scale towards expecting no pain. Values of 0 for both high- and low-pain acquisition biases therefore reflect no influence of initial learning in the reversal block.

3.2.7.2 Placebo and nocebo responses

Our second measure assessed learning by exploring the influence that cue expectations had on intensity ratings. For example, it is widely accepted that when

an individual is expecting an innocuous stimulus a subsequent painful stimulus is perceived as less painful, i.e., placebo responses. In turn, the opposite has also been found, where a subsequent innocuous stimulus is perceived as more painful when an individual is expecting pain, i.e., nocebo responses (Tracey, 2010). As our paradigm encouraged the formation of either a painful (high-pain probability trials) or innocuous (low-pain probability trials) stimulus expectation, we can quantify the extent of the placebo and nocebo response from the intensity ratings of the painful and warm surprise trials, respectively. To calculate this, we did the following for each participant: $\overline{S_{P,b}} - \overline{E_{P,b}}$, where *S*= average intensity ratings of the surprise trials, *E*= average intensity ratings of the expected trials, P=sensory outcome of trial (painful or warm temperature), and *b*=block (acquisition or reversal). If $S_{P,b}$ are painful surprise trials (associated with a low-pain probability cue), then $E_{P,b}$ would be painful expected trials, and vice versa. A subsequent positive value indicates the extent of the nocebo response, reflecting an increase of perceived intensity for the unexpected thermal stimulus. A negative value indicates the extent of the placebo response, reflecting a decrease in intensity ratings. A value of 0, however, reflects no change on the intensity scale, indicating no difference in intensity between expected and surprise trials.

3.2.7.2 Response latency and EMG preparatory activity

In the Active condition, we were able to record from a sub-sample of control participants (*n*=14), EMG activity of the non-dominant forearm from the initial presentation of the object cue to the end of each trial, i.e., after the participant had made their intensity rating (~15000 ms; see *Figure 3.2.B*). This allowed the calculation of response latencies between the presentation of the ‘Go’ cue and the

execution of the object-specific movement (i.e., when the previously defined EMG threshold is reached; see *Electromyographic recording* above). Using this detailed EMG data, we were also able to quantify any modulation in muscle activity 1 second (s) prior to the 'Go' cues presentation. To quantify this preparatory activity, the EMG signal (*fs*=2000 Hz) was band-pass (20 – 500 Hz) and bandstop (49 – 51 Hz) filtered to exclude sampling noise and mains interference. It was then rectified with a low-pass filter of 6 Hz to extract the EMG envelope (Hermens et al., 1999). An average of the signal was then taken across all sampling channels to reflect average muscle activity 1 s prior to the 'Go' cue. Previous research has demonstrated that when a CS+ is displayed, movements are slower in execution (Meulders et al., 2011), and muscle activity increases in the limb of the receiving, painful temperature (Diesch & Flor, 2007; Zhang et al., 2016). Thus, by tracking response latencies and EMG amplitudes across the paradigm, it may provide an objective measure of learning, with responses to high-pain probability cues increasing in latency and preparatory amplitude as the expectation is learnt.

3.2.8 Behavioural data modelling

To assess differences in learning between Active and Passive conditions and across groups, we also fit computational learning models (Rescorla-Wagner and Pearce-Hall hybrid) to participant's trial-by-trial expectancy ratings. As our above learning measures are based on cue and block averages, modelling allows us to use a more sensitive measure of learning.

3.2.8.1 Model descriptions

We initially fit a basic Rescorla-Wagner model (*Equations 1-2*) with a constant learning rate (*a*) as our baseline model. Here, the model's predicted value (*V*) updated on a given trial (*t*) based on the preceding trial's prediction error (δ). A trials' prediction error reflects the difference between the actual sensory outcome (*R*), i.e., whether the trial was painful (0=warm; 1=painful), and the expected outcome (*V*). Learning within this model is error-driven, and characterised by the presented pain sequence only, regardless of the cue shown.

$$V_{t+1} = V_t + a \cdot \delta_t \quad (1)$$

$$\delta_t = R_t - V_t \quad (2)$$

We next fitted another Rescorla-Wagner model which updated the predicted model's value (*V*) on a given trial, dependent on the cue shown (x_t) and the preceding trial's prediction error (*Equations 3-4*). The value for the cues not observed on trial, *t*, remained unchanged.

$$V_{t+1}(x_t) = V_t(x_t) + a \cdot \delta_t(x_t) \quad (3)$$

$$\delta_t(x_t) = R_t - V_t(x_t) \quad (4)$$

For both Rescorla-Wagner models, initial value (V_0) was set at 0.5 and one free parameter, *a* ($0 \leq a \leq 1$), the learning rate, was fitted.

We also fitted a hybrid Rescorla-Wagner and Pearce-Hall model (*Equations 5-6*), as they have been extensively used before in reversal paradigms (Atlas et al., 2016; Boll et al., 2013; Li et al., 2011; Taylor et al., 2017; Zhang et al., 2016). Whereas the Rescorla-Wagner model treats the learning rate value update as constant, the hybrid model substitutes this with an associability term (*a*), which dynamically updates the learning rate based on the preceding trial's prediction

error, weighted by a constant term (η). Here if preceding trials are less reliable, i.e., the prediction error is large, then associability increases. The associability term, therefore, can be viewed as an uncertainty signal. Learning within the hybrid model is therefore driven by error (Rescorla-Wagner) and uncertainty (Pearce-Hall associability).

$$V_{t+1}(x_t) = V_t(x_t) + K \cdot a_t(x_t) \cdot \delta_t(x_t) \quad (5)$$

$$a_{t+1}(x_t) = \eta|\delta_t(x_t)| + (1 - \eta) \cdot a_t(x_t) \quad (6)$$

The initial value (V_0) was set to 0.5 and the initial associability (a_0) was set to 1.0, as we believed learning to be maximal at the start of the paradigm (Zhang et al., 2016, 2018), with free parameters including K ($0 \leq K \leq 1$) and η ($0 \leq \eta \leq 1$).

3.2.8.2 Model fitting

Model fitting was carried out on the single-subject level, with model predicted values fitted to actual trial-by-trial expectancy ratings. The model fitting procedure minimised participant's negative log likelihood for each model, based on residuals from a linear regression (*Equation 7*) that predicted participant's ratings using model predictors (p_t):

$$y_t \sim \beta_0 + \beta_1 \cdot p_t(M_i, \theta_i) + \varepsilon \quad (7)$$

where y_t are participant rated expectancies, M_i is the ith candidate model and β_0, β_1 and θ_i are free parameters to be fitted, and ε is normally distributed noise added to avoid fitting errors (Maheu et al., 2019; Mancini et al., 2021).

To estimate the model free parameters from the data, the Bayesian information criterion (BIC) value was calculated as:

$$BIC = n \cdot \log\hat{\sigma}_{\varepsilon}^2 + k \cdot \log n \quad (7)$$

$$\hat{\sigma}_{\varepsilon}^{2} = \min \frac{1}{n}\sum_{t-1}^{n}(y_t - \hat{y}_t) \quad (8)$$

where $\hat{\sigma}^2$ is the mean squared residual from the linear regression relating participant's expectancy ratings to model predicted values, and *k* is the number of free parameters fitted. *Fmincon* in MATLAB was used to minimise the BIC for each participant and model. The procedure was repeated 100 times with different parameter initialisation. The mean of the 100 repetitions was taken as the fitted parameter and minimised log likelihoods (see *Table 3.2* for means and standard deviations of fitted parameters).

Model	Parameter	Mean (*SD*)	Initial states	Log likelihood
		Active		
(1) Pain	Learning rate, *a*	0.638 (0.967)	V_0=0.5	292.151 (3.359)
(2) Cue	Learning rate, *a*	0.316 (0.821)	V_0=0.5	339.394 (15.626)
(3) Associability	Free parameter, K	0.522 (0.888)	V_0=0.5, *a*=1	341.100 (10.956)
	Free parameter, η	0.432 (0.918)		
		Passive		
(1) Pain	Learning rate, *a*	0.483 (0.980)	V_0=0.5	285.381 (2.639)
(2) Cue	Learning rate, *a*	0.411 (0.595)	V_0=0.5	325.762 (12.809)
(3) Associability	Free parameter, K	0.605 (0.917)	V_0=0.5, *a*=1	326.140 (11.214)
	Free parameter, η	0.373 (0.939)		

Table 3.2. *Model fitting parameters means and standard deviations.* Average and standard deviation of fitted parameter(s) calculated for each model across control participants (*n*=28): (1) Rescorla-Wagner; Pain sequence (baseline), (2) Rescorla-Wagner; Cue sequence, (3) Pearce-Hall Hybrid. Standard deviations are reported in brackets for fitted parameters and log likelihoods.

3.2.8.4 Model comparison

We next conducted a random effects model comparison with the VBA toolbox (Daunizeau et al., 2014). Fitted log likelihoods for each participant/model pair was treated as model evidence, and models were allowed to vary between subjects

(random effects) based on an unknown population distribution. This approach generates the following comparison statistics: model frequency (how often is a given model used by participants), model exceedance probability (how likely it is that any given model is more frequent than all the other models in the comparison set), and protected exceedance probability (corrected exceedance probability for observations due to chance; Rigoux et al., 2014; Stephan et al., 2009). All three values were considered together when selecting the 'winning' model.

3.2.9 Statistical analyses

All statistical analyses were carried out using jamovi (v1.6.23.0). Outliers were classified as +/- 3 standard deviations above the mean. Assessment of normality was carried out by inspection of Q-Q plots and Shapiro-Wilk tests. Where normality assumptions are violated, non-parametric test statistics are reported. Repeated Measures Analysis of Variance (ANOVA) was used to explore learning differences between Conditions (Active x Passive) and Block (Acquisition x Reversal). An additional repeated measures factor of either Cue (H-L x L-H), Acquisition Bias (High-pain x Low-pain) or Response (Nocebo x Placebo) was added, dependent on analysis. A between-groups covariate was also added to control for type of passive sequence administered (matched x unmatched surprise trials). Planned comparisons were conducted if significant interactions with Condition were reported in order to clarify the directionality of the results. Subsequent correlations were used to assess the relationship within each learning measure (e.g., high and low-pain acquisition biases, and placebo and nocebo responses), with 95% confidence intervals reported to allow qualitative comparisons between Active and Passive correlations, and to assess the

relationship to questionnaire measures (depression, anxiety and pain catastrophising). Note that as the 50-50 cue was used to control for floor/ceiling effects and did not generate directional expectations for pain, we analysed its' expectancy and intensity ratings separately. Paired Sample *t*-tests were also used to explore differences between Active and Passive conditions in learning rates fitted by the 'winning' computational model.

Furthermore, a 2 x 2 Repeated Measures ANOVA, including within-subject factors of Block (Acquisition x Reversal) and Cue (H-L x L-H), was conducted to assess learning differences for response latencies and preparatory activity for each cue across the paradigm in the Active condition for a sub-sample of participants (n=14; see *Response latencies and preparatory activity* above). As no significant main effects or interactions were found for both response latencies and preparatory activity (see *Supplementary Figures 7-8*) the results from these analyses will not be discussed further in this study, and all main analyses will focus on the learning measures cited above.

We also reported the corresponding Bayes Factor (BF_{10}), defined as the relative support for the alternative hypothesis, for all reported results (excluding planned and post-hoc comparisons which were conducted on estimated marginal means whilst controlling for the passive sequence covariate). Note that Bayes Factors reported for interactions reflect the model as a whole (main effects and interactions). Subsequent Bayes Inclusion Factors were reported for main effects and interactions individually, which quantify how much the observed data are more probable under models that include the predictor relative to models that do

not. We used the threshold of $BF < 1/3$ as positive evidence in support of the null, consistent with others in the field (Dienes, 2014; Wetzels et al., 2011; though see Kass & Raftery, 1995), and the Cauchy prior width was set as 0.707 (jamovi's default).

3.3 Results

3.3.1 Participants were able to successfully learn pain contingencies with and without movements

We first carried out a few sanity checks to ensure that participants were able to learn successfully within our experimental paradigm. Firstly, we confirmed that there were no differences between the Active and Passive conditions in the thresholded temperatures for warm ($t_{(27)}$=-0.724, p=0.475, d=-0.137, BF_{10}=0.255) and painful trials ($t_{(27)}$=-1.426, p=0.165, d=-0.269, BF_{10}=0.497; see *Table 3.3* for averages), therefore any resulting differences in expectancy and intensity ratings between conditions are not likely to be due to differences in the actual temperature of the stimuli.

	Warm	**Pain**
Active	45.1°C (.07°C)	53.3°C (.08°C)
Passive	45.2°C (.07°C)	53.4°C (.08°C)
AA01	48.5°C	54.5°C
AA02	50°C	57°C
AA04	46.5°C	51°C

Table 3.3. *Temperatures used for warm and painful trials for controls and amputees.* Standard error of the mean in brackets for control participants. Note AA04 reported the highest levels of PLP within this sample, followed by AA01 and then AA02, with the lowest level of PLP.

We next assessed the extent of learning with a Repeated Measures ANOVA, including within-subjects factors of Condition (Active x Passive), Cue (H-L x L-H)

and Block (Acquisition x Reversal), on expectancy and intensity ratings (excluding surprise trials) for control participants. Here we predicted that learning would be evidenced by a difference in expectancy ratings for each cue and block, as exemplified in a Cue x Block interaction e.g., higher expectancy ratings in acquisition block for the H-L cue which lower in the reversal block (and vice versa for the L-H cue). We would also expect to see a similar trend in intensity ratings, with the average ratings following the change in pain probabilities across the experimental paradigm. Furthermore, we predicted that the extent of learning (e.g., expectancy rating change across cues and blocks) would be increased in the Active condition, due to the influence of increased controllability and attention within this condition. We further predicted that the perceived intensity of trials in the Active condition would be less painful than Passive, reflected in a main effect of Condition. If the beneficial effects of the Active condition are specific to a certain learning phase, this would be reflected in a three-way interaction of Condition x Cue x Block. We first found no evidence of overall learning differences between conditions, however, with a non-significant three-way interaction (Condition x Cue x Block) for expectancy and intensity ratings (expectancy: $F_{(1,26)}$=2.30349, p=0.141, η^2_p=0.081, BF_{10}=1.27$_{e+30}$, $BF_{Inclusion}$=0.367; intensity: $F_{(1,26)}$=1.704, p=0.203, η^2_p=0.061, BF_{10}=9.38$_{e+86}$, $BF_{Inclusion}$=0.249; controlling for passive sequence type; see *Supplementary Tables 10-11* for all main effects and interactions). Thus, the overall extent of learning did not change with or without movement inclusion, nor did movement foster a specific reduction in intensity ratings for a cue or learning phase.

We did, however, report a significant Cue x Block interaction for expectancy ($F_{(1,26)}$=45.96193, p<.001, η^2_p=0.639, BF_{10}=4.25$_{e+32}$, $BF_{Inclusion}$=5.52$_{e+31}$) and intensity ($F_{(1,26)}$=245.975, p<.001, η^2_p=0.904, BF_{10}=1.03$_{e+89}$, $BF_{Inclusion}$=5.02$_{e+90}$) ratings, reflecting evidence of substantial learning across both conditions (Active and Passive). Confirmatory comparisons, as shown in *Figure 3.3*, indicated predicted learning trends, with expectancy ratings for the H-L cue in the acquisition block significantly decreasing in the reversal block ($t_{(26)}$=6.979, p<.001). A similar pattern was shown in the reported intensity ratings ($t_{(26)}$=18.36, p<.001), demonstrating that participants were able to correctly follow the change in pain probabilities for the H-L cue across the paradigm. In contrast, expectancy ($t_{(26)}$=-9.287, p<.001) and intensity ($t_{(26)}$=-21.74, p<.001) ratings for the L-H cue significantly increased in the reversal block. Importantly, we can also trace a similar (qualitative) pattern of learning in our amputee sample, with all three individuals demonstrating successful learning of the cues in the acquisition block and adaptation to each cues' pain probability switch in the reversal block, in both their expectancy and intensity ratings.

When assessing our prediction of a generalised reduction in intensity ratings in the Active condition, we did, however, find that thermal stimuli were generally perceived as significantly less intense in the Passive (M=3.72, SE=0.145) not Active (M=3.83, SE=0.155) condition, reflected in a main effect of Condition ($F_{(1,26)}$=12.098, p=0.002, η^2_p=0.318, BF_{10}=0.176, $BF_{Inclusion}$=0.546). However, as our Bayes Factor (including Bayes Inclusion factor) indicated anecdotal support for the null, and the main effect interacted significantly with our passive sequence covariate ($F_{(1,26)}$=11.234, p=0.002, η^2_p=0.302), exploratory post-hoc comparisons

were warranted (corrected alpha=.016; uncorrected *p*-values in text). Here we found that the overall difference in intensity ratings between Conditions were not significantly different regardless of passive sequence type ($t_{(26)}$=1.01, p=0.323), i.e., when considering passive sequences on average, or when the passive sequences' surprise trials were unmatched ($t_{(26)}$=-1.504, p=0.145). However, we do see significantly less intense ratings overall in the Passive condition compared to Active, when the surprise trials were matched in occurrence across conditions ($t_{(26)}$=3.478, p=0.002), validating our inclusion as passive sequence type as a covariate for between condition comparisons.

As our 50-50 cue was included as a learning control, we analysed its expectancy and intensity ratings separately. Intriguingly we found an increase in expectancy ratings for the 50-50 cue in the reversal block in the Active ($t_{(27)}$=-4.48, p<.001, d=-0.847, BF_{10}=219.95) and Passive ($t_{(27)}$=-2.79, p=0.010, d=-0.527, BF_{10}=4.76) conditions. This is also reflected in a small but significant increase of perceived intensity for the 50-50 cue in the reversal block in the Active condition ($t_{(27)}$=-2.2184, p=0.035, d=-0.4192, BF_{10}=1.629). Thus, not only were participants expecting a higher likelihood of painful trials for the 50-50 cue in the reversal block, but they were also perceiving them as more painful as well. This may reflect a general sensitisation effect (although see *Supplementary Figure 9* for pilot data assessing sensitisation/habituation effects within this paradigm). Alternatively, we noted an increased number of consecutively painful trials for the 50-50 cue in the reversal block, (see *Supplementary Figure 10*), which may have also increased the expectancy and intensity ratings. Overall, however, participants and amputees were able to learn, and correctly perceive, both the H-L and L-H cues, as well as

're-learning' the switched pain probabilities in the reversal block, with no noticeable differences so far between Active and Passive conditions.

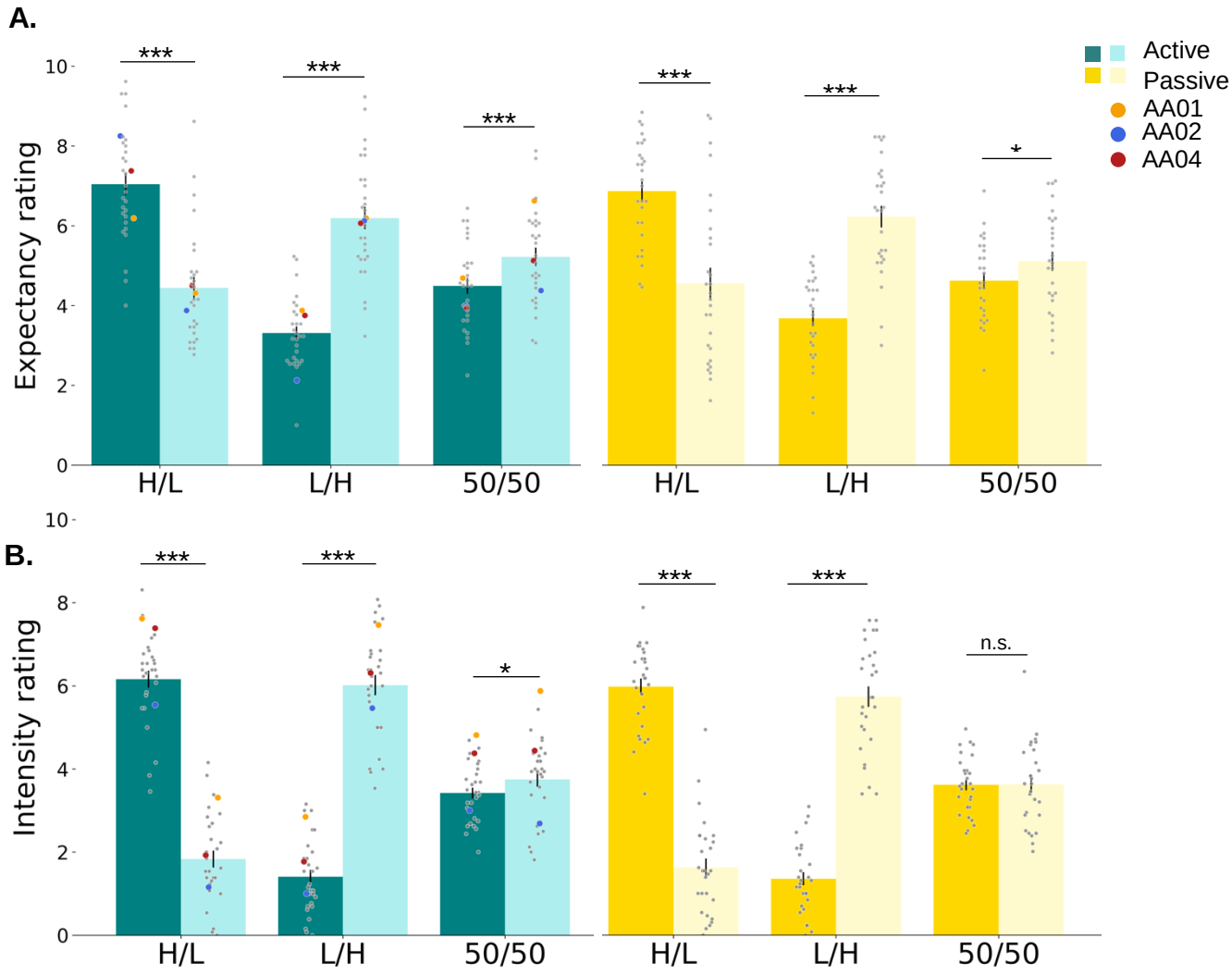


Figure 3.3. *Average expectancy and intensity ratings per cue and block.* Average expectancy **(A)** and intensity **(B)** ratings (*y*-axis) for the H-L, L-H and 50-50 cue (*x*-axis) in the acquisition (darker colours) and reversal (lighter colours) blocks for the Active (teal) and Passive (gold) conditions. We see for the H-L and L-H cue significant expected learning trends across blocks. Standard error of the mean is plotted, along with individual data points in grey. Note the amputees are plotted in three colours – orange (AA01), blue (AA02) and red (AA04) – with each colour relating to their PLP level. *** p<.001; * p<.05; n.s.=non-significant.

3.3.2 Participants demonstrate a generalised bias towards their initial learning

We next wanted to assess the extent that the initial learning of the H-L and L-H cues had on adapting to the pain probability switch in the reversal block. Here we predicted that if learning is enhanced in the Active condition, we would see a generalised reduction in the calculated acquisition biases for both high and low-pain probabilities, reflecting quicker adaptation to the new pain probabilities. We further predicted that amputees would demonstrate an increased sensitivity to expecting painful outcomes across the paradigm. This would be demonstrated in a larger high-pain acquisition bias, reflecting a reluctance to forget a cue associated with a high-pain probability, and a smaller low-pain acquisition bias, indicating quicker adaptation to the high-pain probability in the reversal block.

We first found that the initial learning of the H-L and L-H cue significantly 'carried-over' into the reversal block (see *Figure 3.4.A*) in both conditions. Here control participants displayed a high-pain acquisition bias significantly greater than zero in Active ($t_{(27)}$=4.02, p<.001, d=0.760, BF_{10}=73.09) and Passive ($t_{(27)}$=2.23, p=0.034, d=0.422, BF_{10}=1.67) conditions. We also found that the low-pain acquisition bias was also significantly lower than zero in both Active ($t_{(27)}$=-3.21, p=.003, d=-0.606, BF_{10}=11.50) and Passive ($t_{(27)}$=-2.39, p=0.024, d=-0.451, BF_{10}=2.20) conditions. Amputees also reported acquisition biases anecdotally different from zero for both high and low-pain (although see AA01 for the low-pain acquisition bias and *Discussion*), with no particular exaggeration for the high-pain (and reduction for low-pain biases), as predicted. These results therefore indicate that despite the

pain probabilities associated with each cue changing, expectancy ratings in the reversal block still reflected the cue expectations formed during acquisition. We further found a significant negative relationship between the high- and low-pain acquisition bias in the Active ($r_{(26)}$=-0.403, p=0.033, 95% CI[-0.675, -0.036], BF_{10}=2.02), but not Passive ($r_{(26)}$=-0.167, p=0.394, 95% CI[-0.509, 0.219], BF_{10}=0.332), conditions (see *Figure 3.4.B*). Therefore, some evidence indicates that not only did participants showcase significant biases towards their initial learning, but this was a generalised bias, regardless of whether the original expectation was a high or low-pain probability cue. We anecdotally note a similar trend for our amputee sample, who also seemed to display a generalised bias towards their initial learning of high and low-pain probabilities.

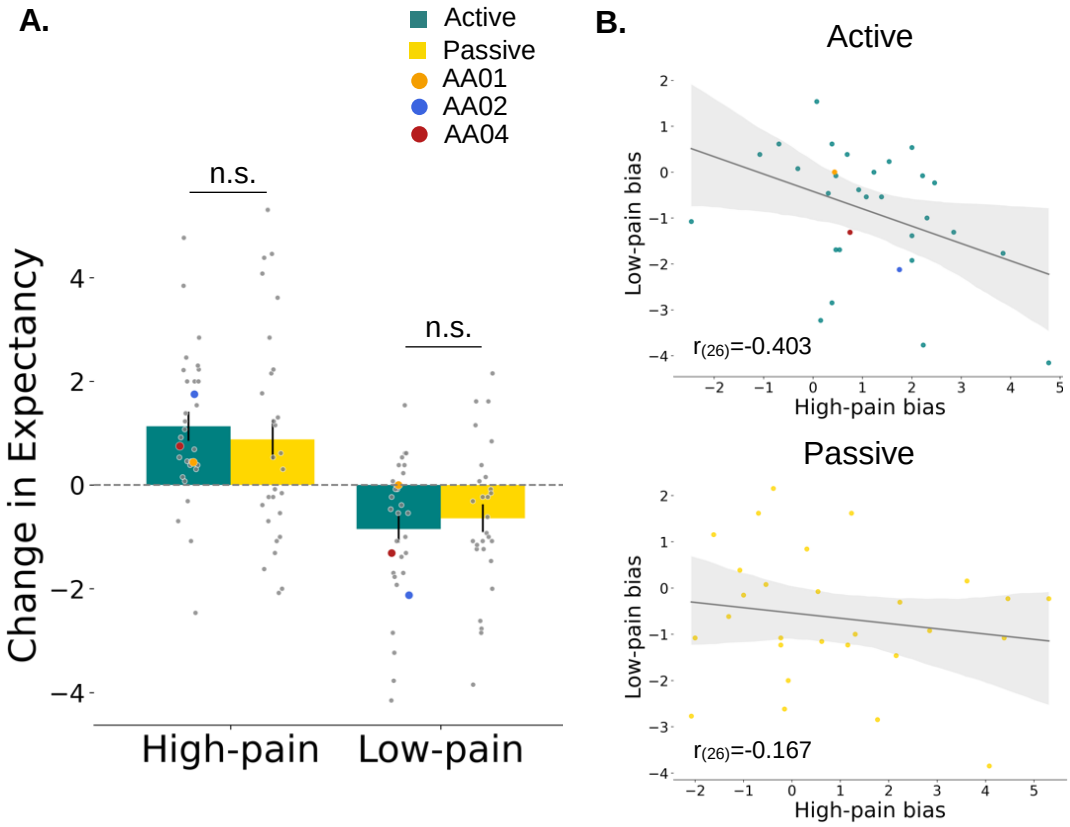


Figure 3.4. *Acquisition biases for high and low-pain probabilities.* **(A)** Average acquisition biases for high-pain and low-pain (*x*-axis) probabilities in Active (teal) and Passive (gold) conditions. Increases in expectancy rating (*y*-axis) indicates greater acquisition bias to initially learnt high-pain probabilities. Decreases in expectancy rating reflect a greater bias towards initially learnt low-pain probabilities. Note, on average, a generalised bias towards both high- and low-pain probabilities. Standard error of the mean and individual data-points are plotted in grey, with amputee data-points highlighted in participant-specific colours. **(B)** Pearson correlations between high- (*x*-axis) and low-pain (*y*-axis) acquisition biases in Active (top row; teal) and Passive (bottom row; gold), with regression line plotted (grey line), along with 95% confidence intervals noted by grey translucent bands around the line. Note a significant correlation between acquisition biases was only found in the Active condition, indicating that participants displayed a generalised bias towards their initial learning in the acquisition block. n.s.=non-significant.

As we found evidence of significant acquisition biases in the reversal block, we then directly compared the extent of these biases between Active and Passive conditions. To do so we used a repeated measures ANOVA with within-subject factors of Condition (Active x Passive) and Acquisition Bias (High-pain x Low-pain), whilst controlling for passive sequence type. Here we found a non-significant interaction ($F_{(1,26)}$=2.126, p=0.157, η^2_p=0.076, BF_{10}=4.722, $BF_{Inclusion}$=0.337) and non-significant main effect of Condition ($F_{(1,26)}$=1.327, p=0.260, η^2_p=0.049, BF_{10}=0.260, $BF_{Inclusion}$=0.276), indicating that both Active and Passive conditions showcased to a similar extent biases towards initial learning of the high and low-pain probabilities (see *Supplementary Table 12* for all main effects). Not only, therefore, are acquisition biases generalised to both high- and low-pain for both controls and amputees, but they are also similar across learning with and without movement. Movement inclusion, therefore, does not seem to lead to quicker adaptation to new pain probabilities, as predicted. Note no significant correlations between acquisition biases (high- and low-pain) and depression, anxiety and pain catastrophising were found in Active (depression and low-pain bias: $_{T}b$=-0.121; anxiety and PCS: -0.074 < r < .259; all p >.184) and Passive (depression: 0.011 < $_{T}b$ < 0.167; anxiety and PCS: -0.175 < r < .167; all p >.205) conditions. Although a significant relationship was found between depression and high-pain acquisition bias in the Active condition ($_{T}b$=0.276, p=0.044, BF_{10}=1.86), whereby higher scores on the BDI led to a greater bias towards initial learning of high-pain probabilities, as the Bayes Factor was inconclusive and the association was not consistent across conditions, we will not interpret this result further.

3.3.3 Movement enhances placebo responses during acquisition

As participants showed significant learning of the paradigm via their expectancy ratings, we next wanted to look at how this may have influenced their perceptual ratings during the task. For example, the perceived intensity of a nociceptive stimulus may vary dependent on what the individual expects to receive, i.e., the nocebo and placebo response. Within our paradigm we can assess the extent of nocebo/placebo responses, and therefore learning of H-L and L-H cues, from the intensity ratings of the surprise trials. If a robust expectation of a high-pain probability has formed, the resulting warm temperatures of the surprise trials will be rated as more painful (nocebo). The opposite is true for low-pain probabilities, whereby more extensive learning will be reflected in rating the painful surprise trials as less painful (placebo). If learning is enhanced within the Active condition, we would expect to see greater placebo and nocebo responses, reflecting more robust formation of pain probability expectations. We would also predict that amputees with PLP would demonstrate a larger nocebo, and reduced placebo, response, reflecting a bias towards heightened expectations of pain.

We first found evidence for nocebo responses significantly greater than zero (i.e., significant increases in intensity ratings for warm surprise trials) in the acquisition block for Active ($t_{(27)}$=-2.3346, p=0.014, d=0.44119, BF_{10}=3.937) and Passive ($t_{(27)}$=3.2600, p=0.002, d=0.61608, BF_{10}=25.703) conditions. This nocebo response subsequently disappeared in the reversal block for the Active condition ($t_{(27)}$=0.5092, p=0.307, d=0.09624, BF_{10}=0.310), but seemed to persist in the Passive condition ($t_{(27)}$=1.9096, p=0.033, d=0.36088, BF_{10}=1.879; note though the inconclusive Bayes Factor), indicating that the influence of high-pain expectations

seems to decrease once the cues had switched pain probabilities. When looking at the placebo, we again find responses significantly smaller than zero (i.e., significant decreases in intensity ratings for painful surprise trials) in the acquisition block for the Active ($t_{(27)}$=-5.8840, p<.001, d=-1.11197, BF_{10}=13396.063) and Passive conditions ($t_{(27)}$=-1.9504, p=0.031, d=-0.36859, BF_{10}=2.009). These placebo responses again disappeared in the reversal block for Active ($t_{(27)}$=-0.0495, p=0.480, d=-0.00936, BF_{10}=0.208), but persisted in the Passive condition ($t_{(27)}$=-2.1999, p=0.018, d=-0.41575, BF_{10}=3.085). These results therefore show that not only do we find evidence of significant nocebo and placebo responses within our paradigm, but that they seem to be more pronounced within the initial phase of learning (although we note a degree of preservation of these responses in the Passive condition).

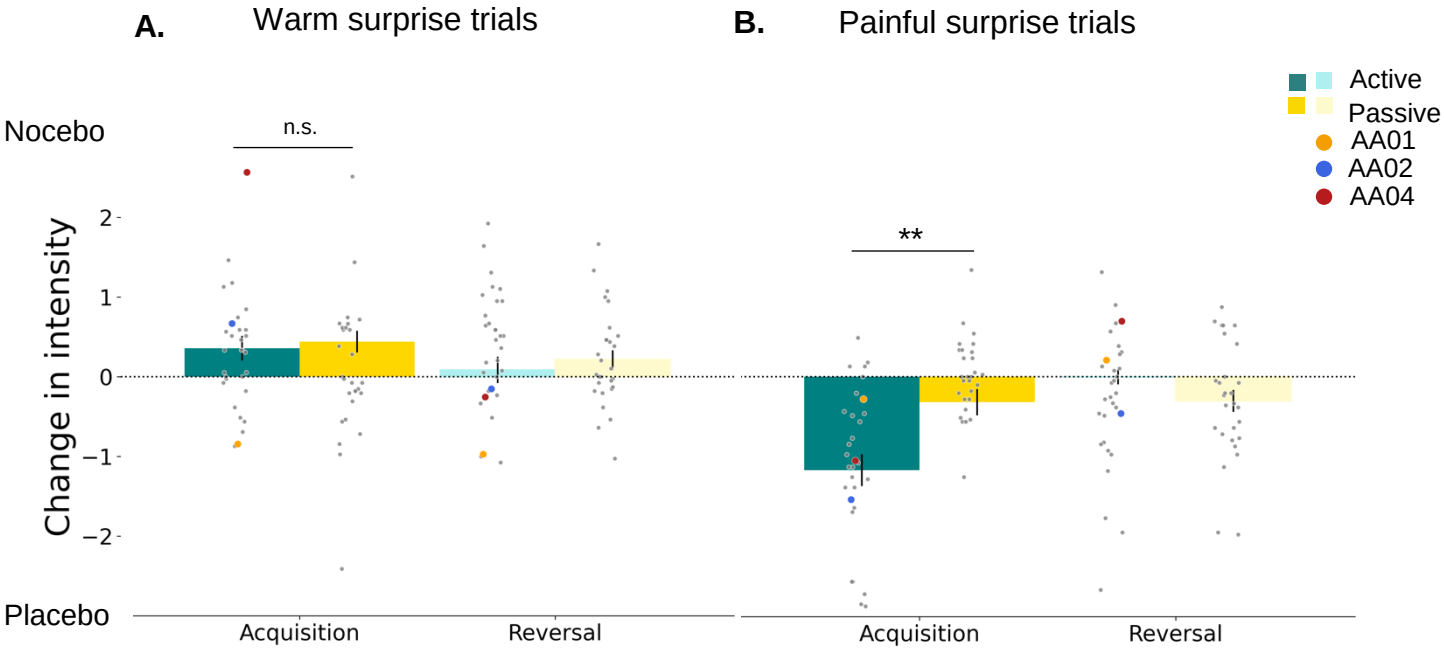


Figure 3.5. *Nocebo and placebo responses for Active and Passive conditions.* Changes in intensity ratings (*y*-axis) for warm **(A)** and painful **(B)** surprise trials in the acquisition (darker colours) and reversal (lighter colours) blocks (*x*-axis) for Active (teal) and Passive (gold) conditions. Increases in intensity ratings for warm surprise trials indicates the presence of a nocebo response, whereas decreases in intensity ratings for painful surprise trials signifies a placebo response. We found significantly enhanced placebo responses in the Active condition during acquisition. Note that in the reversal block, placebo and nocebo responses in the Active condition were not significantly different from zero. Standard error of the mean and individual data-points are plotted in grey, with amputees plotted in participant-specific colours. ** p <.01.

We then explored the extent of the nocebo and placebo responses between Active and Passive conditions using a repeated measures ANOVA with within-subject factors of Condition (Active x Passive) and Response (Nocebo x Placebo) for each learning phase separately (whilst controlling for passive sequence type; see *Supplementary Tables 13-14* for all main effects). If the nocebo/placebo

responses differed between conditions we would expect to find a Condition x Response interaction. When doing so, we did find a significant Condition x Response interaction ($F_{(1,26)}$=7.50, p=0.011, η^2_p=0.224, BF_{10}=9.02e+8, $BF_{Inclusion}$=3.57) in the acquisition, but not reversal block ($F_{(1,26)}$=0.0284, p=0.867, η^2_p=0.001, BF_{10}=0.679, $BF_{Inclusion}$=0.980). Therefore, not only do we find evidence for significant learning in the acquisition block but we find this exemplified in differences between Active and Passive conditions. Subsequent confirmatory comparisons indicated that placebo responses were significantly greater in the Active condition, when compared to Passive ($t_{(26)}$=-3.015, p=0.005) during acquisition (see F*igure 3.5.B*). However, there was no significant differences between conditions for the nocebo response ($t_{(26)}$=-0.483, p=0.633; see *Figure 3.5.A*). These results indicate that including movement when learning about pain probabilities seems to boost the initial formation of low-pain expectations only. It tentatively suggests that movement may aid in relief, not pain, learning (see *Discussion*).

We next wanted to see if participants displayed a general susceptibility to nocebo/placebo responses (e.g., if a participant reports a large nocebo response, then are they also likely to show a large placebo response), or whether these effects were independent of each other. As we only found a significant Condition x Response interaction in the acquisition block, we restricted our analysis to nocebo/placebo responses within this learning phase. When doing so we found non-significant relationships between nocebo and placebo responses for both the Active ($r_{(26)}$=-0.367, p=0.055, 95% CI[-0.651, 0.007], BF_{10}=1.36) and Passive ($r_{(26)}$=0.029, p=0.882, 95% CI[-0.347, 0.398], BF_{10}=0.237) conditions (see *Figure*

3.6). This is in line with previous research which suggests that differential neural mechanisms may underlie both responses (Bingel et al., 2011; Freeman et al., 2015; Fu et al., 2021; although see Petrovic, 2008). Note no significant correlations were found between placebo and nocebo responses in the acquisition block and depression, anxiety, and pain catastrophising measures in Active (depression: -0.013 < $_{T}b$ < 0.027; anxiety and PCS: 0.167 < r < .107; all p >.396) and Passive (depression and placebo: $_{T}b$=-0.197; anxiety and PCS: 0.011 < r < .308; all p >.111) conditions. Although a significant relationship was noted in the Passive condition between nocebo responses and depression ($_{T}b$=0.313, p=0.023, BF_{10}=3.36), whereby those who reported greater scores on the BDI also displayed greater nocebo responses, as suggested by previous work (Corsi & Colloca, 2017). However, as the relationship was not found consistently across conditions it will not be interpreted further in this study.

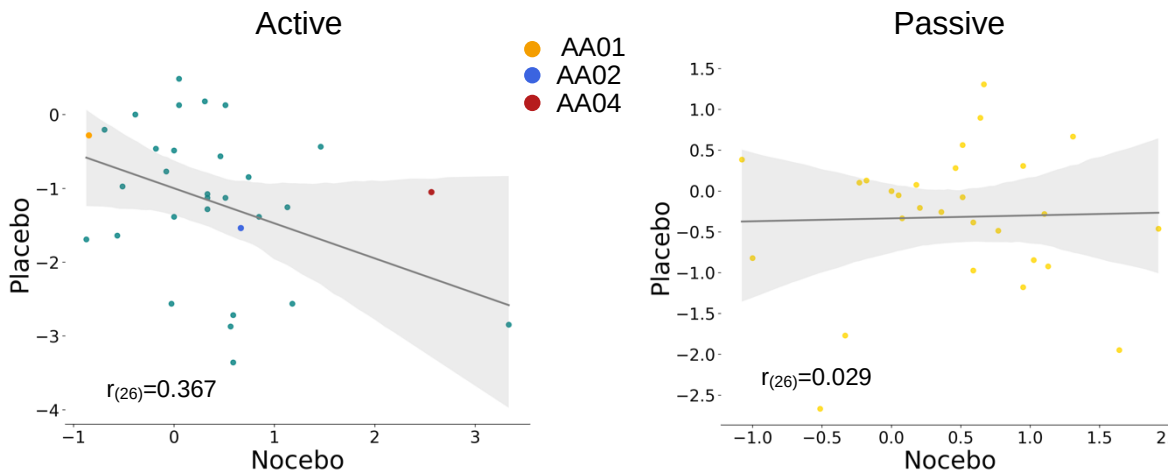


Figure 3.6. *Correlations between nocebo and placebo responses in Active and Passive conditions.* Pearson correlations between placebo (*y*-axis) and nocebo (*x*-axis) for Active (left-hand side; teal) and Passive (right-hand side; gold) conditions during the acquisition block. Note no significant correlations were found. Amputees are plotted for the Active condition only, with participant-specific colours. Regression lines and 95% confidence intervals are plotted in grey.

3.3.4 Participants learn pain probabilities quicker without movement

As the above learning measures were based on cue and block averages, we also fitted each participant's expectancy ratings to a computational model in order to take into account trial-by-trial learning. Here we fitted three reinforcement learning models: a baseline model, Rescorla-Wagner (RW) and Pearce-Hall Hybrid. By doing so we were able to generate learning rates for comparison between Active and Passive conditions, and between our controls and amputee sample (for anecdotal comparison). When assessing model fits using a random-effects model comparison procedure (see *Methods*; see *Supplementary Figure 11* for negative log likelihoods), we found that the RW model which updates the predicted value dependent on the cue shown, was the 'winning' model for Active (model frequency=0.545; exceedance probability=0.774; protected exceedance

probability=0.768) and Passive conditions (model frequency=0.664; exceedance probability=0.969; protected exceedance probability=0.969), compared to alternative models (see *Figure 3.7*).

In the winning, cue-specific RW model, the learning rate reflected the extent to which prediction error (the difference between your expected sensory outcome of a trial and the actual sensory outcome) updates the model's predicted value (in our case, estimated cue probabilities) for the subsequent trial (Atlas et al., 2022). We predicted that, due to enhanced levels of attention and controllability, the Active condition would showcase a higher learning rate than the Passive condition. When testing this comparison, however, we found the contrary – the Passive condition reported a significantly higher learning rate than Active ($t_{(27)}$=-2.70, p=0.012, d=-0.511, BF_{10}=4.03; see *Figure 3.8A*). Participants within the Passive condition, therefore, tended to demonstrate more frequent cue value updates based on prediction errors, and thus larger learning rates, than when learning included movements. In contrast, this tentatively suggests greater stability of estimated cue probabilities, or cue expectations, within the Active condition, as evidenced by the significantly smaller learning rate.

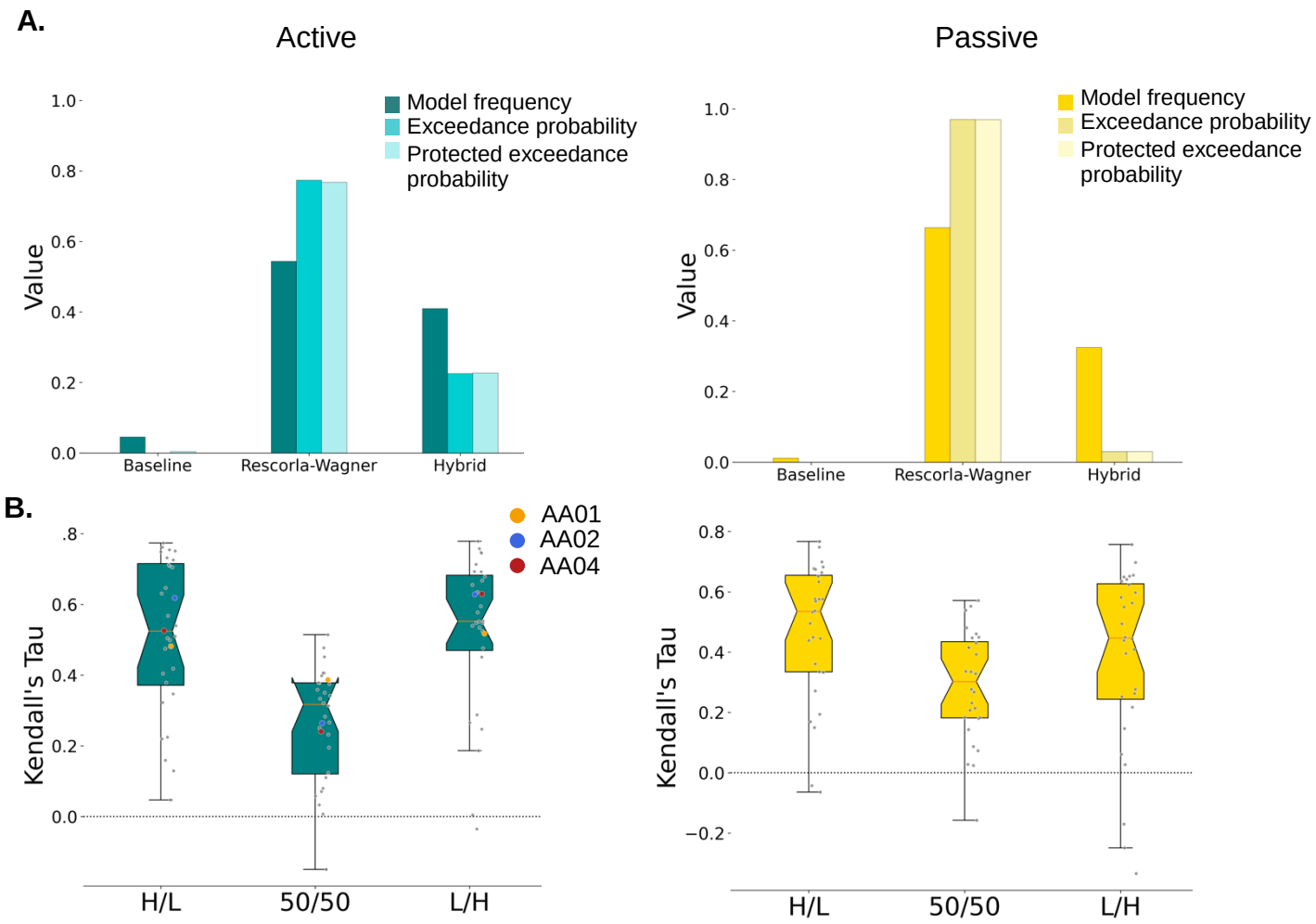


Figure 3.7. *Model comparison statistics and individual correlations between actual and predicted ratings.* **(A)** Model comparison statistics for all three models in Active (teal) and Passive conditions (gold). Note the following comparison statistics (*y*-axis): model frequency, model exceedance probability, and protected exceedance probability, were all higher in the cue-specific Rescorla-Wagner model, when compared to the others (*x*-axis). **(B)** Kendall Tau statistics (*y*-axis) between actual participant expectancy ratings and predicted ratings from the winning model (cue-specific Rescorla-Wagner) in the Active (teal) and Passive (gold) conditions for each cue (*x*-axis). Kendall Tau statistics of 0 are noted by a dashed line, individual data points are plotted in grey, with amputees in the Active condition only plotted in participant-specific colours. The red line inside the boxplot denotes the median, with the notches signifying 95% confidence intervals around the median. See *Supplementary Figure 12* for qualitative comparisons between actual and predicted ratings for participants overall.

As we found a significant difference between placebo responses for Active and Passive conditions in the acquisition block, we next wanted to explore whether this was related to the learning rate. For example, if a smaller learning rate reflects greater stability of cue expectations, we would predict that this might be mirrored in the increased placebo responses in the Active condition. However, we found a non-significant relationship between the learning rate and placebo responses from the acquisition block in both the Active ($r_{(26)}$=0.009, p=0.962, 95% CI[-0.365, 0.381] BF_{10}=0.235) and Passive ($r_{(26)}$=0.173, p=0.379, 95% CI[-0.214, 0.513] BF_{10}=0.340) conditions. Thus, the reported differences in learning rate are not necessarily reflected in subsequent perceptual differences within this paradigm. Anecdotally we note that the learning rates for two of our amputees (AA02 and AA04) are similar to control participants, contrary to our predictions for those with chronic PLP. However, one amputee, AA01, reports an exceptionally high learning rate indicating that this individual may be learning differently, with highly frequent cue value updates, and thus greater sensitivity to prediction errors (see *Discussion*). Note no significant correlations were found between the learning rates in Active and Passive conditions and depression, anxiety and pain catastrophising (depression: -0.214 < $_{T}b$ < -0.132; anxiety and PCS: -0.180 < r < .018; all p >.121).

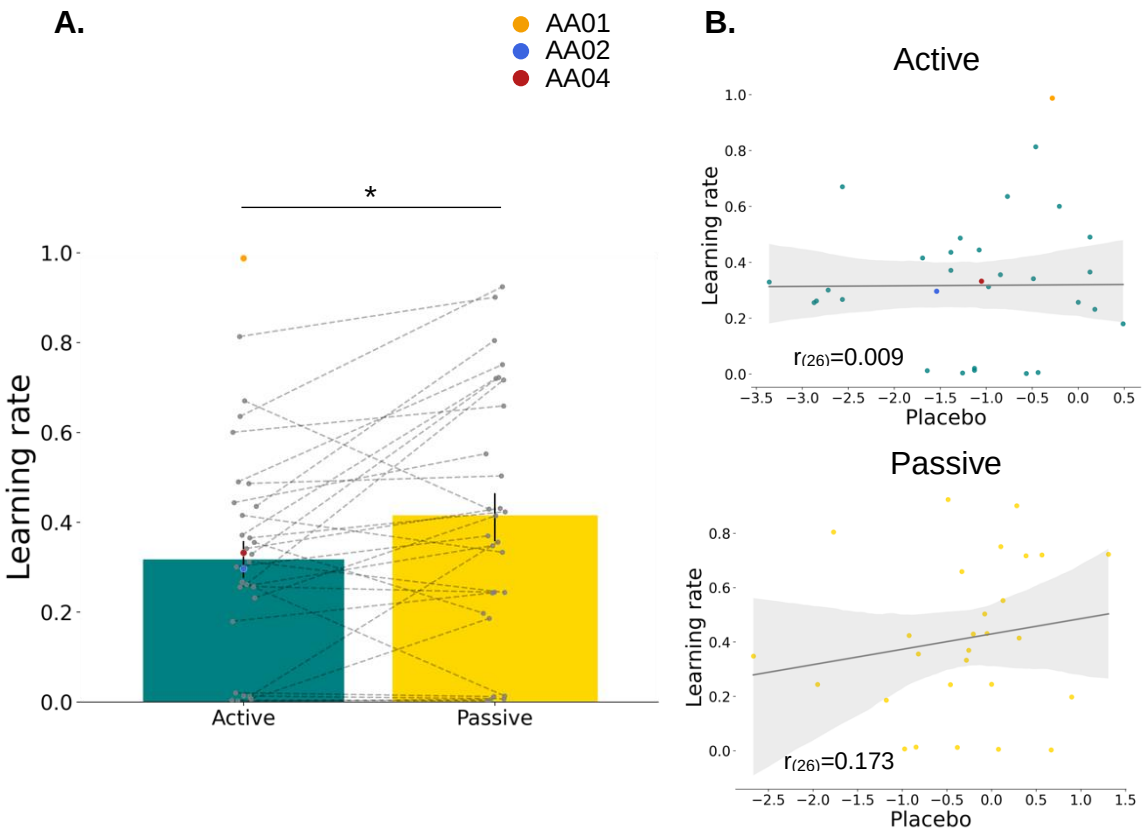


Figure 3.8. *Average learning rates in Active and Passive conditions and the relationship between learning rates and placebo responses.* **(A)** Average learning rates (*y*-axis) generated by the cue-specific Rescorla-Wagner model in Active (teal) and Passive (gold) conditions (*x*-axis). Results indicated significantly higher learning rates in the Passive condition, contrary to predictions. Individual data-points and standard error of the mean plotted in grey, with dashed lines indicating the within-subject comparison. **(B)** Pearson correlations between the learning rate (*y*-axis) and placebo responses (*x*-axis) in the acquisition block for Active (top-row; teal) and Passive (bottom-row; gold) conditions. No significant correlations between the two were found. Regression line and 95% confidence intervals are plotted in grey. Amputees are plotted in all graphs in participant-specific colours.

3.4 Discussion

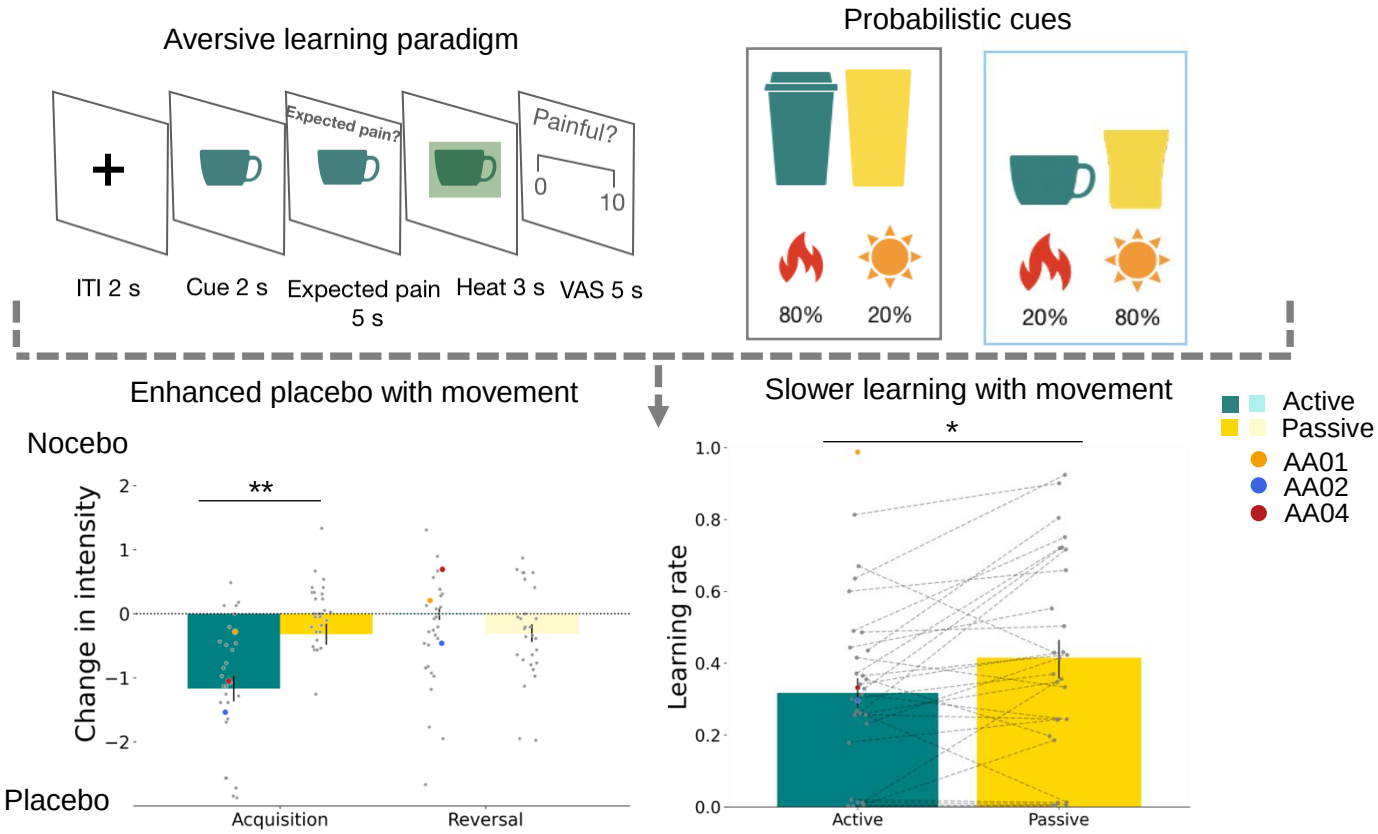


Figure 3.9. *Graphical summary of main findings and methodologies for Chapter 3.* Participants (*n*=28 two-handed controls; *n*=3 upper-limb amputees) partook in an aversive learning paradigm with thermal heat stimuli (painful or warm) associated with three ecologically-valid cues, each with a different probability of painful stimulation. It employed a within-subject's design, whereby control participants completed both an active (teal; movements preceding thermal stimulation) and passive (gold; no movement required) version of the task. It also utilised a reversal learning protocol, where cues with high and low pain probabilities switched associated probabilities halfway through (acquisition block=bold colours; reversal block=lighter colours). Key results demonstrated that including a movement preceding thermal stimulation significantly enhanced a placebo response to unexpected painful trials. Reinforcement modelling of trial-by-trial pain predictions revealed that including movements reduced the overall rate of learning, compared to without movements. Crucially, the subsample of amputees revealed preserved placebo responses, akin to controls.

Forming associations between an action and a subsequent painful experience is fundamental in establishing bodily integrity and threat learning. It is also crucial in the development of chronic pain, with fear avoidance of certain actions and the restriction of movement in learning of innocuous cues thought to be key to the development of a chronic state (Meulders et al., 2011; Vlaeyen et al., 2016). This is particularly highlighted in amputees who develop PLP, whereby painful sensations are localised in their missing phantom limb which is often restricted in terms of movement and sensory feedback. Despite this, most associative aversive learning research has focused on passive paradigms in healthy participants, whereby painful cues are learnt via stationary stimulation and response, or through paradigms using actions such as button presses or joystick movements. In this study, we explored the role of movement in aversive learning with a novel behavioural paradigm in healthy controls and a small sample of amputees with PLP, which included movement or no movement of the non-dominant/phantom limb (within-subjects design) in response to ecologically-valid cues with different pain probabilities (80%, 50% and 20%). We found that the overall extent of learning and the intensity of the pain did not differ between paradigms with and without movement. However, we did find that movement inclusion led to an enhanced placebo response in controls and (anecdotally) amputees in the acquisition block, suggesting that movement in particular aids with relief learning. Furthermore, we found evidence of potentially different learning strategies when movement is included or not, as demonstrated by a significantly higher learning rate in the Passive condition.

One of our main predictions in this paradigm was that learning with movement would be more optimal than learning without movement, due to increased levels of attention, controllability and contextual information of the stimuli (e.g., proprioceptive cues). Surprisingly we found that the beneficial effects of movement were specific, restricted to an enhancement of the placebo response. Previous research has shown that movement itself has analgesic properties, with self-induced stimulation leading to pain relief (Borhani et al., 2017; Bräscher et al., 2016; Lalouni et al., 2021), and higher levels of controllability, usually tied to a movement, also reducing pain (Becker et al., 2015; Salomons et al., 2007; Tang et al., 2019; Wiech, Edwards, et al., 2014; Wiech et al., 2006). However, we did not find a significant reduction of pain intensity ratings in general for the Active condition. Indeed, recent work has reported a lack of pain relief between controllable (e.g., with button presses) and uncontrollable (passive paradigms) conditions (Löffler et al., 2018; Salomons et al., 2004; Wiech, Edwards, et al., 2014), with authors citing the importance of individual differences in believed controllability (Salomons et al., 2007). It is thus not just the 'doing' that is integral to feelings of control, but the level of volition that participants have over the movement itself (Borhani et al., 2017). With this in mind, our lack of generalised pain reduction in the Active condition may result from this decreased feeling of individual choice. For example, participants were required to move on each trial and the type of movement itself was restrained by the cue presented. Choice and exploration were limited. This may have led to reduced levels of perceived controllability, and in turn, reduced generalised pain relief.

If this is the case, then the advantageous effects of movement seemed to emerge when the action coincides with an expectation formation. Instrumental learning paradigms, whereby participants learn about the consequences of action choices which are usually associated with cues, have previously shown analgesic effects associated with relief learning specifically. For example, a recent instrumental paradigm demonstrated that ongoing pain was reduced when there was a greater chance of learning new information associated with relief-predictive cues (Zhang et al., 2018). Within our paradigm, the L-H cue, when associated with a low-pain probability in the acquisition block, could be viewed as relief-predictive – with innocuous outcomes for the majority of the cues' trials. The enhanced placebo response we subsequently report, therefore, may be a parallel of Zhang et al.'s (2018) instrumental relief phenomenon. Why do we then see both the placebo and nocebo responses disappear in the reversal block for the Active condition? Firstly, we found evidence of significant acquisition biases towards the initial learning of high and low-pain probabilities. This 'carry-over' effect, or stubbornness, of initial cue expectations may have subsequently impeded the adaptation to the switched pain probabilities in the reversal block, therefore leading to decreased nocebo and placebo responses. To put it simply, there may not have been long enough in the reversal block for complete extinction of the original learning, followed by efficient 're-learning'.

Previous research in decision-making and uncertainty may also help explain this. Here researchers distinguish between three types of uncertainty – expected uncertainty (a known unreliability of a predictive relationship, e.g., a probabilistic cue), unexpected uncertainty (where sensory observations strongly violate

expectations, e.g., a cue probability switch/reversal) and volatility (the frequency by which cue probabilities change) (Bland & Schaefer, 2012; Yu & Dayan, 2005). In environments with high levels of unexpected uncertainty and volatility, learning rates should be high as participants are required to learn quickly from the new outcomes, and adapt. We would therefore have expected our cue probability switch in the reversal block to encourage faster learning and adaptation. However, this is not what we observe, and if anything, learning is slower in the reversal block as evidenced by the decreased nocebo/placebo responses. A possible reason as to why, is that the levels of unexpected uncertainty and volatility in our paradigm were not only high, but perceived as stochastic. For example, the nature of using probabilistic cues in combination with a contingency reversal, as well as a 50-50 cue, may have created an environment that was merely noisy. Even though a degree of uncertainty and surprise encourages change and adaptation, noisy environments tend to promote a stability of beliefs and slower learning rates (McGuire et al., 2014; Monosov, 2020). Furthermore, at the point of the cue probability switch, participants may have subsequently developed an expectation for further change – this may have also hindered learning in the reversal block in combination with a reluctance to let go of their prior cue expectations.

Our winning computational model, the cue-specific Rescorla-Wagner, can also inform us on how participants responded to uncertainty with and without movement. We are, to the best of our knowledge, one of the first studies directly comparing learning rates within an aversive context for learning with and without movements. Furthermore, as the computational model was applied to trial-by-trial expectancy ratings, this allowed us to generate a more sensitive picture of

participant's learning across the paradigm, contrary to previous learning measures in this study which were calculated on trial and learning block averages. Here we found results contradictive to our predictions, with a significantly higher learning rate in the Passive when compared to Active condition. Learning without movement, therefore, seemed to be quicker, updating estimated cue values on recent prediction errors more often than with movement. Whether this is an optimal way to learn, however, depends on the surrounding context. For example, stable environments with expected uncertainty may benefit from slower learning rates, as it prevents unnecessary updates due to short-term fluctuations in sensory outcomes (Grossman et al., 2022). As the Active condition was shown to have a significantly lower learning rate, this may be why we see an enhanced placebo response in the acquisition block. For example, previous work has argued that the conceptualisation of placebo responses can be framed within a learning context (Colloca & Miller, 2011) . Thus, as participants presumed the initial learning environment to be stable, the lower learning rate would have decreased the influence of surprise trials (i.e., unexpected uncertainty) on the resulting formation of cue expectations, thereby promoting an enhanced placebo response.

However, we did not find a significant correlation between the reported learning rate and placebo responses in the acquisition block, suggesting that other mechanisms may underly the differences in learning rate. Recent work has shown that task design can influence resulting learning rates. For example, providing subjective ratings trial-by-trial can lead to reduced learning rates (Atlas et al., 2022). The authors hypothesise that making explicit ratings trial-by-trial requires concurrent processes of attention, decision-making and probability inference,

which can all gate learning. Within our Active condition the task not only requires the participant to make two explicit ratings each trial, whilst tracking three varying cue pain probabilities all within a short space of time (akin to Passive), but it also requires attending towards the presentation of a 'Go' cue to initiate a movement, and then directing that attention to the relevant physical object to execute a grasp. Task demand and complexity may therefore have been higher in the Active condition which could have, in turn, resulted in significantly lower learning rates. This leaves the question as to why we see enhanced placebo responses in the acquisition block paired with a lower learning rate in the Active condition, which suggests gated learning. As mentioned above, the enhanced placebo response may in fact reflect a particular 'boosting' of instrumental relief learning only when movement is involved, whereas the computed learning rate reflects learning as a whole across the entirety of the Active paradigm. It is difficult to ascertain the underlying mechanisms behind these conflicting findings with the current data, but we encourage future research to explore, and replicate, the inclusion of movement in relief learning only, combined with the modelling of learning rates to answer this outstanding question. Finally, sequential differences may have also contributed to higher/lower learning rates (Mancini et al., 2021), as differing pseudo-randomised cue sequences were presented in Active and Passive conditions. We limited this to an extent by including passive sequence type as a covariate, but we encourage future research to employ a yoked control design, whereby the only differences between conditions would be executing a movement or not.

Our paradigm also addressed potential differences in aversive learning between controls and a small sample of amputees with PLP. We found that, on the whole,

amputees tended to show similar learning to controls in both their average expectancy and intensity ratings. Crucially they all demonstrated intact placebo responses anecdotally similar to our control group, contrary to our prediction. This study was the first of its kind, that we know of, in demonstrating explicitly that analgesic effects can be induced in amputees with PLP as a consequence of associating a phantom movement with a relief-predictive cue (e.g., L-H during acquisition) in an aversive learning paradigm. This demonstrates something vital – amputees with PLP can down-regulate their responses to experimental pain as well as controls. It therefore highlights (speculatively) that previous research using phantom motor execution and imagery, in line with external visual cues such as mirrors and virtual/augmented reality (see Herrador Colmenero et al., 2018 for an overview), may in fact be exploiting a placebo-like mechanism instead of treating the PLP itself. This emphasises the importance of including longitudinal assessment and randomised controls in future clinical trials for PLP treatments, which many currently do not do (Schone et al., 2022). Other work has also shown the preservation of placebo responses in patients with osteoarthritis and fibromyalgia (Power et al., 2020), with authors suggesting this may provide an opportunity for new treatment strategies in those with chronic pain. Future work exploring treatments for PLP, therefore, may want to consider capitalising, as well as controlling for, this preserved endogenous analgesic response.

Two amputees, however, did showcase noticeable (though qualitative) differences from controls. For example, AA04 reported an enhanced nocebo response (see *Figure 3.5*), which was anecdotally higher than controls in the Active condition. This is in line with our predictions, whereby those with chronic pain may report

enlarged nocebo responses due to a bias towards sustaining high-pain probability expectations. It supports previous work suggesting that nocebo-like mechanisms may be involved in the development of a chronic state, where expectation of painful outcomes intersects with altered motor repertoires and impedes subsequent relief learning (Barnes et al., 2021; Hodges & Smeets, 2015; Meulders et al., 2014). Interestingly, AA04 was our amputee who reported the highest levels of PLP within our sample (see *Table 1*), as well as reporting the shortest time since amputation (~ 2 years), which may have predisposed this individual in particular to forming high-pain expectations in the acquisition block.

In contrast, AA01, who had low-to-medium levels of PLP in relation to this sample, reported an almost eradication of the nocebo response, with the unexpected warm trials rated as less intense than expected warm trials (i.e., a 'negative' nocebo). This amputee also displayed an exceedingly high learning rate of 0.988, contrary to prediction, suggesting that this individual may have deployed a different learning strategy to the others. For example, a high learning rate indicates that their expectancy ratings likely reflect the sensory outcome of the most recent trials rather than previously formed expectations (see *Supplementary Figure 13*). In other words, they displayed a greater weighting to prediction errors when estimating cue probabilities. This is in line with previous work on individuals with complex regional pain syndrome, whereby patients were shown to display a greater sensitivity to prediction errors in a tactile spatial learning task. This led to predictions generated by more recent sensory information, rather than the history of previous trial outcomes (Brown et al., 2020). It may also aid in explanation of the inverted nocebo response, whereby utilising this learning strategy would lead

to the surprise trials simply mirroring the warm thermal temperature administered (also note that AA01 reported the lowest levels of high- and low-pain acquisition bias; see *Figure 3.4*). It is currently unclear whether AA01's idiosyncratic learning is typical of amputees due to our small sample, and if so, which characteristics of their condition (e.g., chronicity, cause of amputation, time since injury) are related to such style of aversive learning. Yet it is important to note, and highlight, the idiosyncrasy here – learning in the amputee sample was diverse and unique, with one amputee demonstrating a sensitivity to painful expectations, and another showcasing an almost opposite learning strategy of increased sensitivity to prediction errors. Most importantly, it emphasises the necessity for taking individual differences and experience into account in future studies exploring the origins of, and treatment for, PLP.

To conclude, our novel behavioural study using ecologically-valid cues in a probabilistic aversive learning paradigm found that involving movement aids in relief learning, as evidenced by heightened placebo responses. It further demonstrates that learning with and without movement may also recruit differential learning strategies. Crucially it tentatively suggests that amputees with PLP report intact placebo responses associated with the phantom limb, opening up future avenues for novel treatment approaches. In summary, our results point towards a revision of PLP characterisation as a predominantly cortical phenomenon, with a 'one-size-fits-all' explanation, suggesting that PLP may emerge from a similar phenotype underlying other chronic pain conditions.

Chapter 4 | Is learning of novel nociceptive stimuli associated with probabilistic reasoning?

4.1 Introduction

Perception is widely accepted to be a constructive process, built from an integration of what the individual expects to perceive and incoming sensory input (de Lange et al., 2018). It can be framed as a weighting of 'top-down' predictions and 'bottom-up' sensory information, scaled by precision (i.e., uncertainty), to infer the likely causes of input.

Expectations in particular are known to influence pain perception, with predictions of subsequent relief or increased pain inducing placebo analgesia or nocebo hyperalgesia, respectively (Atlas & Wager, 2012; Tracey, 2010). Importantly, a recent study using drift-diffusion modelling demonstrated that the modulation of pain via expectations may be based on changes in perceptual decision-making, not on altered processing of sensory information (Wiech et al., 2022; Wiech, Vandekerckhove, et al., 2014), indicating that pain predictions may influence subsequent perception via higher-level inference. Recently computational work has not only hypothesised how an incorporation of expectation and sensory information may explain the perception of pain (Büchel et al., 2014; Seymour, 2019; Tabor & Burr, 2019), but also how errors within this inferential process may lead to the development and maintenance of chronic pain (Hechler et al., 2016; Ongaro & Kaptchuk, 2018). Impairments in weighting 'top-down' and 'bottom-up' information have also been suggested to underly the development of disorders such as schizophrenia (Adams et al., 2013; Fletcher & Frith, 2009), autism

(Palmer et al., 2017), functional neurological disorders (Edwards et al., 2012) and depression (Smith et al., 2021), with a recent study suggesting that errors in the precision of sensory information may underly a wide range of psychiatric disorders (Smith et al., 2020).

One of the ways in which these errors may manifest is when individuals integrate new evidence when updating their beliefs. For example, an over-weighting of sensory evidence may lead to the quick formation of 'incorrect' beliefs, and conversely an under-weighting may contribute to the persistence of stubborn beliefs. This is particularly poignant in individuals with schizophrenia and delusions, who have reliably reported a data-gathering bias whereby they require significantly less evidence before making a decision, termed 'jumping-to-conclusions' (JTC).

A common paradigm used within computational psychiatry to assess JTC is the beads task (Garety et al., 1991; Huq et al., 1988). Here two jars (Jar A or Jar B) are presented to participants, each filled with different ratios of coloured beads (e.g., 85% blue beads, 15% red beads, and vice versa). Participants are told that a bead will be drawn, one at a time, from a chosen jar. After each bead withdrawal, the participant must state whether they are certain they know which jar the bead has come from. The number of draws needed to reach certainty is defined as 'draws to decision' (DTD), with DTD of ≤ 2 indicating a JTC bias. It has been found that individuals with schizophrenia and delusional beliefs require significantly less than two beads to reach certainty than healthy or psychiatric

controls (Adams et al., 2018; Dudley et al., 2016; Hayashi et al., 2022; McLean et al., 2017; Ross et al., 2015; So et al., 2016; Strube et al., 2020, 2022).

A graded estimate variant of this task, termed ‘draws to certainty’ (DTC; Adams et al., 2018; Garety et al., 1991; Pareés et al., 2012; Strube et al., 2020, 2022; Young & Bentall, 1997), where participants are required to rate the likelihood that the bead came from Jar A or Jar B at each bead withdrawal, assesses how an individual responds to evidence contrary to an initial hypothesis (e.g., the 1st blue bead in a RRRBR sequence). Here research has shown that schizophrenic participants with delusions are more likely to over-adjust their likelihood ratings in response to this disconfirmatory evidence, compared to healthy and psychiatric controls (McLean et al., 2017; Moritz & Woodward, 2005; although see Fine et al., 2007). A variety of explanations have been suggested for the JTC bias, including overweighting of sensory evidence, (Adams, 2018; McLean et al., 2018; Strube et al., 2020), unstable prior belief formation (Adams et al., 2018; Strube et al., 2020, 2022; note overweighting of sensory evidence and belief formation are not mutually exclusive; Jardri et al., 2017), stochastic decision-making (Adams et al., 2018; Moutoussis et al., 2011) or general probabilistic reasoning deficits (Klein & Pinkham, 2018).

The relationship between JTC and delusional ideation has also been reported in healthy controls (Freeman et al., 2008; Ross et al., 2015), suggesting that the bias may reflect a ‘transdiagnostic phenotype’, manifesting in individuals who are susceptible to, or who have developed, co-occurring neuropsychological disorders (Reininghaus et al., 2019). In support of this, evidence for a JTC bias has also

been found in those with anxiety (Bensi & Giusberti, 2007; Giusti et al., 2018; although see Jacoby et al., 2014), depression (Sastre-Buades et al., 2021; although see So et al., 2016), autism (Jänsch & Hare, 2014; Sahuquillo-Leal et al., 2020; although see Brosnan et al., 2014), Parkinson's disease (de Rezende Costa et al., 2016) and functional neurological disorders (Pareés et al., 2012). However, to our knowledge, only one study so far has administered the beads task in those with chronic pain, finding that a patient group reporting persistent pain demonstrated significantly less DTD (i.e., a JTC bias) than healthy controls (Parkes et al., 2019; note the authors do not state the chronic pain diagnosis).

In this study we aim to further explore the relationship between JTC and a chronic pain patient group in particular – acquired amputees. Here the majority of amputees report the presence of phantom limb pain (PLP) after amputation, which is characterised by chronic painful sensations in the missing limb. As we stated in *Chapter* 3, *Introduction*, the somatosensory landscape of the phantom limb is impoverished, reflecting a stochastic multitude of innocuous and fluctuant painful sensations combined with a limited motor repertoire of the phantom limb. We hypothesise, therefore, that this may lead to difficulties in efficiently gathering and learning from sensory input, which in turn, may impede updating predictions associated with the limb (akin to precision impairments reported in other disorders; Smith et al., 2020). Thus, amputees in particular may be unable to down-regulate (and predict) the stochastic sensory information from the phantom limb, potentially contributing to the development of chronic pain (Hechler et al., 2016; Ongaro & Kaptchuk, 2018), and errors in data-gathering/belief formation.

Our primary aim in this study, therefore, was to assess whether a potential data-gathering impairment in amputees is related to painful information associated with the phantom limb specifically, (i.e., errors in processing nociceptive information only, as explored in *Chapter 3*), or a generalised deficit reflected in a JTC bias. To do so, we recruited thirty-two healthy controls and a small sample of amputees who completed the beads task (including DTD and DTC variants), along with a battery of questionnaires (including depression, trait anxiety and pain catastrophising) and an associative pain learning task (see *Chapter 3*). As previous work has demonstrated JTC biases in those with depression and anxiety (Bensi & Giusberti, 2007; Giusti et al., 2018; Sastre-Buades et al., 2021) and a proportion of those with non-psychotic mental health problems (Dudley et al., 2016), we predicted a significant relationship would be found between depression/anxiety scores and DTD, whereby those with higher scores of depression and anxiety would report less DTD. Furthermore, we predicted that those who are more inclined to catastrophise about pain would also report less DTD (i.e., a JTC bias), reflecting rapid negative belief formation (note, as we are the first study of its kind (to our knowledge) exploring JTC biases and pain catastrophising this prediction is tentative). In addition, we predicted that amputees who reported the presence of PLP would demonstrate a JTC bias, reflected in less DTD than healthy controls. We further predicted they will also report greater sensitivity to disconfirmatory evidence in the DTC task, indicating greater weighting of new sensory evidence when making a decision. Finally, we predicted that DTD's in control participants will be significantly related to the pain learning measures detailed in *Chapter 3* (see *Methods*), indicating the transdiagnostic nature of the JTC bias.

4.2 Methods

4.2.1 Participants

Thirty two-handed controls (age, *M*=36.9, *SE*=2.66; women, *n*=16; left-handers, *n*=3) were recruited for this study and the aversive learning paradigm (see *Chapter 3*). Exclusion criteria included history of psychosis or the presence of a chronic pain condition. Three additional controls who were recruited for the study did not participate in the beads task due to lack of understanding of task instructions (*n*=1), and time constraints (*n*=2). Four additional controls who did complete the beads task but were unable to either complete the set of questionnaires due to time constraints or aversive learning paradigm due to pain thresholding issues (*see Chapter 3*), and so will be excluded from analyses which address the relationship between bead task measures and depression (*n*=1), anxiety and pain catastrophising (*n*=1), and pain learning (*n*=2). Total sample sizes for each analysis will be stated alongside test statistics and significance values.

Four individuals with acquired unilateral upper-limb amputation (age, *M*=41.0, *SE*=6.42; women, *n*=2; missing right hand, *n*=4; hereafter amputees) were also recruited (see *Chapter 3; Table 3.1* for full details). One amputee who was recruited for the study did not participate in the aversive learning paradigm due to issues with task understanding. Procedures were in accordance with NHS National Research Ethics Service approval (18/LO/0474), and written informed consent was obtained.

4.2.2 Experimental procedure

The ‘beads task’ was administered after participants had completed a set of questionnaires (see *Questionnaire* section below) and an aversive learning paradigm (see *Chapter 3* and below). It was split into two sections: Draws to Decision and Draws to Certainty. Participants were always administered the ‘Draws to Decision’ task first. Both tasks were presented to participants on a computer screen and responses were made using the computer keyboard and mouse. PsychoPy v3.2.3 was used for stimulus presentation.

4.2.2.1 Draws to Decision

Participants were first presented with detailed instructions of the task on the computer screen. They were able to discuss with the experimenter at this point if anything was unclear about the task. Instructions were then followed by a two-item comprehension check (McLean, Balzan, et al., 2020; McLean et al., 2018). If participants were unable to answer either question, they were automatically returned to the instructions page to prompt re-reading. If participants failed the comprehension check three times in a row they were excluded from the task (*n*=0 were excluded at this stage). Participants were then shown images of two jars (Jar A and Jar B), filled with beads of two different colours. Jar A contained majority (~85) blue beads and ~15 red beads, whereas Jar B contained the opposite blue:red colour ratio (~15 blue beads and ~85 red beads). For each trial, participants were told that the computer will randomly select either Jar A or Jar B, and will withdraw one bead at a time from the chosen jar in a supposedly random sequence.

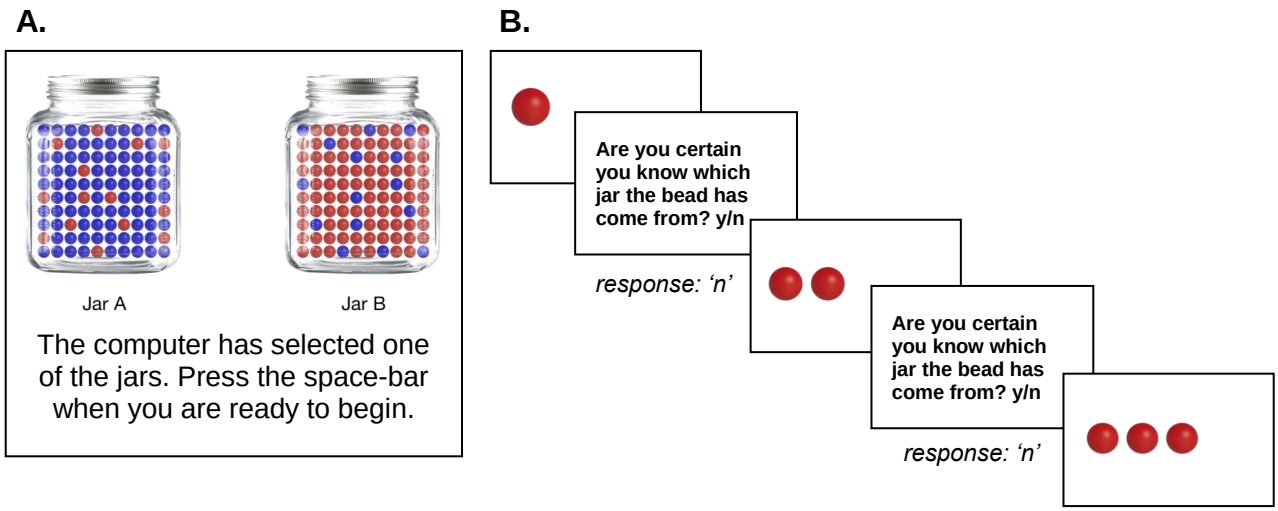


Figure 4.1. *Experimental design for Draws to Decision.* **(A)** Participants were first presented with two jars of coloured beads (Jar A and Jar B) of different ratios (e.g., 85:15 red/bue beads and vice versa). They were then told that the computer will randomly select one of these jars. Beads were then withdrawn from this chosen jar, one at a time **(B)**, and at each bead withdrawal the participant was asked if they were certain they know which jar the bead has come from (required keyboard response: 'y' (yes) or 'n' (no)). If the participants were certain ('y'), the computer either re-selected one of the jars and the next bead withdrawal sequence commenced (target or distractor), or the coloured ratio of beads changed (red/blue, orange/green, yellow/purple) and the subsequent bead withdrawal sequences for those jars commenced. If participants were not certain which jar the bead had come from ('n'), the next bead within the current withdrawal sequence was shown on the screen, along with the history of previous bead withdrawals.

Each trial of the task consisted of 3 pseudo-randomised ‘distractor’ bead sequences (taken from McLean et al., 2018: RRBRRRBRRR, BRRRRBRRRR and RRRRBRRBRR) and one predetermined target sequence (RRRBRRRRRB; Pareés et al., 2012). One distractor sequence was presented before, and two after, the target sequence. The inclusion of ‘distractor’ sequences has been shown to increase task reliability and believability, avoiding repetition effects of target sequence-only paradigms (McLean, Balzan, et al., 2020; McLean et al., 2018; McLean, Mattiske, et al., 2020). There were 3 trials in total, with the colour of the beads changing every trial (blue:red, orange:green, yellow:purple; Ross et al., 2011; Waller et al., 2011).

During the task, each time a bead was withdrawn from the chosen jar it was shown on the computer screen followed by a certainty judgement. Here participants were required to state whether they were certain they know which jar the bead had come from. If they were certain, the number of bead draws was recorded for current sequence (distractor or target). Participants were then told that the computer had now re-selected one of the jars, and the next bead sequence commenced. If participants were not certain, the next bead draw in the current sequence was shown on the screen, along with the history of previous bead withdrawals. This ensured responses were not affected by memory capacity (Freeman et al., 2014). A maximum number of 10 draws was allowed for each sequence (Fear & Healy, 1997). If the maximum number of draws was reached, it was recorded and the next bead sequence was presented automatically. If all bead sequences had been presented (distractors and target) then the next trial began.

Draws-to-decision (DTD), which reflects the amount of information required to make a decision, was calculated by averaging the number of draws across the 3 target sequences. Those who reported DTD ≤ 2 were classified as displaying a 'jumping-to-conclusions' (JTC) bias (McLean, Balzan, et al., 2020; McLean et al., 2018; McLean, Mattiske, et al., 2020; Pareés et al., 2012).

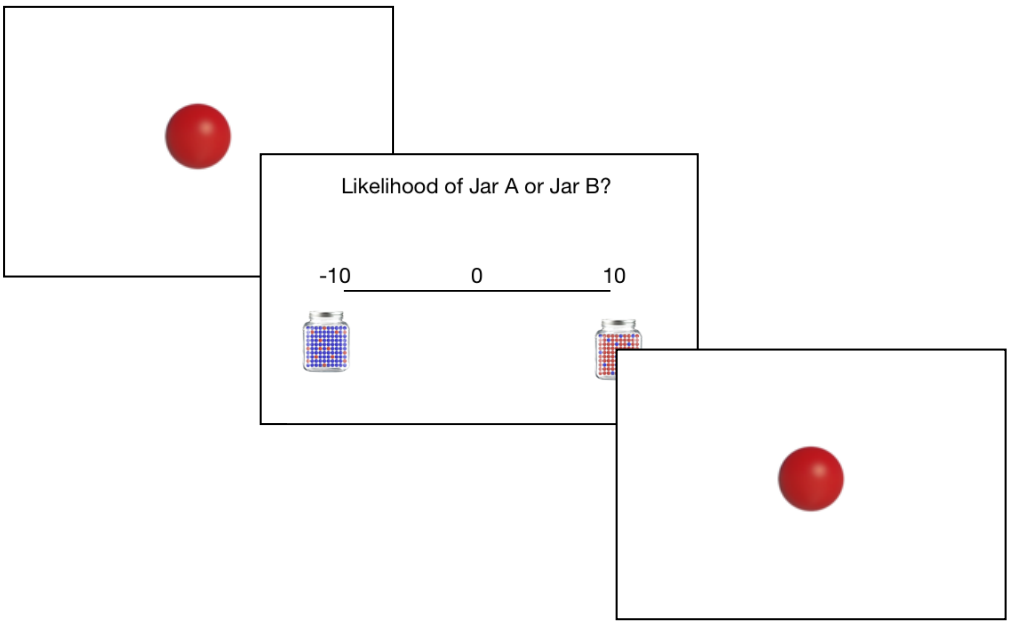


Figure 4.2. *Experimental design for Draws to Certainty.* Participants were instructed that for this part of the experiment, termed Draws to Certainty, the computer would select only one jar (Jar A or Jar B with red/blue beads) for the entirety of the task. A bead at a time was then presented to participants followed by a rating screen. When the rating screen was presented, participants used a computer mouse to mark on -10 (Jar A) to +10 (Jar B) scale the likelihood in which the bead came from either Jar A or Jar B. Crucially, the first 10 beads were predominantly red, supporting the hypothesis that Jar B had been chosen by the computer. The last 10 beads, however, were predominantly blue – supporting the alternative hypothesis of Jar A being chosen.

4.2.2.2 Draws to Certainty

The second part of the task, called 'Draws to Certainty' (Garety et al., 1991; Pareés et al., 2012; Strube et al., 2022; Young & Bentall, 1997), was used to assess how participants responded to confirmatory and disconfirmatory evidence when making probabilistic judgements. To assess this, participants were again shown Jar A and Jar B, filled with 85:15/15:85 (blue:red) of coloured beads, and told that the computer will now select only one of the jars for the entirety of the task. After an initial practice trial, beads were shown one at a time to the participants on the screen followed by a likelihood judgement as to whether the bead had been taken from either Jar A or Jar B. To make their judgements, participants used the computer mouse to place a pointer along a scale ranging from -10 (Jar A) to +10 (Jar B). There were 20 bead draws in total, which followed the sequence: RRRBRRRRBRBBBRBBBBRB. The first 10 bead draws supported the hypothesis that Jar B had been chosen, whilst the last 10 trials supported the alternative – that Jar A had been chosen. In order to assess the influence of dis/confirmatory evidence three measures were computed from the likelihood judgements:

(1) *Confirmatory evidence:* likelihood estimate of the second red bead minus the first red bead. Here more positive values indicate a larger increase in support of Jar B (majority red beads), and thus a greater effect of confirmatory evidence. More negative values indicate a reduction in influence of confirmatory evidence on likelihood judgements, and zero reflects no confirmatory effect at all.

(2) *Disconfirmatory evidence:* likelihood estimate of the first blue bead minus the third red bead. If the resulting value was negative, i.e., a greater change

in likelihood towards Jar A (majority blue beads), this was turned into a positive value in order to reflect the greater influence of disconfirmatory evidence on likelihood judgements. The opposite was applied to resulting positive values, which were switched to negative values, indicating a reduction of disconfirmatory evidence on likelihood judgements.

(3) *Final Decision:* the final likelihood estimate after the last bead draw. Here more positive values indicated support for the initial hypothesis, Jar B (+10), and more negative values indicate support for Jar A (-10).

4.2.3 Questionnaires

To assess the relationship of bead learning measures, e.g., DTD, disconfirmatory evidence, to depression, anxiety and pain catastrophising, three questionnaires were administered to participants before the beads task. These questionnaires consisted of: Beck's Depression Inventory (BDI) (Beck et al., 1961), Trait Anxiety (Spielberger, 1983) and the Pain Catastrophising Scale (PCS) (Sullivan et al., 1995). We initially aimed to use these questionnaires in order to control for potential group differences between controls and amputees. However, as Covid-19 restrictions hindered and stalled recruitment of our patient sample (amputees), we will now aim to explore whether the relationship of a JTC bias to depression, anxiety and pain catastrophising is evident in a healthy control population.

4.2.4 Pain learning measures

In order to assess whether a JTC bias (as classified by DTD) is significantly related to aspects of pain learning we used two measures from our aversive learning paradigm: the learning rate (from the 'winning' computational model; see

Chapter 3, *Results*) and the placebo response (see *Chapter 3, Methods*). The learning rate was generated by fitting a reinforcement learning model to participant trial-by-trial expectancy ratings (i.e., pain probability judgements). It reflected the extent to which the prediction error (e.g., the difference between your expectation and the actual sensory outcome) updated the estimated pain likelihood for each cue, with higher learning rates reflecting more frequent cue value updates. We therefore predicted that participants who have a higher learning rate will also require less DTD before making a judgement. We predicted an opposite relationship between DTD and the placebo response. As the placebo response reflects the influence of expectations on subsequent perception, we predict that larger placebo responses will be associated with a higher number of DTD. Thus, the greater the influence of an expectation, or 'stubborn belief', would be reflected in more DTD, i.e., gathering of sensory evidence, needed to reach certainty/confirm a prediction. As our amputee sample only participated within the Active condition of the aversive learning task, pain learning measures correlated with DTD will be from this condition only. Furthermore, placebo responses will only be taken from the acquisition block due to a lack of a significant response in the reversal block (see *Chapter 3*, *Results*).

4.2.5 Statistical analysis

All statistical analyses were carried out using jamovi (1.6.23). The relationship between DTD and DTC measures and depression, anxiety and pain catastrophising were explored using a multiple linear regression. Assessment of auto-correlation was conducted with a Durbin-Watson test, and collinearity checked by inspection of VIF statistics. Normality was carried out by inspection of

Q-Q plots and Shapiro-Wilk tests on residuals. DTD was found to violate the assumptions of normality. On inspection of data dispersion (see *Figure 4.1*) and the removal of DTD > 6 (*n*=3), normality was reached. Thus, regressions including DTD were carried out both with and without these outliers. Regression statistics reported in the main text include the outliers, with any change of significance reported and results without outliers in *Supplementary Tables 15-21*. As one control participant was unable to complete the BDI due to timing issues, their missing value was replaced with the control sample's median. Age and gender were also included as 'regressors-of-no-interest' in the models, in line with others in the field (Strube et al., 2022), and previous findings demonstrating a significant relationship between age and JTC (Sastre-Buades et al., 2021), and gender and questionnaire measures, e.g., depression (McLean & Anderson, 2009; Piccinelli & Wilkinson, 2000; Sullivan et al., 2000). As our amputee group had a small sample size (*n*=4), no statistical comparisons were made between groups. However, their data-points will be highlighted and visualised, allowing for anecdotal comparisons to the control group.

We also reported the corresponding Bayes Factor (BF_{10}), defined as the relative support for the alternative hypothesis, for each regression model. Bayes Inclusion Factors were subsequently reported for regression coefficients, which quantify how much the observed data are more probable under models that include that predictor, relative to models that do not. We used the threshold of $BF < 1/3$ as positive evidence in support of the null, consistent with others in the field (Dienes, 2014; Wetzels et al., 2011; Kass & Raftery, 1995), and the JZS prior width was set as 0.354 (jamovi's default for Bayesian regression).

4.3 Results

4.3.1 Catastrophising beliefs about pain are tentatively related to 'jumping-to-conclusions'

Control participants reported, on average, a mean DTD of 3.078 (*SEM*=0.307, *SD*=1.683; see *Figure 1A*). Eight controls (~26.7%) displayed a JTC bias, with an average DTD $\leq$ 2 draws. When looking at the relationship between DTD and the questionnaire measures, whilst controlling for age and gender, we found that, overall, depression, anxiety and pain catastrophising did not significantly relate to DTD ($R^2_{adj.}$ =-0.001, $F_{(5,23)}$=0.994, p=0.443, BF_{10}=0.688, n=29; see *Supplementary Tables 15-16* for with and without outliers; note significance of results do not change). However, as the relationship between pain catastrophising and JTC has not been investigated previously, exploratory analyses found that catastrophising reported a negative trend in relation to DTD (β=-0.074, *SE*=0.039, t=-1.902, p=0.070, 95% CI[-0.155, 0.007], BF_{10}=0.874, $BF_{Inclusion}$=1.422), whereby higher pain catastrophising scores were related to lower DTD (see *Figure 4.2.A*). As DTD is thought to reflect the over-weighting of sensory evidence in forming rapid beliefs, it may mirror the formation of catastrophising beliefs in response to little painful information. Yet due to the inconclusive Bayes Factors and insignificant regression model further research with larger sample sizes is needed for robust interpretations to be drawn. Our lack of significant findings for depression and anxiety are in line with previous research in healthy controls which has also reported non-significant relationships between these measures (Parkes et al., 2019), indicating that the relationship between DTD and depression/anxiety is

complex, and may not rely on a continuum of the disorder within the healthy population (see *Discussion*).

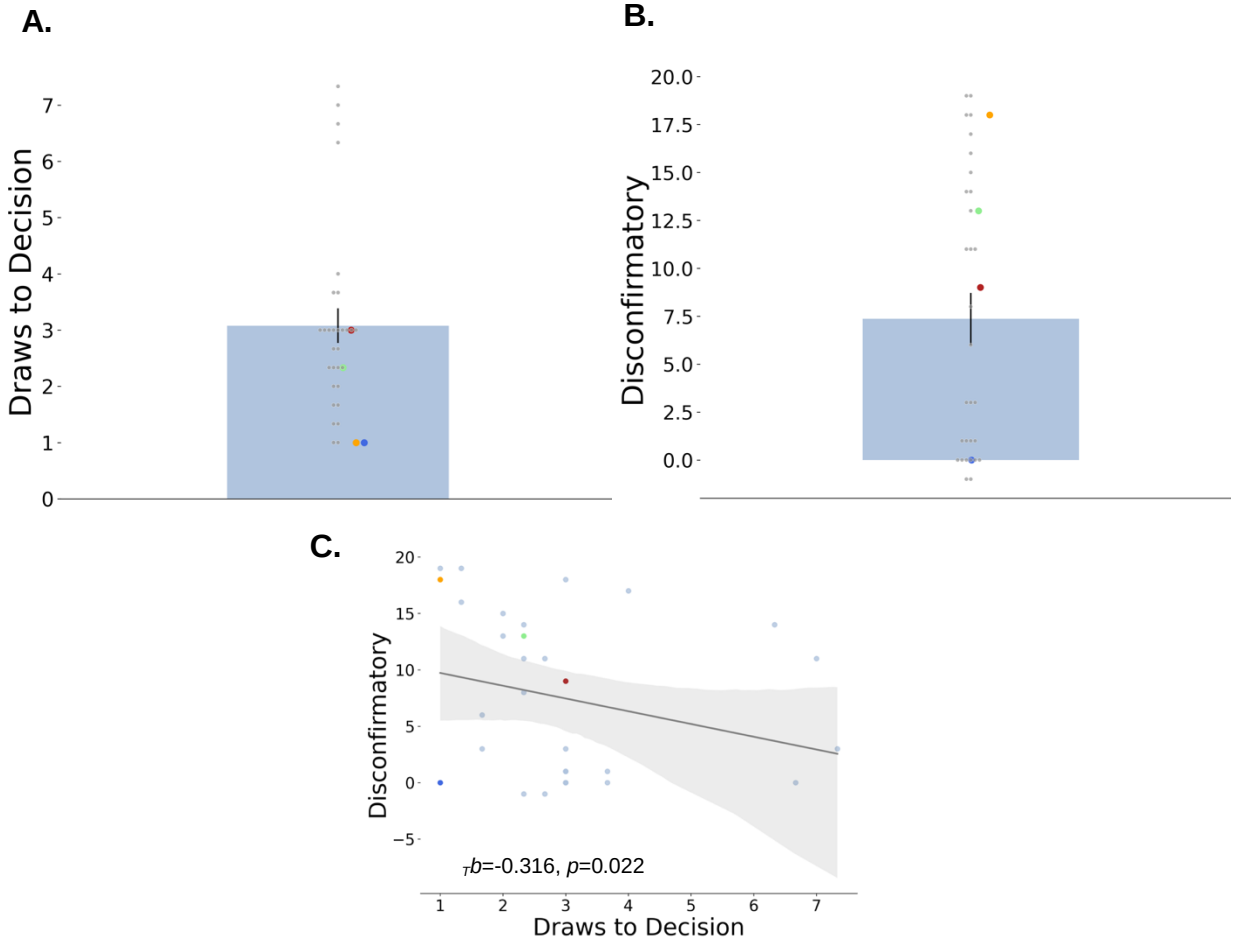


Figure 4.3. *Draws to Decision and Disconfirmatory Evidence for control participants and amputees.* **(A)** Draws to Decision and Disconfirmatory Evidence **(B)** (*y*-axis) average and standard error of the mean for control participants. Individual data-points are plotted in grey. Amputees are plotted in participant-specific colours, in line with *Chapter 3* (e.g., AA01=orange; AA02=blue; AA03=green; AA04=red). **(C)** Significant correlation between Draws to Decision (*x*-axis) and Disconfirmatory Evidence (*y*-axis), indicating a potential similar mechanism underlying both measures. Linear regression line and 95% confidence intervals plotted in grey.

We also found a significant relationship between DTD and Disconfirmatory Evidence (M=7.37, *SD*=7.36, *SE*=1.34; see *Figure 4.1.B*) from the DTC task ($_{\tau}b$=-

0.316, p=0.022, BF_{10}=4.26, n=30; see *Figure 4.1.C*), whereby participants who were more likely to JTC (i.e., have smaller DTD's) were also more likely to weight Disconfirmatory Evidence to a greater extent. No significant relationships between DTD and Confirmatory Evidence ($_{T}b$=0.146, p=0.302, BF_{10}=0.437, n=30) or Final Decision ($_{T}b$=0.120, p=0.382, BF_{10}=0.357, n=30) were found. The significant relationship between DTD and Disconfirmatory Evidence has also been reported in a recent study administering DTD and DTC tasks to schizophrenic patients, patients with major depressive disorder and healthy controls (Strube et al., 2022). It is tempting to hypothesise that both measures likely assess a similar decision-making strategy.

We also found a trend towards a relationship between depression, anxiety and pain catastrophising and Disconfirmatory Evidence ($R^2_{adj.}$=0.190, $F_{(5,23)}$=2.31, p=0.077, BF_{10}=2.403, n=29; see *Supplementary Table 17*). Significant relationships were found for pain catastrophising (β=0.439, SE=0.162, t=2.702, p=0.013, 95% CI[0.103, 0.775], BF_{10}=0.772, $BF_{Inclusion}$=2.750) and trait anxiety (β=-0.563, SE=0.232, t=-1.043, p=0.023, 95% CI[0.103, 0.775], BF_{10}=0.730, $BF_{Inclusion}$=2.428), albeit with opposite directional trends. For example, higher pain catastrophising scores were associated with a greater weighting of Disconfirmatory Evidence, in line with our tentative DTD results. Whereas higher trait anxiety scores were related to lower values of Disconfirmatory Evidence, reflecting that anxious participants were reluctant to update a prior belief in the face of new evidence.

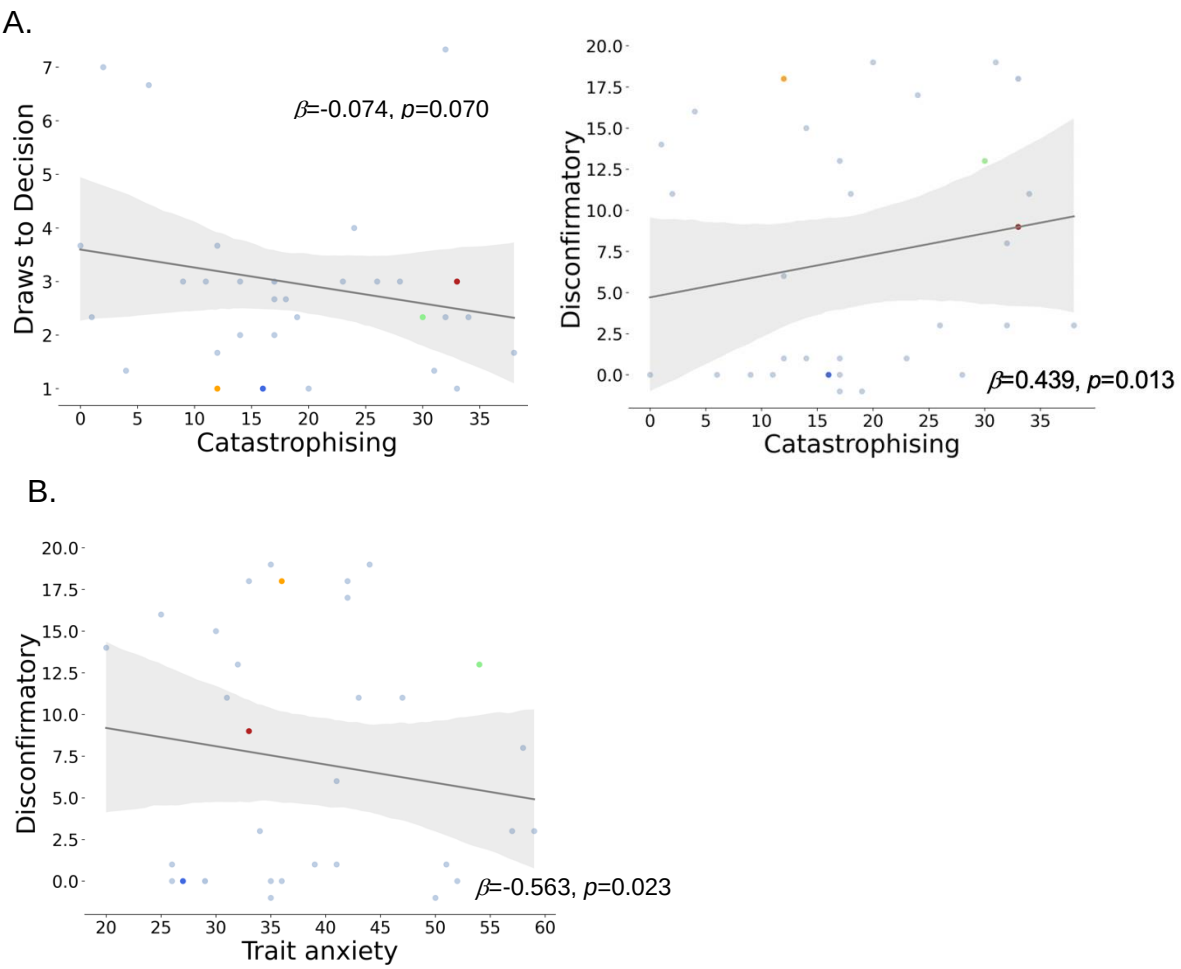


Figure 4.4. *Regressions between questionnaire and bead measures in controls and amputees.* **(A)** Relationship between pain catastrophising (*x*-axis) and Draws to Decision (left-hand side) and Disconfirmatory Evidence (right-hand side) (*y*-axis), as well as the relationship between train anxiety (*x*-axis) and Disconfirmatory Evidence (*y*-axis) **(B)**, in control participants (*n*=29). Note figures include participants who reported DTD > 6, and the regression line plotted denotes the linear regression between variables, as well as the 95% confidence interval. Regression coefficients reported are from the multiple linear regression reported in the main text. Amputees are plotted in participant-specific colours, in line with *Chapter 3* (e.g., AA01=orange; AA02=blue; AA03=green; AA04=red).

We also note a significant relationship with age (β=0.214, *SE*=0.099, *t*=2.152, *p*=0.042, 95% CI[0.008, 0.419], BF_{10}=0.678, $BF_{Inclusion}$=1.266), whereby older participants demonstrated greater weighting of Disconfirmatory Evidence (note, though, the inconclusive Bayes Factors). This relationship has been reported before in previous work, where older individuals were more likely to report a JTC bias (Sastre-Buades et al., 2021). As age was included into our model as a nuisance regressor and we had no prior hypotheses for this as a predictor, we encourage future research to explore the potential relationship further. Note that no significant relationships were found between depression, anxiety and pain catastrophising and Confirmatory Evidence ($R^2_{adj.}$=-0.016, $F_{(5,23)}$=0.908, *p*=0.493, BF_{10}=0.257, *n*=29) or Final Decision ($R^2_{adj.}$=-0.167, $F_{(5,23)}$=0.198, *p*=0.960, BF_{10}=0.236, *n*=29).

4.3.2 No significant relationship was found between nociceptive learning rates and 'jumping-to-conclusions'

As discussed in *Chapter 3*, current theories suggest that associative learning mechanisms may contribute to the development of chronic pain. We therefore predicted that if DTD reflects how an individual gathers and interprets sensory information, this may be, in turn, reflected in measures of aversive learning.

To assess this, we first looked at the relationship between DTD and the fitted learning rate from our winning, cue-specific Rescorla-Wagner model described in *Chapter 3*. When doing so, we found a non-significant relationship between DTD and the learning rate overall ($R^2_{adj.}$=0.0817, $F_{(3,24)}$=1.80, *p*=0.174, BF_{10}=2.30, *n*=28), when controlling for age and gender. When looking at the relationship between the learning rate and DTD only, however, we found a positive

relationship (β=2.907, *SE*=1.382, *t*=2.103, *p*=0.046, 95% CI[0.054, 5.759], BF_{10}=2.30, $BF_{Inclusion}$=2.30), whereby higher learning rates were associated with a higher number of DTD, as predicted. Yet when the regression model was run without DTD outliers (i.e., DTD > 6, *n*=3) to aid in normality of residuals, this significance was lost (*p*=0.428, BF_{10}=0.667; see *Supplementary Tables 18-19* for full model results), indicating that the relationship between the two measures is tenuous, may be spurious and should be interpreted with caution. We found no significant relationship between the learning rate and Disconfirmatory Evidence ($R^2_{adj.}$=-0.0284, $F_{(3,24)}$=0.751, *p*=0.532, BF_{10}=0.567, *n*=28). Furthermore, we found no significant relationships between placebo responses and DTD ($R^2_{adj.}$=-0.0362, $F_{(3,24)}$=0.685, *p*=0.570, BF_{10}=0.819, *n*=28; see *Supplementary Tables 20-21*; note no change in significance of results) or between placebo responses and Disconfirmatory Evidence ($R^2_{adj.}$=-0.006, $F_{(3,24)}$=0.938, *p*=0.438, BF_{10}=0.677, *n*=28), indicating a lack of relationship between pain expectations and JTC. Note, again, no significant relationships between learning rates and placebo responses and Confirmatory Evidence or Final Decision were found (all $R^2_{adj.}$<0.074, all $F_{(3,24)}$<1.72, all *p*>0.190, all BF_{10}< 0.859).

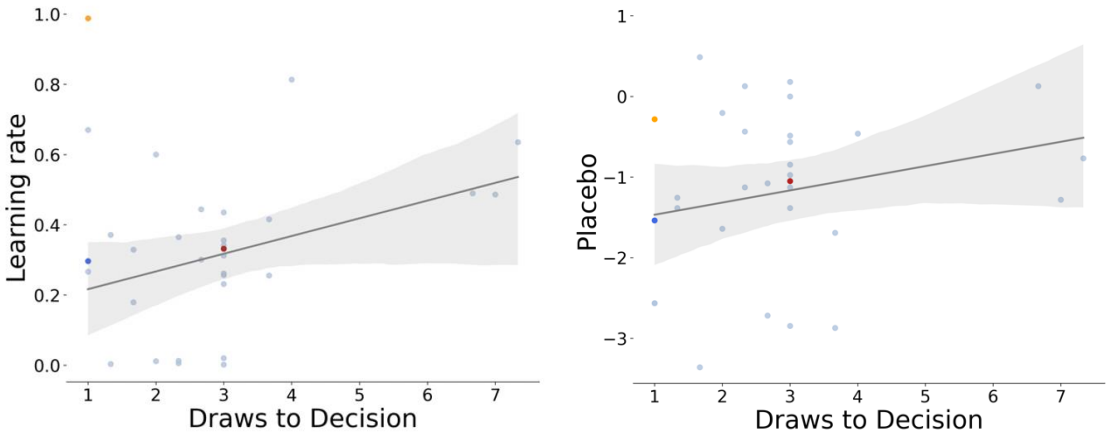


Figure 4.5. *Relationship between Draws to Decision and pain learning measures in control participants.* Draws to Decision (*x*-axis) was not shown to be significantly related to either the aversive learning rate or placebo responses from *Chapter 3* (*y*-axis), indicating that a JTC bias may not necessarily reflect how an individual process nociceptive information. Linear regression line and 95% confidence intervals are plotted in grey. Amputees are plotted in participant-specific colours, in line with *Chapter 3* (e.g., AA01=orange; AA02=blue; AA03=green; AA04=red).

4.3.3 Amputees demonstrate similar responses to the Beads Task as controls

As we did not find a reliable relationship between our bead's measures and controls in terms of learning about pain, we next wanted to explore, anecdotally, whether this relationship would be more poignant in the sample of amputees with PLP, due to the extreme alteration in sensory input from the phantom limb. When comparing the mean DTD for amputees (*M*=1.833, *Median*=1.67, *SD*=1.00) to controls (*M*=3.078, *Median*=3.00, *SD*=1.683), we anecdotally find a lower DTD for our amputee group, in line with previous research into those with persistent pain displaying significant JTC biases (Parkes et al., 2019). However, when looking at

individual values (see *Table 4.1*) we found that the amputee with the highest level of PLP within our sample (AA04) reported the highest DTD within the amputee group. Indeed, conversely one amputee with relatively low levels of chronic PLP (AA02) reported a JTC bias with a DTD of 1.

Amputee	Chronic PLP	DTD	Disconfirmatory Evidence	BDI	Trait Anxiety	PCS
AA01	25	1.00	18	8	36	12
AA02	4	1.00	0	4	27	16
AA03	13.33	2.33	13	24	54	30
AA04	90	3.00	9	11	33	33

Table 4.1. *Task and questionnaire details for amputee sample.* Chronic phantom limb pain (PLP) measures, along with Draws to Decision (DTD) and Disconfirmatory Evidence scores and questionnaires (Becks Depression Inventory (BDI), Trait Anxiety, Pain Catastrophising Scale (PCS)) for the amputee sample (in the above figures; AA01=orange; AA02=blue; AA03=green; AA04=red). Note AA01 and AA02 were classified as 'jumping-to-conclusions'.

We further note that one amputee (AA01), who was categorised as JTC, also demonstrated the greatest weighting of Disconfirmatory Evidence within our amputee sample (see *Figure 4.1.B* and *Table 4.1*), mirroring the significant relationship between DTD and Disconfirmatory Evidence shown in controls. This individual, therefore, seemed to very rapidly make judgments based on recent sensory information – akin to their high learning rate in *Chapter 3* (although we did not find a significant relationship between the two learning measures in controls). However, AA01 does not seem to report values significantly different to our control sample. Our other measures assessing DTC – Confirmatory Evidence and the Final Decision – in amputees also showcased similar distributions to controls (see

Supplementary Figure 14). This tentatively suggests that the presence of chronic pain itself may not be necessary for the occurrence of a JTC bias, contrary to predictions.

4.4 Discussion

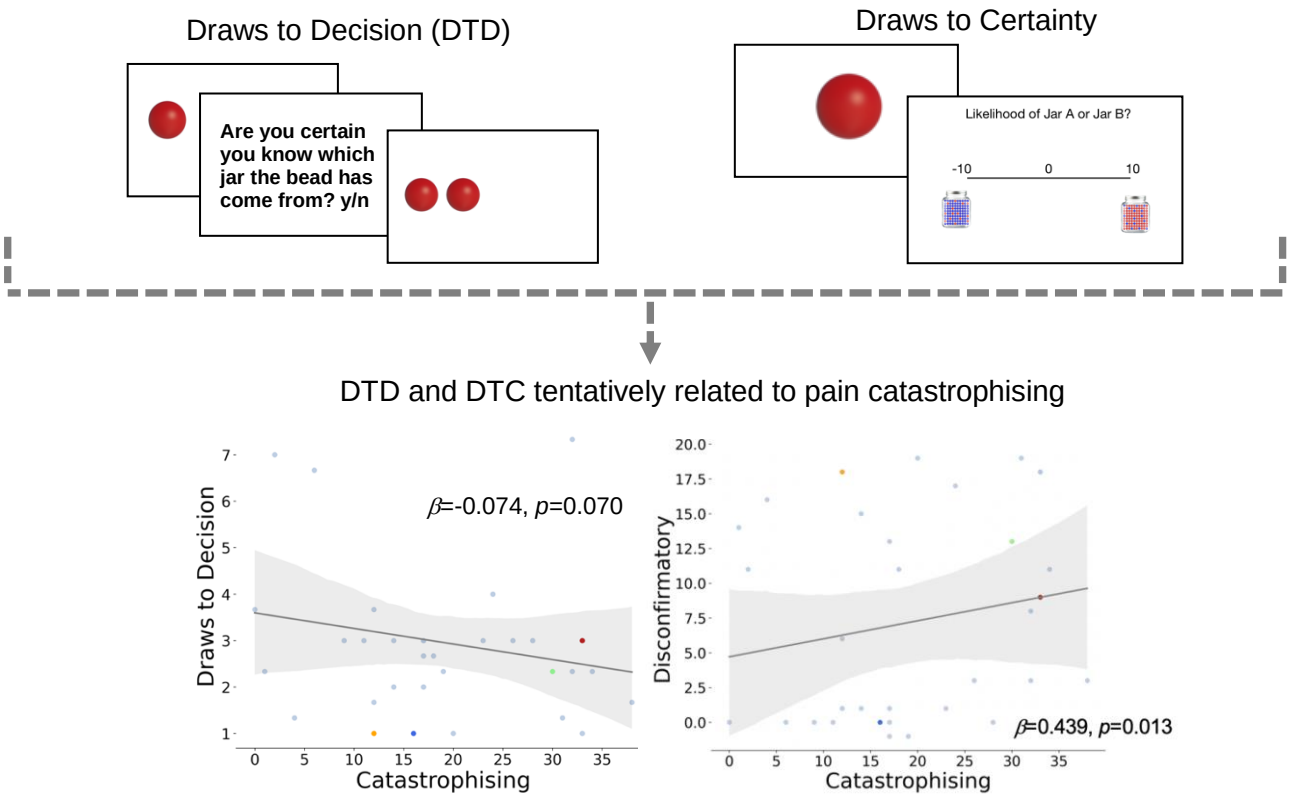


Figure 4.6. *Graphical summary of main findings and methodologies for Chapter 4. n*=32 two-handed controls and *n*=4 upper-limb amputees were recruited to participate in the Beads task, comprising of Draws to Decision (DTD) and Draws to Certainty (DTC) versions. Key results found tentative relationships between pain catastrophising and DTD and DTC, suggesting that those who are more inclined to 'jump-to-conclusions' are also more likely to catastrophise, i.e., rapidly form negative beliefs in response to sensory information. Similar responses between amputees and controls were also found, contrary to our predictions.

In computational psychiatry, a well-known and replicated finding is the 'jumping-to-conclusions' bias (JTC), whereby individuals with schizophrenia and delusions gather less sensory evidence before making a decision than healthy controls (Adams et al., 2018; Dudley et al., 2016; Hayashi et al., 2022; McLean et al., 2017; Ross et al., 2015; So et al., 2016; Strube et al., 2020, 2022). Evidence of this bias has also been reported in those with depression (Sastre-Buades et al., 2021), anxiety (Bensi & Giusberti, 2007), autism (Sahuquillo-Leal et al., 2020) and functional neurological disorders (Pareés et al., 2012), leading some to hypothesise that it may reflect a 'transdiagnostic' phenotype – a common bias in individuals susceptible to, or who have already developed, co-occurring neuropsychological disorders (Reininghaus et al., 2019). An impaired weighting of sensory evidence and prior expectation has also recently been theorised to contribute to the development of chronic pain (Hechler et al., 2016; Ongaro & Kaptchuk, 2018), with recent work demonstrating that the modulation of pain perception from expectation may result from biased perceptual decision-making (Wiech et al., 2022; Wiech, Vandekerckhove, et al., 2014). If JTC does therefore reflect a transdiagnostic trait, could we also find it present in those with chronic pain? To answer this, we used a common experimental paradigm to measure JTC, the beads task, in a particular chronic pain patient group – amputees with PLP, and healthy controls. As amputees often experience stochastic, fluctuant and painful sensations from the phantom limb, potentially leading to difficulties in learning and predicting sensory information originating in the phantom, they may be particularly prone to developing a JTC, or data-gathering, bias. We subsequently found that two amputees within our sample demonstrated a JTC bias, along with ~26.7% of healthy controls. We also found that DTD was

tentatively related to pain catastrophising, whereby lower DTD were associated with higher catastrophising scores. Furthermore, Disconfirmatory Evidence indicated significant relationships with pain catastrophising and trait anxiety, whereby less anxious individuals who tended to catastrophise more often would weight new sensory evidence to a greater extent. We did not find any significant relationships between bead measures and depression. For each bead task measure we found anecdotally similar results between our amputee sample and controls, with no significant and robust relationships found between pain learning (e.g., learning rate and placebo response) and beads measures.

A relatively significant proportion of our control sample (~26.7%) demonstrated DTD $\leq$ 2, indicating the presence of a JTC bias. Our results are in line with previous work, whereby a recent meta-analysis across 55 studies reported 29% of healthy participants and 38% of people with nonpsychotic mental health problems made a decision after 1-2 beads (Dudley et al., 2016; also see Freeman et al., 2008b where 20% of healthy controls JTC). This again supports the notion that JTC may reflect a generalised data-gathering bias in both individuals with schizophrenia (where it is more pronounced) and healthy controls, increasing the susceptibility of the individual towards developing delusional beliefs or non-psychotic mental disorders (Garety & Freeman, 2013). Indeed, a recent longitudinal study demonstrated that the JTC bias is likely present in individuals with both affective disorders (e.g., depression, anxiety) and psychotic experiences (Reininghaus et al., 2019), which not only influenced the development of psychosis, but also the persistence of psychosis over time (Livet et al., 2020; Rauschenberg et al., 2021). Thus, the JTC bias may be present in individuals prior

to the development of long-term symptoms, indicating that it may tentatively reflect a potential risk factor (although note the positive trend in Rauschenberg et al., 2021 for the relative risk ratio). As previous work addressing the JTC bias in other, non-psychotic disorders, including that of chronic pain, is low, it is difficult to ascertain whether JTC may also pose a risk factor in the development of other conditions, or whether it is specific to the formation of delusional beliefs. As we also found a tentative relationship of our bead task measures (in particular Disconfirmatory Evidence) to pain catastrophising and trait anxiety in healthy controls, we are tempted to support the former. However, future work, using longitudinal designs with large sample sizes of non-psychotic patients, are therefore encouraged to reliably clarify this proposition.

Thus, adding to this previous work in psychosis and supporting our initial prediction, we are, to the best of our knowledge, the first study that demonstrated a significant relationship between pain catastrophising and DTD/Disconfirmatory Evidence. As we also found a significant correlation between these two beads measures, we hypothesise that a similar mechanism underlies them both, whereby the individual is more likely to base their judgement on recent sensory evidence, rather than accumulate evidence before forming a belief. The relationship to pain catastrophising, therefore, may reflect individuals rapidly forming catastrophising expectations in response to little sensory input, i.e., rapid and unstable negative belief formation. It demonstrates again the potential transdiagnostic nature of the JTC bias, which may tap into a particular way of inference.

Interestingly, several recent studies have demonstrated the efficacy of cognitive-behavioural therapy (CBT), including metacognitive training, aimed at raising awareness and re-evaluating cognitive biases such as JTC (Moritz et al., 2014, 2022). In support of this, short courses of CBT (between 10 weeks – 3 months) have demonstrated improvement in positive, negative and depressive symptoms in those at risk from psychosis (Kim et al., 2011), and an explicit reduction of the JTC bias in line with improvements in anxious symptoms and paranoid ideation in individuals diagnosed with an anxiety disorder (Giusti et al., 2018). Indeed, one study demonstrated that a course of CBT in a youth at-risk group of psychosis targeted towards cognitive biases, delayed or prevented the transition to psychosis (although note only positive trend for reduction in JTC bias and small sample size; Landa et al., 2016). Recent evidence has also shown that CBT can help reduce pain catastrophising beliefs in those with chronic pain (Gilliam et al., 2021a; Schütze et al., 2018). This is of particular importance as catastrophising tends to develop with co-occurring mental disorders in patients (Slawek et al., 2022), and can increase the likelihood of failure of pain relief interventions (Schumann et al., 2022). Indeed, reductions in pain catastrophising early in treatment have demonstrated subsequent improvements in pain intensity and interference later on in those with neuropathic pain (Racine et al., 2016; although see Buvanendran et al., 2021). Catastrophising has also shown to be an important predicting factor in those with PLP (Richardson et al., 2007; Vase et al., 2011). Potentially the combination of pain catastrophising questionnaires and bead task measures, e.g., Disconfirmatory Evidence, may afford a more holistic approach to classifying cognitive traits in those with chronic pain. In regards to amputees with PLP, it may subsequently help identify individuals who are likely to be predisposed

to making negative, rapid expectations about their PLP and thus who may benefit more from PLP treatments targeting ‘top-down’ beliefs, e.g., CBT, rather than ‘bottom-up’ peripheral interventions. However, these results must be taken with caution. Our regression models were not shown to be significantly different from the null (although we note a positive trend for Disconfirmatory Evidence), and our related Bayes Factors, especially for DTD, were inconclusive. It could be that we simply did not have enough power within this study to draw robust conclusions, and therefore encourage future work, with more participants, to clarify the role, and explanatory power, of pain catastrophising and JTC.

Another possible limitation of the current study is our lack of control for inattention and fatigue during the task. For example, our average DTD of 3.078 bead draws is lower than that reported by previous studies in healthy controls (Hayashi et al., 2022; Pareés et al., 2012; Parkes et al., 2019). We also found that the majority of our controls, on average, had switched their support to Jar A (i.e., they had a score lower than zero on the likelihood scale) by the end of the DTC task in contrast to previous work (Pareés et al., 2012). Thus, participants may have demonstrated speedier decisions in DTD and DTC due to fatigue. The beads task was always administered at the end of the experimental session (after completing the aversive learning paradigm and questionnaires) and so participants may have been keen to finish. We attempted to mitigate these confounding factors to an extent via the two-item comprehension test and practice trials at the beginning of the DTD and DTC tasks, as well as with the presence of an experimenter during the task itself, yet we accept they may have influenced the overall reliability of the results (especially when concerning DTD).

Despite this, we did also find a tentative relationship between Disconfirmatory Evidence and trait anxiety (albeit in the opposite direction to our initial prediction), whereby individuals with higher trait anxiety scores weighted new sensory evidence to a lesser extent. As we believe DTD and Disconfirmatory Evidence reflects a similar inferential characteristic, our results are in line with previous work whereby significant positive correlations between anxiety measures and DTD in healthy controls have been found (McLean, Balzan, et al., 2020; Pareés et al., 2012). Taken together, these results may suggest that more anxious individuals require more DTD and weight new evidence to a lesser degree in forming beliefs. Indeed, previous work has shown that individuals with OCD or high levels of worry tend to require more evidence before making a decision than controls (Tallis et al., 1991; Toffolo et al., 2013).

However, as mentioned in *Chapter 4, Introduction* and in line with our initial prediction, conflicting results have been reported, whereby highly anxious individuals may actually require less DTD than controls (Bensi & Giusberti, 2007; Giusti et al., 2018) due to an intolerance of uncertainty and ambiguous situations. The difficulty in drawing robust conclusions for the directionality of the results may arise from the fact that anxiety measures are usually included within study designs as a control when making between-group comparisons to patients (as we initially intended), and so studies which specifically recruit individuals with anxiety disorders to explore JTC are scarce. This is also the same story for the relationship between JTC and depression. Surprisingly we did not find a significant correlation between DTD and depression in this study, contrary to previous work

and our initial prediction (Dudley et al., 2016; Moritz & Woodward, 2005; Sastre-Buades et al., 2021). Indeed, a recent meta-analysis assessing the relationship between JTC and non-psychotic mental disorders were only able to identify for OCD, anxiety disorders and depression 3-7 studies respectively, and subsequently found small, non-significant effect sizes (So et al., 2016; also see Strube et al., 2022). A possible reason for the heterogeneity of the current results may rest on state-trait dynamic (Strube et al., 2020). For example, a recent study found that those with non-psychotic mental disorders (e.g., depression, anxiety) demonstrated similar unstable belief updating and response stochasticity in the DTC task as schizophrenic patients when unwell. They reported no differences to controls once recovered (Adams et al., 2018; see also So et al., 2008; Freeman et al., 2013 for induction of worry). Therefore, the presence of the JTC bias may only manifest in other non-psychotic mental disorders during acute illness and may explain the tenuous relationships we found between depression and anxiety and bead task measures within this study.

This may also be particularly important in the case of chronic pain. Although we found a tentative relationship between DTD/Disconfirmatory Evidence and pain catastrophising, our amputees with PLP reported similar results to controls throughout. Two amputees did report a JTC bias, but these were individuals with low-to-medium levels of PLP (in relation to our sample), contrary to our predictions. Furthermore, we were unable to find a reliable and significant relationship between the learning rate and placebo responses in *Chapter 3* to any bead task measure. One previous study which had reported JTC in a persistent pain group, did not clarify which condition the patients currently suffered from,

whether they were currently in pain and did not find a significant relationship between DTD and pain severity (Parkes et al., 2019). Taken together, the relationship between the presence of JTC, PLP, and chronic pain in more general, is currently unclear. It may be that an inferential bias does exist in those with PLP, but it is specific to the presence of the pain itself, isolated to the weighting and gathering of nociceptive information only.

Despite this caveat, we do not think it rules out the transdiagnostic nature and usability of JTC – 30% of patients with chronic pain also catastrophise (Dong et al., 2020), and one amputee with PLP in particular, AA01, demonstrated incredibly high learning rates, small placebo responses, very small DTD (e.g., 1) and greater weighting of Disconfirmatory Evidence (although note low catastrophising score; see *Table 4.1*). Clearly for some individuals this way of inferring and interacting with the world is important. Chronic pain, and the development of other mental disorders, is heterogenous and idiosyncratic. A multitude of symptoms and experiences amalgamate together within the individual, developing personalised methods for inferring and gathering data from the world. It could be that this is what the JTC bias identifies – a certain bias in people who may be susceptible to developing a wide range of disorders, dependent on their experience. However, we must be careful not to JTC ourselves, and encourage future research to gather more reliable evidence regarding the suitable of using JTC as a transdiagnostic clinical tool to tailor treatment.

Chapter 5 | Discussion

5.1 Thesis overview

This thesis comprises of a set of experiments designed to assess potential neural mechanisms underlying, and theories behind, phantom limb pain (PLP). To do so, I first evaluated a popular theory of PLP – the maladaptive plasticity model – by testing one of its long-held assumptions using both univariate and multivariate neuroimaging analyses. I then subsequently set out to explore alternative hypotheses of PLP by designing a novel behavioural task and utilising a well-replicated paradigm from computational psychiatry, to quantify how individuals may process and learn about painful information and, anecdotally, how this may subsequently change in those with PLP. Taken together, my aim was to inform the characterisation of PLP beyond that of maladaptive plasticity in the cortex by providing possible future avenues of research.

In *Chapters 1* and *2* I showed that the cortical neighbour to the hand in the primary somatosensory cortex (S1) was likely to be the upper face. I argued that this has profound implications for the maladaptive plasticity model of PLP, which rests on the assumption that the lower face (in particular, the lips) borders the hand area and subsequently shifts into the deprived hand region after upper limb loss, triggering PLP. I also explored for the first time the mapping of the inner mouth, and tongue in particular, in congenital one-handers and amputees, and showed that amputees reported little evidence of somatotopic remapping of the upper and lower face (in particular the lips) in S1. Most importantly, I highlighted that any somatotopic shifts identified in amputees were similar in those with and without

PLP, indicating that pain is not necessarily associated with cortical remapping. In support of this, I also found that congenital one-handers, those born without a hand and who do not experience PLP, displayed significant amounts of facial remapping of both the upper and lower face, into the deprived hand area. In *Chapter 3* I introduced alternative mechanisms that could potentially contribute to the development of chronic PLP. I first introduced a novel behavioural paradigm designed specifically to assess how amputees learn about painful information in relation to movement of their phantom limb. Anecdotal conclusions indicated that amputees displayed a preserved placebo response and idiosyncratic learning styles. Results in control participants also indicated significant learning of probabilistic cues when involving movements, validating the use of such a paradigm for exploring the relationship between associative learning and PLP in future studies. Finally, in *Chapter 4*, I showed that a 'jumping-to-conclusions' (JTC) bias, whereby individuals require little sensory information to form a belief, was tentatively related to pain catastrophising.

These results not only provide an assessment of one of the most common explanations of PLP, but also advance our understanding of the condition by offering novel behavioural paradigms which may allow exploration of PLP mechanisms outside the cortex. I will discuss the broader implications of this work, and in particular, how it may inform future treatment options, below.

5.2 Maladaptive plasticity model – where do we go from here?

Traditionally, maladaptive plasticity in S1 has thought to be a leading factor in triggering PLP (see Flor et al., 2006 for an overview). Indeed, such cortical reorganisation has hypothesised to underly other chronic pain conditions, ranging from complex regional pain syndrome (Maihöfner et al., 2004, 2006; although see Mancini et al., 2019), chronic lower back pain (Flor et al., 1997), dystonia (Burman et al., 2009; Elbert et al., 1998; although see Sadnicka et al., 2021) and spinal cord injury (Wrigley et al., 2009; although see Kikkert et al., 2021). When the chronic pain (regardless of diagnosed condition) is localised to the upper limb, a key measurement of cortical reorganisation is the topographic shift of the lips due to the assumed cortical proximity of the hand and lower face (Flor, Nikolajsen, & Staehelin Jensen, 2006; Maihöfner et al., 2004; Wrigley et al., 2009).

Results presented in *Chapters 1* and *2*, however, demonstrate not only that the cortical neighbour to the hand is likely the upper face, but that there was also very little evidence of cortical remapping of facial parts (upper and lower) in amputees. Indeed, recent work has also begun to question the key assumptions underlying cortical reorganisational theories. For example, a recent paper which used anaesthetic nerve blocks administered to humans' index fingers in order to parallel the seminal reorganisational work carried out in non-human primates (Merzenich et al., 1984), found that resulting 'remapping' could have arisen from methodological restrictions. Specifically, they found that when the anaesthetised fingers' activity was included in a winner-takes-all quantification of the canonical digit map, no significant increase of the neighbouring digit's activity in the deprived area was found, i.e., no cortical remapping. Conversely, when the activity for the

anaesthetised finger was removed from the baseline analysis, results paralleled that of traditional reorganisational studies – neighbouring digits had encroached into the deprived finger area (Wesselink et al., 2022). Interestingly, the authors reported that the induced sensory input loss from the anaesthetised finger actually resulted in a global down-scaling of activity and selectivity across all digits in the hand region, and did not selectively impact the neighbouring representations. This is in line with relatively recent work suggesting that somatotopic organisation in S1 may be more distributed than previously thought. Indeed, even Penfield & Boldrey (1937) reported in their foundational study that the homunculus in S1 contained large overlaps between body part representations. In support of this notion of an overlapping, rather than selective, homunculus, it has been found that information content for different body parts is widely spread across S1 in two-handed controls, with evidence of significant content for different face parts found in the hand area and the non-neighbouring region of the foot (Muret et al., 2022).

In the context of sensory deprivation, cortical remapping in S1 may therefore subsequently emerge from uncovering this pre-existing, distributed latent activity (e.g., shared representational overlap). Following the removal of the map's dominant input, upregulation of the latent activity may manifest as 'remapping', but this process may actually reflect a homeostatic plasticity process, aimed at stabilisation of the system as a whole, and not reorganisation per se (Muret & Makin, 2021). While unmasking has always been considered a key process underlying reorganisation, this perspective suggests that the observed changes to the cortical body map do not represent a functional reallocation of cortical resources, and thus by definition cannot be functionally relevant (i.e.,

maladaptive). In *Chapter 2*, results also showed that remapping for congenital one-handers (and to a lesser extent, amputees) also extended beyond cortical neighbours to the hand, supporting the notion of a distributed somatotopy. Interestingly, the pattern of remapping reported in *Chapter 2* also suggested the influence of adaptive behaviour in shaping the emergent, 'reorganised' maps. For example, in both one-handed groups the forehead was shown to shift away from the deprived hand region (tentatively in amputees), which in turn, displayed increases in lip (one-handers only) and tongue activity, i.e., facial parts which may replace the function of a hand, e.g., using the mouth and/or tongue to manipulate objects. Thus, daily behaviour, and how that individual compensates for upper limb loss, may be subsequently reflected in their cortical somatotopy, possibly via Hebbian-like plasticity (Dempsey-Jones et al., 2019; Hahamy et al., 2017; Makin et al., 2013). This may be exaggerated in those who are born without a hand due to their lack of typical hand representational structure in S1 (Wesselink et al., 2019), thus the employment of other, non-neighbouring body parts mirroring the function of the hand (although see Striem-Amit et al., 2018), may capitalise on latent activity in that cortical area resulting in gross cortical remapping (Muret & Makin, 2021). Subsequent research has demonstrated potentially functional outcomes of this remapping in one-handers, whereby transcranial magnetic stimulation over the missing hand area elicited responses in the foot and mouth (Amoruso et al., 2021; Stoeckel et al., 2009).

However, no conclusive evidence has been found for functional remapping in amputees yet. In fact, this adaptive remapping in amputees is usually denoted by an increase in activity for the intact hand in the deprived hand area (Makin et al.,

2013; Raffin et al., 2016; Valyear et al., 2020), which may reflect inter-hemispheric plasticity and/or homeostatic mechanisms (Muret & Makin, 2021; Valyear et al., 2020), rather than adaptive functional outcomes, i.e., over-use of the intact hand after amputation (although see Makin et al., 2013). As *Chapter 2* found evidence for potential remapping of the tongue (a non-neighbour and non-homologous representation to the hand), as well as a significant decrease in overall facial information content in the intact hemisphere, it is tempting to hypothesise that non-functionally relevant remapping occurs in amputees. However, future research is needed to clarify the adaptive role of cortical remapping in amputees, with a particular focus on thorough mapping of the tongue (see *Discussion, Chapter 2*) and assessing the extent of changes in the intact hemisphere. Maladaptive plasticity, therefore, may reflect a neural mechanism to foster homeostatic stability after sensory deprivation, but is not necessarily maladaptive nor a prerequisite for pain. Using such a model to infer a chronic pain condition or inform treatment options (Moseley & Flor, 2012), may therefore be misguided.

5.3 Phantom limb pain beyond the primary somatosensory cortex

In confirmation of the above, key to my findings in *Chapter 2* was a lack of evidence relating these (small) somatotopic shifts of the face to PLP in amputees. Thus, if maladaptive plasticity may no longer be an informative mechanism of PLP, what alternative explanations exist? In line with computational accounts of pain (Büchel et al., 2014; Seymour, 2019; Tabor & Burr, 2019), imbalances between pain predictions and sensory (nociceptive) information have recently been theorised to contribute to the development of chronic pain (Hechler et al., 2016; Ongaro & Kaptchuk, 2018). Within this computational framework, PLP may

be reframed as the following: sustained and aberrant, ‘bottom-up’ nociceptive firing from the periphery (Nystrom & Hagbarth, 1981) may lead to an over-weighting of ‘top-down’ predictions of perceived bodily threat and robust expectations of pain. Pairing this predictive imbalance with the restricted motor repertoire in amputees, thereby preventing adequate sampling of the environment in order to ‘re-assign’ the weighting between ‘top-down’ expectations and ‘bottom-up’ sensory information, may thus lead to more stubborn and persistent priors (Yon et al., 2019), and the development of a chronic pain state. The below section will thus focus on contextualising this proposition of PLP, tying in previous work on phantom motor control, the periphery, cortical pain regions and associative learning mechanisms, and whether these disparate pieces of evidence fit together to adequately explain PLP (or not).

Firstly, as stated in the *Introduction*, peripheral mechanisms are clearly important in driving PLP, not only in terms of abnormal nociceptive firing (Nystrom & Hagbarth, 1981; Vaso et al., 2014), but also via direct engagement with the phantom limb, e.g., residual muscle contractions and phantom motor control (Gagné et al., 2009; Kikkert et al., 2017; Therrien et al., 2021). Measurements associated to PLP in these studies involved the use of electromyography (EMG) on the residual limb to assess contraction amplitude and movement times, with larger amplitudes and longer movement times associated with PLP. The authors hypothesise that this may reflect either efferent retargeting in the residual limb (Gagné et al., 2009; Therrien et al., 2021), or the preserved nociceptive firing at the periphery (Kikkert et al., 2017), leading to deteriorated motor control, e.g., reduced movement, redistribution of muscular activity and overall reduced

amplitude of contractions (Hodges & Tucker, 2011). These peripheral factors may contribute to an imbalance of predictions/sensory input in two ways. Firstly, efferent retargeting may hinder accurate phantom motor execution, thereby impeding movement that may relieve pain or produce innocuous outcomes (Barnes et al., 2021; Hodges & Smeets, 2015). Thus, in line with the fear avoidance model of pain, sustained avoidance and safety behaviours may ensue, i.e., reducing movement of the phantom, reinforcing top-down expectations of bodily threat and fear. Secondly, nociceptive firing at the periphery may not only directly intersect with motor control adaptations (Hodges & Tucker, 2011), but also reinforce top-down expectations of pain, which increases the likelihood of interpreting innocuous, or 'noisy', interoceptive sensations as more painful than they actually are, e.g., a nocebo-like effect (Hechler et al., 2016; Ongaro & Kaptchuk, 2018), as shown by one amputee in *Chapter 3*. This may be particularly enhanced in amputees due to the stochastic nature of the somatosensory landscape of the phantom limb. Here interoceptive and proprioceptive sensations tend to be dominated by feelings of tingling, itching or numbness, which, due to their unnaturalistic qualia, may be more susceptible to up-regulation (and thus harder to downregulate) by strong, top-down pain predictions. Furthermore, this introduces a state of uncertainty for the individual, as nociceptive firing is likely to be aberrant and unpredictable. States of uncertainty themselves are known to have hyperalgesic effects (Yoshida et al., 2013). It has also been proposed that unpredictable pain can trigger sustained prediction error signalling, i.e., a continuous discrepancy between a prediction and sensory input, which may again be enhanced in amputees due to the stubbornness of predictions as a result of impaired motor control. This persistent prediction error signalling may in turn lead

to perceptual widening and a generalisation of pain (Vlaeyen, 2015). Peripheral mechanisms, therefore, are an important factor in characterising a predictive imbalance. A key implication of this framework is that the exact weighting between expectations and sensory information may differ across individuals (see *Discussion*, *Chapter 3*), dependent on the integrity of the peripheral nerves, optimality of reinnervation and existence of neuromas. These factors amalgamate to produce the overall somatosensory landscape of the phantom limb, and thus the quality and quantity (nociceptive, innocuous and kinaesthetic) of the sensory input into the system.

Movement of the phantom has not only been shown to activate the deprived hand region in S1 (Kikkert et al., 2016, 2018; Makin, Scholz, et al., 2013; Wesselink et al., 2019), as stated in the *Introduction*, but also regions beyond the sensorimotor cortices. For example, when moving the phantom hand activation can be found in typical pain processing and threat detection networks, such as the bilateral insula and the anterior cingulate cortex (ACC) (Kikkert et al., 2018; Makin, Scholz, et al., 2013). The phantom hand area in amputees has also been shown to display increased functional connectivity to the insula at rest, when compared to controls (Kikkert et al., 2019). Furthermore, a recent study demonstrated that upregulation of these pain processing regions, in particular the posterior insula, subsequently led to downregulation of activity in the deprived hand area and PLP relief after a short course of non-invasive brain stimulation over the missing hand region during phantom movements (Kikkert et al., 2019). Interestingly, recent work in pain perception has demonstrated that the processing of pain predictions and prediction errors, including their weighting, is likely to occur in regions such as the

anterior and dorsal posterior insula (Fazeli & Büchel, 2018; Geuter et al., 2017; Horing & Büchel, 2022). In support of this, subsequent neuroimaging work has not only shown activation of the dorsal posterior insula in the generation of tonic pain in healthy controls (Segerdahl et al., 2015), but also of the anterior insula in response to endogenous pain fluctuations of those with a chronic pain condition, e.g., chronic back pain, chronic migraine (Ferraro et al., 2022; Mayr et al., 2022; also see Kaplan et al., 2019 for the importance of posterior insula activation in fibromyalgia). Furthermore, the ACC has previously been implicated in signalling prediction error and surprise (Alexander & Brown, 2019; Roy et al., 2014), and is an important cortical region in pain, cognitive control and negative affect (Shackman et al., 2011; Xiao & Zhang, 2018). Work using rodent pain models has demonstrated the importance of ACC in pain sensitisation of the spinal cord in peripheral nerve injury (Chen et al., 2018), as well as promoting reflexive and active avoidance behaviour towards pain (via the periaqueductal gray; Lee et al., 2022). In humans, activation in the rostral ACC has also been shown to increase in response to spontaneous pain of chronic back pain patients, and was related to the subsequent intensity of the pain (Baliki et al., 2006). Thus, regions outside of S1 shown to activate in amputees are also widely associated with not only predictive processing of pain expectations and prediction error, but also chronic pain more generally. However, despite one study associating insula activity to PLP relief (Kikkert et al., 2019), the direct association of insula and ACC activity to PLP is yet to be shown. Thus, future work using neuroimaging focusing on the above cortical regions-of-interest (as well as other prefrontal regions; see Wiech et al., 2022) in amputees with PLP may be able to ascertain whether robust associations between PLP and cortical activity outside of S1 exist.

There are, however, a few neuroimaging studies which have investigated cortical activation patterns of pain expectations and sensory input in other chronic pain patient groups. One recent study employed a paradigm whereby two cues (red and green) were initially associated with high and low pain stimulation. During the testing phase, the painful stimulation for the green (low-pain) cue was increased. Subsequently, activity in M1 and the anterior insula also increased in patients with fibromyalgia, reflecting the change in noxious stimulation (Sandström et al., 2020). Similar associative learning paradigms have also been used extensively in behavioural studies. Here chronic pain patients have been shown to demonstrate reduced extinction rates (Flor, 2002), potentially indicating more stubborn pain predictions, and sub-optimal learning strategies reflecting greater precision on prediction errors (Brown et al., 2020). Interestingly, a recent study demonstrated that associative threat learning was not only worse in chronic lower back pain patients than controls, but that this was related to pain duration, e.g., the longer the individual was in pain, the greater the reduction in threat learning (Schlitt et al., 2021). Thus, the ability to learn associations between expectations and nociceptive input may not only change, but worsen, the longer that the individual is in pain. PLP has been reported to be relatively stable over time (Schone et al., 2022), however, it could be that the predictive balancing underlying the generation of PLP may fluctuate temporally. For example, in the field of computational psychiatry, a recent study demonstrated that in the early stages of psychosis a decreased sensitivity to perceptual priors may subsequently lead to an over-weighting of cognitive priors needed to explain the incoming sensory information (Haarsma et al., 2020). Could a similar adjustment of weighting be played out in

those with PLP? For example, PLP originates initially from a traumatic nerve injury, i.e., the amputation, which may thus exemplify nociceptive peripheral firing and prediction error, which could in turn lead to the over-weighting of 'top-down' predictions of bodily threat and pain. Indeed, anecdotal results in *Chapter 3* demonstrated that one amputee displayed a sensitivity towards pain expectations and another to sensory input. In further support of this, previous work has demonstrated that risk factors associated with PLP include pre-existing pain, depression, anxiety and pain catastrophising (Fuchs et al., 2018; Larbig et al., 2019; Vase et al., 2011), which may all differ across individuals, and contribute to the emergent formation, and weighting, of pain expectations after amputation.

How can we quantify the above factors in an experimental paradigm for PLP? The utilisation of an associative learning paradigm may be key, as it could provide a richer context in which to situate the individual's pain experience by quantifying expectation biases (of pain or relief, dependent on the associative cue), optimality of learning (via acquisition and extinction rate), and how nociceptive information is processed, i.e., precision weighting (via application of computational models, e.g., reinforcement learning, hierarchical gaussian filter models). The associative learning paradigm proposed in *Chapter 3* (which demonstrated successful learning in controls), would be suited to amputees as the integration of EMG recordings on the residual limb would allow for quantification of motor control and how this may intersect with learning of pain predictions. Future work may want to consider combining the above associative learning paradigm and neuroimaging in amputees with PLP, specifically focusing on processing in regions-of-interest such as the insula and ACC. A within-subject, active versus passive, functional MRI

paradigm would therefore shed some light on how (and if) engagement of phantom movements modulates activity in these regions and predictive processing. In summary, to provide a detailed characterisation of PLP beyond S1, a holistic and individualistic approach is needed, which takes into account the role of the periphery (including motor control) and top-down, cognitive factors (e.g., associative learning), and how these factors interplay across time.

5.4 Future treatment avenues for phantom limb pain

By reframing PLP beyond that of a predominantly cortical phenomenon, this also allows the opportunity for development of novel treatments. A promising avenue stems from findings in *Chapter 3*, which showed that executing a movement not only boosted placebo responses to nociceptive stimuli in two-handed controls, but that all amputees tested displayed similar preserved placebo responses. The consequences of this for treatment are three-fold: the importance of controlling for placebo responses in clinical trials (as discussed in *Chapter 3*), setting adequate treatment expectations and utilising endogenous analgesia for treatment itself. When setting treatment expectations, utilisation of placebo responses may be aid in subsequent treatment success. For example, by presenting a novel treatment in a positive manner, with the patient fully informed regarding the underlying mechanisms and expected outcomes, may consequently enhance a potential successful response to that treatment, i.e., encouraging pain relief (Albu et al., 2022). Indeed, an extreme version of this in practice is open-label placebo (OLP) interventions, whereby patients are prescribed a placebo treatment without deception. Recent work has shown that OLP improved symptoms in those with irritable bowel syndrome, when compared to no treatment, and did not differ in

symptom improvements when compared to a double-blind placebo control group (Lembo et al., 2021). Surprisingly, pain relief for chronic lower back pain patients gained through an OLP intervention were shown to last to up to 5 years after treatment (Carvalho et al., 2021). Thus, utilising the placebo response to tailor treatment expectations may be beneficial in promoting pain relief in individuals with PLP.

Placebo analgesia may also be used in combination with existing treatments for PLP. Results in *Chapter 3* demonstrated that phantom movements, which has previously been related to worsening PLP, can also be associated with the opposite – pain relief. Popular treatment options for PLP currently either require imagined movements of the phantom (e.g., graded motor imagery, mirror therapy; (Thieme et al., 2016) or actual movements using augmented reality (Ortiz-Catalan et al., 2016). However, the aims of such treatment usually include moving the phantom into certain postures, arbitrary associations between a phantom movement and a virtual game (e.g., moving a cursor around a screen), or neglecting moving the phantom at all (e.g., moving the intact hand in a mirror). They focus on engagement with the phantom, but not on the context, or the functional role, of that engagement. Results in *Chapter 3* demonstrated that contextual cues are important and can be a powerful tool in terms of treatment. Thus, subsequent treatment approaches may want to consider using naturalistic phantom movements associated with relief-predictive cues. These movements would not only capitalise on the preserved sensorimotor pathway (central and peripheral) of the phantom, but could also be made in response to everyday objects or interactions (e.g., forming a grasp to open a door). This would situate

the ‘re-training’ of the phantom limb with innocuous responses within a familiar environment that contains meaning to the individual and their pain. For example, if a particular movement is known to induce PLP, by enacting these very same actions with innocuous outcomes (either via peripheral nerve blocks or acute experimental pain to the residual limb) may encourage the re-evaluation, or re-weighting, of the formed association. This could also be done in line with task concurrent non-invasive brain stimulation, which has shown promising pain-relieving outcomes previously (Bolognini et al., 2013, 2015; Kikkert et al., 2019).

As stated in the previous section, however, heterogeneity is important in PLP. A type of treatment which might be beneficial to one individual, may not work as well for another. Thus, future treatments for PLP may want to consider tailoring the treatment offered to the PLP presented (also see *Discussion*, *Chapter 4*). A trait which may be useful in identifying amputees who may particularly benefit from treatment is those who catastrophise. For example, several studies have found that pain catastrophising positively correlates to the magnitude of PLP (Fuchs et al., 2018; Richardson et al., 2007; Vase et al., 2011). Additionally, research has found that catastrophising before amputation significantly predicted PLP six months after amputation, more so than pre-operative pain (Richardson et al., 2007). Identifying patients who catastrophise is particularly important in treating chronic pain because it is known to influence treatment success (Schumann et al., 2022), and may be an indicator of the formation of fear-avoidance beliefs or negative pain priors (see above). In *Chapter 4*, Draws to Decision and Disconfirmatory Evidence in the beads task, which measures how much sensory information individuals need to form a belief, was tentatively shown to correlate

with pain catastrophising in controls. The beads task is a popular, well-replicated task used in computational psychiatry (see *Chapter 4* for full description), and may therefore provide a validated and reliable implicit measurement of pain catastrophising (in addition to questionnaires). As the significant association was identified in controls, it may also allow clinicians to pinpoint individuals who may be predisposed to developing catastrophising beliefs prior to amputation. Furthermore, the beads task also allows identification of individuals who JTC, i.e., those who need less sensory information before forming a rapid belief. By administering the task at different timepoints (e.g., before and after amputation), it could provide a proxy measure of predictive weighting in those with PLP. For example, those who are more sensitive to prediction error may also display a greater JTC bias (see results for AA01 in *Chapter 3* and *Chapter 4*). This could subsequently allow the tailoring of treatment options based on the heterogeneity (or predictive balance) of the PLP presented. However, as associations between beads task measures, pain learning measures and pain catastrophising were only tentative in *Chapter 4*, I strongly encourage future research, with larger sample sizes, to quantify the relationship to PLP, as the potential to use this quick, cheap and easy-to-administer task in clinic is great.

5.5 Concluding remarks

A key question that remains to the field, however, is whether PLP treatment should be targeted towards resolving the mechanisms underlying the pain, or relieving the resulting symptoms. The swathe of treatments aimed to ‘normalise’ maladaptive cortical remapping in S1, including mirror therapy and graded motor imagery, all focused on fixing a mechanism of the pain (Moseley & Flor, 2012).

However, as has been discussed above, cortical reorganisation is unlikely to be associated with emergent pain after amputation. Thus, multiple treatment instantiations stemming from the same concept dominated PLP treatment for decades, with little to no reliable, or clinically significant, pain relief (Aternali & Katz, 2019; Makin, 2021; Richardson & Kulkarni, 2017; Schone et al., 2022). Turning the focus to more symptom-based management of their pain may be more beneficial in the short-term. Indeed, OLP administered in other chronic pain populations look promising and may be a better alternative to long-term pharmacological management of PLP. Furthermore, cognitive behavioural therapy targeted towards managing pain catastrophising beliefs (as well as co-morbid depression and anxiety), have also been related to improved quality of life and pain interference measures (Gilliam et al., 2021). However, perhaps it is not an either/or question, but one that requires a holistic and personalised approach. For example, recent advances in peripheral nerve surgeries, such as targeted muscle reinnervation (TMR) and regenerative peripheral nerve interfaces, which could be done at the time of amputation, are showcasing promising results, with one study reporting that 62% of amputees were without PLP after TMR at the time of amputation compared to 24% of benchmark controls (O'Brien et al., 2021). By integrating treatment options that target potential peripheral mechanisms (e.g., neuromas and aberrant peripheral firing), as well as considering symptom-based management after amputation, may offer the best opportunity for PLP relief in the long-term. Thus, it is only when we step aside from viewing PLP as a homogenous perceptual response to localised cortical remapping, and reframing it as a complex, multifaceted phenomenon which encompasses the whole system

(peripheral, cortical and cognitive) can we then begin to design holistic treatment approaches that foster PLP relief.

References

Abreu, V., Vaz, R., Chamadoira, C., Rebelo, V., Reis, C., Costa, F., Martins, J., Gillies, M. J., Aziz, T. Z., & Pereira, E. A. C. (2022). Thalamic deep brain stimulation for post-traumatic neuropathic limb pain: Efficacy at five years' follow-up and effective volume of activated brain tissue. *Neurochirurgie*, *68*(1), 52–60. https://doi.org/10.1016/J.NEUCHI.2021.06.006

Adams, R. A. (2018). Bayesian Inference, Predictive Coding, and Computational Models of Psychosis. *Computational Psychiatry: Mathematical Modeling of Mental Illness*, 175–195. https://doi.org/10.1016/B978-0-12-809825-7.00007-9

Adams, R. A., Napier, G., Roiser, J. P., Mathys, C., & Gilleen, J. (2018). Attractor-like Dynamics in Belief Updating in Schizophrenia. *Journal of Neuroscience*, *38*(44), 9471–9485. https://doi.org/10.1523/JNEUROSCI.3163-17.2018

Adams, R. A., Stephan, K. E., Brown, H. R., Frith, C. D., & Friston, K. J. (2013). The computational anatomy of psychosis. *Frontiers in Psychiatry*, *4*(May), 1–26. https://doi.org/10.3389/fpsyt.2013.00047

Aiyer, R., Barkin, R. L., Bhatia, A., & Gungor, S. (2017). A systematic review on the treatment of phantom limb pain with spinal cord stimulation. *Pain Management*, *7*(1), 59–69. https://doi.org/10.2217/PMT-2016-0041/ASSET/IMAGES/LARGE/FIGURE1.JPEG

Alaiti, R. K., Zuccolo, P. F., Hunziker, M. H. L., Caneiro, J. P., Vlaeyen, J. W. S., & Fernandes da Costa, M. (2020). Pain can be conditioned to voluntary movements through associative learning: an experimental study in healthy participants. *Pain*, *161*(10), 2321–2329. https://doi.org/10.1097/J.PAIN.0000000000001919

Albu, S., Linsenbardt, H., & Meagher, M. W. (2022). Cognitive-affective modulation of pain: The placebo and nocebo phenomena and their impact on pain treatment. *The Neurobiology, Physiology, and Psychology of Pain*, 375–386. https://doi.org/10.1016/B978-0-12-820589-1.00033-6

Alexander, W. H., & Brown, J. W. (2019). The Role of the Anterior Cingulate Cortex in Prediction Error and Signaling Surprise. *Topics in Cognitive Science*, *11*(1), 119–135. https://doi.org/10.1111/TOPS.12307

Amoruso, E., Kromm, M., Spampinato, D., Kop, B., Muret, D., Rothwell, J., Rocchi, L., & Makin, T. R. (2021). Stimulating the deprived motor 'hand' area causes facial muscle responses in one-handers. *Brain Stimulation*. https://doi.org/10.1016/j.brs.2021.01.022

Anani, A., & Körner, L. (1979). Discrimination of phantom hand sensations elicited by afferent electrical nerve stimulation in below-elbow amputees. *Medical Progress through Technology*, *6*(3), 131–135.

Andersson, J. L. R., Jenkinson, M., & Smith, S. (2010). *Non-linear registration, aka spatial normalization (FMRIB technical report TR07JA2)*. *June*.

Andoh, J., Milde, C., Diers, M., Bekrater-Bodmann, R., Trojan, J., Fuchs, X., Becker, S., Desch, S., & Flor, H. (2020). Assessment of cortical reorganization and preserved function in phantom limb pain: a methodological perspective. *Scientific Reports*, *10*(1), 1–15. https://doi.org/10.1038/s41598-020-68206-9

Andoh, J., Milde, C., Tsao, J. W., & Flor, H. (2018). Cortical plasticity as a basis of phantom limb pain: Fact or fiction? *Neuroscience*, *387*, 85–91. https://doi.org/10.1016/j.neuroscience.2017.11.015

Ariani, G., Pruszynski, J. A., & Diedrichsen, J. (2022). Motor planning brings human primary somatosensory cortex into action-specific preparatory states. *Elife*, *11*, e69517.

Aternali, A., & Katz, J. (2019). Recent advances in understanding and managing phantom limb pain. *F1000Research*, *8*, 1167. https://doi.org/10.12688/F1000RESEARCH.19355.1

Atlas, L. Y., Doll, B. B., Li, J., Daw, N. D., & Phelps, E. A. (2016). Instructed knowledge shapes feedback- driven aversive learning in striatum and orbitofrontal cortex, but not the amygdala. *ELife*, *5*(MAY2016), 1–26. https://doi.org/10.7554/eLife.15192

Atlas, L. Y., Sandman, C. F., & Phelps, E. A. (2022). Rating expectations can slow aversive reversal learning. *Psychophysiology*, *59*(3), 1–15. https://doi.org/10.1111/psyp.13979

Atlas, L. Y., & Wager, T. D. (2012). How expectations shape pain. *Neuroscience Letters*, *520*(2), 140–148. https://doi.org/10.1016/J.NEULET.2012.03.039

Balakhanlou, E., Webster, J., Borgia, M., & Resnik, L. (2021). Frequency and Severity of Phantom Limb Pain in Veterans with Major Upper Limb Amputation: Results of a National Survey. *PM&R*, *13*(8), 827–835. https://doi.org/10.1002/PMRJ.12485

Baliki, M. N., Chialvo, D. R., Geha, P. Y., Levy, R. M., Harden, R. N., Parrish, T. B., & Apkarian, A. V. (2006). Chronic Pain and the Emotional Brain: Specific Brain Activity Associated with Spontaneous Fluctuations of Intensity of Chronic Back Pain. *Journal of Neuroscience*, *26*(47), 12165–12173. https://doi.org/10.1523/JNEUROSCI.3576-06.2006

Barbin, J., Seetha, V., Casillas, J. M., Paysant, J., & Pérennou, D. (2016). The effects of mirror therapy on pain and motor control of phantom limb in amputees: A systematic review. *Annals of Physical and Rehabilitation Medicine*, *59*(4), 270–275. https://doi.org/10.1016/J.REHAB.2016.04.001

Barnes, K., McNair, N. A., Harris, J. A., Sharpe, L., & Colagiuri, B. (2021). In anticipation of pain: expectancy modulates corticospinal excitability, autonomic response, and pain perception. *Pain*, *162*(8), 2287–2296. https://doi.org/10.1097/J.PAIN.0000000000002222

Barroso, J., Branco, P., & Apkarian, A. V. (2021). Brain mechanisms of chronic pain: critical role of translational approach. *Translational Research*, *238*, 76–89. https://doi.org/10.1016/J.TRSL.2021.06.004

Beck, A. T., Ward, C. H., Mendelson, M., Mock, J., & Erbaugh, J. (1961). An Inventory for Measuring Depression. *Archives of General Psychiatry*, *4*(6), 561–571. https://doi.org/10.1001/ARCHPSYC.1961.01710120031004

Becker, S., Gandhi, W., Kwan, S., Ahmed, A. K., & Schweinhardt, P. (2015). Doubling Your Payoff: Winning Pain Relief Engages Endogenous Pain Inhibition. *ENeuro*, *2*(4). https://doi.org/10.1523/ENEURO.0029-15.2015

Beckler, K. (2010). State-Trait Anxiety Inventory for Adults Sampler Set Manual, Instrument and Scoring Guide. *1983 Consulting Psychologists Press, Inc. Mind Garden, Inc.*, 0–78. https://doi.org/10.1037/T06496-000

Bedwell, S. A., Billett, E. E., Crofts, J. J., & Tinsley, C. J. (2014). The topology of connections between rat prefrontal, motor and sensory cortices. *Frontiers in*

Systems Neuroscience, *8*, 177. https://doi.org/10.3389/FNSYS.2014.00177/BIBTEX

Bensi, L., & Giusberti, F. (2007). Trait anxiety and reasoning under uncertainty. *Personality and Individual Differences*, *43*(4), 827–838. https://doi.org/10.1016/J.PAID.2007.02.007

Berlot, E., Prichard, G., O'Reilly, J., Ejaz, N., & Diedrichsen, J. (2019). Ipsilateral finger representations in the sensorimotor cortex are driven by active movement processes, not passive sensory input. *Journal of Neurophysiology*, *121*(2), 418–426. https://doi.org/10.1152/JN.00439.2018/ASSET/IMAGES/LARGE/Z9K0011949240005.JPEG

Bestmann, S., Oliviero, A., Voss, M., Dechent, P., Lopez-Dolado, E., Driver, J., & Baudewig, J. (2006). Cortical correlates of TMS-induced phantom hand movements revealed with concurrent TMS-fMRI. *Neuropsychologia*, *44*(14), 2959–2971. https://doi.org/10.1016/J.NEUROPSYCHOLOGIA.2006.06.023

Bingel, U., Wanigasekera, V., Wiech, K., Mhuircheartaigh, R. N., Lee, M. C., Ploner, M., & Tracey, I. (2011). The effect of treatment expectation on drug efficacy: Imaging the analgesic benefit of the opioid remifentanil. *Science Translational Medicine*, *3*(70). https://doi.org/10.1126/SCITRANSLMED.3001244/SUPPL_FILE/3-70RA14_SM.PDF

Birbaumer, N., Lutzenberger, W., Montoya, P., Larbig, W., Unertl, K., Töpfner, S., Grodd, W., Taub, E., & Flor, H. (1997). Effects of regional anesthesia on phantom limb pain are mirrored in changes in cortical reorganization. *The Journal of Neuroscience : The Official Journal of the Society for Neuroscience*, *17*(14), 5503–5508. http://www.ncbi.nlm.nih.gov/pubmed/9204932

Bittar, R. G., Otero, S., Carter, H., & Aziz, T. Z. (2005). Deep brain stimulation for phantom limb pain. *Journal of Clinical Neuroscience*, *12*(4), 399–404. https://doi.org/10.1016/J.JOCN.2004.07.013

Bland, A. R., & Schaefer, A. (2012). Different varieties of uncertainty in human decision-making. *Frontiers in Neuroscience*, *0*(JUN), 85. https://doi.org/10.3389/FNINS.2012.00085/BIBTEX

Boll, S., Gamer, M., Gluth, S., Finsterbusch, J., & Büchel, C. (2013). Separate amygdala subregions signal surprise and predictiveness during associative fear learning in humans. *European Journal of Neuroscience*, *37*(5), 758–767. https://doi.org/10.1111/ejn.12094

Bolognini, N., Olgiati, E., Maravita, A., Ferraro, F., & Fregni, F. (2013). Motor and parietal cortex stimulation for phantom limb pain and sensations. *PAIN*®, *154*(8), 1274–1280. https://doi.org/10.1016/J.PAIN.2013.03.040

Bolognini, N., Spandri, V., Ferraro, F., Salmaggi, A., Molinari, A. C. L., Fregni, F., & Maravita, A. (2015). Immediate and Sustained Effects of 5-Day Transcranial Direct Current Stimulation of the Motor Cortex in Phantom Limb Pain. *The Journal of Pain*, *16*(7), 657–665. https://doi.org/10.1016/J.JPAIN.2015.03.013

Borghi, B., D'Addabbo, M., & Borghi, R. (2014). Can neural blocks prevent phantom limb pain? *Http://Dx.Doi.Org/10.2217/Pmt.14.17*, *4*(4), 261–266. https://doi.org/10.2217/PMT.14.17

Borghi, B., D'Addabbo, M., White, P. F., Gallerani, P., Toccaceli, L., Raffaeli, W., Tognù, A., Fabbri, N., & Mercuri, M. (2010). The use of prolonged peripheral

neural blockade after lower extremity amputation: The effect on symptoms associated with phantom limb syndrome. *Anesthesia and Analgesia*, *111*(5), 1308–1315. https://doi.org/10.1213/ANE.0b013e3181f4e848
Borhani, K., Beck, B., & Haggard, P. (2017). Choosing, Doing, and Controlling: Implicit Sense of Agency Over Somatosensory Events. *Psychological Science*, *28*(7), 882–893. https://doi.org/10.1177/0956797617697693
Borsook, D., Burstein, R., & Becerra, L. (2004). *Functional Imaging of the Human Trigeminal System : Opportunities for New Insights into Pain Processing in Health and Disease ABSTRACT :* https://doi.org/10.1002/neu.20085
Boström, K. J., de Lussanet, M. H. E., Weiss, T., Puta, C., & Wagner, H. (2014). A computational model unifies apparently contradictory findings concerning phantom pain. *Scientific Reports*, *4*, 1–9. https://doi.org/10.1038/srep05298
Bramati, I. E., Rodrigues, E. C., Simões, E. L., Melo, B., Höfle, S., Moll, J., Lent, R., & Tovar-Moll, F. (2019). Lower limb amputees undergo long-distance plasticity in sensorimotor functional connectivity. *Scientific Reports 2019 9:1*, *9*(1), 1–10. https://doi.org/10.1038/s41598-019-39696-z
Bräscher, A. K., Becker, S., Hoeppli, M. E., & Schweinhardt, P. (2016). Different brain circuitries mediating controllable and uncontrollable pain. *Journal of Neuroscience*, *36*(18), 5013–5025. https://doi.org/10.1523/JNEUROSCI.1954-15.2016
Breivik, H., Collett, B., Ventafridda, V., Cohen, R., & Gallacher, D. (2006). Survey of chronic pain in Europe: Prevalence, impact on daily life, and treatment. *European Journal of Pain*, *10*(4), 287–333. https://doi.org/10.1016/J.EJPAIN.2005.06.009
Brooks, J. C. W., Zambreanu, L., Godinez, A., Craig, A. D., & Tracey, I. (2005). Somatotopic organisation of the human insula to painful heat studied with high resolution functional imaging. *NeuroImage*, *27*(1), 201–209. https://doi.org/10.1016/j.neuroimage.2005.03.041
Brosnan, M., Chapman, E., & Ashwin, C. (2014). Adolescents with autism spectrum disorder show a circumspect reasoning bias rather than "jumping-to-conclusions." *Journal of Autism and Developmental Disorders*, *44*(3), 513–520. https://doi.org/10.1007/S10803-013-1897-5/FIGURES/2
Brown, C. A., Scholtes, I., Shenker, N., & Lee, M. C. (2020). Suboptimal learning of tactile-spatial predictions in patients with complex regional pain syndrome. *Pain*, *161*(2), 369–378. https://doi.org/10.1097/j.pain.0000000000001730
Bruno, V., Ronga, I., Fossataro, C., Capozzi, F., & Garbarini, F. (2019). Suppressing movements with phantom limbs and existing limbs evokes comparable electrophysiological inhibitory responses. *Cortex*, *117*, 64–76. https://doi.org/10.1016/J.CORTEX.2019.02.024
Bruurmijn, L. C. M., Raemaekers, M., Branco, M. P., Vansteensel, M. J., & Ramsey, N. F. (2021). Decoding attempted phantom hand movements from ipsilateral sensorimotor areas after amputation. *Journal of Neural Engineering*, *18*(5), 056037. https://doi.org/10.1088/1741-2552/AC20E4
Bruurmijn, M. L. C. M., Pereboom, I. P. L., Vansteensel, M. J., Raemaekers, M. A. H., & Ramsey, N. F. (2017). Preservation of hand movement representation in the sensorimotor areas of amputees. *Brain*, *140*(12), 3166–3178. https://doi.org/10.1093/brain/awx274
Büchel, C., Geuter, S., Sprenger, C., & Eippert, F. (2014). Placebo Analgesia: A Predictive Coding Perspective. *Neuron*, *81*(6), 1223–1239. https://doi.org/10.1016/J.NEURON.2014.02.042

Buonomano, D. v., & Merzenich, M. M. (1998). Cortical plasticity: From synapses to maps. *Annual Review of Neuroscience*, *21*, 149–186. https://doi.org/10.1146/annurev.neuro.21.1.149

Burman, D. D., Lie-Nemeth, T., Brandfonbrener, A. G., Parisi, T., & Meyer, J. R. (2009). Altered finger representations in sensorimotor cortex of musicians with focal dystonia: Precentral cortex. *Brain Imaging and Behavior*, *3*(1), 10–23. https://doi.org/10.1007/S11682-008-9046-Z/TABLES/4

Buvanendran, A., Sremac, A. C., Merriman, P. A., della Valle, C. J., Burns, J. W., & McCarthy, R. J. (2021). Preoperative cognitive–behavioral therapy for reducing pain catastrophizing and improving pain outcomes after total knee replacement: a randomized clinical trial. *Regional Anesthesia & Pain Medicine*, *46*(4), 313–321. https://doi.org/10.1136/RAPM-2020-102258

Carvalho, C., Pais, M., Cunha, L., Rebouta, P., Kaptchuk, T. J., & Kirsch, I. (2021). Open-label placebo for chronic low back pain: a 5-year follow-up. *Pain*, *162*(5), 1521–1527. https://doi.org/10.1097/J.PAIN.0000000000002162

Castillo, R. C., Wegener, S. T., Heins, S. E., Haythornthwaite, J. A., Mackenzie, E. J., & Bosse, M. J. (2013). Longitudinal relationships between anxiety, depression, and pain: Results from a two-year cohort study of lower extremity trauma patients. *PAIN*®, *154*(12), 2860–2866. https://doi.org/10.1016/J.PAIN.2013.08.025

Cerkevich, C. M., Qi, H.-X., & Kaas, J. H. (2013). Thalamic input to representations of the teeth, tongue, and face in somatosensory area 3b of macaque monkeys. *The Journal of Comparative Neurology*, *521*, 3954–3971. https://doi.org/10.1002/cne.23386

Chand, P., & Jain, N. (2015). Intracortical and thalamocortical connections of the hand and face representations in somatosensory area 3b of macaque monkeys and effects of chronic spinal cord injuries. *Journal of Neuroscience*, *35*(39), 13475–13486. https://doi.org/10.1523/JNEUROSCI.2069-15.2015

Chen, C. fu, Kreutz-Delgado, K., Sereno, M. I., & Huang, R. S. (2017). Validation of periodic fMRI signals in response to wearable tactile stimulation. *NeuroImage*, *150*, 99–111. https://doi.org/10.1016/J.NEUROIMAGE.2017.02.024

Chen, T., Taniguchi, W., Chen, Q. Y., Tozaki-Saitoh, H., Song, Q., Liu, R. H., Koga, K., Matsuda, T., Kaito-Sugimura, Y., Wang, J., Li, Z. H., Lu, Y. C., Inoue, K., Tsuda, M., Li, Y. Q., Nakatsuka, T., & Zhuo, M. (2018). Top-down descending facilitation of spinal sensory excitatory transmission from the anterior cingulate cortex. *Nature Communications 2018 9:1*, *9*(1), 1–17. https://doi.org/10.1038/s41467-018-04309-2

Cohen, L. G., Bandinelli, S., Findley, T. W., & Hallett, M. (1991). MOTOR REORGANIZATION AFTER UPPER LIMB AMPUTATION IN MANA STUDY WITH FOCAL MAGNETIC STIMULATION. *Brain*, *114*(1), 615–627. https://doi.org/10.1093/BRAIN/114.1.615

Cohen, S. P., Vase, L., & Hooten, W. M. (2021). Chronic pain: an update on burden, best practices, and new advances. *The Lancet*, *397*(10289), 2082–2097. https://doi.org/10.1016/S0140-6736(21)00393-7

Collins, K. L., Russell, H. G., Schumacher, P. J., Robinson-Freeman, K. E., O'Conor, E. C., Gibney, K. D., Yambem, O., Dykes, R. W., Waters, R. S., & Tsao, J. W. (2018). A review of current theories and treatments for phantom limb pain. *Journal of Clinical Investigation*, *128*(6), 2168–2176. https://doi.org/10.1172/JCI94003

Colloca, L., & Miller, F. G. (2011). How placebo responses are formed: a learning perspective. *Philosophical Transactions of the Royal Society B: Biological Sciences*, *366*(1572), 1859–1869. https://doi.org/10.1098/RSTB.2010.0398

Coq, J.-O., Qi, H., Collins, C. E., & Kaas, J. H. (2004). Anatomical and functional organization of somatosensory areas of the lateral fissure of the New World titi monkey (Callicebus moloch). *The Journal of Comparative Neurology*, *476*(4), 363–387. https://doi.org/10.1002/cne.20237

Corniani, G., & Saal, H. P. (2020). Tactile innervation densities across the whole body. *Journal of Neurophysiology*, *124*(4), 1229–1240. https://doi.org/10.1152/JN.00313.2020/ASSET/IMAGES/LARGE/AJ-NEUR200020F003.JPEG

Corsi, N., & Colloca, L. (2017). Placebo and nocebo effects: The advantage of measuring expectations and psychological factors. *Frontiers in Psychology*, *8*(MAR), 308. https://doi.org/10.3389/FPSYG.2017.00308/BIBTEX

Crapse, T. B., & Sommer, M. A. (2008). Corollary discharge across the animal kingdom. *Nature Reviews Neuroscience 2008 9:8*, *9*(8), 587–600. https://doi.org/10.1038/nrn2457

Cusick, C. G., Wall, J. T., & Kaas, J. H. (1986). Representations of the face, teeth and oral cavity in areas 3b and 1 of somatosensory cortex in squirrel monkeys. *Brain Research*, *370*(2), 359–364. https://doi.org/10.1016/0006-8993(86)90494-4

Custead, R., Oh, H., Wang, Y., & Barlow, S. (2017). Brain encoding of saltatory velocity through a pulsed pneumotactile array in the lower face. *Brain Research*, *1677*, 58–73. https://doi.org/10.1016/J.BRAINRES.2017.09.025

Damercheli, S., Ramne, M., & Ortiz-Catalan, M. (2022). transcranial Direct Current Stimulation (tDCS) for the treatment and investigation of Phantom Limb Pain (PLP). *Psychoradiology*, *2*(1), 23–31. https://doi.org/10.1093/PSYRAD/KKAC004

D'Anna, E., Petrini, F. M., Artoni, F., Popovic, I., Simanić, I., Raspopovic, S., & Micera, S. (2017). A somatotopic bidirectional hand prosthesis with transcutaneous electrical nerve stimulation based sensory feedback. *Scientific Reports 2017 7:1*, *7*(1), 1–15. https://doi.org/10.1038/s41598-017-11306-w

Darnall, B. D., Ephraim, P., Wegener, S. T., Dillingham, T., Pezzin, L., Rossbach, P., & MacKenzie, E. J. (2005). Depressive symptoms and mental health service utilization among persons with limb loss: Results of a national survey. *Archives of Physical Medicine and Rehabilitation*, *86*(4), 650–658. https://doi.org/10.1016/J.APMR.2004.10.028

DaSilva, A. F. M., Becerra, L., Makris, N., Strassman, A. M., Gonzalez, R. G., Geatrakis, N., & Borsook, D. (2002). Somatotopic activation in the human trigeminal pain pathway. *The Journal of Neuroscience*, *22*(18), 8183–8192.

Daunizeau, J., Adam, V., & Rigoux, L. (2014). VBA: A Probabilistic Treatment of Nonlinear Models for Neurobiological and Behavioural Data. *PLOS Computational Biology*, *10*(1), e1003441. https://doi.org/10.1371/JOURNAL.PCBI.1003441

de Lange, F. P., Heilbron, M., & Kok, P. (2018). How Do Expectations Shape Perception? *Trends in Cognitive Sciences*, *22*(9), 764–779. https://doi.org/10.1016/j.tics.2018.06.002

De Nunzio, A. M., Schweisfurth, M. A., Ge, N., Falla, D., Hahne, J., Gödecke, K., Petzke, F., Siebertz, M., Dechent, P., Weiss, T., Flor, H., Graimann, B.,

Aszmann, O. C., & Farina, D. (2018). Relieving phantom limb pain with multimodal sensory-motor training. *Journal of Neural Engineering*, *15*(6). https://doi.org/10.1088/1741-2552/aae271

de Rezende Costa, F. H., Averbeck, B., O'Sullivan, S. S., Vincent, M. B., Rosso, A. L., Lees, A. J., & Djamshidian, A. (2016). Jumping to conclusions in untreated patients with Parkinson's disease. *Neuropsychologia*, *85*, 19–23. https://doi.org/10.1016/J.NEUROPSYCHOLOGIA.2016.03.002

Dempsey-Jones, H., Wesselink, D. B., Friedman, J., & Makin, T. R. (2019). Organized Toe Maps in Extreme Foot Users. *Cell Reports*, *28*(11), 2748-2756.e4. https://doi.org/10.1016/J.CELREP.2019.08.027

Dhillon, G. S. (2005). Effects of Short-Term Training on Sensory and Motor Function in Severed Nerves of Long-Term Human Amputees. *Journal of Neurophysiology*, *93*(5), 2625–2633. https://doi.org/10.1152/jn.00937.2004

Dhillon, G. S., Lawrence, S. M., Hutchinson, D. T., & Horch, K. W. (2004). Residual function in peripheral nerve stumps of amputees: Implications for neural control of artificial limbs. *Journal of Hand Surgery*, *29*(4), 605–615. https://doi.org/10.1016/j.jhsa.2004.02.006

Diedrichsen, J., Yokoi, A., & Arbuckle, S. A. (2018). Pattern component modeling: A flexible approach for understanding the representational structure of brain activity patterns. *NeuroImage*, *180*(July 2017), 119–133. https://doi.org/10.1016/j.neuroimage.2017.08.051

Dienes, Z. (2014). Using Bayes to get the most out of non-significant results. *Frontiers in Psychology*, *5*(July), 1–17. https://doi.org/10.3389/fpsyg.2014.00781

Diers, M., Christmann, C., Koeppe, C., Ruf, M., & Flor, H. (2010). Mirrored, imagined and executed movements differentially activate sensorimotor cortex in amputees with and without phantom limb pain. *PAIN*®, *149*(2), 296–304. https://doi.org/10.1016/J.PAIN.2010.02.020

Diers, M., Kamping, S., Kirsch, P., Rance, M., Bekrater-Bodmann, R., Foell, J., Trojan, J., Fuchs, X., Bach, F., Maaß, H., Çakmak, H., & Flor, H. (2015). Illusion-related brain activations: A new virtual reality mirror box system for use during functional magnetic resonance imaging. *Brain Research*, *1594*, 173–182. https://doi.org/10.1016/J.BRAINRES.2014.11.001

Diers, M., Krumm, B., Fuchs, X., Bekrater-Bodmann, R., Milde, C., Trojan, J., Foell, J., Becker, S., Rümenapf, G., & Flor, H. (2022). The Prevalence and Characteristics of Phantom Limb Pain and Non-Painful Phantom Phenomena in a Nationwide Survey of 3,374 Unilateral Limb Amputees. *The Journal of Pain*, *23*(3), 411–423. https://doi.org/10.1016/J.JPAIN.2021.09.003

Diesch, E., & Flor, H. (2007). Alteration in the response properties of primary somatosensory cortex related to differential aversive Pavlovian conditioning. *Pain*, *131*(1–2), 171–180. https://doi.org/10.1016/J.PAIN.2007.01.016

Dong, H. J., Gerdle, B., Bernfort, L., Levin, L. Å., & Dragioti, E. (2020). Pain Catastrophizing in Older Adults with Chronic Pain: The Mediator Effect of Mood Using a Path Analysis Approach. *Journal of Clinical Medicine 2020, Vol. 9, Page 2073*, *9*(7), 2073. https://doi.org/10.3390/JCM9072073

Draganski, B., Moser, T., Lummel, N., Gänssbauer, S., Bogdahn, U., Haas, F., & May, A. (2006). Decrease of thalamic gray matter following limb amputation. *NeuroImage*, *31*(3), 951–957. https://doi.org/10.1016/j.neuroimage.2006.01.018

Dreyer, D. A., Loe, P. R., Metz, C. B., & Whitsel, B. L. (1975). Representation of head and face in postcentral gyrus of the macaque. *Journal of Neurophysiology*, *38*(3), 714–733. https://doi.org/10.1152/jn.1975.38.3.714
Dudley, R., Taylor, P., Wickham, S., & Hutton, P. (2016). Psychosis, Delusions and the "Jumping to Conclusions" Reasoning Bias: A Systematic Review and Meta-analysis. *Schizophrenia Bulletin*, *42*(3), 652–665. https://doi.org/10.1093/SCHBUL/SBV150
Dumanian, G. A., Potter, B. K., Mioton, L. M., Ko, J. H., Cheesborough, J. E., Souza, J. M., Ertl, W. J., Tintle, S. M., Nanos, G. P., Valerio, I. L., Kuiken, T. A., Apkarian, A. V., Porter, K., & Jordan, S. W. (2019). Targeted Muscle Reinnervation Treats Neuroma and Phantom Pain in Major Limb Amputees: A Randomized Clinical Trial. *Annals of Surgery*, *270*(2), 238–246. https://doi.org/10.1097/SLA.0000000000003088
Edin, B. B., & Abbs, J. H. (1991). Finger movement responses of cutaneous mechanoreceptors in the dorsal skin of the human hand. *Journal of Neurophysiology*, *65*(3), 657–670. https://doi.org/10.1152/jn.1991.65.3.657
Edwards, M. J., Adams, R. A., Brown, H., Pareés, I., & Friston, K. J. (2012). A Bayesian account of "hysteria." *Brain*, *135*(11), 3495–3512. https://doi.org/10.1093/brain/aws129
Ehde, D. M., Czerniecki, J. M., Smith, D. G., Campbell, K. M., Edwards, W. T., Jensen, M. P., & Robinson, L. R. (2000). Chronic phantom sensations, phantom pain, residual limb pain, and other regional pain after lower limb amputation. *Archives of Physical Medicine and Rehabilitation*, *81*(8), 1039–1044. https://doi.org/10.1053/APMR.2000.7583
Eichert, N., Papp, D., Mars, R. B., & Watkins, K. E. (2020). Mapping human laryngeal motor cortex during vocalization. *Cerebral Cortex*, *30*(12), 6254–6269. https://doi.org/10.1093/cercor/bhaa182
Ejaz, N., Hamada, M., & Diedrichsen, J. (2015). Hand use predicts the structure of representations in sensorimotor cortex. *Nature Neuroscience*, *18*(7), 1034–1040.
Elbert, T., Candia, C. A. V., Altenmüller, E., Rau, H., Sterr, A., Rockstroh, B., Pantev, C., & Taub, E. (1998). *9858362*. *9*(16), 3571–3575.
Erlenwein, J., Diers, M., Ernst, J., Schulz, F., & Petzke, F. (2021). Clinical updates on phantom limb pain. *Pain Reports*, *6*(1), e888. https://doi.org/10.1097/PR9.0000000000000888
Fairhurst, M., Wiech, K., Dunckley, P., & Tracey, I. (2007). Anticipatory brainstem activity predicts neural processing of pain in humans. *Pain*, *128*(1–2), 101–110. https://doi.org/10.1016/j.pain.2006.09.001
Fayaz, A., Croft, P., Langford, R. M., Donaldson, L. J., & Jones, G. T. (2016). Prevalence of chronic pain in the UK: a systematic review and meta-analysis of population studies. *BMJ Open*, *6*(6), e010364. https://doi.org/10.1136/BMJOPEN-2015-010364
Fazeli, S., & Büchel, C. (2018). Pain-related expectation and prediction error signals in the anterior insula are not related to aversiveness. *Journal of Neuroscience*, *38*(29), 6461–6474. https://doi.org/10.1523/JNEUROSCI.0671-18.2018
Fear, C. F., & Healy, D. (1997). Probabilistic reasoning in obsessive–compulsive and delusional disorders. *Psychological Medicine*, *27*(1), 199–208. https://doi.org/10.1017/S0033291796004175

Ferraro, S., Klugah-Brown, B., Tench, C. R., Yao, S., Nigri, A., Demichelis, G., Pinardi, C., Bruzzone, M. G., & Becker, B. (2022). Dysregulated anterior insula reactivity as robust functional biomarker for chronic pain—Meta-analytic evidence from neuroimaging studies. *Human Brain Mapping*, *43*(3), 998–1010. https://doi.org/10.1002/HBM.25702

Fine, C., Gardner, M., Craigie, J., & Gold, I. (2007). Hopping, skipping or jumping to conclusions? Clarifying the role of the JTC bias in delusions. *Http://Dx.Doi.Org/10.1080/13546800600750597*, *12*(1), 46–77. https://doi.org/10.1080/13546800600750597

Flesher, S. N., Collinger, J. L., Foldes, S. T., Weiss, J. M., Downey, J. E., Tyler-Kabara, E. C., Bensmaia, S. J., Schwartz, A. B., Boninger, M. L., & Gaunt, R. A. (2016). Intracortical microstimulation of human somatosensory cortex. *Science Translational Medicne*, 1–11. https://doi.org/10.1126/scitranslmed.aaf8083

Flesher, S. N., Downey, J. E., Weiss, J. M., Hughes, C. L., Herrera, A. J., Tyler-Kabara, E. C., Boninger, M. L., Collinger, J. L., & Gaunt, R. A. (2019). Restored tactile sensation improves neuroprosthetic arm control. *BioRxiv*, 653428. https://doi.org/10.1101/653428

Fletcher, P. C., & Frith, C. D. (2009). Perceiving is believing: A Bayesian approach to explaining the positive symptoms of schizophrenia. *Nature Reviews Neuroscience*, *10*(1), 48–58. https://doi.org/10.1038/nrn2536

Flor, H. (2002). Phantom-limb pain: Characteristics, causes, and treatment. *Lancet Neurology*, *1*(3), 182–189. https://doi.org/10.1016/S1474-4422(02)00074-1

Flor, H., Braun, C., Elbert, T., & Birbaumer, N. (1997). Extensive reorganization of primary somatosensory cortex in chronic back pain patients. *Neuroscience Letters*, *224*(1), 5–8. https://doi.org/10.1016/S0304-3940(97)13441-3

Flor, H., Denke, C., Schaefer, M., & Grüsser, S. (2001). Effect of sensory discrimination training on cortical reorganisation and phantom limb pain. *The Lancet*, *357*(9270), 1763–1764. https://doi.org/10.1016/S0140-6736(00)04890-X

Flor, H., Diers, M., & Andoh, J. (2013). The neural basis of phantom limb pain. *Trends in Cognitive Sciences*, *17*(7), 307–308. https://doi.org/10.1016/j.tics.2013.04.007

Flor, H., Elbert, T., Knecht, S., Wienbruch, C., Pantev, C., Birbaumer, N., Larbig, W., & Taub, E. (1995). Phantom-limb pain as a perceptual correlate of cortical reorganization following arm amputation. *Nature*, *375*(6531), 482–484.

Flor, H., Knost, B., & Birbaumer, N. (2002). The role of operant conditioning in chronic pain: an experimental investigation. *Pain*, *95*(1–2), 111–118. https://doi.org/10.1016/S0304-3959(01)00385-2

Flor, H., Nikolajsen, L., Jensen, T. S., Staehelin Jensen, T., & Jensen, T. S. (2006). Phantom limb pain: a case of maladaptive CNS plasticity? *Nature Reviews. Neuroscience*, *7*(11), 873–881. https://doi.org/10.1038/nrn1991

Florence, S. L., Taub, H. B., & Kaas, J. H. (1998). Large-scale sprouting of cortical connections after peripheral injury in adult Macaque monkeys. *Science*, *282*(5391), 1117–1121. https://doi.org/10.1126/SCIENCE.282.5391.1117/ASSET/A66907E3-0936-4A6E-87E7-C452AF26139B/ASSETS/GRAPHIC/SE4686992003.JPEG

Foell, J., Bekrater-Bodmann, R., Diers, M., & Flor, H. (2014). Mirror therapy for phantom limb pain: Brain changes and the role of body representation.

European Journal of Pain (United Kingdom), *18*(5), 729–739. https://doi.org/10.1002/j.1532-2149.2013.00433.x

Franke, L. K., Miedl, S. F., Danböck, S. K., Grill, M., Liedlgruber, M., Kronbichler, M., Flor, H., & Wilhelm, F. H. (2022). Neuroscientific evidence for pain being a classically conditioned response to trauma- and pain-related cues in humans. In *Pain: Vol. Publish Ah*. https://doi.org/10.1097/j.pain.0000000000002621

Freeman, D., Pugh, K., & Garety, P. (2008). Jumping to conclusions and paranoid ideation in the general population. *Schizophrenia Research*, *102*(1–3), 254–260. https://doi.org/10.1016/J.SCHRES.2008.03.020

Freeman, D., Startup, H., Dunn, G., Černis, E., Wingham, G., Pugh, K., Cordwell, J., & Kingdon, D. (2013). The interaction of affective with psychotic processes: A test of the effects of worrying on working memory, jumping to conclusions, and anomalies of experience in patients with persecutory delusions. *Journal of Psychiatric Research*, *47*(12), 1837–1842. https://doi.org/10.1016/J.JPSYCHIRES.2013.06.016

Freeman, D., Startup, H., Dunn, G., Černis, E., Wingham, G., Pugh, K., Cordwell, J., Mander, H., & Kingdon, D. (2014). Understanding jumping to conclusions in patients with persecutory delusions: working memory and intolerance of uncertainty. *Psychological Medicine*, *44*(14), 3017–3024. https://doi.org/10.1017/S0033291714000592

Freeman, R., Emir, B., & Parsons, B. (2015). Predictors of placebo response in peripheral neuropathic pain: Insights from pregabalin clinical trials. *Journal of Pain Research*, *8*, 257–268. https://doi.org/10.2147/JPR.S78303

Friston, K. J., Fletcher, P., Josephs, O., Holmes, A., Rugg, M. D., & Turner, R. (1998). Event-related fMRI: Characterizing differential responses. *NeuroImage*, *7*(1), 30–40. https://doi.org/10.1006/nimg.1997.0306

Fu, J., Wu, S., Liu, C., Camilleri, J. A., Eickhoff, S. B., & Yu, R. (2021). Distinct neural networks subserve placebo analgesia and nocebo hyperalgesia. *NeuroImage*, *231*(February), 117833. https://doi.org/10.1016/j.neuroimage.2021.117833

Fuchs, X., Bekrater-Bodma, R., & Flor, H. (2015). Phantom pain: The role of maladaptive plasticity and emotional and cognitive variables. *Pain, Emotion and Cognition: A Complex Nexus*, 189–207. https://doi.org/10.1007/978-3-319-12033-1_12/COVER

Fuchs, X., Flor, H., & Bekrater-Bodmann, R. (2018). Psychological factors associated with phantom limb pain: A review of recent findings. *Pain Research and Management*, *2018*. https://doi.org/10.1155/2018/5080123

Gagné, M., Reilly, K. T., & Hétu, S. (2009). MOTOR CONTROL OVER THE PHANTOM LIMB IN ABOVE-ELBOW AMPUTEES AND ITS RELATIONSHIP WITH PHANTOM LIMB PAIN. *NSC*, *162*(1), 78–86. https://doi.org/10.1016/j.neuroscience.2009.04.061

Garcia-Pallero, M. Á., Cardona, D., Rueda-Ruzafa, L., Rodriguez-Arrastia, M., & Roman, P. (2022). Central nervous system stimulation therapies in phantom limb pain: a systematic review of clinical trials. *Neural Regeneration Research*, *17*(1), 59. https://doi.org/10.4103/1673-5374.314288

Gardner, E. P., Ro, J. Y., Srinivasa Babu, K., & Ghosh, S. (2007). Neurophysiology of prehension. II. Response diversity in primary somatosensory (S-I) and motor (M-I) cortices. *Journal of Neurophysiology*, *97*(2), 1656–1670.

https://doi.org/10.1152/JN.01031.2006/ASSET/IMAGES/LARGE/Z9K0020779480010.JPEG
Garety, P. A., & Freeman, D. (2013). The past and future of delusions research: from the inexplicable to the treatable. *The British Journal of Psychiatry*, *203*(5), 327–333. https://doi.org/10.1192/BJP.BP.113.126953
Garety, P. (1991). Reasoning and delusions*. The British Journal of Psychiatry,* 159(S14), 14-18.
Geuter, S., Boll, S., Eippert, F., & Büchel, C. (2017). Functional dissociation of stimulus intensity encoding and predictive coding of pain in the insula. *ELife*, *6*, 1–22. https://doi.org/10.7554/eLife.24770
Gilliam, W. P., Schumann, M. E., Cunningham, J. L., Evans, M. M., Luedtke, C. A., Morrison, E. J., Sperry, J. A., & Vowles, K. E. (2021). Pain catastrophizing as a treatment process variable in cognitive behavioural therapy for adults with chronic pain. *European Journal of Pain*, *25*(2), 339–347. https://doi.org/10.1002/EJP.1671
Giusti, L., Ussorio, D., Salza, A., Malavolta, M., Aggio, A., Bianchini, V., Casacchia, M., & Roncone, R. (2018). Preliminary study of effects on paranoia ideation and jumping to conclusions in the context of group treatment of anxiety disorders in young people. *Early Intervention in Psychiatry*, *12*(6), 1072–1080. https://doi.org/10.1111/EIP.12415
Glasser, M. F., Coalson, T. S., Robinson, E. C., Hacker, C. D., Harwell, J., Yacoub, E., Ugurbil, K., Andersson, J., Beckmann, C. F., Jenkinson, M., Smith, S. M., & Van Essen, D. C. (2016). A multi-modal parcellation of human cerebral cortex. *Nature*, *536*(7615), 171–178. https://doi.org/10.1038/nature18933
Gracely, R. H., Lota, L., Walter, D. J., & Dubner, R. (1988). A multiple random staircase method of psychophysical pain assessment. *Pain*, *32*(1), 55–63. https://doi.org/10.1016/0304-3959(88)90023-1
Graham, A., Ryan, C. G., MacSween, A., Alexanders, J., Livadas, N., Oatway, S., Atkinson, G., & Martin, D. J. (2020). Sensory discrimination training for adults with chronic musculoskeletal pain: a systematic review. *Https://Doi.Org/10.1080/09593985.2020.1830455*. https://doi.org/10.1080/09593985.2020.1830455
Grahl, A., Onat, S., & Büchel, C. (2018). The periaqueductal gray and Bayesian integration in placebo analgesia. *ELife*, *7*, 1–20. https://doi.org/10.7554/eLife.32930
Granata, G., di Iorio, R., Romanello, R., Iodice, F., Raspopovic, S., Petrini, F., Strauss, I., Valle, G., Stieglitz, T., Čvančara, P., Andreu, D., Divoux, J. L., Giraud, D., Wauters, L., Hiairrassary, A., Jensen, W., Micera, S., & Rossini, P. M. (2018). Phantom somatosensory evoked potentials following selective intraneural electrical stimulation in two amputees. *Clinical Neurophysiology*, *129*(6), 1117–1120. https://doi.org/10.1016/J.CLINPH.2018.02.138
Graziano, M. S. A. (2016). Ethological Action Maps: A Paradigm Shift for the Motor Cortex. *Trends in Cognitive Sciences*, *20*(2), 121–132. https://doi.org/10.1016/J.TICS.2015.10.008
Graziano, M. S. A., & Aflalo, T. N. (2007). Mapping behavioral repertoire onto the cortex. *Neuron*, *56*(2), 239–251. https://doi.org/10.1016/j.neuron.2007.09.013
Greve, D. N., & Fischl, B. (2009). Accurate and robust brain image alignment using boundary-based registration. *NeuroImage*, *48*(1), 63–72. https://doi.org/10.1016/j.neuroimage.2009.06.060

Grossman, C. D., Bari, B. A., & Cohen, J. Y. (2022). Serotonin neurons modulate learning rate through uncertainty. *Current Biology*, *32*(3), 586-599.e7. https://doi.org/10.1016/j.cub.2021.12.006

Grüsser, S. M., Winter, C., Mühlnickel, W., Denke, C., Karl, A., Villringer, K., & Flor, H. (2001). The relationship of perceptual phenomena and cortical reorganization in upper extremity amputees. *Neuroscience*, *102*(2), 263–272. https://doi.org/10.1016/S0306-4522(00)00491-7

Gunduz, M. E., Pacheco-Barrios, K., Bonin Pinto, C., Duarte, D., Vélez, F. G. S., Gianlorenco, A. C. L., Teixeira, P. E. P., Giannoni-Luza, S., Crandell, D., Battistella, L. R., Simis, M., & Fregni, F. (2021). Effects of Combined and Alone Transcranial Motor Cortex Stimulation and Mirror Therapy in Phantom Limb Pain: A Randomized Factorial Trial. *Neurorehabilitation and Neural Repair*, *35*(8), 704–716. https://doi.org/10.1177/15459683211017509

Haarsma, J., Knolle, F., Griffin, J. D., Taverne, H., Mada, M., Goodyer, I. M., Fletcher, P. C., & Murray, G. K. (2020). Influence of prior beliefs on perception in early psychosis: Effects of illness stage and hierarchical level of belief. *Journal of Abnormal Psychology*, *129*(6), 581. https://doi.org/10.1037/ABN0000494

Hahamy, A., Macdonald, S. N., van den Heiligenberg, F., Kieliba, P., Emir, U., Malach, R., Johansen-Berg, H., Brugger, P., Culham, J. C., & Makin, T. R. (2017). Representation of Multiple Body Parts in the Missing-Hand Territory of Congenital One-Handers. *Current Biology*, *27*(9), 1350–1355. https://doi.org/10.1016/j.cub.2017.03.053

Hahamy, A., & Makin, T. (2019). Remapping in cerebral and cerebellar cortices is not restricted by somatotopy. *J Neurosci*, *39*(47), 9328–9342. https://doi.org/10.1101/439356

Hall, N., & Eldabe, S. (2017). Phantom limb pain: a review of pharmacological management. *British Journal of Pain*, 204946371774730. https://doi.org/10.1177/2049463717747307

Harding-Forrester, S., & Feldman, D. E. (2018). Somatosensory maps. *Handbook of Clinical Neurology*, *151*, 73–102. https://doi.org/10.1016/B978-0-444-63622-5.00004-8

Harris, A. J. (1999). Cortical origin of pathological pain. *Lancet*, *354*(9188), 1464–1466. https://doi.org/10.1016/S0140-6736(99)05003-5

Hayashi, R., Kuroda, K., & Inadomi, H. (2022). Jumping to conclusions correlates with negative symptoms, poor response inhibition, and impaired functioning in individuals diagnosed with schizophrenia. *Asian Journal of Psychiatry*, *71*, 103068. https://doi.org/10.1016/J.AJP.2022.103068

Hechler, T., Endres, D., & Thorwart, A. (2016). Why harmless sensations might hurt in individuals with chronic pain: About heightened prediction and perception of pain in the mind. *Frontiers in Psychology*, *7*(OCT), 1638. https://doi.org/10.3389/FPSYG.2016.01638/BIBTEX

Henderson, W. R., & Smyth, G. E. (1948). Phantom limbs. *Journal of Neurology, Neurosurgery and Psychiatry*.

Hermens, H. J., Freriks, B., Merletti, R., Stegeman, D., Blok, J., Rau, G., Disselhorst-Klug, C., & Hägg, G. (n.d.). *European Recommendations for Surface ElectroMyoGraphy Results of the SENIAM project*.

Herrador Colmenero, L., Perez Marmol, J. M., Martí-García, C., Querol Zaldivar, M. de los Á., Tapia Haro, R. M., Castro Sánchez, A. M., & Aguilar-Ferrándiz, M. E. (2018). Effectiveness of mirror therapy, motor imagery, and virtual

feedback on phantom limb pain following amputation: A systematic review. *Prosthetics and Orthotics International*, *42*(3), 288–298. https://doi.org/10.1177/0309364617740230

Hess, C. W., Mills, K. R., & Murray, N. M. F. (1986). Magnetic stimulation of the human brain: Facilitation of motor responses by voluntary contraction of ipsilateral and contralateral muscles with additional observations on an amputee. *Neuroscience Letters*, *71*(2), 235–240. https://doi.org/10.1016/0304-3940(86)90565-3

Hodges, P. W., & Smeets, R. J. (2015). Interaction between pain, movement, and physical activity: Short-term benefits, long-term consequences, and targets for treatment. *Clinical Journal of Pain*, *31*(2), 97–107. https://doi.org/10.1097/AJP.0000000000000098

Hodges, P. W., & Tucker, K. (2011). Moving differently in pain: A new theory to explain the adaptation to pain. *Pain*, *152*(SUPPL.3). https://doi.org/10.1016/J.PAIN.2010.10.020

Horgan, O., & MacLachlan, M. (2009). Psychosocial adjustment to lower-limb amputation: A review. *Https://Doi.Org/10.1080/09638280410001708869*, *26*(14–15), 837–850. https://doi.org/10.1080/09638280410001708869

Horing, B., & Büchel, C. (2022). The human insula processes both modality-independent and pain-selective learning signals. *PLOS Biology*, *20*(5), e3001540. https://doi.org/10.1371/JOURNAL.PBIO.3001540

Huang, R. S., Chen, C. fu, & Sereno, M. I. (2017). Mapping the complex topological organization of the human parietal face area. *NeuroImage*, *163*, 459–470. https://doi.org/10.1016/J.NEUROIMAGE.2017.09.004

Huang, R. S., & Sereno, M. I. (2007). Dodecapus: An MR-compatible system for somatosensory stimulation. *NeuroImage*, *34*(3), 1060–1073. https://doi.org/10.1016/J.NEUROIMAGE.2006.10.024

Huq, S. F., Garety, P. A., & Hemsley, D. R. (1988). Probabilistic Judgements in Deluded and Non-Deluded Subjects. *The Quarterly Journal of Experimental Psychology Section A*, *40*(4), 801–812. https://doi.org/10.1080/14640748808402300

Iannetti, G. D., Porro, C. A., Pantano, P., Romanelli, P. L., Galeotti, F., & Cruccu, G. (2003). Representation of different trigeminal divisions within the primary and secondary human somatosensory cortex. *NeuroImage*, *19*(3), 906–912. https://doi.org/10.1016/S1053-8119(03)00139-3

Ilfeld, B. M., Khatibi, B., Maheshwari, K., Madison, S. J., Esa, W. A. S., Mariano, E. R., Kent, M. L., Hanling, S., Sessler, D. I., Eisenach, J. C., Cohen, S. P., Mascha, E. J., Ma, C., Padwal, J. A., & Turan, A. (2021). Ambulatory continuous peripheral nerve blocks to treat postamputation phantom limb pain: a multicenter, randomized, quadruple-masked, placebo-controlled clinical trial. *Pain*, *162*(3), 938. https://doi.org/10.1097/J.PAIN.0000000000002087

Ingram, J. N., Körding, K. P., Howard, I. S., & Wolpert, D. M. (2008). The statistics of natural hand movements. *Experimental Brain Research*, *188*(2), 223–236. https://doi.org/10.1007/S00221-008-1355-3/FIGURES/6

Jacoby, R. J., Abramowitz, J. S., Buck, B. E., & Fabricant, L. E. (2014). How is the Beads Task related to intolerance of uncertainty in anxiety disorders? *Journal of Anxiety Disorders*, *28*(6), 495–503. https://doi.org/10.1016/J.JANXDIS.2014.05.005

Jain, N. J., Catania, K. C., & Kaas, J. H. (1997). Deafferentation and reactivation of somatosensory cortex after dorsal spinal cord injury. *Nature*, *386*, 495–498.
Jain, N., Qi, H. X., Collins, C. E., & Kaas, J. H. (2008). Large-Scale Reorganization in the Somatosensory Cortex and Thalamus after Sensory Loss in Macaque Monkeys. *Journal of Neuroscience*, *28*(43), 11042–11060. https://doi.org/10.1523/JNEUROSCI.2334-08.2008
Jain, N., Qi, H.-X., Catania, K. C., & Kaas, J. H. (2001). Anatomic correlates of the face and oral cavity representations in the somatosensory cortical area 3b of monkeys. *The Journal of Comparative Neurology*, *429*(3), 455–468. https://doi.org/10.1002/1096-9861(20010115)429:3<455::AID-CNE7>3.0.CO;2-F
Jänsch, C., & Hare, D. J. (2014). An Investigation of the “jumping to conclusions” data-gathering bias and paranoid thoughts in asperger syndrome. *Journal of Autism and Developmental Disorders*, *44*(1), 111–119. https://doi.org/10.1007/S10803-013-1855-2/FIGURES/4
Jardri, R., Duverne, S., Litvinova, A. S., & Denève, S. (2017). Experimental evidence for circular inference in schizophrenia. *Nature Communications 2017 8:1*, *8*(1), 1–13. https://doi.org/10.1038/ncomms14218
Jenkinson, M., Bannister, P., Brady, M., & Smith, S. (2002). Improved Optimization for the Robust and Accurate Linear Registration and Motion Correction of Brain Images. *NeuroImage*, *17*(2), 825–841. https://doi.org/10.1006/nimg.2002.1132
Jones, E. C., & Pons, T. P. (1998). Thalamic and brainstem contributions to large-scale plasticity of primate somatosensory cortex. *Science*, *282*(5391), 1121–1125. https://doi.org/10.1126/SCIENCE.282.5391.1121/ASSET/4309CF71-E3C3-4DFD-8C0C-03009007EF8F/ASSETS/GRAPHIC/SE4686987004.JPEG
Kaas, J. H., Qi, H. X., Burish, M. J., Gharbawie, O. A., Onifer, S. M., & Massey, J. M. (2008). Cortical and subcortical plasticity in the brains of humans, primates, and rats after damage to sensory afferents in the dorsal columns of the spinal cord. *Experimental Neurology*, *209*(2), 407–416. https://doi.org/10.1016/J.EXPNEUROL.2007.06.014
Kaplan, C. M., Schrepf, A., Vatansever, D., Larkin, T. E., Mawla, I., Ichesco, E., Kochlefl, L., Harte, S. E., Clauw, D. J., Mashour, G. A., & Harris, R. E. (2019). Functional and neurochemical disruptions of brain hub topology in chronic pain. *Pain*, *160*(4), 973. https://doi.org/10.1097/J.PAIN.0000000000001480
Karl, A., Birbaumer, N., Lutzenberger, W., Cohen, L. G., & Flor, H. (2001). Reorganization of motor and somatosensory cortex in upper extremity amputees with phantom limb pain. *The Journal of Neuroscience : The Official Journal of the Society for Neuroscience*, *21*(10), 3609–3618. https://doi.org/21/10/3609 [pii]
Kass, R. E., & Raftery, A. E. (1995). Bayes factors. *Journal of the American Statistical Association*, *90*(430), 773–795. https://doi.org/10.1080/01621459.1995.10476572
Kazemi, H., Ghassemi, S., Feres, S. M., Amini, A., Kolivand, P. H., & Doroudi, T. (2013). Anxiety and Depression in Patients with Amputated Limbs Suffering from Phantom Pain: A Comparative Study with Non-Phantom Chronic Pain. *International Journal of Preventive Medicine*, *4*(2), 218. /pmc/articles/PMC3604856/

Kikkert, S., Johansen-Berg, H., Tracey, I., & Makin, T. R. (2018). Reaffirming the link between chronic phantom limb pain and maintained missing hand representation. *Cortex*, *106*, 174–184. https://doi.org/10.1016/j.cortex.2018.05.013

Kikkert, S., Kolasinski, J., Jbabdi, S., Tracey, I., Beckmann, C. F., Berg, H. J., & Makin, T. R. (2016). Revealing the neural fingerprints of a missing hand. *ELife*, *5*(AUGUST), e15292. https://doi.org/10.7554/eLife.15292

Kikkert, S., Mezue, M., Henderson Slater, D., Johansen-Berg, H., Tracey, I., & Makin, T. R. (2017). Motor correlates of phantom limb pain. *Cortex*, *95*, 29–36. https://doi.org/10.1016/j.cortex.2017.07.015

Kikkert, S., Mezue, M., O'Shea, J., Henderson Slater, D., Johansen-Berg, H., Tracey, I., & Makin, T. R. (2019). Neural basis of induced phantom limb pain relief. *Annals of Neurology*, *85*(1), 59–73. https://doi.org/10.1002/ana.25371

Kikkert, S., Pfyffer, D., Verling, M., Freund, P., & Wenderoth, N. (2021). Finger somatotopy is preserved after tetraplegia but deteriorates over time. *ELife*, *10*. https://doi.org/10.7554/ELIFE.67713

Kikkert, S., Sonar, H. A., Freund, P., Paik, J., & Wenderoth, N. (2022). Hand and face somatotopy shown using MRI-safe vibrotactile stimulation with a novel Soft Pneumatic Actuator (SPA)-Skin interface. *BioRxiv*, 2021.10.27.465604. https://doi.org/10.1101/2021.10.27.465604

Kim, K. R., Lee, S. Y., Kang, J. I., Kim, B. R., Choi, S. H., Park, J. Y., Lee, E., An, S. K., & Kwon, J. S. (2011). Clinical efficacy of individual cognitive therapy in reducing psychiatric symptoms in people at ultra-high risk for psychosis. *Early Intervention in Psychiatry*, *5*(2), 174–178. https://doi.org/10.1111/J.1751-7893.2011.00267.X

Klein, H. S., & Pinkham, A. E. (2018). Examining reasoning biases in schizophrenia using a modified "Jumping to Conclusions" probabilistic reasoning task. *Psychiatry Research*, *270*, 180–186. https://doi.org/10.1016/J.PSYCHRES.2018.09.020

Knotkova, H., Hamani, C., Sivanesan, E., le Beuffe, M. F. E., Moon, J. Y., Cohen, S. P., & Huntoon, M. A. (2021). Neuromodulation for chronic pain. *The Lancet*, *397*(10289), 2111–2124. https://doi.org/10.1016/S0140-6736(21)00794-7

Kolasinski, X., Makin, T. R., Jbabdi, S., Clare, S., Stagg, C. J., & Johansen-Berg, H. (2016). Investigating the stability of fine-grain digit somatotopy in individual human participants. *Journal of Neuroscience*, *36*(4), 1113–1127. https://doi.org/10.1523/JNEUROSCI.1742-15.2016

Kopietz, R., Sakar, V., Albrecht, J., Kleemann, A. M., Schöpf, V., Yousry, I., Linn, J., Fesl, G., & Wiesmann, M. (2009). Activation of primary and secondary somatosensory regions following tactile stimulation of the face. *Clinical Neuroradiology*, *19*(2), 135–144. https://doi.org/10.1007/s00062-009-8022-3

Lalouni, M., Fust, J., Vadenmark-Lundqvist, V., Ehrsson, H. H., Kilteni, K., & Birgitta Jensen, K. (2021). Predicting pain: differential pain thresholds during self-induced, externally induced, and imagined self-induced pressure pain. *Pain*, *162*(5), 1539. https://doi.org/10.1097/J.PAIN.0000000000002151

Landa, Y., Mueser, K. T., Wyka, K. E., Shreck, E., Jespersen, R., Jacobs, M. A., Griffin, K. W., van der Gaag, M., Reyna, V. F., Beck, A. T., Silbersweig, D. A., & Walkup, J. T. (2016). Development of a group and family-based cognitive behavioural therapy program for youth at risk for psychosis. *Early Intervention in Psychiatry*, *10*(6), 511–521. https://doi.org/10.1111/EIP.12204/SUPPINFO

Larbig, W., Andoh, J., Huse, E., Stahl-Corino, D., Montoya, P., Seltzer, Z., & Flor, H. (2019). Pre- and postoperative predictors of phantom limb pain. *Neuroscience Letters*, *702*, 44–50. https://doi.org/10.1016/J.NEULET.2018.11.044

Lee, J.-Y., You, T., Lee, C.-H., Im, G. H., Seo, H., Woo, C.-W., & Kim, S.-G. (2022). Role of anterior cingulate cortex inputs to periaqueductal gray for pain avoidance. *Current Biology*. https://doi.org/10.1016/J.CUB.2022.04.090

Leknes, S., Brooks, J. C. W., Wiech, K., & Tracey, I. (2008). Pain relief as an opponent process: A psychophysical investigation. *European Journal of Neuroscience*, *28*(4), 794–801. https://doi.org/10.1111/j.1460-9568.2008.06380.x

Lembo, A., Kelley, J. M., Nee, J., Ballou, S., Iturrino, J., Cheng, V., Rangan, V., Katon, J., Hirsch, W., Kirsch, I., Hall, K., Davis, R. B., & Kaptchuk, T. J. (2021). Open-label placebo vs double-blind placebo for irritable bowel syndrome: a randomized clinical trial. *Pain*, *162*(9), 2428–2435. https://doi.org/10.1097/J.PAIN.0000000000002234

Li, J., Schiller, D., Schoenbaum, G., Phelps, E. A., & Daw, N. D. (2011). Differential roles of human striatum and amygdala in associative learning. *Nature Neuroscience 2011 14:10*, *14*(10), 1250–1252. https://doi.org/10.1038/nn.2904

Li, L., Gainey, M. A., Goldbeck, J. E., & Feldman, D. E. (2014). Rapid homeostasis by disinhibition during whisker map plasticity. *Proceedings of the National Academy of Sciences of the United States of America*, *111*(4), 1616–1621. https://doi.org/10.1073/PNAS.1312455111

Limakatso, K., Bedwell, G. J., Madden, V. J., & Parker, R. (2019). The prevalence and risk factors for phantom limb pain in people with amputations: A systematic review and meta-analysis. *Systematic Reviews*, *8*(17). https://doi.org/10.1101/19008961

Limakatso, K., Bedwell, G. J., Madden, V. J., & Parker, R. (2020). The prevalence and risk factors for phantom limb pain in people with amputations: A systematic review and meta-analysis. *PLOS ONE*, *15*(10), e0240431. https://doi.org/10.1371/JOURNAL.PONE.0240431

Limakatso, K., Madden, V. J., Manie, S., & Parker, R. (2020). The effectiveness of graded motor imagery for reducing phantom limb pain in amputees: a randomised controlled trial. *Physiotherapy*, *109*, 65–74. https://doi.org/10.1016/J.PHYSIO.2019.06.009

Lin, L. D., & Sessle, B. J. (1994). Functional properties of single neurons in the primate face primary somatosensory cortex. III. Modulation of responses to peripheral stimuli during trained orofacial motor behaviors. *Journal of Neurophysiology*, *71*(6), 2401–2413. https://doi.org/10.1152/jn.1994.71.6.2401

Livet, A., Navarri, X., Potvin, S., & Conrod, P. (2020). Cognitive biases in individuals with psychotic-like experiences: A systematic review and a meta-analysis. *Schizophrenia Research*, *222*, 10–22. https://doi.org/10.1016/J.SCHRES.2020.06.016

Löffler, M., Kamping, S., Brunner, M., Bustan, S., Kleinböhl, D., Anton, F., & Flor, H. (2018). Impact of controllability on pain and suffering. *Pain Reports*, *3*(6). https://doi.org/10.1097/PR9.0000000000000694

Lotze, M., Flor, H., Grodd, W., Larbig, W., & Birbaumer, N. (2001). Phantom movements and pain. An fMRI study in upper limb amputees. *Brain*, *124*(Pt 11), 2268–2277. https://doi.org/10.1093/brain/124.11.2268

Lyu, Y., Guo, X., Bekrater-Bodmann, R., Flor, H., & Tong, S. (2016). Phantom limb perception interferes with motor imagery after unilateral upper-limb amputation. *Scientific Reports*, *6*, 2–11. https://doi.org/10.1038/srep21100

MacIver, K., Lloyd, D. M., Kelly, S., Roberts, N., & Nurmikko, T. (2008). Phantom limb pain, cortical reorganization and the therapeutic effect of mental imagery. *Brain*, *131*(8), 2181–2191. https://doi.org/10.1093/brain/awn124

Maheu, M., Dehaene, S., & Meyniel, F. (2019). Brain signatures of a multiscale process of sequence learning in humans. *ELife*, *8*. https://doi.org/10.7554/ELIFE.41541

Maihöfner, C., Handwerker, H. O., Neundörfer, B., & Birklein, F. (2004). Cortical reorganization during recovery from complex regional pain syndrome. *Neurology*, *63*(4), 693–701. https://doi.org/10.1212/01.WNL.0000134661.46658.B0

Maihöfner, C., Neundörfer, B., Birklein, F., & Handwerker, H. O. (2006). Mislocalization of tactile stimulation in patients with complex regional pain syndrome. *Journal of Neurology 2006 253:6*, *253*(6), 772–779. https://doi.org/10.1007/S00415-006-0117-Z

Makin, T. R. (2021). Phantom limb pain: Thinking outside the (mirror) box. *Brain*, *2021*. https://doi.org/10.1093/brain/awab139

Makin, T. R., & Bensmaia, S. J. (2017). Stability of Sensory Topographies in Adult Cortex. *Trends in Cognitive Sciences*, *21*(3), 195–204. https://doi.org/10.1016/j.tics.2017.01.002

Makin, T. R., Cramer, A. O., Scholz, J., Hahamy, A., Henderson Slater, D., Tracey, I., & Johansen-Berg, H. (2013). Deprivation-related and use-dependent plasticity go hand in hand. *ELife*, *2*, 1–15. https://doi.org/10.7554/eLife.01273

Makin, T. R., & Flor, H. (2020). Brain (re)organisation following amputation: Implications for phantom limb pain. *NeuroImage*, *218*(September 2019), 116943. https://doi.org/10.1016/j.neuroimage.2020.116943

Makin, T. R., Scholz, J., Filippini, N., Henderson Slater, D., Tracey, I., & Johansen-Berg, H. (2013). Phantom pain is associated with preserved structure and function in the former hand area. *Nature Communications*, *4*, 1570–1578. https://doi.org/10.1038/ncomms2571

Makin, T. R., Scholz, J., Henderson Slater, D., Johansen-Berg, H., & Tracey, I. (2015). Reassessing cortical reorganization in the primary sensorimotor cortex following arm amputation. *Brain*, *138*(8), 2140–2146. https://doi.org/10.1093/brain/awv161

Mancini, F., Wang, A. P., Schira, M. M., Isherwood, Z. J., McAuley, J. H., Iannetti, G. D., Sereno, M. I., Moseley, G. L., & Rae, C. D. (2019). Fine-Grained Mapping of Cortical Somatotopies in Chronic Complex Regional Pain Syndrome. *Journal of Neuroscience*, *39*(46), 9185–9196. https://doi.org/10.1523/JNEUROSCI.2005-18.2019

Mancini, F., Zhang, S., & Seymour, B. (2021). Learning the statistics of pain : computational and neural mechanisms. *BioRxiv*.

Manger, P. R., Woods, T. M., & Jones, E. G. (1995). Representation of the face and intraoral structures in area 3b of the squirrel monkey (Saimiri sciureus) somatosensory cortex, with special reference to the ipsilateral representation.

The Journal of Comparative Neurology, *362*(4), 597–607. https://doi.org/10.1002/cne.903620412
Mayr, A., Jahn, P., Stankewitz, A., Deak, B., Winkler, A., Witkovsky, V., Eren, O., Straube, A., & Schulz, E. (2022). Patients with chronic pain exhibit individually unique cortical signatures of pain encoding. *Human Brain Mapping*, *43*(5), 1676–1693. https://doi.org/10.1002/HBM.25750
McCormick, Z., Chang-Chien, G., Marshall, B., Huang, M., & Harden, R. N. (2014). Phantom Limb Pain: A Systematic Neuroanatomical-Based Review of Pharmacologic Treatment. *Pain Medicine*, *15*(2), 292–305. https://doi.org/10.1111/PME.12283
McGuire, J. T., Nassar, M. R., Gold, J. I., & Kable, J. W. (2014). Functionally Dissociable Influences on Learning Rate in a Dynamic Environment. *Neuron*, *84*(4), 870–881. https://doi.org/10.1016/j.neuron.2014.10.013
McLean, B. F., Balzan, R. P., & Mattiske, J. K. (2020). Jumping to conclusions in the less-delusion-prone? Further evidence from a more reliable beads task. *Consciousness and Cognition*, *83*, 102956. https://doi.org/10.1016/J.CONCOG.2020.102956
McLean, B. F., Mattiske, J. K., & Balzan, R. P. (2017). Association of the Jumping to Conclusions and Evidence Integration Biases With Delusions in Psychosis: A Detailed Meta-analysis. *Schizophrenia Bulletin*, *43*(2), 344–354. https://doi.org/10.1093/SCHBUL/SBW056
McLean, B. F., Mattiske, J. K., & Balzan, R. P. (2018). Towards a reliable repeated-measures beads task for assessing the jumping to conclusions bias. *Psychiatry Research*, *265*, 200–207. https://doi.org/10.1016/J.PSYCHRES.2018.04.043
McLean, B. F., Mattiske, J. K., & Balzan, R. P. (2020). Jumping to conclusions in the less-delusion-prone? Preliminary evidence from a more reliable beads task. *Journal of Behavior Therapy and Experimental Psychiatry*, *68*(January), 101562. https://doi.org/10.1016/j.jbtep.2020.101562
McLean, C. P., & Anderson, E. R. (2009). Brave men and timid women? A review of the gender differences in fear and anxiety. *Clinical Psychology Review*, *29*(6), 496–505. https://doi.org/10.1016/J.CPR.2009.05.003
Mercier, C., Reilly, K. T., Vargas, C. D., Aballea, A., & Sirigu, A. (2006). Mapping phantom movement representations in the motor cortex of amputees. *Brain*, *129*(8), 2202–2210. https://doi.org/10.1093/brain/awl180
Merzenich, M. M., Kaas, J. H., Sur, M., & Lin, C. -S. (1978). Double representation of the body surface within cytoarchitectonic area 3b and 1 in “SI” in the owl monkey (aotus trivirgatus). *Journal of Comparative Neurology*, *181*(1), 41–73. https://doi.org/10.1002/cne.901810104
Merzenich, M. M., Kaas, J. H., Wall, J., Nelson, R. J., Sur, M., & Felleman, D. (1983). Topographic reorganization of somatosensory cortical areas 3b and 1 in adult monkeys following restricted deafferentation. *Neuroscience*, *8*(1), 33–55. https://doi.org/10.1016/0306-4522(83)90024-6
Merzenich, M. M., Nelson, R. J., Kaas, J. H., Stryker, M. P., Jenkins, W. M., Zook, J. M., Cynader, M. S., & Schoppmann, A. (1987). Variability in hand surface representations in areas 3b and 1 in adult owl and squirrel monkeys. *Journal of Comparative Neurology*, *258*(2), 281–296. https://doi.org/10.1002/CNE.902580208
Merzenich, M. M., Nelson, R. J., Stryker, M. P., Cynader, M. S., Schoppmann, A., & Zook, J. M. (1984). Somatosensory cortical map changes following digit

amputation in adult monkeys. *Journal of Comparative Neurology*, *224*(4), 591–605. https://doi.org/10.1002/CNE.902240408
Meulders, A., Franssen, M., Fonteyne, R., & Vlaeyen, J. W. S. (2016). Acquisition and extinction of operant pain-related avoidance behavior using a 3 degrees-of-freedom robotic arm. *Pain*, *157*(5), 1094–1104. https://doi.org/10.1097/J.PAIN.0000000000000483
Meulders, A., Harvie, D. S., Bowering, J. K., Caragianis, S., Vlaeyen, J. W. S., & Moseley, G. L. (2014). Contingency learning deficits and generalization in chronic unilateral hand pain patients. *Journal of Pain*, *15*(10), 1046–1056. https://doi.org/10.1016/j.jpain.2014.07.005
Meulders, A., Vansteenwegen, D., & Vlaeyen, J. W. S. (2011). The acquisition of fear of movement-related pain and associative learning: A novel pain-relevant human fear conditioning paradigm. *PAIN*, *152*(11), 2460–2469. https://doi.org/10.1016/J.PAIN.2011.05.015
Miall, R. C., & Wolpert, D. M. (1996). Forward Models for Physiological Motor Control. *Neural Networks*, *9*(8), 1265–1279. https://doi.org/10.1016/S0893-6080(96)00035-4
Monosov, I. E. (2020). How Outcome Uncertainty Mediates Attention, Learning, and Decision-Making. *Trends in Neurosciences*, *43*(10), 795–809. https://doi.org/10.1016/j.tins.2020.06.009
Moritz, S., Andreou, C., Schneider, B. C., Wittekind, C. E., Menon, M., Balzan, R. P., & Woodward, T. S. (2014). Sowing the seeds of doubt: a narrative review on metacognitive training in schizophrenia. *Clinical Psychology Review*, *34*(4), 358–366. https://doi.org/10.1016/J.CPR.2014.04.004
Moritz, S., Menon, M., Balzan, R., Todd, ·, & Woodward, S. (2022). Metacognitive training for psychosis (MCT): past, present, and future. *European Archives of Psychiatry and Clinical Neuroscience 2022*, *1*, 1–7. https://doi.org/10.1007/S00406-022-01394-9
Moritz, S., & Woodward, T. S. (2005). Jumping to conclusions in delusional and non-delusional schizophrenic patients. *British Journal of Clinical Psychology*, *44*(2), 193–207. https://doi.org/10.1348/014466505X35678
Morley, S., Williams, A., & Eccleston, C. (2013). Examining the evidence about psychological treatments for chronic pain: Time for a paradigm shift? *Pain*, *154*(10), 1929–1931. https://doi.org/10.1016/J.PAIN.2013.05.049
Moseley, G. L. (2006). Graded motor imagery for pathologic pain. *Neurology*, *67*(12), 2129–2134. https://doi.org/10.1212/01.WNL.0000249112.56935.32
Moseley, G. L., & Flor, H. (2012). Targeting cortical representations in the treatment of chronic pain: A review. *Neurorehabilitation and Neural Repair*, *26*(6), 646–652. https://doi.org/10.1177/1545968311433209
Moseley, G. L., Gallace, A., & Spence, C. (2008). Is mirror therapy all it is cracked up to be? Current evidence and future directions. *Pain*, *138*(1), 7–10. https://doi.org/10.1016/J.PAIN.2008.06.026
Moulton, E. A., Pendse, G., Morris, S., Aiello-Lammens, M., Becerra, L., & Borsook, D. (2009). Segmentally arranged somatotopy within the face representation of human primary somatosensory cortex. *Human Brain Mapping*, *30*(3), 757–765. https://doi.org/10.1002/hbm.20541
Moutoussis, M., Bentall, R. P., El-Deredy, W., & Dayan, P. (2011). Bayesian modelling of Jumping-to-Conclusions bias in delusional patients. *Http://Dx.Doi.Org/10.1080/13546805.2010.548678*, *16*(5), 422–447. https://doi.org/10.1080/13546805.2010.548678

Muret, D., & Makin, T. R. (2021). The homeostatic homunculus : rethinking deprivation-triggered reorganisation. *Current Opinion in Neurobiology*, *67*, 115–122. https://doi.org/10.1016/j.conb.2020.08.008

Muret, D., Root, V., Kieliba, P., Clode, D., & Makin, T. R. (2022). Beyond body maps: Information content of specific body parts is distributed across the somatosensory homunculus. *Cell Reports*, *38*(11), 110523. https://doi.org/10.1016/J.CELREP.2022.110523

Nardone, R., Höller, Y., Brigo, F., Seidl, M., Christova, M., Bergmann, J., Golaszewski, S., & Trinka, E. (2013). Functional brain reorganization after spinal cord injury: Systematic review of animal and human studies. *Brain Research*, *1504*, 58–73. https://doi.org/10.1016/j.brainres.2012.12.034

Nelson, R. J., Sur, M., Felleman, D. J., & Kaas, J. H. (1980). Representations of the body surface in postcentral parietal cortex of Macaca fascicularis. *The Journal of Comparative Neurology*, *192*, 611–643. https://doi.org/10.1002/cne.901920402

Nguyen, B. T., Tran, T. D., Hoshiyama, M., Inui, K., & Kakigi, R. (2004). Face representation in the human primary somatosensory cortex. *Neuroscience Research*, *50*(2), 227–232. https://doi.org/10.1016/j.neures.2004.07.004

Nguyen, J. P., Nizard, J., Keravel, Y., & Lefaucheur, J. P. (2011). Invasive brain stimulation for the treatment of neuropathic pain. *Nature Reviews Neurology 2011 7:12*, *7*(12), 699–709. https://doi.org/10.1038/nrneurol.2011.138

Nili, H., Wingfield, C., Walther, A., Su, L., Marslen-Wilson, W., & Kriegeskorte, N. (2014). A Toolbox for Representational Similarity Analysis. *PLoS Computational Biology*, *10*(4). https://doi.org/10.1371/journal.pcbi.1003553

Nystrom, B., & Hagbarth, K. E. (1981). Microelectrode recordings from transected nerves in amputees with phantom limb pain. *Neuroscience Letters*, *27*(2), 211–216. https://doi.org/10.1016/0304-3940(81)90270-6

O'Brien, A. L., Jordan, S. W., West, J. M., Mioton, L. M., Dumanian, G. A., & Valerio, I. L. (2021). Targeted Muscle Reinnervation at the Time of Upper-Extremity Amputation for the Treatment of Pain Severity and Symptoms. *The Journal of Hand Surgery*, *46*(1), 72.e1-72.e10. https://doi.org/10.1016/J.JHSA.2020.08.014

Ongaro, G., & Kaptchuk, T. J. (2018). Symptom perception, placebo effects, and the Bayesian brain. *Pain*, *160*(1), 1. https://doi.org/10.1097/00006396-900000000-98882

Ortiz-Catalan, M. (2018). The stochastic entanglement and phantom motor execution hypotheses: A theoretical framework for the origin and treatment of Phantom limb pain. *Frontiers in Neurology*, *9*(SEP), 1–16. https://doi.org/10.3389/fneur.2018.00748

Ortiz-Catalan, M., Guðmundsdóttir, R. A., Kristoffersen, M. B., Zepeda-Echavarria, A., Caine-Winterberger, K., Kulbacka-Ortiz, K., Widehammar, C., Eriksson, K., Stockselius, A., Ragnö, C., Pihlar, Z., Burger, H., & Hermansson, L. (2016). Phantom motor execution facilitated by machine learning and augmented reality as treatment for phantom limb pain: a single group, clinical trial in patients with chronic intractable phantom limb pain. *The Lancet*, *388*(10062), 2885–2894. https://doi.org/10.1016/S0140-6736(16)31598-7

Osumi, M., Inomata, K., Inoue, Y., Otake, Y., Morioka, S., & Sumitani, M. (2019). Characteristics of Phantom Limb Pain Alleviated with Virtual Reality Rehabilitation. *Pain Medicine*, *20*(5), 1038–1046. https://doi.org/10.1093/PM/PNY269

Palmer, C. J., Lawson, R. P., & Hohwy, J. (2017). Bayesian approaches to autism: Towards volatility, action, and behavior. *Psychological Bulletin*, *143*(5), 521–542. https://doi.org/10.1037/BUL0000097

Pareés, I., Kassavetis, P., Saifee, T. A., Sadnicka, A., Bhatia, K. P., Fotopoulou, A., & Edwards, M. J. (2012). 'Jumping to conclusions' bias in functional movement disorders. *Journal of Neurology, Neurosurgery & Psychiatry*, *83*(4), 460–463. https://doi.org/10.1136/JNNP-2011-300982

Parkes, C., Bezzina, O., Chapman, A., Luteran, A., Freeston, M. H., & Robinson, L. J. (2019). Jumping to conclusions in persistent pain using a somatosensory modification of the beads task. *Journal of Psychosomatic Research*, *126*, 109819. https://doi.org/10.1016/J.JPSYCHORES.2019.109819

Penfield, W., & Boldrey, E. (1937). Somatic Motor and Sensory Representation in Man. *Brain*, 389–443.

Penfield, W., & Rasmussen, T. (1950). The Cerebral Cortex of Man. A Clinical Study of Localization of Function.pdf. In *Academic Medicine* (Vol. 25, p. 375). https://doi.org/10.1097/00001888-195009000-00037

Petrovic, P. (2008). Placebo analgesia and nocebo hyperalgesia - Two sides of the same coin? *Pain*, *136*(1–2), 5–6. https://doi.org/10.1016/J.PAIN.2008.03.004

Phelps, C. E., Navratilova, E., & Porreca, F. (2021). Cognition in the Chronic Pain Experience: Preclinical Insights. *Trends in Cognitive Sciences*, *25*(5), 365–376. https://doi.org/10.1016/J.TICS.2021.01.001

Philip, B. A., & Frey, S. H. (2014). Compensatory Changes Accompanying Chronic Forced Use of the Nondominant Hand by Unilateral Amputees. *Journal of Neuroscience*, *34*(10), 3622–3631. https://doi.org/10.1523/JNEUROSCI.3770-13.2014

Philip, B., Valyear, K., Cirstea, C., & Frey, S. (2017). Reorganization of primary somatosensory cortex after upper limb amputation may lack functional significance. *Archives of Physical Medicine and Rehabilitation*, *98*(10), e103. https://doi.org/10.1016/j.apmr.2017.08.331

Piccinelli, M., & Wilkinson, G. (2000). Gender differences in depression: Critical review. *The British Journal of Psychiatry*, *177*(6), 486–492. https://doi.org/10.1192/BJP.177.6.486

Pons, T. P., Garraghty, P. E., Ommaya, A. K., Kaas, J. H., Taub, E., & Mishkin, M. (1991). Massive cortical reorganization after sensory deafferentation in adult macaques. *Science, New Series*, *252*(5014), 1857–1860.

Power, A., Brown, C. A., Sivan, M., Lenton, A., Rainey, T., El-Deredy, W., Jones, A. K. P., & Watson, A. (2020). Individuals with chronic pain have the same response to placebo analgesia as healthy controls in terms of magnitude and reproducibility. *Pain*, *161*(12), 2720–2730. https://doi.org/10.1097/j.pain.0000000000001966

Prsa, M., Morandell, K., Cuenu, G., & Huber, D. (2019). Feature-selective encoding of substrate vibrations in the forelimb somatosensory cortex. *Nature*, *567*(7748), 384–388. https://doi.org/10.1038/s41586-019-1015-8

Racine, M., Moulin, D. E., Nielson, W. R., Morley-Forster, P. K., Lynch, M., Clark, A. J., Stitt, L., Gordon, A., Nathan, H., Smyth, C., Ware, M. A., & Jensen, M. P. (2016). The reciprocal associations between catastrophizing and pain outcomes in patients being treated for neuropathic pain: A cross-lagged panel analysis study. *Pain*, *157*(9), 1946–1953. https://doi.org/10.1097/J.PAIN.0000000000000594

Raffin, E., Giraux, P., & Reilly, K. T. (2012). The moving phantom: Motor execution or motor imagery? *Cortex*, *48*(6), 746–757. https://doi.org/10.1016/j.cortex.2011.02.003

Raffin, E., Mattout, J., Reilly, K. T., & Giraux, P. (2012). Disentangling motor execution from motor imagery with the phantom limb. *Brain*, *135*(2), 582–595. https://doi.org/10.1093/brain/awr337

Raffin, E., Richard, N., Giraux, P., & Reilly, K. T. (2016). Primary motor cortex changes after amputation correlate with phantom limb pain and the ability to move the phantom limb. *NeuroImage*, *130*, 134–144. https://doi.org/10.1016/j.neuroimage.2016.01.063

https://doi.org/10.1016/j.neuroimage.2016.01.063

Raja, S. N., Carr, D. B., Cohen, M., Finnerup, N. B., Flor, H., Gibson, S., Keefe, F. J., Mogil, J. S., Ringkamp, M., Sluka, K. A., Song, X. J., Stevens, B., Sullivan, M. D., Tutelman, P. R., Ushida, T., & Vader, K. (2020). The revised International Association for the Study of Pain definition of pain: concepts, challenges, and compromises. *Pain*, *161*(9), 1976–1982. https://doi.org/10.1097/J.PAIN.0000000000001939

Rajendram, C., Ken-Dror, G., Han, T., & Sharma, P. (2022). Efficacy of mirror therapy and virtual reality therapy in alleviating phantom limb pain: a meta-analysis and systematic review. *BMJ Mil Health*, *168*(2), 173–177. https://doi.org/10.1136/BMJMILITARY-2021-002018

Ramachandran, V. S., & Hirstein, W. (1998a). The perception of phantom limbs. The D. O. Hebb lecture. *Brain*, *121*(9), 1603–1630. https://doi.org/10.1093/brain/121.9.1603

Ramachandran, V. S., & Hirstein, W. (1998b). The perception of phantom limbs. The D. O. Hebb lecture. *Brain*, *121*(9), 1603–1630. https://doi.org/10.1093/brain/121.9.1603

Ramachandran, V. S., Rogers-Ramachandran, D., & Cobb, S. (1995). Touching the phantom limb. *Nature 1995 377:6549*, *377*(6549), 489–490. https://doi.org/10.1038/377489a0

Rauschenberg, C., Reininghaus, U., ten Have, M., de Graaf, R., van Dorsselaer, S., Simons, C. J. P., Gunther, N., Henquet, C., Pries, L. K., Guloksuz, S., Bak, M., & van Os, J. (2021). The jumping to conclusions reasoning bias as a cognitive factor contributing to psychosis progression and persistence: findings from NEMESIS-2. *Psychological Medicine*, *51*(10), 1696–1703. https://doi.org/10.1017/S0033291720000446

Recanzone, G. H., Merzenich, M. M., Jenkins, W. M., Grajski, K. A., & Dinse, H. R. (1992). Topographic reorganization of the hand representation in cortical area 3b of owl monkeys trained in a frequency-discrimination task. *Journal of Neurophysiology*, *67*(5), 1031–1056. https://doi.org/10.1152/jn.1992.67.5.1031

Reilly, K. T., Mercier, C., Schieber, M. H., & Sirigu, A. (2006). Persistent hand motor commands in the amputees' brain. *Brain*, *129*(8), 2211–2223. https://doi.org/10.1093/brain/awl154

Reininghaus, U., Rauschenberg, C., ten Have, M., de Graaf, R., van Dorsselaer, S., Simons, C. J. P., Gunther, N., Pries, L. K., Guloksuz, S., Radhakrishnan, R., Bak, M., & van Os, J. (2019). Reasoning bias, working memory performance and a transdiagnostic phenotype of affective disturbances and psychotic experiences in the general population. *Psychological Medicine*, *49*(11), 1799–1809. https://doi.org/10.1017/S0033291718002209

Richardson, C., Glenn, S., Horgan, M., & Nurmikko, T. (2007). A Prospective Study of Factors Associated With the Presence of Phantom Limb Pain Six Months After Major Lower Limb Amputation in Patients With Peripheral Vascular Disease. *The Journal of Pain*, *8*(10), 793–801. https://doi.org/10.1016/J.JPAIN.2007.05.007

Richardson, C., & Kulkarni, J. (2017). A review of the management of phantom limb pain: challenges and solutions. *Journal of Pain Research*, *10*, 1861. https://doi.org/10.2147/JPR.S124664

Rigoux, L., Stephan, K. E., Friston, K. J., & Daunizeau, J. (2014). Bayesian model selection for group studies — Revisited. *NeuroImage*, *84*, 971–985. https://doi.org/10.1016/J.NEUROIMAGE.2013.08.065

Ross, K., Freeman, D., Dunn, G., & Garety, P. (2011). A Randomized Experimental Investigation of Reasoning Training for People With Delusions. *Schizophrenia Bulletin*, *37*(2), 324–333. https://doi.org/10.1093/SCHBUL/SBN165

Ross, R. M., McKay, R., Coltheart, M., & Langdon, R. (2015). Jumping to Conclusions About the Beads Task? A Meta-analysis of Delusional Ideation and Data-Gathering. *Schizophrenia Bulletin*, *41*(5), 1183–1191. https://doi.org/10.1093/SCHBUL/SBU187

Roux, F. E., Djidjeli, I., & Durand, J. B. (2018). Functional architecture of the somatosensory homunculus detected by electrostimulation. *Journal of Physiology*, *596*(5), 941–956. https://doi.org/10.1113/JP275243

Roy, M., Shohamy, D., Daw, N., Jepma, M., Wimmer, G. E., & Wager, T. D. (2014). Representation of aversive prediction errors in the human periaqueductal gray. *Nature Neuroscience 2014 17:11*, *17*(11), 1607–1612. https://doi.org/10.1038/nn.3832

Ruben, J., Schwiemann, J., Deuchert, M., Meyer, R., Krause, T., Curio, G., Villringer, K., Kurth, R., & Villringer, A. (2001). Somatotopic organization of human secondary somatosensory cortex. *Cerebral Cortex*, *11*(5), 463–473. https://doi.org/10.1093/cercor/11.5.463

Sadnicka, A., Wiestler, T., Butler, K., Altenmüller, E., Edwards, M. J., Ejaz, N., & Diedrichsen, J. (2021). Intact finger representation within primary sensorimotor cortex of Musician's Dystonia. *MedRxiv*, 2021.12.01.21266860. https://doi.org/10.1101/2021.12.01.21266860

Sahuquillo-Leal, R., Ghosn, F., Moreno-Giménez, A., Almansa, B., Serrano-Lozano, E., Ferrín, M., Cañada-Martínez, A., Vento, M., & García-Blanco, A. (2020). Jumping to conclusions in autism: integration of contextual information and confidence in decision-making processes. *European Child and Adolescent Psychiatry*, *29*(7), 959–968. https://doi.org/10.1007/S00787-019-01409-2/FIGURES/4

Salomons, T. v., Johnstone, T., Backonja, M. M., & Davidson, R. J. (2004). Perceived Controllability Modulates the Neural Response to Pain. *Journal of Neuroscience*, *24*(32), 7199–7203. https://doi.org/10.1523/JNEUROSCI.1315-04.2004

Salomons, T. v., Johnstone, T., Backonja, M. M., Shackman, A. J., & Davidson, R. J. (2007). Individual Differences in the Effects of Perceived Controllability on Pain Perception: Critical Role of the Prefrontal Cortex. *Journal of Cognitive Neuroscience*, *19*(6), 993–1003. https://doi.org/10.1162/JOCN.2007.19.6.993

Sanders, Z.-B., Wesselink, D., Dempsey-Jones, H., & Makin, T. (2019). *Similar somatotopy for active and passive digit representation in primary somatosensory cortex*. 1–36. https://doi.org/10.1101/754648

Sandström, A., Ellerbrock, I., Tour, J., Kadetoff, D., Jensen, K. B., & Kosek, E. (2020). Neural correlates of conditioned pain responses in fibromyalgia subjects indicate preferential formation of new pain associations rather than extinction of irrelevant ones. *Pain*, *161*(9), 2079–2088. https://doi.org/10.1097/j.pain.0000000000001907

Sastre-Buades, A., Ochoa, S., Lorente-Rovira, E., Barajas, A., Grasa, E., López-Carrilero, R., Luengo, A., Ruiz-Delgado, I., Cid, J., González-Higueras, F., Sánchez-Alonso, S., Baca-García, E., Barrigón, M. L., Acevedo, A., Anglès, J., Argany, M. A., Barajas, A., Barrigón, M. L., Beltrán, M., … Villellas, R. (2021). Jumping to conclusions and suicidal behavior in depression and psychosis. *Journal of Psychiatric Research*, *137*, 514–520. https://doi.org/10.1016/J.JPSYCHIRES.2021.03.024

Sato, K., Nariai, T., Sasaki, S., Yazawa, I., Mochida, H., Miyakawa, N., Momose-Sato, Y., Kamino, K., Ohta, Y., Hirakawa, K., & Ohno, K. (2002). Intraoperative intrinsic optical imaging of neuronal activity from subdivisions of the human primary somatosensory cortex. *Cerebral Cortex*, *12*(3), 269–280.

Sato, K., Nariai, T., Tanaka, Y., Maehara, T., Miyakawa, N., Sasaki, S., Momose-Sato, Y., & Ohno, K. (2005). Functional representation of the finger and face in the human somatosensory cortex: Intraoperative intrinsic optical imaging. *NeuroImage*, *25*(4), 1292–1301. https://doi.org/10.1016/j.neuroimage.2004.12.049

Schellekens, W., Bakker, C., Ramsey, N. F., & Petridou, N. (2022). Moving in on human motor cortex. Characterizing the relationship between body parts with non-rigid population response fields. *PLOS Computational Biology*, *18*(4), e1009955. https://doi.org/10.1371/JOURNAL.PCBI.1009955

Schieber, M. H. (2001). Constraints on somatotopic organization in the primary motor cortex. *Journal of Neurophysiology*, *86*(5), 2125–2143. https://doi.org/10.1152/jn.2001.86.5.2125

Schley, M. T., Wilms, P., Toepfner, S., Schaller, H. P., Schmelz, M., Konrad, C. J., & Birbaumer, N. (2008). Painful and nonpainful phantom and stump sensations in acute traumatic amputees. *Journal of Trauma - Injury, Infection and Critical Care*, *65*(4), 858–864. https://doi.org/10.1097/TA.0B013E31812EED9E

Schlitt, F., Schmidt, K., Merz, C. J., Wolf, O. T., Kleine-Borgmann, J., Elsenbruch, S., Wiech, K., Forkmann, K., & Bingel, U. (2021). Impaired pain-related threat and safety learning in patients with chronic back pain. *Pain*, *Publish Ah*(00). https://doi.org/10.1097/j.pain.0000000000002544

Schone, H. R., Baker, C. I., Katz, J., Nikolajsen, L., Limakatso, K., Flor, H., & Makin, T. R. (2022). Making sense of phantom limb pain. *Journal of Neurology, Neurosurgery & Psychiatry*, jnnp-2021-328428. https://doi.org/10.1136/JNNP-2021-328428

Schumann, M. E., Coombes, B. J., Gascho, K. E., Geske, J. R., McDermott, M. C., Morrison, E. J., Reynolds, A. L., Bernau, J. L., & Gilliam, W. P. (2022). Pain Catastrophizing and Pain Self-Efficacy Mediate Interdisciplinary Pain Rehabilitation Program Outcomes at Posttreatment and Follow-Up. *Pain Medicine*, *23*(4), 697–706. https://doi.org/10.1093/PM/PNAB271

Schütze, R., Rees, C., Smith, A., Slater, H., Campbell, J. M., & O'Sullivan, P. (2018). How Can We Best Reduce Pain Catastrophizing in Adults With Chronic Noncancer Pain? A Systematic Review and Meta-Analysis. *The Journal of Pain*, *19*(3), 233–256. https://doi.org/10.1016/J.JPAIN.2017.09.010

Schwartz, T. H., Li, M. C., Friedman, R. M., Spencer, D. D., & Roe, A. W. (2004). Intraoperative optical imaging of human face cortical topography: A case study. *NeuroReport*, *15*(9), 1527–1531. https://doi.org/10.1097/01.wnr.0000131006.59315.2f

Scientifi, A. (2014). The Simple Difference Formula: An Approach to Teaching Nonparametric Correlation1: *Http://Dx.Doi.Org/10.2466/11.IT.3.1*, *3*(1), 11.IT.3.1. https://doi.org/10.2466/11.IT.3.1

Segerdahl, A. R., Mezue, M., Okell, T. W., Farrar, J. T., & Tracey, I. (2015). The dorsal posterior insula subserves a fundamental role in human pain. *Nature Neuroscience 2015 18:4*, *18*(4), 499–500. https://doi.org/10.1038/nn.3969

Senra, H., Oliveira, R. A., Leal, I., & Vieira, C. (2012). Beyond the body image: A qualitative study on how adults experience lower limb amputation. *Clinical Rehabilitation*, *26*(2), 180–191. https://doi.org/10.1177/0269215511410731/ASSET/IMAGES/LARGE/10.1177_0269215511410731-FIG1.JPEG

Serino, A., Akselrod, M., Salomon, R., Martuzzi, R., Blefari, M. L., Canzoneri, E., Rognini, G., van der Zwaag, W., Iakova, M., Luthi, F., Amoresano, A., Kuiken, T., & Blanke, O. (2017). Upper limb cortical maps in amputees with targeted muscle and sensory reinnervation. *Brain*, *140*(11), 2993–3011. https://doi.org/10.1093/BRAIN/AWX242

Serra, J., Duan, W. R., Locke, C., Solà, R., Liu, W., & Nothaft, W. (2015). Effects of a T-type calcium channel blocker, ABT-639, on spontaneous activity in C-nociceptors in patients with painful diabetic neuropathy: a randomized controlled trial. *Pain*, *156*(11), 2175–2183. https://doi.org/10.1097/j.pain.0000000000000249

Servos, P., Engel, S. a, Gati, J., & Menon, R. (1999). fMRI evidence for an inverted face representation in human somatosensory cortex. *Neuroreport*, *10*(7), 1393–1395. https://doi.org/10.1097/00001756-199905140-00002

Seymour, B. (2019). Pain: A Precision Signal for Reinforcement Learning and Control. *Neuron*, *101*(6), 1029–1041. https://doi.org/10.1016/J.NEURON.2019.01.055

Seymour, B., & Mancini, F. (2020). Hierarchical models of pain: Inference, information-seeking, and adaptive control. *NeuroImage*, *222*(July), 117212. https://doi.org/10.1016/j.neuroimage.2020.117212

Shackman, A. J., Salomons, T. v., Slagter, H. A., Fox, A. S., Winter, J. J., & Davidson, R. J. (2011). The integration of negative affect, pain and cognitive control in the cingulate cortex. *Nature Reviews Neuroscience 2011 12:3*, *12*(3), 154–167. https://doi.org/10.1038/nrn2994

Shukla, G. D., Sahu, S. C., Tripathi, R. P., & Gupta, D. K. (1982a). A Psychiatric Study of Amputees. *The British Journal of Psychiatry*, *141*(1), 50–53. https://doi.org/10.1192/BJP.141.1.50

Shukla, G. D., Sahu, S. C., Tripathi, R. P., & Gupta, D. K. (1982b). Phantom Limb: A Phenomenological Study. *The British Journal of Psychiatry*, *141*(1), 54–58. https://doi.org/10.1192/BJP.141.1.54

Slawek, D. E., Syed, M., Cunningham, C. O., Zhang, C., Ross, J., Herman, M., Sohler, N., Minami, H., Levin, F. R., Arnsten, J. H., & Starrels, J. L. (2022).

Pain catastrophizing and mental health phenotypes in adults with refractory chronic pain: A latent class analysis. *Journal of Psychiatric Research*, *145*, 102–110. https://doi.org/10.1016/J.JPSYCHIRES.2021.12.001

Smith, R., Badcock, P., & Friston, K. J. (2021). Recent advances in the application of predictive coding and active inference models within clinical neuroscience. *Psychiatry and Clinical Neurosciences*, *75*(1), 3–13. https://doi.org/10.1111/pcn.13138

Smith, R., Kuplicki, R., Feinstein, J., Forthman, K. L., Stewart, J. L., Paulus, M. P., & Khalsa, S. S. (2020). A Bayesian computational model reveals a failure to adapt interoceptive precision estimates across depression, anxiety, eating, and substance use disorders. *PLOS Computational Biology*, *16*(12), e1008484. https://doi.org/10.1371/JOURNAL.PCBI.1008484

Smith, S. M. (2002). Fast robust automated brain extraction. *Human Brain Mapping*, *17*(3), 143–155. https://doi.org/10.1002/hbm.10062

Smith, S. M., & Nichols, T. E. (2009). Threshold-free cluster enhancement: Addressing problems of smoothing, threshold dependence and localisation in cluster inference. *NeuroImage*, *44*(1), 83–98. https://doi.org/10.1016/j.neuroimage.2008.03.061

So, S. H. W., Freeman, D., & Garety, P. (2008). Impact of state anxiety on the jumping to conclusions delusion bias. *Australian and New Zealand Journal of Psychiatry*, *42*(10), 879–886. https://doi.org/10.1080/00048670802345466

So, S. H. wai, Siu, N. Y. fan, Wong, H. lam, Chan, W., & Garety, P. A. (2016). 'Jumping to conclusions' data-gathering bias in psychosis and other psychiatric disorders — Two meta-analyses of comparisons between patients and healthy individuals. *Clinical Psychology Review*, *46*, 151–167. https://doi.org/10.1016/J.CPR.2016.05.001

Sonar, H. A., Huang, J.-L., & Paik, J. (2021). Soft Touch using Soft Pneumatic Actuator–Skin as a Wearable Haptic Feedback Device. *Advanced Intelligent Systems*, *3*(3), 2000168. https://doi.org/10.1002/aisy.202000168

Stankevicius, A., Wallwork, S. B., Summers, S. J., Hordacre, B., & Stanton, T. R. (2021). Prevalence and incidence of phantom limb pain, phantom limb sensations and telescoping in amputees: A systematic rapid review. *European Journal of Pain*, *25*(1), 23–38. https://doi.org/10.1002/EJP.1657

Stephan, K. E., Penny, W. D., Daunizeau, J., Moran, R. J., & Friston, K. J. (2009). Bayesian model selection for group studies. *NeuroImage*, *46*(4), 1004–1017. https://doi.org/10.1016/J.NEUROIMAGE.2009.03.025

Stepniewska, I., Preuss, T. M., & Kaas, J. H. (1993). Architectionis, somatotopic organization, and ipsilateral cortical connections of the primary motor area (M1) of owl monkeys. *Journal of Comparative Neurology*, *330*(2), 238–271. https://doi.org/10.1002/CNE.903300207

Stoeckel, M. C., Seitz, R. J., & Buetefisch, C. M. (2009). Congenitally altered motor experience alters somatotopic organization of human primary motor cortex. *Proceedings of the National Academy of Sciences*, *106*(7), 2395–2400. https://doi.org/10.1073/pnas.0803733106

Striem-Amit, E., Vannuscorps, G., & Caramazza, A. (2018). Plasticity based on compensatory effector use in the association but not primary sensorimotor cortex of people born without hands. *Proceedings of the National Academy of Sciences*, 201803926. https://doi.org/10.1073/pnas.1803926115

Strube, W., Cimpianu, C. L., Ulbrich, M., Öztürk, Ö. F., Schneider-Axmann, T., Falkai, P., Marshall, L., Bestmann, S., & Hasan, A. (2022). Unstable Belief

Formation and Slowed Decision-making: Evidence That the Jumping-to-Conclusions Bias in Schizophrenia Is Not Linked to Impulsive Decision-making. *Schizophrenia Bulletin*, *48*(2), 347–358. https://doi.org/10.1093/SCHBUL/SBAB108

Strube, W., Marshall, L., Quattrocchi, G., Little, S., Cimpianu, C. L., Ulbrich, M., Schneider-Axmann, T., Falkai, P., Hasan, A., & Bestmann, S. (2020). Glutamatergic Contribution to Probabilistic Reasoning and Jumping to Conclusions in Schizophrenia: A Double-Blind, Randomized Experimental Trial. *Biological Psychiatry*, *88*(9), 687–697. https://doi.org/10.1016/J.BIOPSYCH.2020.03.018

Sullivan, M. J. L., Bishop, S. R., & Pivik, J. (1995). The Pain Catastrophizing Scale: Development and Validation. *Psychological Assessment*, *7*(4), 524–532. https://doi.org/10.1037/1040-3590.7.4.524

Sullivan, M. J. L., Tripp, D. A., & Santor, D. (2000). Gender Differences in Pain and Pain Behavior: The Role of Catastrophizing. *Cognitive Therapy and Research 2000 24:1*, *24*(1), 121–134. https://doi.org/10.1023/A:1005459110063

Sun, F., Zhang, G., Ren, L., Yu, T., Ren, Z., Gao, R., & Zhang, X. (2021). Functional organization of the human primary somatosensory cortex: A stereo-electroencephalography study. *Clinical Neurophysiology*, *132*(2), 487–497. https://doi.org/10.1016/J.CLINPH.2020.11.032

Sur, M., Nelson, R. J., & Kaas, J. H. (1982). Representations of the body surface in cortical areas 3b and 1 of squirrel monkeys: Comparisons with other primates. *Journal of Comparative Neurology*, *211*(2), 177–192. https://doi.org/10.1002/cne.902110207

Tabor, A., & Burr, C. (2019). Bayesian Learning Models of Pain: A Call to Action. *Current Opinion in Behavioral Sciences*, *26*, 54–61. https://doi.org/10.1016/J.COBEHA.2018.10.006

Tabor, A., Keogh, E., & Eccleston, C. (2017). Embodied pain - Negotiating the boundaries of possible action. *Pain*, *158*(6), 1007–1011. https://doi.org/10.1097/j.pain.0000000000000875

Tallis, F., Eysenck, M., & Mathews, A. (1991). Elevated evidence requirements and worry. *Personality and Individual Differences*, *12*(1), 21–27. https://doi.org/10.1016/0191-8869(91)90128-X

Tan, D. W., Schiefer, M. A., Keith, M. W., Anderson, J. R., Tyler, J., & Tyler, D. J. (2014). A neural interface provides long-term stable natural touch perception. *Science Translational Medicine*, *6*(257), 257ra138-257ra138. https://doi.org/10.1126/scitranslmed.3008669

Tang, B., Geers, A., Barnes, K., & Colagiuri, B. (2019). Instrumental Control Enhances Placebo Analgesia. *The Journal of Pain*, *20*(12), 1486–1497. https://doi.org/10.1016/J.JPAIN.2019.05.013

Taylor, V. A., Chang, L., Rainville, P., & Roy, M. (2017). Learned expectations and uncertainty facilitate pain during classical conditioning. *Pain*, *158*(8), 1528–1537. https://doi.org/10.1097/j.pain.0000000000000948

Therrien, A. S., Howard, C., & Buxbaum, L. J. (2021). Aberrant activity in an intact residual muscle is associated with phantom limb pain in above-knee amputees. *Journal of Neurophysiology*, *125*(6), 2135–2143. https://doi.org/10.1152/JN.00482.2020/ASSET/IMAGES/LARGE/JN.00482.2020_F004.JPEG

Thieme, H., Morkisch, N., Rietz, C., Dohle, C., & Borgetto, B. (2016). The Efficacy of Movement Representation Techniques for Treatment of Limb Pain—A Systematic Review and Meta-Analysis. *The Journal of Pain*, *17*(2), 167–180. https://doi.org/10.1016/J.JPAIN.2015.10.015

Toda, T., & Taoka, M. (2004). Converging patterns of inputs from oral structures in the postcentral somatosensory cortex of conscious macaque monkeys. *Experimental Brain Research*, *158*(1), 43–49. https://doi.org/10.1007/s00221-004-1869-2

Toffolo, M. B. J., van den Hout, M. A., Hooge, I. T. C., Engelhard, I. M., & Cath, D. C. (2013). Mild Uncertainty Promotes Checking Behavior in Subclinical Obsessive-Compulsive Disorder: *Https://Doi.Org/10.1177/2167702612472487*, *1*(2), 103–109. https://doi.org/10.1177/2167702612472487

Tracey, I. (2010). Getting the pain you expect: Mechanisms of placebo, nocebo and reappraisal effects in humans. *Nature Medicine*, *16*(11), 1277–1283. https://doi.org/10.1038/nm.2229

Treede, R. D., Rief, W., Barke, A., Aziz, Q., Bennett, M. I., Benoliel, R., Cohen, M., Evers, S., Finnerup, N. B., First, M. B., Giamberardino, M. A., Kaasa, S., Korwisi, B., Kosek, E., Lavand'Homme, P., Nicholas, M., Perrot, S., Scholz, J., Schug, S., … Wang, S. J. (2019). Chronic pain as a symptom or a disease: The IASP Classification of Chronic Pain for the International Classification of Diseases (ICD-11). *Pain*, *160*(1), 19–27. https://doi.org/10.1097/J.PAIN.0000000000001384

Turk, D. C. (2002). Clinical effectiveness and cost-effectiveness of treatments for patients with chronic pain. *Clinical Journal of Pain*, *18*(6), 355–365. https://doi.org/10.1097/00002508-200211000-00003

Umeda, T., Koizumi, M., Katakai, Y., Saito, R., & Seki, K. (2019). Decoding of muscle activity from the sensorimotor cortex in freely behaving monkeys. *NeuroImage*, *197*, 512–526. https://doi.org/10.1016/J.NEUROIMAGE.2019.04.045

Valerio, I. L., Dumanian, G. A., Jordan, S. W., Mioton, L. M., Bowen, J. B., West, J. M., Porter, K., Ko, J. H., Souza, J. M., & Potter, B. K. (2019). Preemptive Treatment of Phantom and Residual Limb Pain with Targeted Muscle Reinnervation at the Time of Major Limb Amputation. *Journal of the American College of Surgeons*, *228*(3), 217–226. https://doi.org/10.1016/J.JAMCOLLSURG.2018.12.015

Valyear, K. F., Philip, B. A., Cirstea, C. M., Chen, P. W., Baune, N. A., Marchal, N., & Frey, S. H. (2020). Interhemispheric transfer of post-amputation cortical plasticity within the human somatosensory cortex. *NeuroImage*, *206*(September 2019), 116291. https://doi.org/10.1016/j.neuroimage.2019.116291

van der Schans, C. P., Geertzen, J. H. B., Schoppen, T., & Dijkstra, P. U. (2002). Phantom Pain and Health-Related Quality of Life in Lower Limb Amputees. *Journal of Pain and Symptom Management*, *24*(4), 429–436. https://doi.org/10.1016/S0885-3924(02)00511-0

Vase, L., Egsgaard, L. L., Nikolajsen, L., Svensson, P., Jensen, T. S., & Arendt-Nielsen, L. (2012). Pain catastrophizing and cortical responses in amputees with varying levels of phantom limb pain: A high-density EEG brain-mapping study. *Experimental Brain Research*, *218*(3), 407–417. https://doi.org/10.1007/S00221-012-3027-6/TABLES/4

Vase, L., Nikolajsen, L., Christensen, B., Egsgaard, L. L., Arendt-Nielsen, L., Svensson, P., & Staehelin Jensen, T. (2011). Cognitive-emotional sensitization contributes to wind-up-like pain in phantom limb pain patients. *PAIN*®, *152*(1), 157–162. https://doi.org/10.1016/J.PAIN.2010.10.013

Vaso, A., Adahan, H. M., Gjika, A., Zahaj, S., Zhurda, T., Vyshka, G., & Devor, M. (2014). Peripheral nervous system origin of phantom limb pain. *PAIN*®, *155*(7), 1384–1391. https://doi.org/10.1016/J.PAIN.2014.04.018

Vlaeyen, J. W. S. (2015). Learning to predict and control harmful events: Chronic pain and conditioning. *Pain*, *156*(4), S86–S93. https://doi.org/10.1097/j.pain.0000000000000107

Vlaeyen, J. W. S., Crombez, G., & Linton, S. J. (2016). The fear-avoidance model of pain. *Pain*, *157*(8), 1588–1589. https://doi.org/10.1097/J.PAIN.0000000000000574

Waller, H., Freeman, D., Jolley, S., Dunn, G., & Garety, P. (2011). Targeting reasoning biases in delusions: A pilot study of the Maudsley Review Training Programme for individuals with persistent, high conviction delusions. *Journal of Behavior Therapy and Experimental Psychiatry*, *42*(3), 414–421. https://doi.org/10.1016/J.JBTEP.2011.03.001

Walther, A., Nili, H., Ejaz, N., Alink, A., Kriegeskorte, N., & Diedrichsen, J. (2016). Reliability of dissimilarity measures for multi-voxel pattern analysis. *NeuroImage*, *137*, 188–200. https://doi.org/10.1016/j.neuroimage.2015.12.012

Wang, F., Zhang, R., Zhang, J., Li, D., Wang, Y., Yang, Y. H., & Wei, Q. (2021). Effects of mirror therapy on phantom limb sensation and phantom limb pain in amputees: A systematic review and meta-analysis of randomized controlled trials. *Clinical Rehabilitation*, *35*(12), 1710–1721. https://doi.org/10.1177/02692155211027332

Wang, X., Merzenlch, M. M., Sameshlma, K., & Jenkins, W. M. (1995). *Timing of Tactile Stimulation*. *378*(November), 71–75.

Wesselink, D. B., Heiligenberg, F. M. van den, Ejaz, N., Dempsey-Jones, H., Cardinali, L., Tarall-Jozwiak, A., Diedrichsen, J., & Makin, T. R. (2019). Obtaining and maintaining cortical hand representation as evidenced from acquired and congenital handlessness. *ELife*, *8*, 1–19. https://doi.org/10.7554/eLife.37227

Wesselink, D. B., & Maimon-Mor, R. O. (2018). *RSA toolbox extension for FSL*.

Wesselink, D. B., Sanders, Z.-B., Edmondson, L. R., Dempsey-Jones, H., Kieliba, P., Kikkert, S., Themistocleous, A. C., Emir, U., Diedrichsen, J., Saal, H. P., & Makin, T. R. (2022). Malleability of the cortical hand map following a finger nerve block. *Science Advances*, *8*(16), 2393. https://doi.org/10.1126/SCIADV.ABK2393

Wetzels, R., Matzke, D., Lee, M. D., Rouder, J. N., Iverson, G. J., & Wagenmakers, E. J. (2011). Statistical evidence in experimental psychology: An empirical comparison using 855 t tests. *Perspectives on Psychological Science*, *6*(3), 291–298. https://doi.org/10.1177/1745691611406923

Whyte, A. S., & Niven, C. A. (2001). Variation in Phantom Limb Pain: Results of a Diary Study. *Journal of Pain and Symptom Management*, *22*(5), 947–953. https://doi.org/10.1016/S0885-3924(01)00356-6

Wiech, K. (2016). Deconstructing the sensation of pain: The influence of cognitive processes on pain perception. *Science*, *354*(6312), 584–587. https://doi.org/10.1126/science.aaf8934

Wiech, K., Edwards, R., Moseley, G. L., Berna, C., Ploner, M., & Tracey, I. (2014). Dissociable Neural Mechanisms Underlying the Modulation of Pain and Anxiety? An fMRI Pilot Study. *PLOS ONE*, *9*(12), e110654. https://doi.org/10.1371/JOURNAL.PONE.0110654

Wiech, K., Eippert, F., Vandekerckhove, J., Zaman, J., Placek, K., Tuerlinckx, F., Vlaeyen, J. W. S., & Tracey, I. (2022). Cortico-Brainstem Mechanisms of Biased Perceptual Decision-Making in the Context of Pain. *The Journal of Pain*, *23*(4), 680–692. https://doi.org/10.1016/J.JPAIN.2021.11.006

Wiech, K., Jbabdi, S., Lin, C. S., Andersson, J., & Tracey, I. (2014). Differential structural and resting state connectivity between insular subdivisions and other pain-related brain regions. *Pain*, *155*(10), 2047–2055. https://doi.org/10.1016/j.pain.2014.07.009

Wiech, K., Kalisch, R., Weiskopf, N., Pleger, B., Stephan, K. E., & Dolan, R. J. (2006). Anterolateral Prefrontal Cortex Mediates the Analgesic Effect of Expected and Perceived Control over Pain. *Journal of Neuroscience*, *26*(44), 11501–11509. https://doi.org/10.1523/JNEUROSCI.2568-06.2006

Wiech, K., Vandekerckhove, J., Zaman, J., Tuerlinckx, F., Vlaeyen, J. W. S., & Tracey, I. (2014). Influence of prior information on pain involves biased perceptual decision-making. *Current Biology*, *24*(15), R679–R681. https://doi.org/10.1016/J.CUB.2014.06.022

Wiestler, T., & Diedrichsen, J. (2013). Skill learning strengthens cortical representations of motor sequences. *ELife*, *2013*(2), 1–20. https://doi.org/10.7554/eLife.00801

Wiestler, T., McGonigle, D. J., & Diedrichsen, J. (2011). Integration of sensory and motor representations of single fingers in the human cerebellum. *Journal of Neurophysiology*, *105*(6), 3042–3053. https://doi.org/10.1152/JN.00106.2011/ASSET/IMAGES/LARGE/Z9K0061107940008.JPEG

Willoughby, W. R., Thoenes, K., & Bolding, M. (2021). Somatotopic Arrangement of the Human Primary Somatosensory Cortex Derived From Functional Magnetic Resonance Imaging. *Frontiers in Neuroscience*, *14*, 1397. https://doi.org/10.3389/FNINS.2020.598482/BIBTEX

Winkler, A. M., Ridgway, G. R., Webster, M. A., Smith, S. M., & Nichols, T. E. (2014). Permutation inference for the general linear model. *NeuroImage*, *92*, 381–397. https://doi.org/10.1016/j.neuroimage.2014.01.060

Wise, R. G., Rogers, R., Painter, D., Bantick, S., Ploghaus, A., Williams, P., Rapeport, G., & Tracey, I. (2002). Combining fMRI with a pharmacokinetic model to determine which brain areas activated by painful stimulation are specifically modulated by remifentanil. *NeuroImage*, *16*(4), 999–1014. https://doi.org/10.1006/nimg.2002.1146

Wrigley, P. J., Press, S. R., Gustin, S. M., Macefield, V. G., Gandevia, S. C., Cousins, M. J., Middleton, J. W., Henderson, L. A., & Siddall, P. J. (2009). Neuropathic pain and primary somatosensory cortex reorganization following spinal cord injury. *PAIN®*, *141*(1–2), 52–59. https://doi.org/10.1016/J.PAIN.2008.10.007

Xiao, X., & Zhang, Y. Q. (2018). A new perspective on the anterior cingulate cortex and affective pain. *Neuroscience & Biobehavioral Reviews*, *90*, 200–211. https://doi.org/10.1016/J.NEUBIOREV.2018.03.022

Yanagisawa, T., Fukuma, R., Seymour, B., Hosomi, K., Kishima, H., Shimizu, T., Yokoi, H., Hirata, M., Yoshimine, T., Kamitani, Y., & Saitoh, Y. (2016).

Induced sensorimotor brain plasticity controls pain in phantom limb patients. *Nature Communications 2016 7:1*, *7*(1), 1–11. https://doi.org/10.1038/ncomms13209

Yang, T. T., Gallen, C. C., Schwartz, B. J., & Bloom, F. E. (1993). Noninvasive somatosensory homunculus mapping in humans by using a large- array biomagnetometer. *Proceedings of the National Academy of Sciences of the United States of America*, *90*(7), 3098–3102. https://doi.org/10.1073/pnas.90.7.3098

Yon, D., de Lange, F. P., & Press, C. (2019). The Predictive Brain as a Stubborn Scientist. *Trends in Cognitive Sciences*, *23*(1), 6–8. https://doi.org/10.1016/J.TICS.2018.10.003

Yoshida, W., Seymour, B., Koltzenburg, M., & Dolan, R. J. (2013). Uncertainty Increases Pain: Evidence for a Novel Mechanism of Pain Modulation Involving the Periaqueductal Gray. *Journal of Neuroscience*, *33*(13), 5638–5646. https://doi.org/10.1523/JNEUROSCI.4984-12.2013

Young, H. F., & Bentall, R. P. (1997). Probabilistic reasoning in deluded, depressed and normal subjects: Effects of task difficulty and meaningful versus non-meaningful material. *Psychological Medicine*, *27*(2), 455–465. https://doi.org/10.1017/S0033291796004540

Yu, A. J., & Dayan, P. (2005). Uncertainty, Neuromodulation, and Attention. *Neuron*, *46*(4), 681–692. https://doi.org/10.1016/J.NEURON.2005.04.026

Zhang, S., Mano, H., Ganesh, G., Robbins, T., & Seymour, B. (2016). Dissociable Learning Processes Underlie Human Pain Conditioning. *Current Biology*, *26*(1), 52–58. https://doi.org/10.1016/j.cub.2015.10.066

Zhang, S., Mano, H., Lee, M., Yoshida, W., Kawato, M., Robbins, T. W., & Seymour, B. (2018). The control of tonic pain by active relief learning. *ELife*, *7*, 1–30. https://doi.org/10.7554/eLife.31949

Appendices

6.1 Supplementary Materials Chapter 1

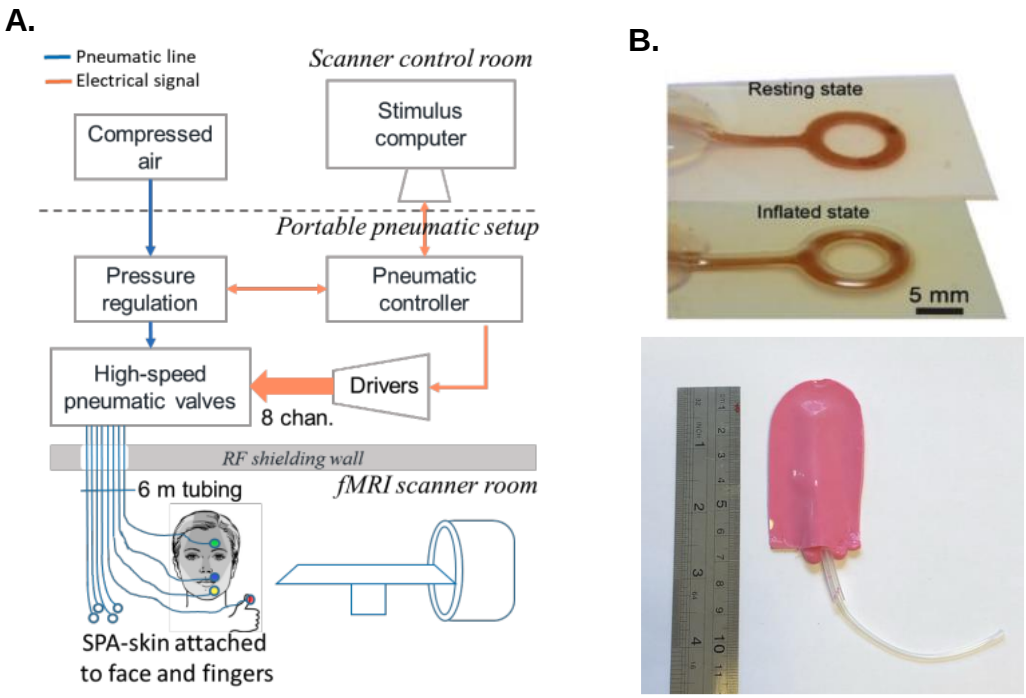
6.1.1 Supplementary Methods

The SPA-skin is made of MR-safe silicone that has a similar stiffness as the human skin. The actuators consist of an elastomeric membrane that can be pneumatically inflated with pressure input, and has a total thickness of 1 mm. It utilises closed-loop feedback control, to ensure accurate tactile stimulation and has an actuation bandwidth 15 – 35 Hz, and pressure of 80 kPa. The SPA-skin set-up involved: a computer, portable air compressor, portable pneumatic control circuit model, and corresponding pneumatic tubes and actuators (up to 8). The air compressor (Implotex, Germany) produced the airflow to the pressure regulator (ITV1050, SMC Corp., USA) that was controlled by the microcontroller in the control circuit. The stimulation intensity could thus be adjusted by modulating the airflow via the pressure regulator, which in turn, could be controlled by serial commands from the computer. This allowed real time manipulation of stimulation intensity and frequency. See *Supplementary Figure 1.A* for a schematic illustration of the set-up.

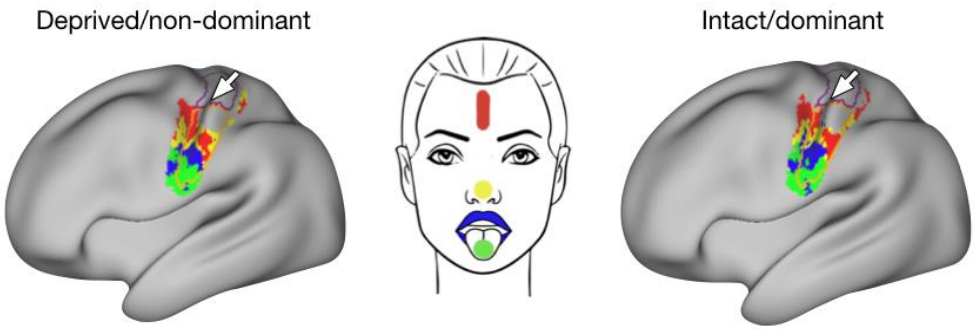
Actuators were attached to the body using micropore surgical tape. In order to constrain and direct the inflation of the actuators towards the skin, 3D-printed small pads, just larger than the actuators inflatable ring, were made of PLA (Polylactic acid - biodegradable thermoplastic) and placed behind the actuators before taping them onto the skin. To stimulate the tongue, a flexible disposable pouch made of biocompatible dental silicone (Turboflex Light Fast R&S) was made with a disposable actuator placed inside and sealed (see *Supplementary*

Figure 1.B). The participant then placed the actuator pouch on the top of their tongue, with the pneumatic tube between the lips, preventing choking. Thus, when pressure was sent to the actuator, the silicon pouch inflated at the same speed and intensity, stimulating the tongue. Each participant had a new biocompatible dental silicone pouch created for them.

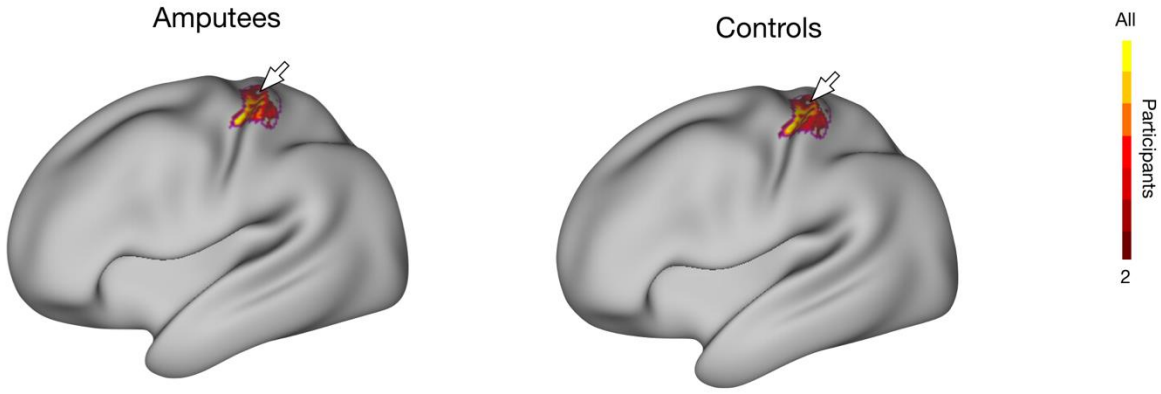
6.1.2 Supplementary Figures



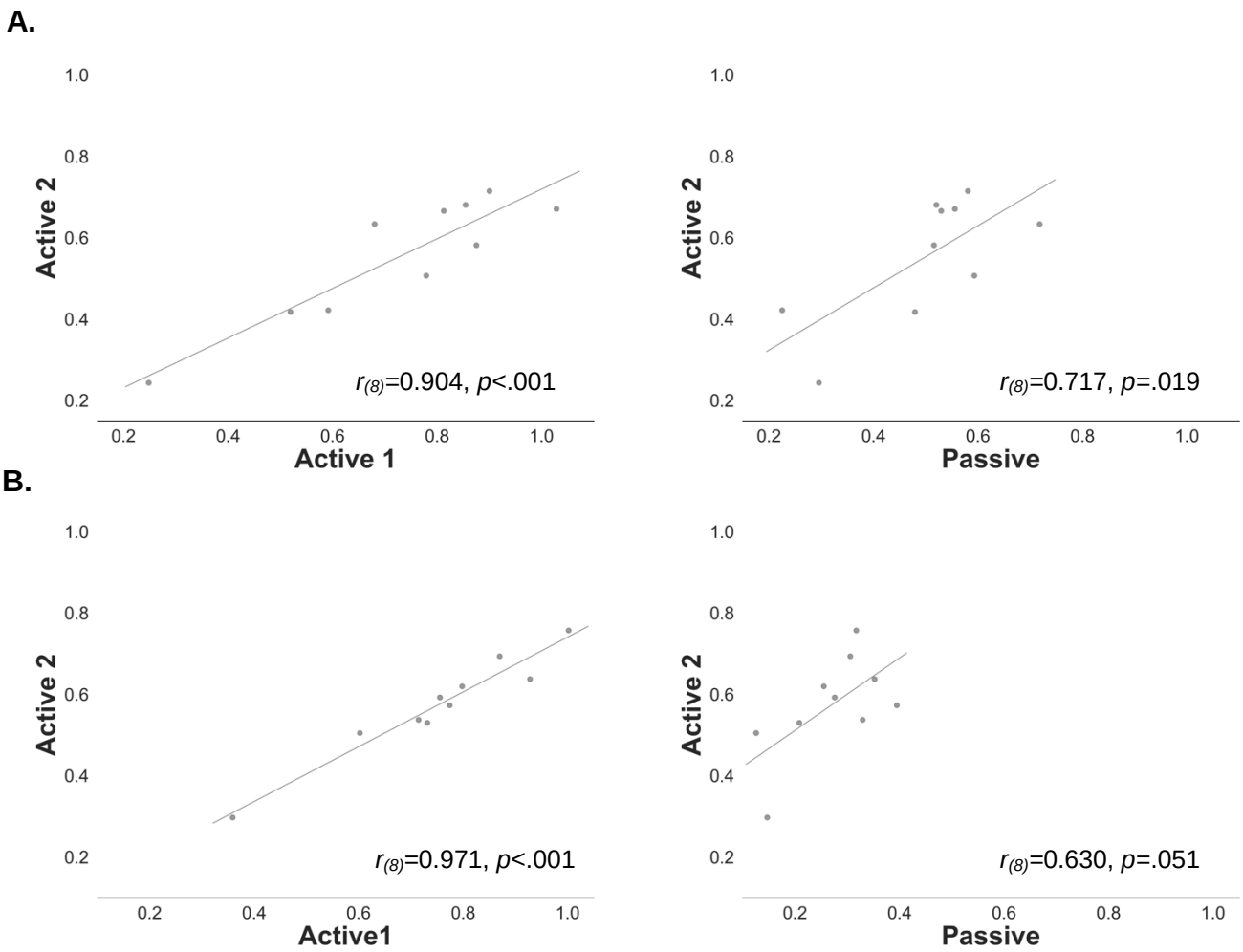
Supplementary Figure 1. Schematic illustration and examples of actuators used for the passive stimulation protocol. (A) Here is a schematic illustration of the SPA-skin set-up in the scanner and scanner control room. Note this schematic was taken from Kikkert et al., (2022) and so minor details differed to our protocol, e.g., stimulation sites. **(B)** On the top row is an example picture (also taken from Kikkert et al., 2022) of the SPA-skin's actuators both in a resting and inflated state. By modulating the amount of pressure and speed of inflation different stimulation intensities and frequencies can be achieved. On the bottom row is an example of the dental silicone pouch we created, which contained an actuator, in order to stimulate the tongue within our passive stimulation protocol.



Supplementary Figure 2. *Group-level activity maps of two-handed control participants with nose movements.* Group average activity for the forehead (red), nose (yellow), lips (blue) and tongue (green) movements, contrasted to rest, in the deprived/non-dominant hemisphere and intact/dominant hemisphere for controls (*n* = 22). All clusters were created using a threshold-free cluster enhancement procedure with a sensorimotor pre-threshold mask (defined using the Harvard Cortical Atlas), and thresholded at $p < .01$. The hand and face ROIs are outlined in purple and orange respectively, and the central sulcus is denoted with a white arrow.



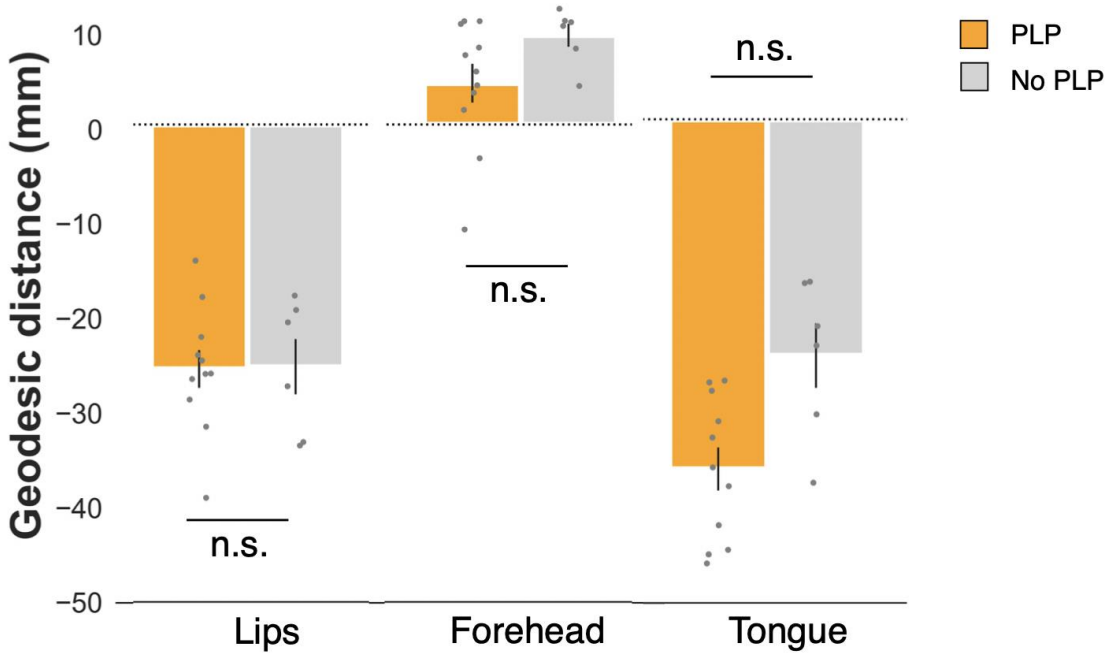
Supplementary Figure 3. *Phantom and non-dominant thumb representation in the deprived hemisphere of amputees and controls.* Group-level consistency map for the phantom/non-dominant thumb in the hand ROI for amputees (n = 17) and controls (n = 22). Note the percentage of surface area coverage of the deprived/non-dominant hand ROI was not significantly different for the phantom (*M*=69.448%; *SE*=3.752%) compared to the non-dominant thumb of controls (*M*=63.989%; *SE*=3.594 %; *U*=225.000, *p*=0.292, *d*=0.203, BF_{10}=0.579). The colour gradient represents participant agreement for maximally activating that particular voxel, relative to the face movements (winner-takes-all approach). The hand ROI is outlined in purple and central sulcus denoted by the white arrow.



Supplementary Figure 4. *Correlations between sessions (Active and Passive) for two control case studies in the intact hemisphere.* **(A)** Pearson correlations for CTR 01. Significant correlations between Active 1 and Active 2 ($r_{(8)}$=0.904, p<.001, 95% CI[0.64, 0.98], BF_{10}=97.268), and Active 2 and Passive ($r_{(8)}$=0.717, p=.019, 95% CI[0.16, 0.93], BF_{10}=4.239), were found between pairwise distances in the face ROI of the intact hemisphere. **(B)** Pearson correlations for CTR 02. Again, significant correlations were found for Active 1 and Active 2 ($r_{(8)}$=0.971, p<.001, 95% CI[0.88, 0.99], BF_{10}=3657.947), as well as strong positive trend for Active 2 and Passive ($r_{(8)}$=0.630, p=.051, 95% CI[0.0, 0.9], BF_{10}=2.094), for pairwise distances in the face ROI of the intact hemisphere.

6.2 Supplementary Materials Chapter 2

6.2.1 Supplementary Figures



Supplementary Figure 5. *Comparison of cortical distances in the deprived hemisphere of amputees.* Cortical (geodesic) distances were compared between amputees who reported the presence of PLP (n=11; orange) and amputees without PLP (n=6; grey) using a one-tailed Independent Samples *t*-test. Non-significant differences were found for the lips ($t_{(15)}$=-0.068, p=0.527, d=-0.035, BF_{10}=0.414), forehead ($t_{(15)}$=-1.720, p=0.947, d=-0.873, BF_{10}=0.203) and tongue ($t_{(15)}$=-3.018, p=0.996, d=-1.532, BF_{10}=0.156). Contrary to popular theories of brain plasticity and phantom limb pain (PLP; see *Chapter 2, Introduction*), these results demonstrate that individuals with PLP do not exhibit greater instances of cortical remapping in the deprived hemisphere of the tested facial parts, including both the traditional marker of plasticity – the lips – and the cortical neighbour – the forehead.

6.2.2 Supplementary Tables

Within Subjects Effects

Cases	Sum of Squares	df	Mean Square	F	p	η^2_p
Hemisphere	0.003	1	0.003	1.910e -4	0.989	5.307e -6
Hemisphere ✻ group	0.053	1	0.053	0.003	0.954	9.566e -5
Hemisphere ✻ brainVol	0.092	1	0.092	0.006	0.939	1.661e -4
Residuals	553.654	36	15.379			

Note. Type III Sum of Squares

Between Subjects Effects

Cases	Sum of Squares	df	Mean Square	F	p	η^2_p
group	67.225	1	67.225	1.821	0.186	0.048
brainVol	245.659	1	245.659	6.655	0.014	0.156
Residuals	1328.857	36	36.913			

Note. Type III Sum of Squares

Supplementary Table 1. *Main effects and interaction for comparison of geodesic distances between amputees and controls for the lips.*

Within Subjects Effects

Cases	Sum of Squares	df	Mean Square	F	p	η^2_p
Hemisphere	4.987	1	4.987	0.290	0.593	0.007
Hemisphere ✻ group	93.236	1	93.236	5.419	0.025	0.119
Hemisphere ✻ brainVol	0.920	1	0.920	0.053	0.818	0.001
Residuals	688.253	40	17.206			

Note. Type III Sum of Squares

Between Subjects Effects

Cases	Sum of Squares	df	Mean Square	F	p	η^2_p
group	7.777	1	7.777	0.194	0.662	0.005
brainVol	550.077	1	550.077	13.725	< .001	0.255
Residuals	1603.114	40	40.078			

Note. Type III Sum of Squares

Supplementary Table 2. *Main effects and interaction for comparison of geodesic distances between one-handers and controls for the lips.*

Within Subjects Effects

Cases	Sum of Squares	df	Mean Square	F	p	η^2_p
Hemisphere	4.254	1	4.254	0.229	0.635	0.006
Hemisphere ✻ group	17.380	1	17.380	0.935	0.340	0.025
Hemisphere ✻ brainVol	2.752	1	2.752	0.148	0.703	0.004
Residuals	668.911	36	18.581			

Note. Type III Sum of Squares

Between Subjects Effects

Cases	Sum of Squares	df	Mean Square	F	p	η^2_p
group	14.117	1	14.117	0.634	0.431	0.017
brainVol	92.715	1	92.715	4.164	0.049	0.104
Residuals	801.643	36	22.268			

Note. Type III Sum of Squares

Supplementary Table 3. *Main effects and interaction for comparison of geodesic distances between amputees and controls for the forehead.*

Within Subjects Effects

Cases	Sum of Squares	df	Mean Square	F	p	η^2_p
Hemisphere	0.070	1	0.070	0.005	0.941	1.367e -4
Hemisphere ✻ group	106.153	1	106.153	8.287	0.006	0.172
Hemisphere ✻ brainVol	0.134	1	0.134	0.010	0.919	2.620e -4
Residuals	512.392	40	12.810			

Note. Type III Sum of Squares

Between Subjects Effects

Cases	Sum of Squares	df	Mean Square	F	p	η^2_p
group	68.526	1	68.526	2.575	0.116	0.060
brainVol	50.946	1	50.946	1.914	0.174	0.046
Residuals	1064.519	40	26.613			

Note. Type III Sum of Squares

Supplementary Table 4. *Main effects and interaction for comparison of geodesic distances between one-handers and controls for the forehead.*

Within Subjects Effects

Cases	Sum of Squares	df	Mean Square	F	p	η^2_p
Hemisphere	0.164	1	0.164	0.011	0.918	2.995e -4
Hemisphere ✻ group	38.760	1	38.760	2.546	0.119	0.066
Hemisphere ✻ brainVol	0.794	1	0.794	0.052	0.821	0.001
Residuals	548.070	36	15.224			

Note. Type III Sum of Squares

Between Subjects Effects

Cases	Sum of Squares	df	Mean Square	F	p	η^2_p
group	106.146	1	106.146	0.797	0.378	0.022
brainVol	285.276	1	285.276	2.142	0.152	0.056
Residuals	4795.420	36	133.206			

Note. Type III Sum of Squares

Supplementary Table 5. *Main effects and interaction for comparison of geodesic distances between amputees and controls for the tongue.*

Within Subjects Effects

Cases	Sum of Squares	df	Mean Square	F	p	η^2_p
Hemisphere	39.972	1	39.972	1.493	0.229	0.036
Hemisphere ✻ group	191.346	1	191.346	7.149	0.011	0.152
Hemisphere ✻ brainVol	25.683	1	25.683	0.960	0.333	0.023
Residuals	1070.656	40	26.766			

Note. Type III Sum of Squares

Between Subjects Effects

Cases	Sum of Squares	df	Mean Square	F	p	η^2_p
group	174.848	1	174.848	1.732	0.196	0.042
brainVol	441.349	1	441.349	4.373	0.043	0.099
Residuals	4037.482	40	100.937			

Note. Type III Sum of Squares

Supplementary Table 6. *Main effects and interaction for comparison of geodesic distances between one-handers and controls for the tongue.*

Fixed Effect Omnibus tests

	F	Num df	Den df	p
Group	2.2211	1	37.0	0.145
Hemisphere	1.8462	1	259.0	0.175
faceThumbPairs	3.4735	3	259.0	0.017
Group ✻ Hemisphere	0.0571	1	259.0	0.811
Group ✻ faceThumbPairs	0.7404	3	259.0	0.529
Hemisphere ✻ faceThumbPairs	0.3653	3	259.0	0.778
Group ✻ Hemisphere ✻ faceThumbPairs	0.5692	3	259.0	0.636

Note. Satterthwaite method for degrees of freedom

Supplementary Table 7. *Results from the linear mixed model used to explore differences in the face-thumb pairwise distances in the hand ROI for amputees and controls.*

Fixed Effect Omnibus tests

	F	Num df	Den df	p
Group	2.409	2	56.0	0.099
Hemisphere	27.059	1	627.0	< .001
FacePairs	22.380	5	627.0	< .001
Age	0.286	1	56.0	0.595
Group ✻ Hemisphere	14.544	2	627.0	< .001
Group ✻ FacePairs	0.881	10	627.0	0.551
Hemisphere ✻ FacePairs	1.056	5	627.0	0.384
Group ✻ Hemisphere ✻ FacePairs	0.572	10	627.0	0.837

Note. Satterthwaite method for degrees of freedom

Supplementary Table 8. *Results from the linear mixed model used to explore differences in the face-face pairwise distances in the hand ROI for amputees, one-handers and controls.*

Fixed Effect Omnibus tests

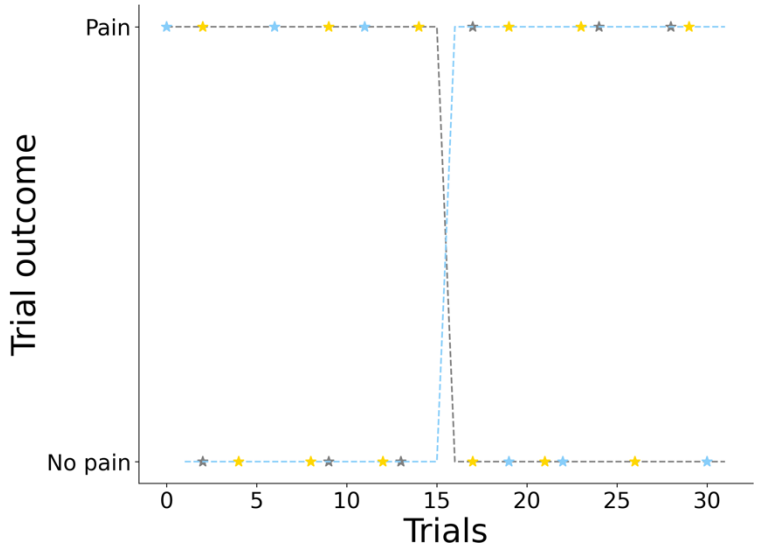
	F	Num df	Den df	p
Group	1.010	2	56.0	0.371
Hemisphere	1.301	1	627.0	0.254
FacePairs	268.322	5	627.0	< .001
Age	0.282	1	56.0	0.598
Group ✻ Hemisphere	0.626	2	627.0	0.535
Group ✻ FacePairs	1.462	10	627.0	0.150
Hemisphere ✻ FacePairs	0.222	5	627.0	0.953
Group ✻ Hemisphere ✻ FacePairs	0.136	10	627.0	0.999

Note. Satterthwaite method for degrees of freedom

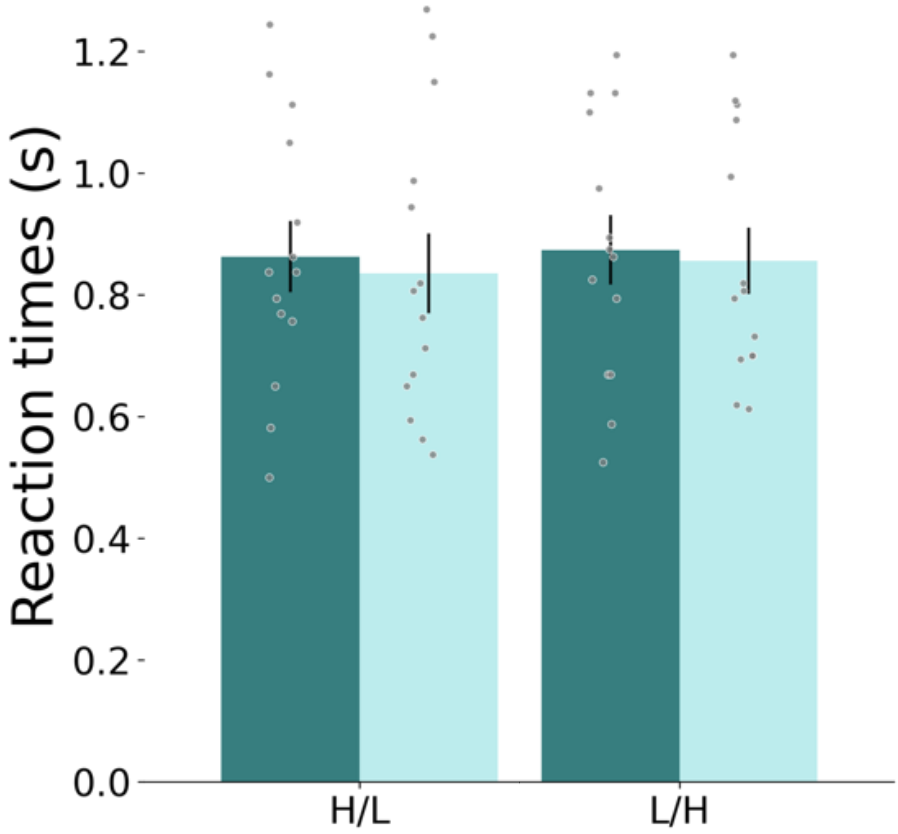
Supplementary Table 9. *Results from the linear mixed model used to explore differences in the face-face pairwise distances in the face ROI for amputees, one-handers and controls.*

6.3 Supplementary Materials Chapter 3

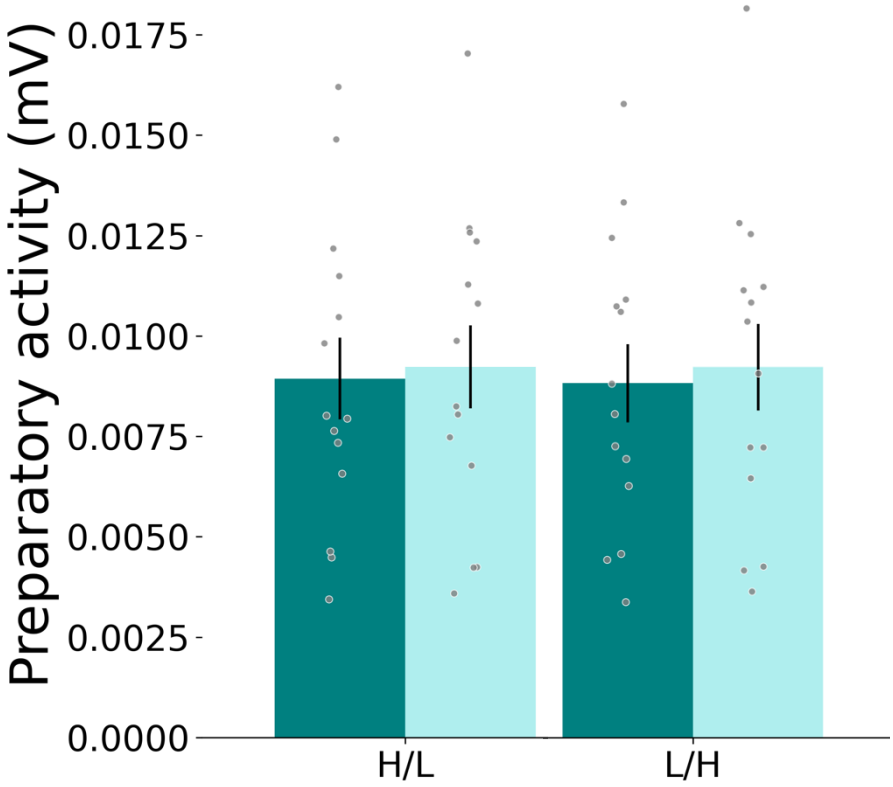
6.3.1 Supplementary Figures



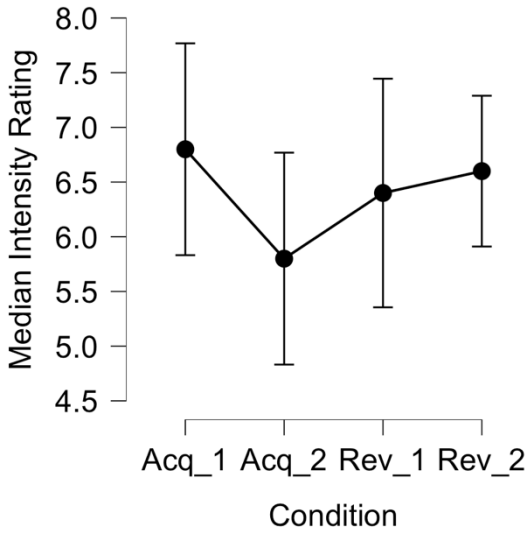
Supplementary Figure 6. *Schematic outline for the H-L and L-H sequence in Active and Passive (matched and unmatched) conditions.* Trial outcome (pain/no pain) is on the *y*-axis and trial number is on the *x*-axis, with the H-L cue (grey) switching to a low-pain probability halfway through, and vice versa for the L-H cue (light blue) for Active and Passive (matched) conditions. Surprise trials are denoted by stars for each cue (grey and light blue). Note that gold stars indicate the 'unmatched' surprise trials for each cue in the Passive condition, which was administered to *n*=11 participants.



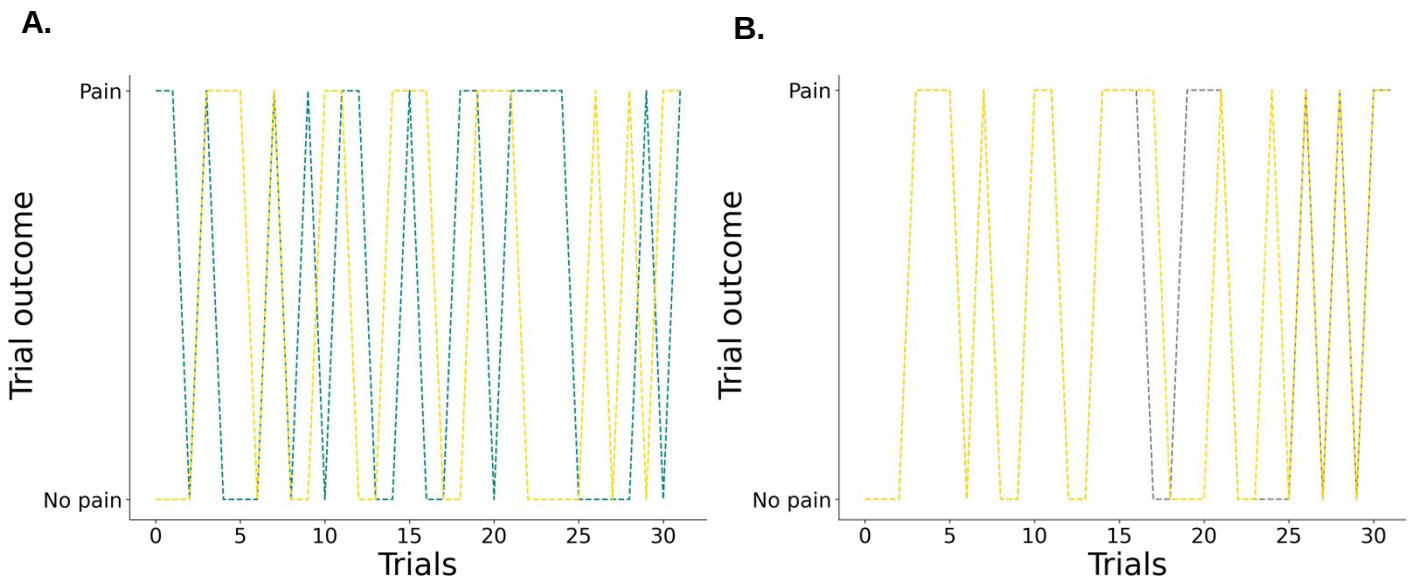
Supplementary Figure 7. *Response latencies recorded for a sub-sample of control participants.* Non-significant main effect of Cue (H-L x L-H) ($F_{(1,13)}$=0.0114, p=0.917, η^2_p=0.001, BF_{10}=0.2656, $BF_{Inclusion}$=0.264), Block (Acquisition x Reversal) ($F_{(1,13)}$=0.1915, p=0.669, η^2_p=0.015, BF_{10}=0.2880, $BF_{Inclusion}$=0.287) or Cue x Block interaction ($F_{(1,13)}$=1.9551, p=0.185, η^2_p=0.131, BF_{10}=0.1048, $BF_{Inclusion}$=1.402) was found for response latencies (*y*-axis; time (seconds) between 'Go' cue and movement initiation) in sub-sample of control participants (n=14) for each cue (*x*-axis). Results therefore indicate, contrary to predictions, that participants did not display response delays to the high-pain probability cue across the paradigm. Timings in acquisition block are in darker colours, reversal block in lighter colours, with individual data points and standard error of the mean plotted in grey.



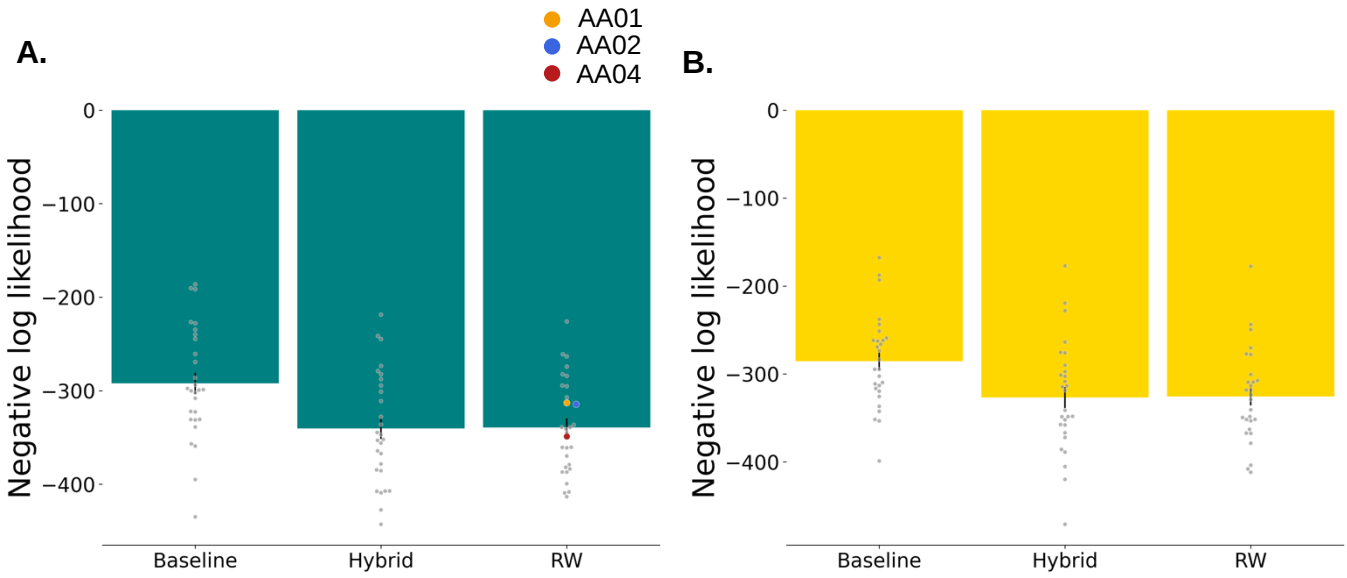
Supplementary Figure 8. *Preparatory activity recorded for a sub-sample of control participants.* Non-significant main effect of Cue (H-L x L-H) ($F_{(1,13)}$=1.0777, p=0.318, η^2_p=0.077, BF_{10}=0.2756, $BF_{Inclusion}$=0.274), Block (Acquisition x Reversal) ($F_{(1,13)}$=0.0142, p=0.907, η^2_p=0.001, BF_{10}=0.4411, $BF_{Inclusion}$=0.439) or Cue x Block interaction ($F_{(1,13)}$=3.0543, p=0.104, η^2_p=0.190, BF_{10}=0.0412, $BF_{Inclusion}$=0.347) was found for preparatory activity (y-axis; millivolts (mV)) in sub-sample of control participants (n=14) for each cue (x-axis). Results therefore indicate, contrary to predictions, that participants did not display increases in muscular amplitude to the high-pain probability cue across the paradigm. Muscle activity in acquisition block is denoted by darker colours, reversal block in lighter colours, with individual data points and standard error of the mean plotted in grey.



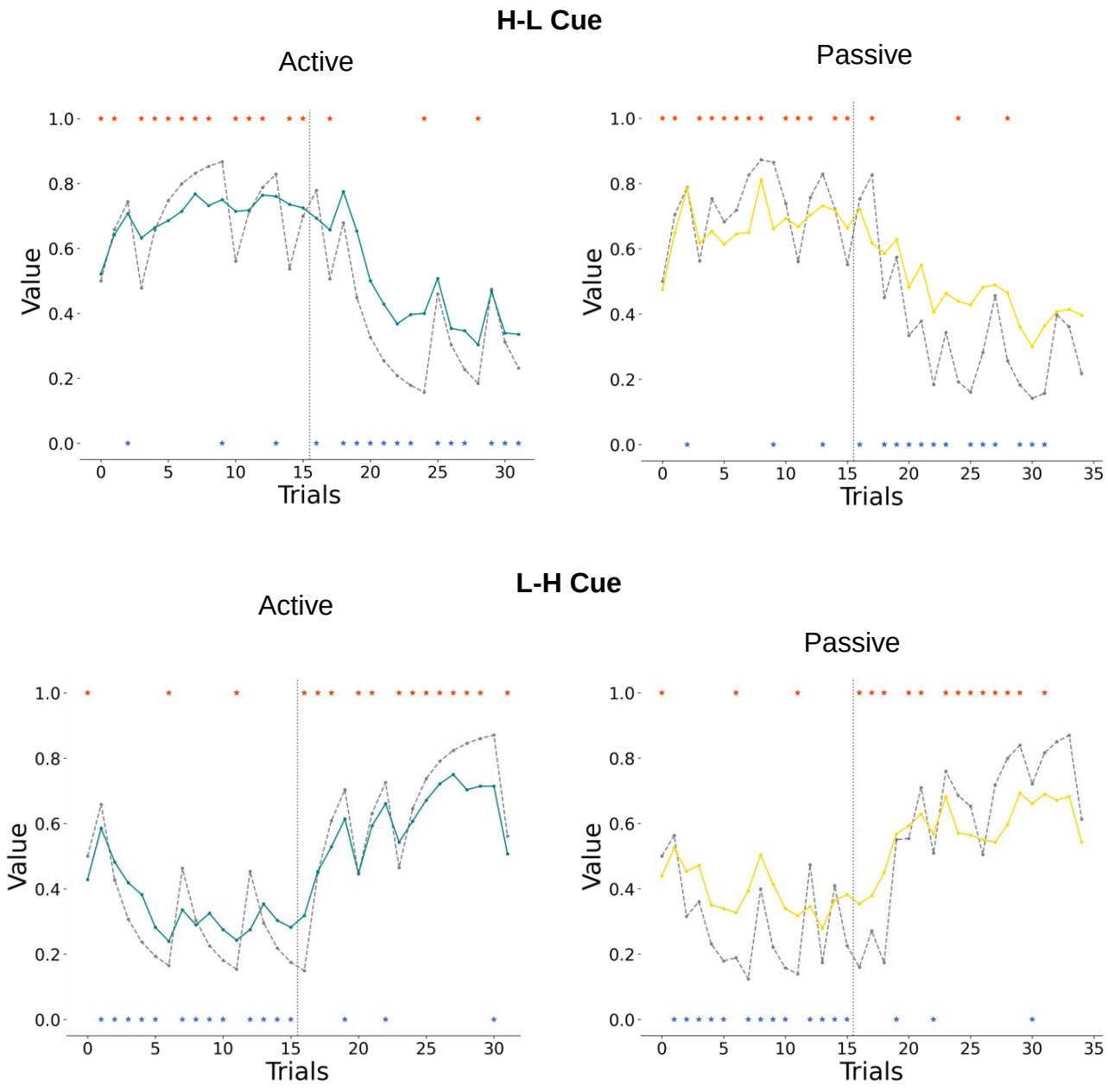
Supplementary Figure 9. *Data from sensitisation/habituation pilots in n=5 control participants.* To assess for sensitisation/habituation effects in the experimental paradigm *n*=5 healthy controls (age: *M*=25.2 years, *SD*=6.3 years; 3 females; 1 left-handed) were recruited to complete a modified version of the task. Each participant went through a shortened pain thresholding procedure whereby the target pain rating of '6' was achieved by using ascending/descending staircases. The task consisted of 96 trials spilt into 4 blocks, with the acquisition and reversal block presented in halves (Acq 1-2; Rev 1-2). Each trial started with the presentation of a geometric shape during administration of the painful temperature for 3 seconds, followed by a verbal intensity rating (0=no pain at all; 10=worst pain imaginable; 3 seconds) and an inter-trial-interval of 20 seconds. Thus, the time between each administration of the thermal stimulus to the same stimulation site was ~23 seconds (in the main experimental paradigm this was increased to ~31 seconds). This allowed us to assess how variable the intensity ratings were for a painful temperature across the length of a similar paradigm. A resulting Friedman test (within-subjects factor of Block (Acq_1 x Acq_2 x Rev_1 x Rev_2)) demonstrated that intensity ratings did not significantly vary across acquisition and reversal blocks ($\chi_{2(3)}$=4.214, *p*=0.237, *W*=0.882), indicating that sensitisation/habituation effects are not likely to occur within this paradigm.



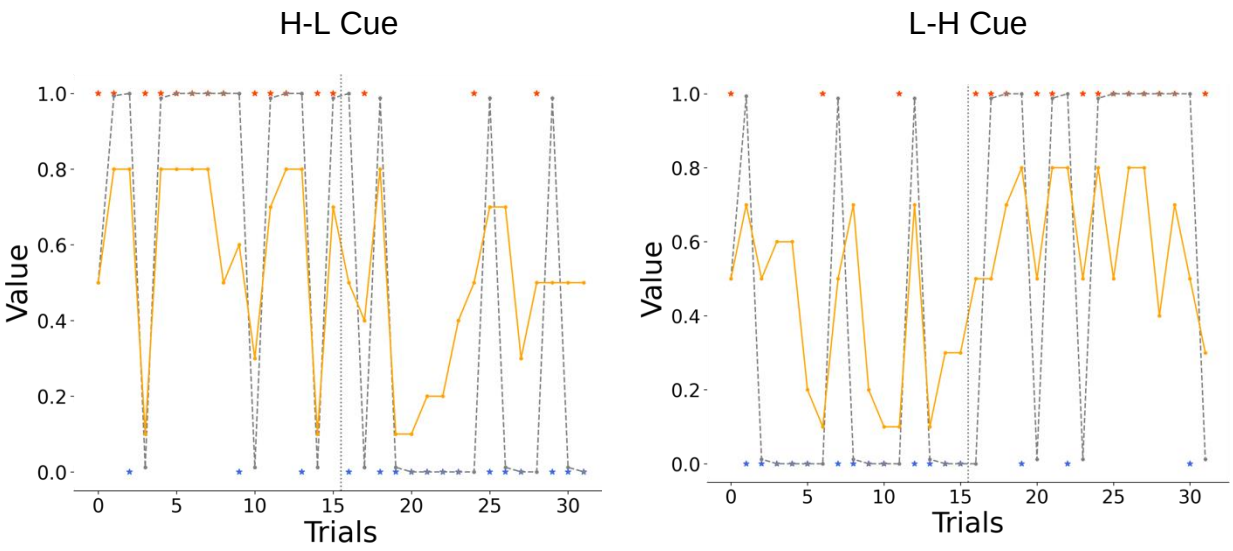
Supplementary Figure 10. *Sequences for the 50-50 cue in Active and Passive conditions.* **(A)** 50-50 sequence for Active (teal) and Passive (gold) conditions. Number of trials is on the *x*-axis (32 trials in total; 16 trials per block), and the trial's sensory outcome, whether it is painful or not, is on the *y*-axis. Note the prolonged number of painful trials in the reversal block for the Active condition (trial 21 – 25). **(B)** 50-50 sequences for the passive condition with matched surprise trials of the H-L and L-H cues to Active (grey) and unmatched surprise trials (gold). Note only slight differences to the 50-50 sequence when matching the surprise trials due to ensuring a painful temperature was not administered to the same stimulation site twice.



Supplementary Figure 11. *Negative log likelihood of model fits*. Average negative log likelihoods (*y*-axis) of model fits for all models (*x*-axis): baseline (Rescorla-Wagner; Pain sequence), Hybrid (Pearce-Hall Hybrid) and RW (Rescorla-Wagner; Cue Sequence). Note for Active (teal; **(A)**) and Passive (gold; **(B)**) conditions, the negative log likelihoods for Hybrid and RW model were not significantly different from each other (Active: $t_{(27)}$=0.366, p=0.717, d=0.0692, BF_{10}=0.213; Passive: W=169, p=0.451, r_{bs}=-0.1675, BF_{10}=0.208). However, when using a more sensitive model comparison procedure (see main text in *Chapter 3*) based on model log evidence (i.e., the absolute of the negative log likelihoods), the RW was found to be the 'winning' model. Standard error of the mean and individual data-points are plotted in grey. Amputee data-points are only plotted for the Active RW model, and are coloured using participant-specific colours (AA01=orange, AA02=blue, AA04=red).



Supplementary Figure 12. *Actual and predicted average expectancy ratings for control participants.* Actual and predicted (grey) average expectancy ratings (y-axis) are plotted for the H-L cue (top row) and L-H cue (bottom row) for Active (teal) and Passive (matched surprise trials; gold) conditions. Painful trials are denoted in red stars and warm trials in blue stars, with the vertical dashed line separating the acquisition and reversal block.



Supplementary Figure 13. *Actual and predicted expectancy ratings for AA01.* Plotted actual (orange) and predicted (grey) expectancy ratings (y-axis) from AA01 using the fitted learning rate of 0.988 for the H-L and L-H cue (number of trials along the x-axis). Painful trials are denoted red stars and warm trials are denoted by blue stars, with the acquisition and reversal block separated by a vertical dashed line. Note that AA01's ratings dramatically shift after a surprise trial (particularly for the H-L cue), demonstrating the greater reliance this individual placed on recent sensory outcomes of the previous trial (i.e., prediction error).

6.3.2 Supplementary Tables

Within Subjects Effects

	Sum of Squares	df	Mean Square	F	p	η^2_p
Task	0.00116	1	0.00116	0.00103	0.975	0.000
Task ✻ PassiveSeq	0.77008	1	0.77008	0.68099	0.417	0.026
Residual	29.40145	26	1.13083			
Cue	17.97923	1	17.97923	6.55303	0.017	0.201
Cue ✻ PassiveSeq	1.90558	1	1.90558	0.69454	0.412	0.026
Residual	71.33493	26	2.74365			
Block	0.00102	1	0.00102	8.59e-4	0.977	0.000
Block ✻ PassiveSeq	1.36527	1	1.36527	1.15355	0.293	0.042
Residual	30.77187	26	1.18353			
Task ✻ Cue	1.26975	1	1.26975	2.12576	0.157	0.076
Task ✻ Cue ✻ PassiveSeq	0.51705	1	0.51705	0.86561	0.361	0.032
Residual	15.53029	26	0.59732			
Task ✻ Block	0.96377	1	0.96377	1.32678	0.260	0.049
Task ✻ Block ✻ PassiveSeq	2.12789	1	2.12789	2.92937	0.099	0.101
Residual	18.88635	26	0.72640			
Cue ✻ Block	207.68781	1	207.68781	45.96193	< .001	0.639
Cue ✻ Block ✻ PassiveSeq	1.15614	1	1.15614	0.25586	0.617	0.010
Residual	117.48600	26	4.51869			
Task ✻ Cue ✻ Block	3.05154	1	3.05154	2.30349	0.141	0.081
Task ✻ Cue ✻ Block ✻ PassiveSeq	1.82380	1	1.82380	1.37672	0.251	0.050
Residual	34.44346	26	1.32475			

Note. Type 3 Sums of Squares

Supplementary Table 10. *Repeated measures ANOVA statistics, with within-subject factors of Task/Condition (Active x Passive), Cue (H-L x L-H) and Block (Acquisition x Reversal), controlling for passive sequence type (PassiveSeq), for expectancy ratings in control participants (n=28).*

Within Subjects Effects

	Sum of Squares	df	Mean Square	F	p	η^2_p
Task	8.4233	1	8.4233	12.098	0.002	0.318
Task ✻ PassiveSeq	7.8214	1	7.8214	11.234	0.002	0.302
Residual	18.1026	26	0.6963			
Cue	0.6690	1	0.6690	2.517	0.125	0.088
Cue ✻ PassiveSeq	1.4547	1	1.4547	5.472	0.027	0.174
Residual	6.9114	26	0.2658			
Block	0.1364	1	0.1364	0.350	0.559	0.013
Block ✻ PassiveSeq	1.7533	1	1.7533	4.501	0.044	0.148
Residual	10.1274	26	0.3895			
Task ✻ Cue	0.0341	1	0.0341	0.146	0.706	0.006
Task ✻ Cue ✻ PassiveSeq	0.1839	1	0.1839	0.786	0.383	0.029
Residual	6.0848	26	0.2340			
Task ✻ Block	0.8528	1	0.8528	1.824	0.189	0.066
Task ✻ Block ✻ PassiveSeq	0.7505	1	0.7505	1.605	0.216	0.058
Residual	12.1583	26	0.4676			
Cue ✻ Block	572.6759	1	572.6759	245.975	< .001	0.904
Cue ✻ Block ✻ PassiveSeq	8.0288	1	8.0288	3.449	0.075	0.117
Residual	60.5328	26	2.3282			
Task ✻ Cue ✻ Block	0.9022	1	0.9022	1.704	0.203	0.061
Task ✻ Cue ✻ Block ✻ PassiveSeq	0.9207	1	0.9207	1.739	0.199	0.063
Residual	13.7691	26	0.5296			

Note. Type 3 Sums of Squares

Supplementary Table 11. *Repeated measures ANOVA statistics, with within-subject factors of Task/Condition (Active x Passive), Cue (H-L x L-H) and Block (Acquisition x Reversal), controlling for passive sequence type (PassiveSeq), for intensity ratings in control participants (n=28).*

Within Subjects Effects

	Sum of Squares	df	Mean Square	F	p	η^2_p
Task	1.93	1	1.93	1.327	0.260	0.049
Task ✻ PassiveSeq	4.26	1	4.26	2.929	0.099	0.101
Residual	37.77	26	1.45			
Cue_Bias	35.96	1	35.96	6.553	0.017	0.201
Cue_Bias ✻ PassiveSeq	3.81	1	3.81	0.695	0.412	0.026
Residual	142.67	26	5.49			
Task ✻ Cue_Bias	2.54	1	2.54	2.126	0.157	0.076
Task ✻ Cue_Bias ✻ PassiveSeq	1.03	1	1.03	0.866	0.361	0.032
Residual	31.06	26	1.19			

Note. Type 3 Sums of Squares

Supplementary Table 12. *Repeated measures ANOVA statistics, with within-subject factors of Task/Condition (Active x Passive) and Cue_Bias (High-pain x Low-pain), controlling for passive sequence type (PassiveSeq), for acquisition biases in control participants (n=28).*

Within Subjects Effects

	Sum of Squares	df	Mean Square	F	p	η^2_p
Task	6.82	1	6.822	14.29	< .001	0.355
Task ✻ PassiveSeq	1.23	1	1.225	2.57	0.121	0.090
Residual	12.41	26	0.477			
Response	11.78	1	11.784	22.62	< .001	0.465
Response ✻ PassiveSeq	4.17	1	4.166	8.00	0.009	0.235
Residual	13.54	26	0.521			
Task ✻ Response	7.87	1	7.866	7.50	0.011	0.224
Task ✻ Response ✻ PassiveSeq	3.81	1	3.805	3.63	0.068	0.122
Residual	27.27	26	1.049			

Note. Type 3 Sums of Squares

Supplementary Table 13. *Repeated measures ANOVA statistics, with within-subject factors of Task/Condition (Active x Passive) and Response (Placebo x Nocebo), controlling for passive sequence type (PassiveSeq), for intensity ratings of surprise trials in the acquisition block in control participants (n=28).*

Within Subjects Effects

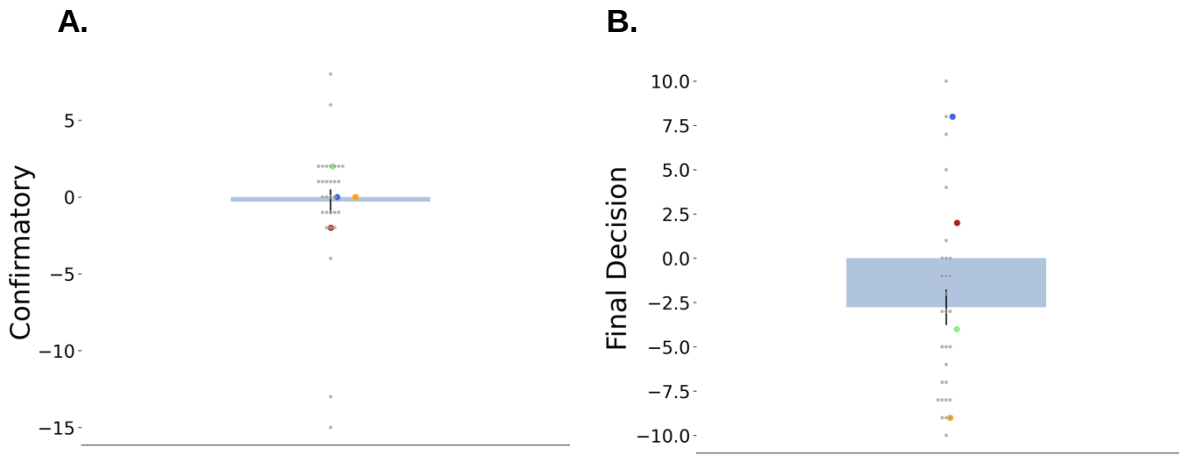
	Sum of Squares	df	Mean Square	F	p	η^2_p
Task	0.3238	1	0.3238	1.2665	0.271	0.046
Task ✻ PassiveSeq	0.1315	1	0.1315	0.5145	0.480	0.019
Residual	6.6471	26	0.2557			
Response	2.7881	1	2.7881	3.6049	0.069	0.122
Response ✻ PassiveSeq	0.4291	1	0.4291	0.5547	0.463	0.021
Residual	20.1091	26	0.7734			
Task ✻ Response	0.0132	1	0.0132	0.0284	0.867	0.001
Task ✻ Response ✻ PassiveSeq	2.5864	1	2.5864	5.5551	0.026	0.176
Residual	12.1054	26	0.4656			

Note. Type 3 Sums of Squares

Supplementary Table 14. *Repeated measures ANOVA statistics, with within-subject factors of Task/Condition (Active x Passive) and Response (Placebo x Nocebo), controlling for passive sequence type (PassiveSeq), for intensity ratings of surprise trials in the reversal block in control participants (n=28).*

6.4 Supplementary Materials Chapter 4

6.4.1 Supplementary Figures



Supplementary Figure 14. *Confirmatory evidence and Final Decision in the Draws to Certainty task in control participants and amputees.* Average Confirmatory Evidence **(A)** and Final Decision **(B)** (*y*-axis) for controls (*n*=30) and amputees (*n=4*). Note the small influence of Confirmatory Evidence within this sample, as well as the majority of the sample switching their support to Jar A at the end of the task. Individual data points and standard error of the mean plotted in grey. Amputees are plotted in participant-specific colours, in line with *Chapter 3* (e.g., AA01=orange; AA02=blue; AA03=green; AA04=red).

6.4.2 Supplementary Tables

Model Fit Measures

				Overall Model Test			
Model	**R**	**R²**	**Adjusted R²**	**F**	**df1**	**df2**	**p**
1	0.422	0.178	-0.00103	0.994	5	23	0.443

Model Coefficients - mean_DTD

			95% Confidence Interval			
Predictor	**Estimate**	**SE**	**Lower**	**Upper**	**t**	**p**
Intercept [a]	2.6582	1.4432	-0.3272	5.64374	1.842	0.078
BDI	0.0228	0.0951	-0.1739	0.21945	0.240	0.813
PCS	-0.0742	0.0390	-0.1550	0.00652	-1.902	0.070
Trait anxiety	0.0540	0.0558	-0.0614	0.16936	0.968	0.343
Age	-0.0216	0.0238	-0.0709	0.02776	-0.904	0.375
Gender:						
M – F	0.4829	0.7028	-0.9709	1.93670	0.687	0.499

[a] Represents reference level

Supplementary Table 15. *Regression model predicting Draw's to Decision (DTD) in control participants (n=29), including those who reported DTD > 6, with explanatory variables of depression, anxiety and pain catastrophising (including nuisance regressors of age and gender). Note the positive trend for pain catastrophising coefficient, despite the non-significant overall regression model. BDI=Becks Depression Inventory; PCS=Pain Catastrophising Scale.*

Model Fit Measures

				Overall Model Test			
Model	**R**	**R^2**	**Adjusted R^2**	**F**	**df1**	**df2**	**p**
1	0.477	0.228	0.0350	1.18	5	20	0.353

Model Coefficients - mean_DTD

			95% Confidence Interval			
Predictor	**Estimate**	**SE**	**Lower**	**Upper**	**t**	**p**
Intercept [a]	2.9283	0.7399	1.3848	4.4718	3.9575	< .001
BDI	-0.0389	0.0483	-0.1396	0.0618	-0.8053	0.430
PCS	-0.0320	0.0204	-0.0745	0.0105	-1.5726	0.131
Trait anxiety	0.0364	0.0283	-0.0226	0.0954	1.2877	0.213
Age	-0.0251	0.0124	-0.0510	8.97e-4	-2.0139	0.058
Gender:						
M – F	-0.0188	0.3616	-0.7731	0.7355	-0.0520	0.959

[a] Represents reference level

Supplementary Table 16. *Regression model predicting Draw's to Decision (DTD) in control participants (n=26), excluding those who reported DTD > 6, with explanatory variables of depression, anxiety and pain catastrophising (including nuisance regressors of age and gender). BDI=Becks Depression Inventory; PCS=Pain Catastrophising Scale.*

Model Fit Measures

				Overall Model Test			
Model	**R**	**R^2**	**Adjusted R^2**	**F**	**df1**	**df2**	**p**
1	0.579	0.335	0.190	2.31	5	23	0.077

Model Coefficients - likelihood2

			95% Confidence Interval			
Predictor	**Estimate**	**SE**	**Lower**	**Upper**	**t**	**p**
Intercept [a]	11.076	6.0053	-1.34657	23.4994	1.844	0.078
BDI	0.319	0.3956	-0.49974	1.1371	0.805	0.429
PCS	0.439	0.1624	0.10294	0.7749	2.702	0.013
Trait anxiety	-0.563	0.2321	-1.04329	-0.0832	-2.427	0.023
Age	0.214	0.0992	0.00831	0.4187	2.152	0.042
Gender:						
M – F	-1.259	2.9244	-7.30832	4.7907	-0.430	0.671

[a] Represents reference level

Supplementary Table 17. *Regression model predicting Disconfirmatory Evidence in control participants (n=29), with explanatory variables of depression, anxiety and pain catastrophising (including nuisance regressors of age and gender). Note the significant predictors of pain catastrophising and trait anxiety coefficient, despite the non-significant (but positive trend) overall regression model. BDI=Becks Depression Inventory; PCS=Pain Catastrophising Scale.*

Model Fit Measures

				Overall Model Test			
Model	**R**	**R²**	**Adjusted R²**	**F**	**df1**	**df2**	**p**
1	0.429	0.184	0.0817	1.80	3	24	0.174

Model Coefficients - mean_DTD

			95% Confidence Interval			
Predictor	**Estimate**	**SE**	**Lower**	**Upper**	**t**	**p**
Intercept [a]	2.6314	0.8812	0.8127	4.4502	2.986	0.006
Age	-0.0209	0.0205	-0.0633	0.0214	-1.021	0.317
Gender:						
M – F	0.4090	0.6073	-0.8445	1.6624	0.673	0.507
Alpha_Active	2.9065	1.3822	0.0539	5.7592	2.103	0.046

[a] Represents reference level

Supplementary Table 18. *Regression model predicting Draws to Decision in control participants (n=28), including those with DTD > 6, with explanatory variables of aversive learning rate (from the 'winning' computational model; see Chapter 3 Method and Results), and controlling for age and gender. Note the significant predictor of the learning rate (Alpha_Active).*

Model Fit Measures

				Overall Model Test			
Model	**R**	**R²**	**Adjusted R²**	**F**	**df1**	**df2**	**p**
1	0.375	0.140	0.0175	1.14	3	21	0.355

Model Coefficients - mean_DTD

			95% Confidence Interval			
Predictor	**Estimate**	**SE**	**Lower**	**Upper**	**t**	**p**
Intercept [a]	2.9916	0.4835	1.9862	3.99703	6.188	< .001
Age	-0.0198	0.0114	-0.0434	0.00392	-1.736	0.097
Gender:						
M – F	0.1090	0.3362	-0.5902	0.80824	0.324	0.749
Alpha_Active	0.6393	0.7910	-1.0056	2.28430	0.808	0.428

[a] Represents reference level

Supplementary Table 19. *Regression model predicting Draws to Decision in control participants (n=28), excluding those with DTD > 6, with explanatory variables of aversive learning rate (from the 'winning' computational model; see Chapter 3 Method and Results), and controlling for age and gender. Note the significance of the learning rate (Alpha_Active) is lost.*

Model Fit Measures

				Overall Model Test			
Model	**R**	**R^2**	**Adjusted R^2**	**F**	**df1**	**df2**	**p**
1	0.281	0.0789	-0.0362	0.685	3	24	0.570

Model Coefficients - mean_DTD

			95% Confidence Interval			
Predictor	**Estimate**	**SE**	**Lower**	**Upper**	**t**	**p**
Intercept [a]	3.7998	0.8982	1.9460	5.6536	4.230	< .001
Age	-0.0161	0.0218	-0.0611	0.0290	-0.737	0.468
Gender:						
M – F	0.3314	0.6483	-1.0066	1.6695	0.511	0.614
Active_Placebo_Acq	0.3311	0.3039	-0.2961	0.9583	1.089	0.287

[a] Represents reference level

Supplementary Table 20. *Regression model predicting Draws to Decision in control participants (n=28), including those with DTD > 6, with explanatory variable of the placebo response during the acquisition block of the aversive learning paradigm (see Chapter 3, Results), whilst controlling for age and gender.*

Model Fit Measures

				Overall Model Test			
Model	**R**	**R²**	**Adjusted R²**	**F**	**df1**	**df2**	**p**
1	0.376	0.141	0.0185	1.15	3	21	0.352

Model Coefficients - mean_DTD

			95% Confidence Interval			
Predictor	**Estimate**	**SE**	**Lower**	**Upper**	**t**	**p**
Intercept [a]	3.2983	0.4802	2.2997	4.29692	6.869	< .001
Age	-0.0185	0.0113	-0.0420	0.00511	-1.628	0.118
Gender:						
M – F	0.0869	0.3367	-0.6133	0.78709	0.258	0.799
Active_Placebo_Acq	0.1282	0.1559	-0.1959	0.45239	0.823	0.420

[a] Represents reference level

Supplementary Table 21. *Regression model predicting Draws to Decision in control participants (n=28), excluding those with DTD > 6, with explanatory variable of the placebo response during the acquisition block of the aversive learning paradigm (see Chapter 3, Results), whilst controlling for age and gender.*